Synthesis, properties and applications of all-*cis*-pentafluorocyclohexane 'Janus' ring building blocks

Joshua Clark

A thesis submitted for the degree of PhD
at the
University of St Andrews

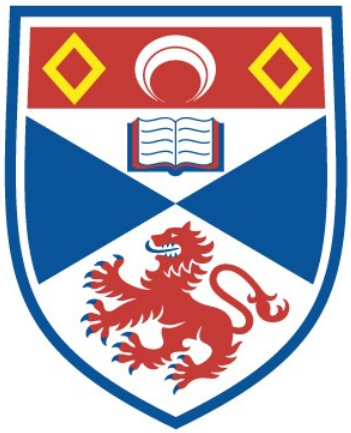

2022

DOI: https://doi.org/10.17630/sta/720

Candidate's declaration

I, Joshua Clark, do hereby certify that this thesis, submitted for the degree of PhD, which is approximately 43,000 words in length, has been written by me, and that it is the record of work carried out by me, or principally by myself in collaboration with others as acknowledged, and that it has not been submitted in any previous application for any degree. I confirm that any appendices included in my thesis contain only material permitted by the 'Assessment of Postgraduate Research Students' policy.

I was admitted as a research student at the University of St Andrews in September 2016.

I received funding from an organisation or institution and have acknowledged the funder(s) in the full text of my thesis.

Date 15th January 2022 Signature of candidate

Supervisor's declaration

I hereby certify that the candidate has fulfilled the conditions of the Resolution and Regulations appropriate for the degree of PhD in the University of St Andrews and that the candidate is qualified to submit this thesis in application for that degree. I confirm that any appendices included in the thesis contain only material permitted by the 'Assessment of Postgraduate Research Students' policy.

Date 15th January 2022 Signature of supervisor

Permission for publication

In submitting this thesis to the University of St Andrews we understand that we are giving permission for it to be made available for use in accordance with the regulations of the University Library for the time being in force, subject to any copyright vested in the work not being affected thereby. We also understand, unless exempt by an award of an embargo as

requested below, that the title and the abstract will be published, and that a copy of the work may be made and supplied to any bona fide library or research worker, that this thesis will be electronically accessible for personal or research use and that the library has the right to migrate this thesis into new electronic forms as required to ensure continued access to the thesis.

I, Joshua Clark, confirm that my thesis does not contain any third-party material that requires copyright clearance.

The following is an agreed request by candidate and supervisor regarding the publication of this thesis:

Printed copy

No embargo on print copy.

Electronic copy

No embargo on electronic copy.

Date 15th January 2022 Signature of candidate

Date 15th January 2022 Signature of supervisor

Underpinning Research Data or Digital Outputs

Candidate's declaration

I, Joshua Clark, understand that by declaring that I have original research data or digital outputs, I should make every effort in meeting the University's and research funders' requirements on the deposit and sharing of research data or research digital outputs.

Date 15th January 2022 Signature of candidate

Permission for publication of underpinning research data or digital outputs

We understand that for any original research data or digital outputs which are deposited, we are giving permission for them to be made available for use in accordance with the requirements of the University and research funders, for the time being in force.

We also understand that the title and the description will be published, and that the underpinning research data or digital outputs will be electronically accessible for use in accordance with the license specified at the point of deposit, unless exempt by award of an embargo as requested below.

The following is an agreed request by candidate and supervisor regarding the publication of underpinning research data or digital outputs:

No embargo on underpinning research data or digital outputs.

Date 15th January 2022 Signature of candidate

Date 15th January 2022 Signature of supervisor

Abstract

Strategically fluorinated compounds such as the all-*cis*-pentafluorocyclohexane 'Janus' rings, the subject of this research, can have strong molecular dipole moments because the electronegative fluorines polarise the geminal hydrogens rendering them electropositive.

In Chapter 1, a general discussion of the dominant interactions associated with organofluorine compounds is given. This is followed by an examination of the variety of fluorination methods available. The role of fluorine in medicinal chemistry is explored including in positron emission tomography (PET). A summary of previous work from the St Andrews group provides the contextual basis on which the following chapters build.

Chapter 2 explores a recently reported Rh-catalysed hydrogenation reaction of fluoroarenes to access all-*cis*-fluorocyclohexanes in excellent diastereoselectivity. The scope of this reaction is expanded to generate novel cyclohexane products such as alcohol **2.47** and methyl ester **2.60**. Derivatisation of these products has furnished a library of all-*cis*-pentafluorocyclohexane building blocks for further study. These include alkyl bromide **2.82**, organoazide **2.83** and aldehyde **2.87**.

In Chapter 3, the elaboration of these building blocks to higher order molecular structures is explored. Ugi 4-component reactions (Ugi-4CR) with aldehyde **2.87** provide combinatorial access to medicinally relevant *bis*-amides **3.20**-**3.27**. The Ugi-4CR, optimised by microwave assistance, can be completed within 45 mins. Using an HPLC method the Log P of three of these Ugi products (**3.23**, **3.25** and **3.27**) was measured and in each case the Log P value reduced relative to phenyl ring analogues. This finding suggests a potential application of the 'Janus' ring as an arene isostere in medicinal chemistry. Other methods of elaboration explored in Chapter 3 include amide coupling, Wittig and CuAAC 'click' reactions.

Chapter 4 reports the preparation of 'Janus' ring bearing novel amphiphiles, the long chain carboxylic acid **4.1** and alcohol **4.2** as well as analogous hydrocarbon reference compounds **4.4** and **4.5**. A Langmuir isotherm study examined the influence of the ring system on phase behaviour at the air-water interface. Evidence is presented of molecular self-assembly for the long chain **4.1** and **4.2,** unlike the classical behaviour observed for the hydrocarbon counterparts **4.4** and **4.5**. This analysis is supported by a thorough examination of X-ray crystal structures and presents a platform for the further development of the 'Janus' ring motif for supramolecular chemistry.

Finally, Chapter 5 summarises the findings of the previous chapters and explores possible avenues for future work such as the development of a 'pull-down' assay using biotinylated affinity probes **5.1** and **5.2** to better understand interactions between the 'Janus' ring and proteins of interest.

Acknowledgements

First and foremost, I want to thank my supervisor Prof David O'Hagan for all his support and guidance throughout my PhD. I am very grateful to him for the opportunity to work in such a unique research group. David's enthusiasm for science and intellectual curiosity have helped me to persist in the face of challenges both in and out of the lab throughout my PhD.

Thank you to all the members of the DOH group past and present. It has been a pleasure to work alongside so many intelligent and talented people from all around the world. I want to thank Phil especially for being a patient mentor right at the start of my PhD when I was fearful of doing everything wrong. Thanks also to Prof Andrew Smith and Dr Kevin Jones of the CRITICAT CDT for all their work to provide an enriching program. Kevin, thank you for being a listening ear whenever I wanted to talk.

I want to thank the many staff of the department for their help especially Tomas and Siobhan for all their help with NMR, David and Alex for solving the many X-ray crystal structures and Caroline for running the mass spectrometry facilities. Thank you to Prof Andrew Smith and Dr Gordon Florence for allowing me to work temporarily in your labs in the aftermath of the BMS fire. Thank you to our many collaborators especially Dr Stefan Guldin and Dr Alaric Taylor at UCL for providing me with a fascinating hands-on experience with your Langmuir trough, just in time before COVID-19 made such things impossible. Also thank you to Prof Cormac Murphy and Dr Mohd Khan of UCD and to Prof. Rodrigo Cormanich and Bruno Piscelli of the University of Campinas for their studies which have informed this work.

Thanks to my family, especially my parents and my sister Zoë for their unconditional love and support, I couldn't have done any of this without them. Thank you for all those hours helping with revision and driving the length of the country to open days. Thank you for always being there for me whenever I've needed you and for always believing in me.

À Teresa, obrigado pelo teu amor. Tens sido uma luz brilhante nos meus momentos mais escuros e a minha amiga mais próxima. E agora, mais forte do que nunca, vamos começar mais uma aventura juntos. Mal posso esperar.

Finally, I want to thank all my friends for their support. My Horsham friends, you made the lockdowns bearable with hours of zoom calls and so many terrible movies. Will, you've been like a brother, thanks for the memories. Maybe we'll get the band back together for karaoke sometime soon. This thesis is dedicated to the memory of Scott Stinson, a great person and friend who is deeply missed. I feel lucky to have had him in my life.

The research underpinning this thesis has received funding from the EPSRC Centre for Doctoral Training in Critical Resource Catalysis (CRITICAT, Grant Number EP/L016419/1). Research data underpinning this thesis are available at
https://doi.org/10.17630/edc5d01f-7743-4349-9c50-7fcb0529f1ac

Abbreviations

Å	Angstrom
α	Optical rotation
δ	Chemical shift
ε'	Dielectric constant
ε''	Dielectric loss constant
µ	Micro
A	Area
Ac	Acetyl
AlkylFluor	1,3-Bis(2,6-diisopropylphenyl)-2-fluoro-1H-imidazol-3-ium tetrafluoroborate
Ax	Axial
Bn	Benzyl
Boc	*tert*-Butyloxycarbonyl
br	Broad
Bz	Benzoyl
c	Centi
CAAC	Cyclic(alkyl)(amino)carbene
Cat	Catalyst
COD	1,5-Cyclooctadiene
COSY	Correlation spectroscopy
4CR	Four component reaction
18-crown-6	1,4,7,10,13,16-Hexaoxacyclooctadecane
CuAAC	Copper-catalysed alkyne-azide cycloaddition
2D	Two-dimensional
d	Doublet
D	Debye
DABCO	1,4-Diazabicyclo[2.2.2]octane
DAST	Diethylaminosulfur trifluoride
1,2-DCE	1,2-Dichloroethane
Deoxofluor	Bis(2-methoxyethyl)aminosulfur trifluoride
Dipp	Diisopropylphenyl
DFI	2,2-Difluoro-1,3-dimethylimidazolidine
DFMBA	*N*,*N*-Diethyl-α,α-difluoro-3-methylbenzylamine
DFT	Density-functional theory

DIBAlH	Diisobutylaluminium hydride
DMAP	4-Dimethylaminopyridine
DMF	*N*,*N*-Dimethylformamide
DMSO	Dimethylsulfoxide
DOPr	Δ-Opiod receptor
E1cB	Elimination unimolcular conjugate base
E2	Bimolecular elimination
EC_{50}	Half maximal effective concentration
ED_{50}	Median effective dose
Ee	Enantiomeric excess
EI	Electron impact
Eq	Equatorial
ESI	Electrospray
Et	Ethyl
eV	Electronvolt
FAR	Fluoroamino reagent
5'-FDA	5'-Fluorodeoxyadenosine
FDG	2-Deoxy-2-[^{18}F]fluoro-D-glucose
g	Gram
G	Giga
Glu	Glutamic acid
h	Hours
[H]	Reduction
HATU	1-[Bis(dimethylamino)methylene]-1H-1,2,3-triazolo[4,5-b]pyridinium 3-oxide hexafluorophosphate
HF.Pyr	Pyridine hydrofluoride, Olah's reagent
HMBC	Heteronuclear multiple bond correlation spectroscopy
HMDS	Hexamethyldisilazane
HPLC	High performance liquid chromatography
HSQC	Heteronuclear single-quantum correlation spectroscopy
HOMO	Highest occupied molecular orbital
HRMS	High-resolution mass spectrometry
5-HT_{2a}	5-Hydroxytryptamine receptor 2a

HWE	Horner-Wadsworth-Emmons
Hz	Hertz
^{i}Bu	Isobutyl
IC_{50}	Half maximal inhibitory concentration
IMCR	Isocyanide multicomponent reaction
^{i}Pr	Isopropyl
IR	Infrared
J	Spin-spin coupling constant
k	Capacity factor
K_a	Acid dissociation constant
K_a	Association constant
K_i	Inhibitor constant
L	Litre
LDA	Lithium diisopropylamide
Leu	Leucine
Log D	Distribution coefficient
Log P	Partition coefficient
LUMO	Lowest unoccupied molecular orbital
m	Multiplet
m	Milli
M	Molar
M	Mega
mCPBA	*meta*-Chloroperbenzoic acid
MCR	Multicomponent reactions
Me	Methyl
Morpho-DAST	Morpholinosulfur trifluoride
mins	Minutes
m.p.	Melting point
MOF	Metal-organic-framework
Ms	Mesyl
MS	Molecular sieves
MW	Microwave
m/z	Mass:charge ratio
N	Normal
^{n}Bu	Butyl
NFSI	*N*-Fluorobenzenesulfonimide

NHC	*N*-Heterocyclic carbene
NLO	Non-linear optical
NMR	Nuclear magnetic resonance
NOESY	Nuclear overhauser effect spectroscopy
OPA	Oxaphosphetane
PET	Positron emission tomography
pH	Potential of hydrogen
Ph	Phenyl
Phenofluor	1,3-Bis(2,6-diisopropylphenyl)-2,2-difluoro-2,3-dihydro-1H-imidazole
Phenofluor mix	Ceasium Fluoride.2-chloro-1,3-bis(2,6-diisopropylphenyl)-1H-imidazol-3-ium chloride
pK_a	Negative log of K_a
PTFE	Poly(tetrafluoroethylene)
*p*TSA	*p*-Toluenesulfonic acid
PVDF	Poly(vinylidene fluoride)
Pyfluor	2-Pyridinesulfonyl Fluoride
q	Quartet
quant.	Quantitative yield
r	Radius
Ref	Reference
Rf	Retention factor
r.t.	Room temperature
s	Singlet
SAM	*S*-Adenosyl methionine
Selectfluor	1-Chloromethyl-4-fluoro-1,4-diazoniabicyclo[2.2.2]octane bis(tetrafluoroborate)
S_NAr	Nucleophilic aromatic substitution
S_N2	Bimolecular nucleophilic substitution
SPS	Solvent purification system
SSRI	Selective serotonin reuptake inhibitor
$t_{1/2}$	Half life
t	Triplet
tan δ	Loss tangent
TBAF	Tetra-n-butylammonium fluoride
TBS/TBDMS	*tert*-Butyldimethylsilyl

^{t}Bu	*tert*-Butyl
tert	Tertiary
Tf	Trifluoromethanesulfonyl
TFA	Trifluoroacetic acid
TFEDMA	1,1,2,2-Tetrafluoro-*N*,*N*-dimethylethylamine
THF	Tetrahydrofuran
THP	Tetrahydropyran
TLC	Thin-layer chromatography
TMS	Tetramethylsilane
TREAT-HF	Triethylamine trihydrofluoride
tRNA	Transfer ribonucleic acid
Ts	Tosyl
UV	Ultraviolet
v	Volume
VdW	Van der Waals
v_{max}	Maximum absorption

Contents

1. Introduction

The origins of fluorine chemistry can be traced to the serendipitous production of hydrofluoric acid (HF) from the reaction of sulfuric acid with feldspar (CaF_2). The first studies of HF were conducted by Carl William Scheele following its earlier description by Andreas Sigismund Marggraf in the 18th century.[1] Following isolation, HF was to find an application in the etching of glass for decorative purposes. Today, commercially available sources of HF are stored in plastic bottles to avoid corrosion. Elemental fluorine (F_2) was first isolated by the electrolysis of hydrofluoric acid in 1886 by Henri Moissan.[1] Moissan was awarded the 1906 Nobel Prize for his work.

The first organofluorine compounds were reported by Frédéric Swarts beginning in 1892 with the isolation of trichlorofluoromethane ($CFCl_3$).[2] Swarts' employed halogen exchange reactions between chlorocarbons and metal fluoride salts such as antimony trifluoride (SbF_3).[2] Using this reaction, Swarts reported dozens more organofluorine compounds including dichlorodifluoromethane (CF_2Cl_2) which subsequently found mass commercialisation as Freon-12 in domestic refrigeration in the 1950s. The use of Freon-12 and other ozone-depleting chlorofluorocarbons was later prohibited in all but exceptional circumstances under the Montreal Protocol in 1987.

Since these early forays, organofluorine chemistry has proved relevant to numerous fields of chemical science. Today, around a fifth of all licensed pharmaceuticals contain one or more fluorine atom.[3] Likewise in agrochemistry, a quarter of globally licensed herbicides are fluorine-containing compounds.[4] Organofluorine compounds have found diverse applications also in polymer and materials science, for example the fluorinated polymer Teflon™ which is widely utilised as a non-stick coating for cookware, exemplifies the unusual properties of highly fluorinated materials.[5]

1.1. Atomic fluorine

As the most electronegative element in the Periodic Table, fluorine exhibits unique electronic properties. The electronegativity of fluorine ($1s^2 2s^2 2p^5$) is a consequence of its high nuclear charge and small atomic radius. Oxidation of the fluorine atom to form F^+ is highly endothermic (−401.2 kcal mol^{-1}) whereas the reduction of the fluorine atom is exothermic (+78.3 kcal mol^{-1}). In the latter case the additional electron fills the 2p shell which is particularly well stabilised by the positive charge of the nucleus. The fluorine atom has a Van der Waals radius lying between those of oxygen and hydrogen and it is often utilised in drug discovery as an isostere for either atom.

	H	O	F
Electronegativity (Pauling)	2.1	3.5	4.0
Van der Waals radius / Å	1.2	1.52	1.47
C-X bond length / Å	1.09	1.43	1.35
C-X bond dissociation energy / kcal mol^{-1}	98.8	84.0	105.4

Table 1.1 Comparing properties of hydrogen, oxygen and fluorine.

1.2. The carbon-fluorine bond

The carbon-fluorine single bond is the strongest in organic chemistry as a consequence of the electrostatic attraction between the electronegative fluorine atom and the electropositive carbon. Electron density is highly concentrated on the fluorine atom of the C-F bond. The carbon-fluorine bond therefore has a significant ionic component and a strong dipole moment. Dolbier *et al*.,[6] demonstrated the preference of fluorine to bonds to sp^3 over sp^2 carbons by exploring the equilibrium of the Cope rearrangement as illustrated in Scheme 1.1. Carbon atoms with sp^3 hybridisation have electrons with greater p-character. These are more polarisable than those in sp^2 orbitals. Fluorine makes more thermodynamically favourable bonds with sp^3 carbons due to its ability to draw more electron density from the carbon, which strengthens the bond.

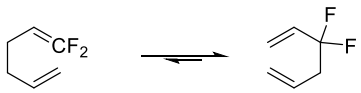

1.1 1.2

Scheme 1.1 Cope rearrangement as reported by Dolbier *et al*..[6]

The carbon-fluorine bond displays unusually slow reactivity, for instance the rate of S_N2 reactions with alkyl fluorides are an order of magnitude slower than alkyl chlorides and three orders of magnitude slower than alkyl bromides and iodides (Scheme 1.2).[7] Although the carbon of the C-F bond is strongly electropositive, the strength of the carbon-fluorine bond means there is a significant barrier to cleavage.

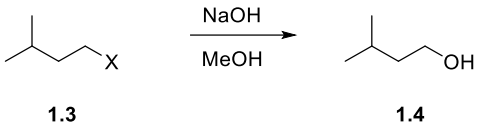

1.3 **1.4**

X	Relative rate
F	1
Cl	71
Br	3500
I	4500

Scheme 1.2 The relative rates of alkyl halides to S_N2 reactions.[7]

The C-F bond is vulnerable to cleavage in S_NAr reactions where aryl fluorides are often better electrophiles than the analogous aryl halides (Scheme 1.3). In the example of halo-substituted 2,4-dinitrobenzenes **1.5** Senger *et al*.,[8] found a 400-fold increase in relative rate for the fluorine containing electrophile versus the bromo- and chloro- analogues. The rate enhancement is due to the acceleration of the typically rate-limiting addition step and then, stabilisation of the intermediate anion **1.6** by the fluorine atom.

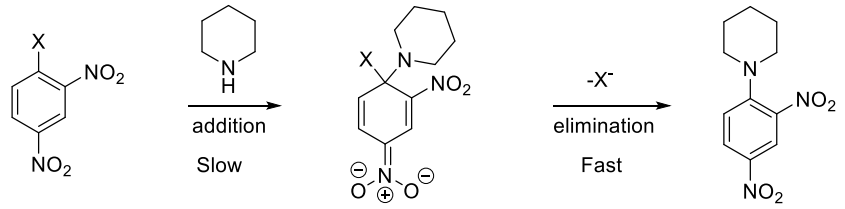

1.5 **1.6** **1.7**

X	Relative rate
F	1613
Cl	4
Br	4
I	1

Scheme 1.3 The relative rates of electron-deficient aryl halides to S_NAr reported by Senger *et al*..[8]

Base-sensitivity of fluoroalkanes is often problematic in the syntheses of organofluorine compounds. Kinetic analysis by Ryberg *et al*., of the base-promoted HF elimination from **1.8** showed that the elimination pathway involves an E1cB process (Scheme 1.4).[9] Under basic conditions, the β-carbon is deprotonated as the resultant carbanion **1.9** is stabilised by the inductive effect of the fluorine atom. Then **1.9** can form a π-bond and eliminate fluoride to give the alkene product **1.10**.

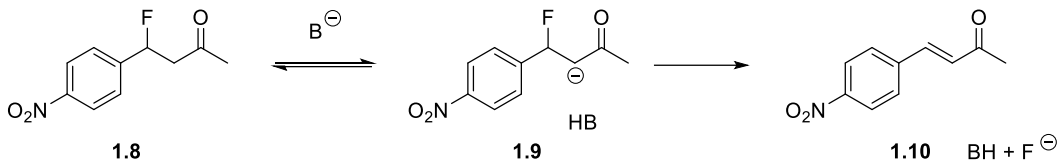

Scheme 1.4 E1cB elimination of fluoride under basic conditions.[9]

1.3. Stereoelectronic and conformational effects of the C-F bond

1.3.1. Hyperconjugation

The low-lying LUMO of the C-F bond (σ*) readily accepts electrons from electron rich bonding orbitals such as a C-H (σ) bond in stabilising hyperconjugation interactions (Figure 1.1). This is an important interaction in organofluorine chemistry and underpins the anomeric and *gauche* effects.

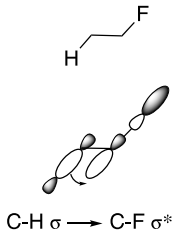

Figure 1.1 Hyperconjugation from C-H (σ) to C-F (σ*).

1.3.2. The anomeric effect

The anomeric effect explains the frequently observed axial preference for heteroatom substituents in the 2-position of tetrahydropyrans (Figure 1.2). In the axial (α-) conformer of **1.11** (**1.11a**) hyperconjugation occurs from the non-bonding oxygen lone pair to the LUMO C-O (σ*). This hyperconjugation is not possible in the equatorial (β-) conformer (**1.11b**) due to poor orbital overlap. Similarly, the anomeric effect has been predicted by DFT to be even stronger in 2-fluorotetrahydropyran **1.12**, with ΔE increasing from 0.78 kcal mol^{-1} in **1.11** to 2.89 kcal mol^{-1} in **1.12**.[10]

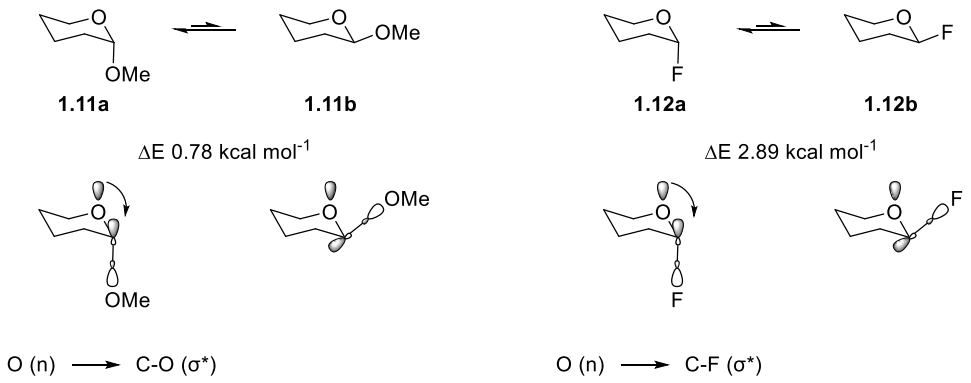

Figure 1.2 The anomeric effect showing hyperconjugation interactions supporting a preference for the α-conformer in 2-methoxytetrahydropyran **1.11** and 2-fluorotetrahydropyran **1.12**.

1.3.3. The '*gauche* effect'

Vicinal difluoroalkanes such as 1,2-difluoroethane preferentially adopt a *gauche* conformation. By contrast, 1,2-dichloro-, 1,2-dibromo- and 1,2-diiodo-ethane (**1.13**) adopt an *anti* conformation on steric grounds (Figure 1.3A). The unusual stability of the *gauche* conformer of 1,2-difluoroethane **1.14** has been termed the '*gauche* effect' and is explained by hyperconjugation stabilising the *gauche* conformer.[7] The stability derived from hyperconjugation in the *gauche* conformer outweighs the Pauli repulsion between the fluorine lone pairs due to the relatively small size of fluorine.[11]

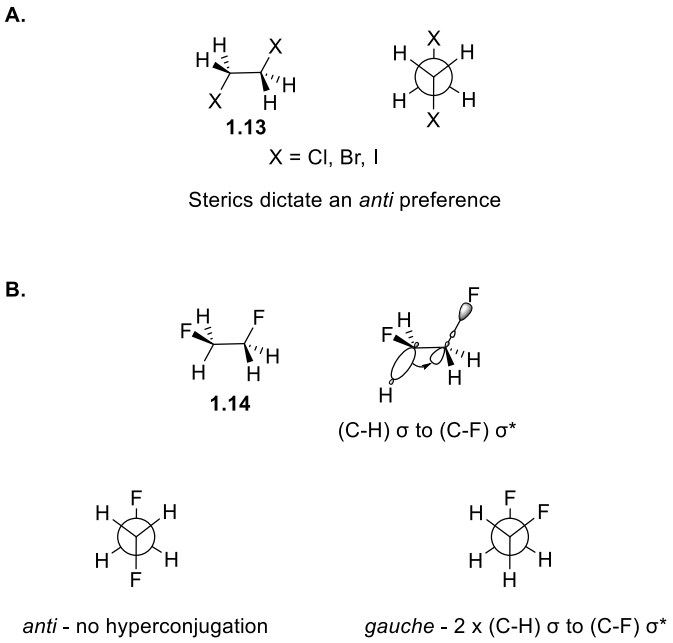

Figure 1.3 A. Preference for *anti* conformer in 1,2-dichloro-, 1,2-dibromo- and 1,2-diiodo-ethane (**1.13**). **B**. Preference for *gauche* conformer in 1,2-difluoroethane **1.14** due to hyperconjugation.

Alternative explanations for the observed '*gauche* effect' have been proposed. A 'bent bonds' hypothesis reported by Wilberg *et al*. argues that the relative stability of the *gauche* conformer of 1,2-difluoroethane derives from the avoidance of unfavourable orbital overlap present in the *anti* conformer.[12] More recently Thacker *et al.* have utilised an 'interacting quantum atoms' method to propose that 1,3 C···F electrostatic polarisation interactions are the dominant contribution accounting for the '*gauche* effect'.[13] The true nature of the fluorine '*gauche* effect' remains a subject of investigation in which both hyperconjugation and electrostatic interactions play a role.

1.3.4. Dipole-dipole interactions

Although hyperconjugation has been much discussed, its overall contribution to conformational stability can be low. For example, in the case of 1,3-difluoropropane the least stable of the four vicinally staggered conformers, **1.18**, is highest in energy by > 3 kcal mol^{-1} due to 1,3-dipolar repulsion between the fluorine atoms. Conformers **1.16** and **1.17**, which have lower molecular dipole moments, are lower in energy despite reduced hyperconjugation interactions. The most stable conformer **1.15** facilitates favourable hyperconjugation and minimises 1,3-dipolar repulsion.

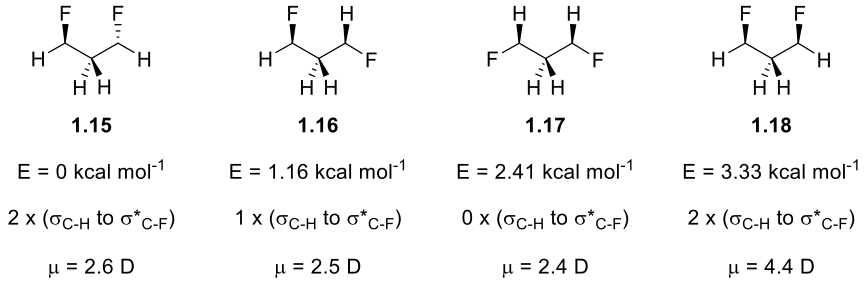

Figure 1.4 Relative energy of various conformers of 1,3-difluoropropane (**1.15**-**1.18**) as reported by Wu *et al*..[14]

Compounds with a fluorine substituent α- to a carbonyl display a preference for *anti* conformations in the gas phase.[7] By adopting the *anti* conformer, the dipole moments of the C-F bond and the carbonyl are antiparallel, and the molecular dipole moment is minimised (Scheme 1.5A). The dipolar repulsion effect typically persists in the solution phase for non-polar solvents but as solvent polarity increases, the *syn* conformer becomes more dominant due to dipole alignment to the solvent. In the case of α-fluoroacetone, the *anti* conformer is favoured (ΔE = +2.9 kcal mol^{-1}) in the gas phase and the *syn* conformer is favoured (ΔE = −1.3 kcal mol^{-1}) in solution when DMSO is the solvent (Scheme 1.5B).[15]

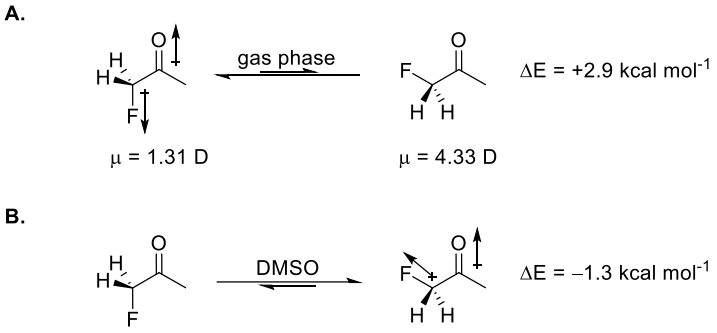

Scheme 1.5A Dipolar repulsion favouring *anti* conformation in α-fluoroacetone in the gas phase. **B** Dipolar alignment favouring *syn* conformation in α-fluoroacetone in the solution phase (DMSO).[15]

1.3.5. Charge-dipole interactions

The C-F bond can also form strong interactions with positively charged groups as shown by the axial preference of the C-F bond in 3-fluoropiperidines **1.19** and **1.20**.[16] The axial preference occurs because the C-F dipole lies *anti* parallel to the N-H dipole. There is also an electrostatic attraction between the diaxial atoms.

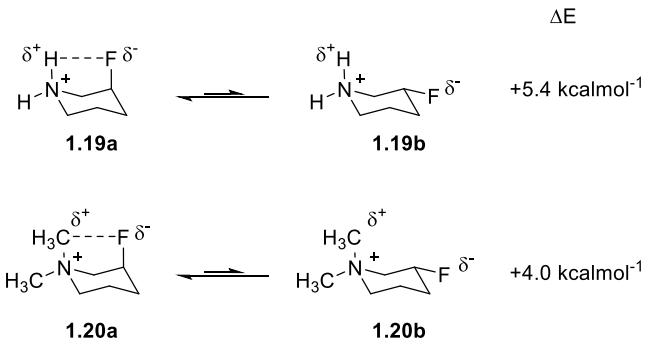

Scheme 1.6 Axial preference of the C-F bond in 3-fluoropiperidines **1.19** and **1.20** stabilised by charge-dipole interactions.[16]

1.4. Fluorination of organic compounds

1.4.1. Electrophilic fluorinating agents

Electrophilic fluorinations of both aromatic and aliphatic substrates are typically achieved utilising *N*-fluoro species (Figure 1.5). Initially these consisted of pyridinium fluoride salts such as **1.21** and **1.22** first reported by Umemoto.[17] These reagents have largely been superseded by more specific and effective DABCO-based reagents including Selectfluor. Also important are the neutral *N*-fluorosulfonamide reagents such as NFSI. The reactivity of each reagent can be tuned by varying substituents in the core structures.

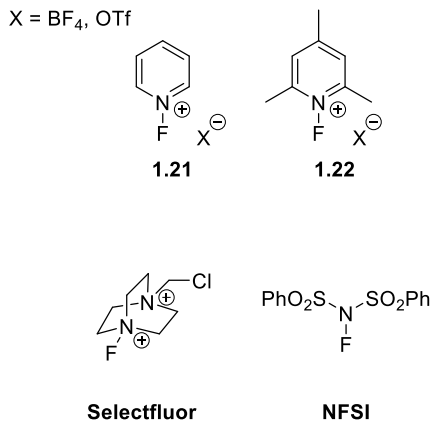

Figure 1.5 Electrophilic *N*-fluoro fluorination reagents.

1.4.2. Nucleophilic fluorination

Fluoride anions are poor nucleophiles in protic solvents as they are readily solvated. Metal fluoride salts (NaF, CsF, KF) are typically insoluble in polar solvents due to tight ion-pairing. The use of complexing agents such as crown ethers can improve the solubility of metal fluoride salts in aprotic solvents. For example, Scheme 1.7 shows the fluorination of alkyl tosylate **1.23** to give a fluorinated vitamin D3 derivative **1.24**. Here, the use of 18-crown-6 facilitated the solubility of KF in DMF.[18]

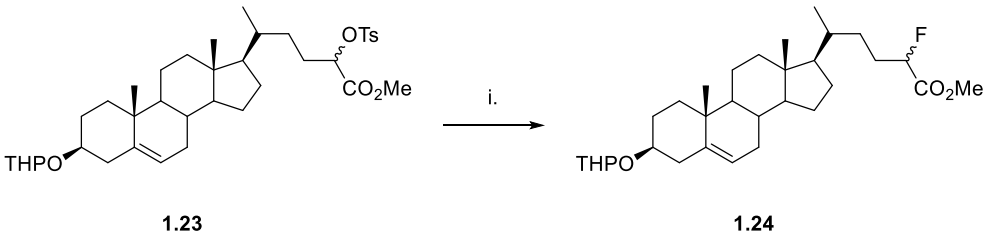

Scheme 1.7 The fluorination of vitamin D3 derivative **1.23** to give **1.24**; i. KF, 18-crown-6, DMF, 70 °C, 73%.[18]

Similarly, the solubility and nucleophilicity of metal fluoride salts can be increased by hydrogen bonding as demonstrated by Gouverneur.[19–21] Using chiral *bis*-urea phase-transfer catalysts **1.25** and **1.26** and KF/CsF as a nucleophile the highly enantioselective preparation of β-fluorosulfides, β-fluoroamines and γ-fluoroamines by the fluorination of *in-situ* formed heterocyclic cations has been reported (Scheme 1.8). The chiral *bis*-urea catalysts form a tridentate hydrogen-bonding complex to fluoride which forms an ion-pair with the cationic electrophile thereby facilitating asymmetric fluorination (Scheme 1.8).[19–21]

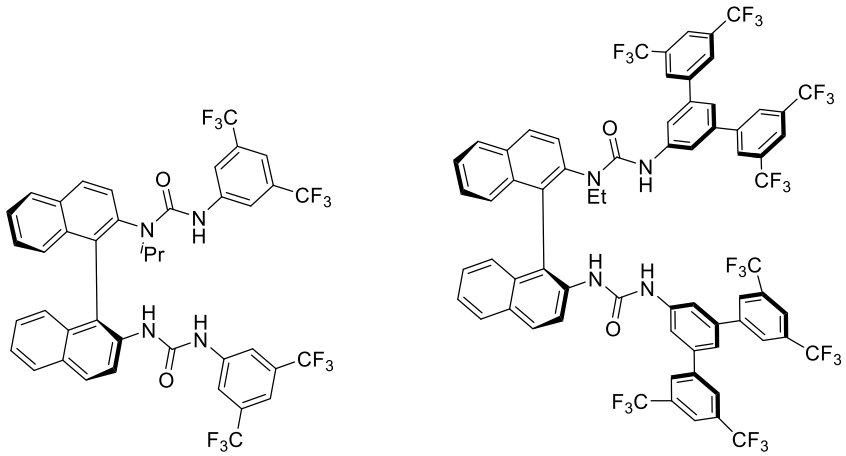

1.25 **1.26**

Figure 1.6 Hydrogen bonding phase transfer catalysts for enantioselective fluorination **1.25** and **1.26**.

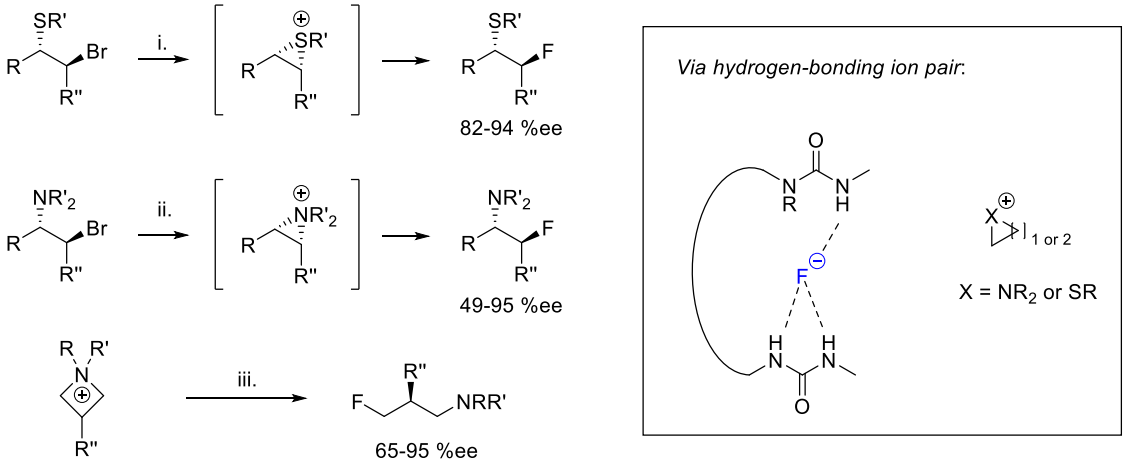

Scheme 1.8 Enantioselective fluorination by Hydrogen-bonding phase transfer catalysis; i. **1.25** (10 mol%), CsF (2 eq.), 1,2-difluorobenzene, −30 °C to r.t., 24-72 h; ii. **1.26** (5 mol%), KF (3 eq.), $CHCl_3$, −15 °C, 24 h; iii. **1.25** (5-10 mol%), CsF (2 eq.), 1,2-DCE, r.t., 24-72 h.[19–21]

The use of a fluoride salt with a soft counterion such as TBAF in an aprotic polar solvent has also proven to be an effective way to achieve nucleophilic fluorination. For example, the S_NAr reaction of **1.27** with TBAF proceeds in excellent yield under mild conditions (Scheme 1.9).[22]

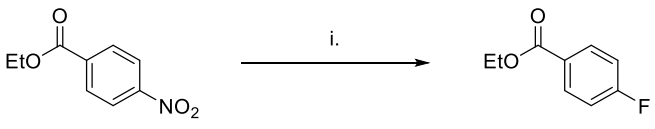

1.27 **1.28**

Scheme 1.9 The S_NAr reaction of ethyl 4-nitrobenzoate **1.27** with TBAF to give ethyl 4-fluorobenzoate **1.28**; i. TBAF, DMSO, 20 °C, 30 min, >95%.[22]

A limitation of reagents such as TBAF is their vulnerability to E2 elimination, especially at elevated temperatures. Maintaining anhydrous conditions is essential during the preparation and manipulation of tetraalkylammonium fluorides. Exposure to water leads to the generation of hydroxide which is implicated in the elimination reaction (Scheme 1.10).[23]

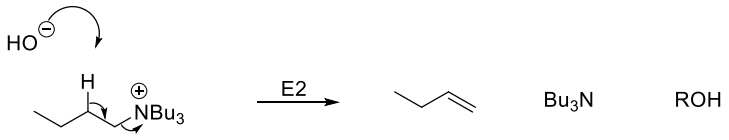

Scheme 1.10 The E2 elimination of TBAF which proceeds by the generation of hydroxide on exposure to moisture to give 1-butene and tributylamine.

Hydrogen fluoride (HF) which has a boiling point of 20 °C, is both challenging and hazardous to use in synthetic procedures. A stable liquid can be obtained by the complexation of HF with various Lewis bases, particularly pyridine (Olah's reagent) or triethylamine (TREAT-HF). Olah's reagent,[24] was first reported in 1963 and is more acidic than TREAT-HF, therefore the latter can be a more selective reagent in some circumstances. For example, reaction of **1.29** with TREAT-HF results in the desired epoxide opening to give 1,3-difluoroalkane **1.30** (Scheme 1.11). Treatment of **1.29** with Olah's reagent gives the tetrahydrofuran **1.32** resulting from the cyclisation of the reactive alkoxide-phenonium intermediate **1.31** (Scheme 1.11).[25]

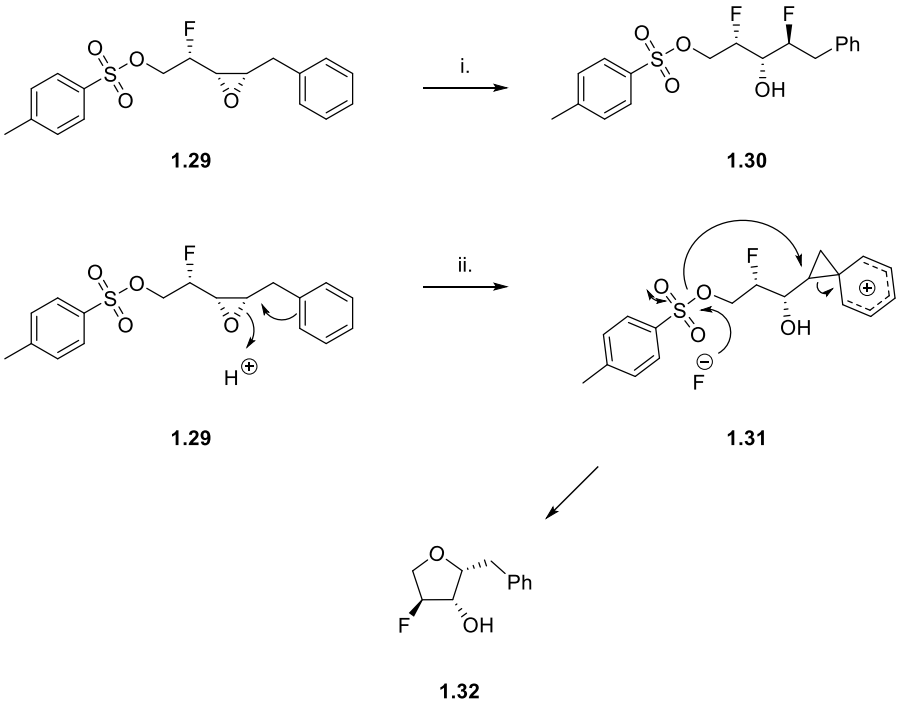

Scheme 1.11 The reactions of epoxide **1.29** with TREAT-HF and Olah's reagent; i. $Et_3N.3HF$, $CHCl_3$, 100 °C, 58%; ii. HF.Pyr, CH_2Cl_2, 0 °C, 33%.[25]

1.4.3. Deoxyfluorination

Deoxyfluorination, whereby an alcohol is converted to an alkyl fluoride or a carbonyl to a geminal difluoride is a powerful tool in organofluorine synthesis. Diethylaminosulfur trifluoride (DAST) which was first reported in 1975,[26] is synthesised by the reaction of sulfur tetrafluoride with diethylaminotrimethylsilane (Scheme 1.12). DAST and similar S-F reagents convert alcohols to alkyl fluorides. The mechanism typically proceeds with inversion of stereochemistry (Scheme 1.12).[27]

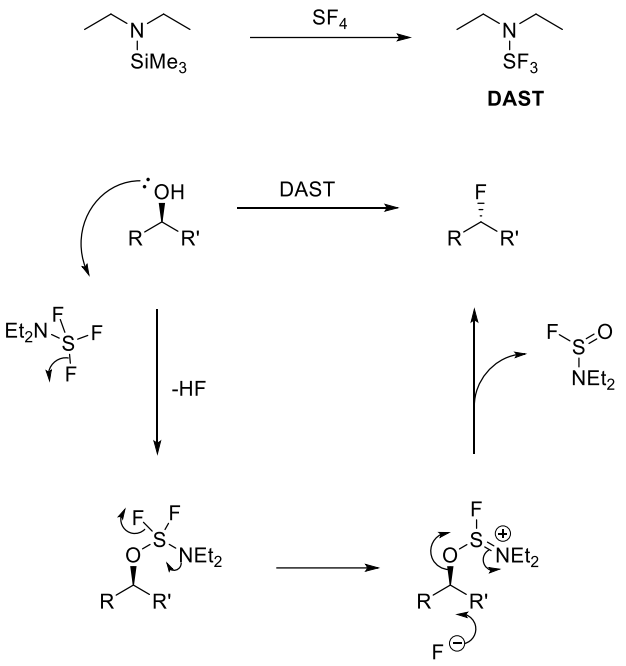

Scheme 1.12 Preparation of diethylaminosulfur trifluoride (DAST) and mechanism of deoxyfluorination.

Although it remains popular in research environments, DAST is a hazardous material for process development, as it detonates upon heating. Second generation S-F reagents have been developed which have greater thermal stability, examples of which are shown in Figure 1.7.[28–31]

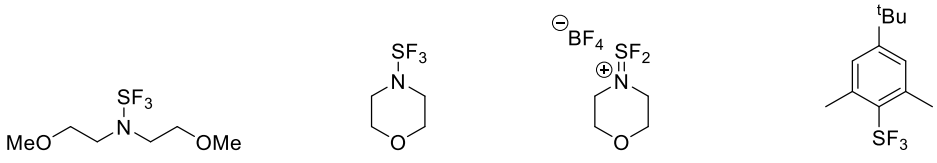

Figure 1.7 Second generation S-F reagents.

Another established class of deoxyfluorination reagents are the fluoroamino reagents (FARs). The first reported FAR was Yarovenko's reagent which is generated from diethylamine and chlorotrifluoroethylene. The mechanism is outlined in Scheme 1.13.[32]

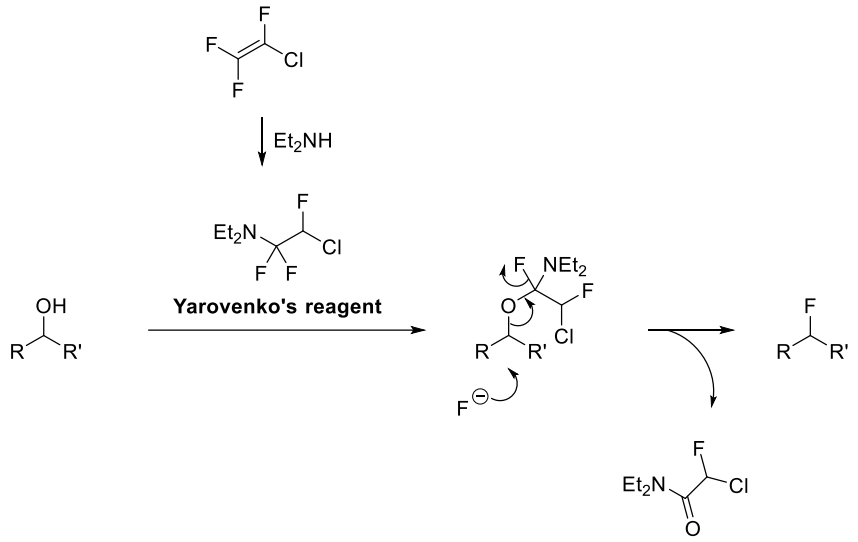

Scheme 1.13 Deoxyfluorination with Yarovenko's reagent.

Yarovenko's reagent suffers from instability and has been superseded by more stable FAR reagents (Figure 1.8), particularly Ishikawa's reagent (prepared from diethylamine and hexafluoropropene).[33] An alternative FAR is TFEDMA (prepared from diethylamine and tetrafluoroethylene), the volatile by-products of which are easily purged from the reaction mixture.[34] Another stable FAR, DFMBA (prepared by the deoxyfluorination of the parent amide) is usually used at elevated temperatures and can effect unique transformations such as the conversion of epoxides to vicinal difluorides as well as deoxyfluorination.[35]

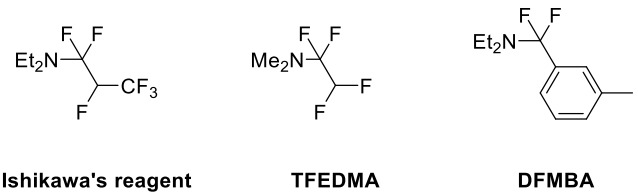

Figure 1.8 Second generation fluoroamino reagents (FAR).

A third class of deoxyfluorination reagents, the fluoroimidazolines have been the subject of recent attention. The first of these to be reported was DFI (Figure 1.9) which is suitable for reaction at reduced temperature but which is unstable above 0 °C.[36] Subsequently, the Ritter group reported the more stable PhenoFluor (Figure 1.9).[37,38] Despite the improved stability, PhenoFluor is vulnerable to hydrolysis and more recently the analogues, PhenoFluor Mix and

AlkylFluor have been developed with greater tolerance to moisture.[39,40] A mechanism of deoxyfluorination by fluoroimidazolinium reagents is shown in Scheme 1.14.

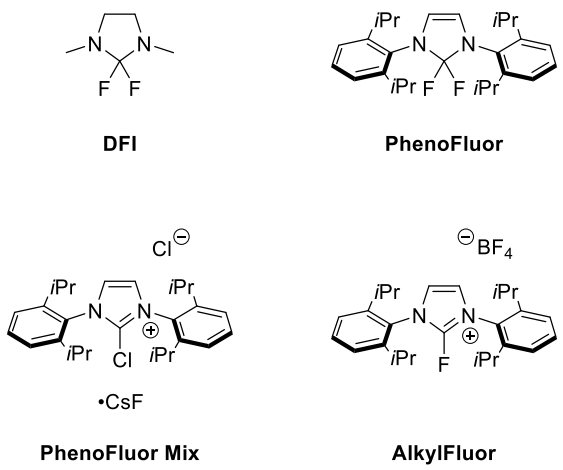

Figure 1.9 Fluoroimidazolinium reagents for deoxyfluorination.

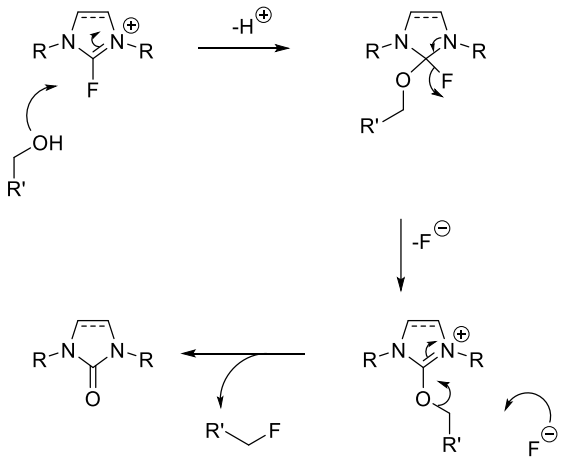

Scheme 1.14 The mechanism of deoxyfluorination by fluoroimidazolinium reagents.

Pyfluor is a sulfonyl fluoride reagent for deoxyfluorination reported by Doyle in 2015.[41] Pyfluor is a bench stable reagent with selectivity for primary and secondary alcohols and is readily prepared in one step from 2-mercaptopyridine **1.33** (Scheme 1.15). The cost is therefore much less than other stable alternatives (e.g. Pyfluor - £10.52 per gram, AlkylFluor - £289.00 per gram).[42]

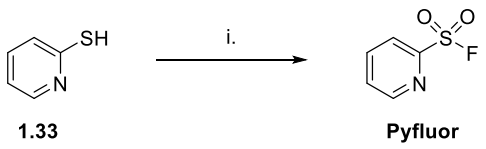

Scheme 1.15 Synthesis of Pyfluor from **1.33**; i. 13% NaOCl, H_2SO_4, 0 °C, 4h then KHF_2, MeCN, r.t., 20 min, 73%.

1.5. Fluorine in medicinal chemistry

Since the first fluorine-containing drugs were introduced in the 1950s, the role of fluorine in medicinal chemistry has increased dramatically.[43] Fluorine-containing drugs represent an estimated 20-25% of approved drugs today.[3] Two of the first such drugs to be approved were the tumour-inhibitor 5-fluorouracil **1.34** and the steroid fludrocortisone **1.35** (Figure 1.10).[44,45] Both result from the substitution of a hydrogen for a fluorine atom in a known parent compound (cortisone and uracil respectively). The fluorine atom has proven to be an excellent bioisostere for hydrogen, meaning that the two are recognised similarly in biological systems and drug activity is generally retained on substitution. Fluoxetine (Prozac ®) **1.36**, also shown in Figure 1.10 is a selective serotonin reuptake inhibitor (SSRI) which remains among the most prescribed anti-depressants on the market. Selective fluorination has proven to have subtle and often advantageous effects on the pharmacokinetic and physicochemical properties of lead compounds. Some of these effects are described below.

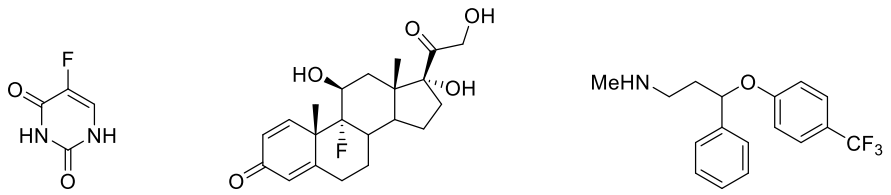

1.34 **1.35** **1.36**

Figure 1.10 The structure of 5-fluorouracil **1.34**, fludrocortisone **1.35** and fluoxetine **1.36**.

1.5.1. The effect of fluorine on pK_a

The effect of fluorination on molecular pK_a is dependent on the structure of the parent molecule. For example, the basicity of piperidines can be moderated by the inductive effect of fluorine (Figure 1.11). It was found that fluorination of the antipsychotic 3-piperidinylindole **1.37** at the γ-position to give **1.38** reduced the pK_a from 10.4 to 8.5. This significantly increased oral bioavailability (F) from negligible levels to a moderate 18% in rats. Binding affinity for 5-HT_{2a} was measured by the ability of the compound to displace [^{3}H]-ketanserin from human 5-HT_{2a} receptors. These assays showed a slight increase in binding affinity to 5-HT_{2a} for **1.38** relative to **1.37**. Further optimisation by derivatisation of the indole of **1.38** resulted in increased binding affinity to 5-HT_{2a} receptors and bioavailability in rats.[46]

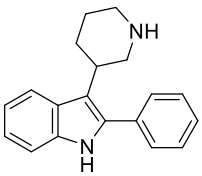

1.37

pK_a = 10.4
F = poor
Affinity 5-HT$_{2a}$ = 0.99 nM

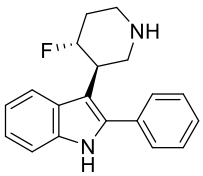

1.38

pK_a = 8.5
F = 18%
Affinity 5-HT$_{2a}$ = 0.43 nM

Figure 1.11 The utilisation of fluorine to tune pK_a.[46]

The pK_a of carboxylic acids can be decreased by fluorine substitution at the α-position. This is apparent when comparing the pK_a of acetic acid (3.75) and fluoroacetic acid (2.66). The rheumatoid arthritis drug, methotrexate **1.39** has an associated toxicity arising from polyglutamylation of the terminal carboxylic acid. Fluorine substitution α- to the terminal carboxylic acid to give **1.40**, resulted in a reduction in toxicity and a 15-fold increase in the lethal dose (defined as the dose resulting in the death of one mouse). The reduced toxicity was attributed to a reduction in polyglutamylation in normal cells due to the decrease in the pK_a (Figure 1.12).[47]

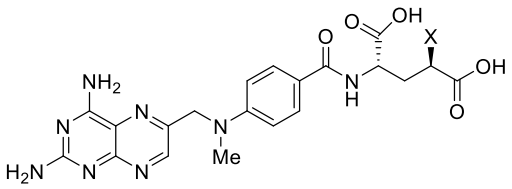

	1.39 (X = H)	**1.40** (X = F)
Mitogen response IC_{50} (T cell proliferation) / ng mL^{-1}	6.1	25.9
Mitogen response IC_{50} (B cell proliferation) / ng mL^{-1}	12.5	21.0
Lethal dose (mouse)/ mg kg^{-1}	40	600

Figure 1.12 Methotrexate **1.39** and fluoromethotrexate **1.40**.[47]

1.5.2. Effect of fluorine on lipophilicity

Lipophilicity is an important parameter used in medicinal chemistry to predict oral bioavailability of a drug. Lipinski's rules hold that Log P (derived from the degree of partitioning between an aqueous and *n*-octanol phase) or Log D (identical to Log P but recorded at pH = 7.4 and taking account of ionized and non-ionized forms of the compound) of a candidate drug molecule should not exceed 5.[48] In the drug optimisation stage, a chemist may seek to either increase or decrease lipophilicity while preserving target-binding properties. The strategic introduction of one or more fluorine atoms can increase or decrease lipophilicity (depending

on the chemical environment). As fluorine atoms are comparable in size to hydrogen, binding affinities to targets after selective fluorination are often comparable to the parent compounds. The selective fluorination of alkanes generally decreases lipophilicity relative to the parent compound as is the case for *n*-pentane (Figure 1.13) as the fluorine polarises geminal hydrogens. In the case of aromatic hydrocarbons fluorination increases lipophilicity as shown for benzene (Figure 1.14) as there are no geminal hydrogens. The effect of fluorination on more complex structures with heteroatoms can be difficult to predict but generally fluorination increases Log P if geminal hydrogens are not present.

In 2004,[49] Böhm *et al* investigated the effect of fluorination on Log D in 293 proprietary compounds from the Roche in-house database. On average, they found that Log D increased by 0.25 for each hydrogen to fluorine substitution.

	1.41	**1.42**
Log P	3.11	2.33

Figure 1.13 Log P of pentane **1.41** and 1-fluoropentane **1.42**.

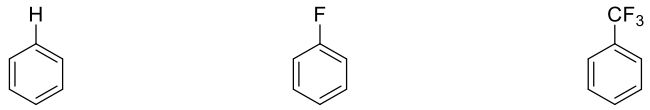

	1.43	**1.44**	**1.45**
Log P	2.1	2.3	3.0

Figure 1.14 Log P of benzene **1.43**, fluorobenzene **1.44** and trifluoromethylbenzene **1.45**.

1.5.3. Metabolic effects

All drugs are actively metabolised *in vivo* as the body tries to remove the foreign entity. Of particular importance to drug metabolism are P450 monooxygenase enzymes which reside mostly in the liver. The P450 monooxygenases are responsible for the oxidation of drug molecules, which increases their hydrophilicity and facilitates their removal by the urinary tract. A common issue in drug development is an insufficient half life due to the presence of one or more metabolically labile C-H bonds, and a common strategy involves substituting a labile C-H bond for an inert C-F bond. This strategy was successfully employed in the lead optimisation of the cholesterol absorption inhibitor, Ezetimibe **1.48** (Figure 1.15). A dual fluorine substitution of the initially reported inhibitor **1.46** to give **1.47** led to a 3-fold reduction in the median effective dose (ED_{50}) by increasing the metabolic stability. Further optimisation (benzylic

oxidation and demethylation) resulted in Ezetimibe **1.48** and a 50-fold reduction in ED_{50} from the initial inhibitor **1.46**.[50]

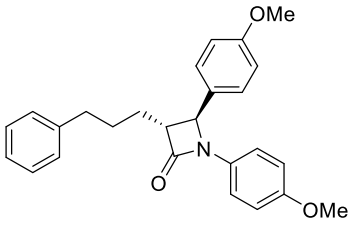

1.46

ED_{50} = 2.2 mg kg^{-1}

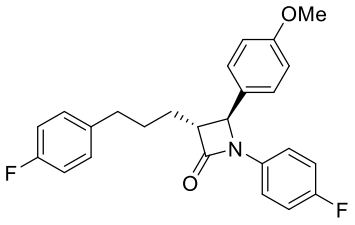

1.47

ED_{50} = 0.7 mg kg^{-1}

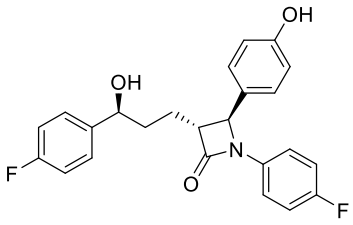

1.48

ED_{50} = 0.04 mg kg^{-1}

Figure 1.15 Lead optimisation towards Ezetimibe **1.48**.

1.5.4. Isosterism

Isosteres are atoms or functional groups which share physical and chemical properties while also exhibiting similar biological activity. The replacement of a labile hydrogen atom with a metabolically inert fluorine has already been discussed. The similar size of the two atoms frequently avoids perturbation of biological activity on substitution but the versatility of fluorine in isosterism extends still further.

The isosteric replacement of a carbonyl bond in an ester, ketone or carboxylic acid with a C-F bond preserves the dipole moment of the parent compound and has been a successful strategy in drug discovery programs. For example, camptothecin **1.49** is an inhibitor of Topoisomerase I (EC_{50} = < 1 μM) and prevents tumour cell proliferation (Figure 1.16). However, the lactone ring of **1.49** is vulnerable to chemical and metabolic hydrolysis and the product of hydrolysis is inactive. The half life of **1.49** at pH 7.4 was reported to be less than 6 h. The replacement of the lactone carbonyl of **1.49** with an α-fluoro ether was found to greatly increase the lifetime of the drug at physiological pH (4% loss; 6 h, pH 7.4). The inhibitory activity of the fluorinated analogues **1.50** and **1.51** were reduced, particularly the (2*R*)-isomer

but the derivatisation of the quinoline core by incorporation of a cyclohexyl moiety to give **1.52**, restored activity to that of the parent compound across three cell lines (Figure 1.16).[51]

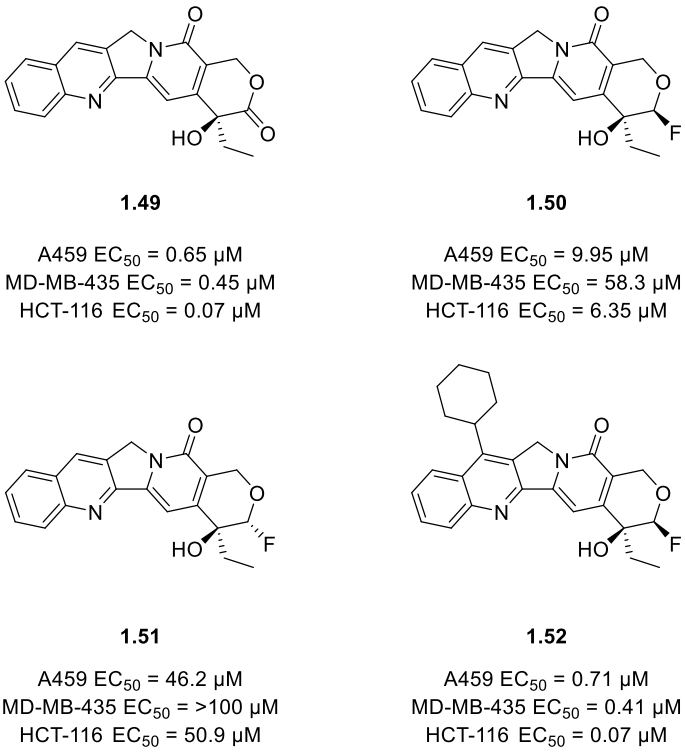

Figure 1.16 Activity profiles of camptothecin **1.49** and derivatives **1.50**-**1.52**.

The polarisation of the C-F bond results in a similar dipole moment to that observed in some carbonyl groups. The amide bond however has a larger dipole moment (μ ~ 3.6 D) and although fluoroalkene (μ ~ 1.4 D) and trifluoromethylalkene (μ ~ 2.3 D) derivatives have been suggested as amide isosteres as they have a similar geometry, their dipole moments are not analogous (Figure 1.17).[52]

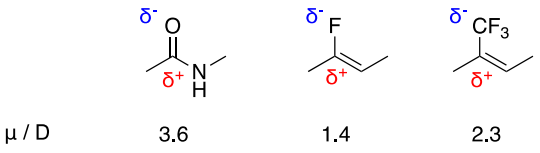

Figure 1.17 The dipole moments of amide isosteres.

Nevertheless, in some circumstances this difference has a minimal impact on the effectiveness of a drug candidate. This was the case in the optimisation of the pentapeptide Leu-Enkephalin **1.53** known to activate the Δ-opiod receptor (DOPr) in the brain. Despite its activity **1.53** does not produce the expected analgesic effects when administered intravenously partly because of its low lipophilicity which prevents it crossing the blood-brain

barrier. After identifying an amide bond in **1.53** which did not participate in essential H-bond donation, the fluoroalkene derivative **1.54** was prepared. It was found to increase lipophilicity while maintaining strong bioactivity in vitro, demonstrating the utility of this approach to improve pharmacokinetic profiles of drug candidates. Additionally, the fluoroalkene motif is inert to proteolysis in contrast to the amide bond which is metabolically labile to this process. In comparison, the unfluorinated alkene **1.55** gave a similar increase in lipophilicity as seen for **1.54** but a greatly diminished activity (Figure 1.18).[53]

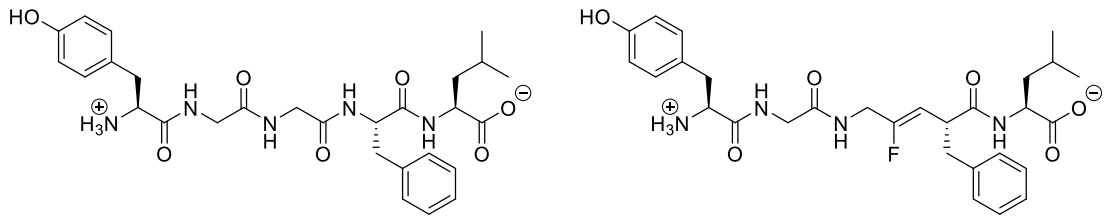

1.53
K_i = 6.9 ± 2.3 nM
$LogD_{7.4}$ = -0.95

1.54
K_i = 43 ± 14 nM
$LogD_{7.4}$ = -0.11

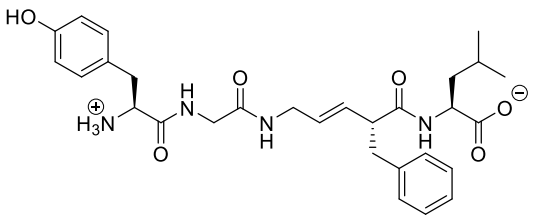

1.55
K_i = 587 ± 19 nM
$LogD_{7.4}$ = -0.07

Figure 1.18 The structure and properties of Leu-Enkephalin **1.53** and derivatives.

1.5.5. ^{18}F Positron emission tomography (PET)

Positron emission tomography (PET) is an imaging technique in nuclear medicine which utilises radiotracers with affinity for a biological target of interest and bearing a positron emitting radionuclide (e.g. ^{11}C, ^{13}N, ^{15}O and ^{18}F). Radiotracers are designed to have high selectivity and affinity for their biological targets and can therefore be administered on the nanogram scale. This reduces side effects and makes PET a non-invasive technique.[53] Following administration, detection of γ-rays resulting from the annihilation of the emitted positrons allows a three-dimensional image to be generated. From this, quantification of the radiotracer at specific sites can be determined (Figure 1.19).[54]

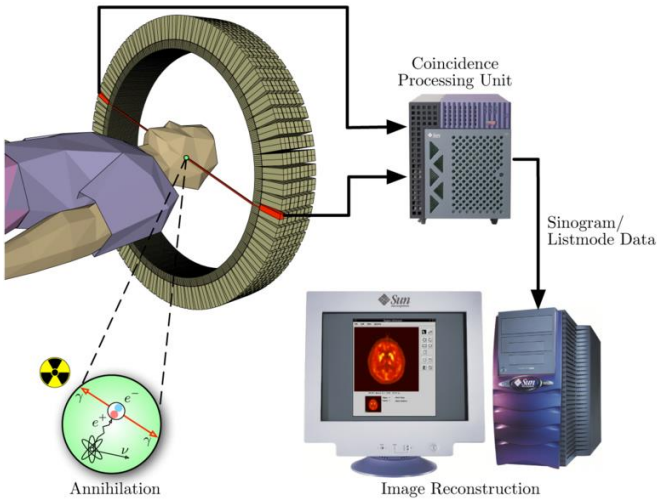

Figure 1.19. Illustration of the use of PET in nuclear medicine (image used with permission).[55]

Fluorine-18 (^{18}F) is generated by the bombardment of oxygen-18 enriched water ($^{18}OH_2$) with high energy protons. ^{18}F is widely utilised in PET and its use has advantages over other positron-emitting radionuclides. Although fluorine does not occur in mammalian biological systems, the bioisosteric replacement of for example hydrogen with fluorine and the stability of the C-F bond has been discussed. The half life of ^{18}F is 110 min, which although short, is longer than many other commonly used radionuclides (Table 1.2), and gives sufficient time for the generation and radiotracer synthesis prior to administration.[3,54]

Radionuclide	Half life ($t_{1/2}$) / min	E_{max} of positron / MeV
^{15}O	2	1.74
^{13}N	10	1.20
^{11}C	20	0.97
^{68}Ga	68	1.90
^{18}F	110	0.64
^{64}Cu	762	0.66
^{76}Br	972	4.00
^{124}I	60,192	2.14

Table 1.2 Commonly used positron-emitting radionuclides by half life.

The most widespread PET radiotracer is 2-deoxy-2-[^{18}F]fluoro-D-glucose (FDG). In FDG the 2-hydroxyl group in D-glucose has been substituted for a fluorine-18 atom. Just as for D-glucose, FDG is incorporated in many cells in the body where it is phosphorylated at O-6, and its distribution can be monitored by a PET scanner. High glucose-using cells such as those of cancer tissue accumulate FDG in high concentrations and FDG has found wide use for the

diagnosis and monitoring of cancers.[56] Other applications of FDG include the research and diagnosis of dementia,[57] and the monitoring of cardiac and vascular inflammation.[58]

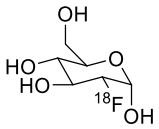

FDG

Figure 1.20. The structure of 2-deoxy-2-[^{18}F]fluoro-D-glucose (FDG).

1.6. Fluorinated natural products

Despite its high relative abundance (13th most abundant element) in the Earth's crust, fluorine-containing natural products are very rare. The majority of these are derived from the reaction of the fluorinase enzyme which was isolated from the actinomycete bacteria, *Streptomyces cattleya*. The fluorinase, first reported in 2002, catalyses the reversible S_N2 reaction of *S*-adenosyl methionine (SAM) **1.56** and a fluoride ion to give 5'-fluorodeoxyadenosine (5'-FDA) **1.57**.[59] The metabolism of **1.57** gives rise to the two fluorinated natural products **1.58** and **1.59** in *S. cattleya* and **1.60** has been isolated from *Streptomyces M.A.*. Fluoroacetate **1.58** also accumulates in a variety of plant species and this results in the production of further secondary metabolites.[60,61] In plants the toxin, (*2R*,*3R*)-2-fluorocitrate **1.61** arises from the metabolism of **1.58** by the action of citrate synthase. Following dehydration **1.61** is an efficient inhibitor of aconitase, an enzyme of the citric acid cycle, and this results in toxicity. Additionally, ω-fluorooleic acid **1.62** and related fatty acids have been isolated from the West-African plant *Datura toxicarium*. These fatty acids appear to arise from the incorporation of fluoroacetate **1.58** as a starter unit in the fatty acid biosynthetic pathway.

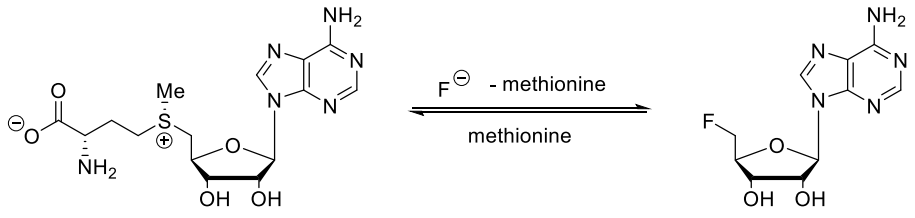

1.56 **1.57**

Scheme 1.16. Fluorinase-catalysed reaction of SAM **1.56** with fluoride to give 5'-FDA **1.57**.

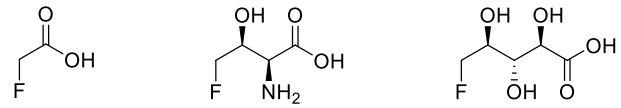

1.58 **1.59** **1.60**

Figure 1.21 Fluorinated natural products isolated from soil bacteria.

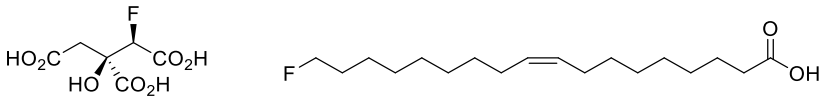

1.61 **1.62**

Figure 1.22. Fluorinated natural products arising from the metabolism of **1.58** in plants.

The final class of fluorine-containing natural products are those which do not derive from 5'-FDA **1.57** by the action of the fluorinase. Nucleocidin **1.63** is a potent antibiotic which was first isolated from the bacterium *Streptomyces calvus* in 1957.[62] Despite its antibiotic properties nucleocidin has not received wide attention due to its mammalian toxicity and fickle production. Indeed, **1.63** could not be re-isolated in cultures of *S. calvus* for decades until a complementation with *bldA*-encoded Leu-tRNA^{UUA} was recently reported to correct a mutation and restore production.[63] Subsequent efforts to elucidate the biosynthesis of **1.63** have resulted in the detection of two glycosylated fluorometabolites **1.64** and **1.65**.[64] Efforts towards the elucidation of the biosynthetic pathway of **1.63** are ongoing.

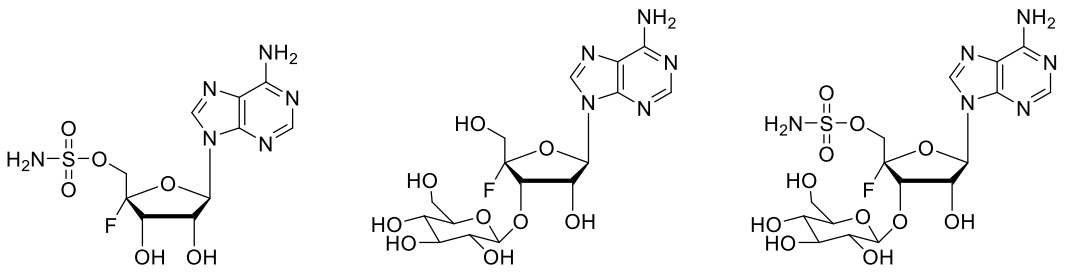

1.63 **1.64** **1.65**

Figure 1.23 Nucleocidin **1.63** and related fluorometabolites **1.64** and **1.65**.

1.7. Multi-vicinal fluorinated compounds

The conformation of alkyl chains with multiple vicinal fluorine substituents is dominated by the repulsion between 1,3 fluorine atoms. The *gauche* effect has a less significant influence on their conformations. The effect of 1,3-dipolar repulsion can be seen in the two stereoisomers **1.66** and **1.67** (Figure 1.24).[65] Isomer **1.66** adopts a helical conformation to avoid parallel alignment of 1,3-fluorine substituents whereas isomer **1.67** adopts the linear *anti*-zig-zag

conformation (Figure 1.24). Both conformations also facilitate hyperconjugation interactions observed in the *gauche* effect (C-H σ to C-F σ*).

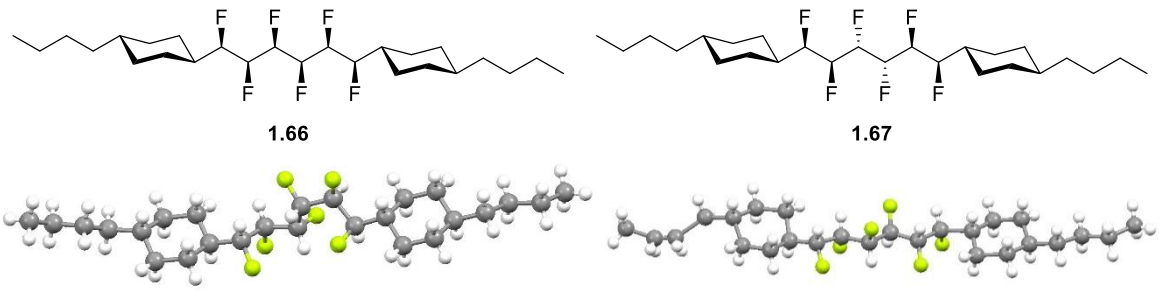

Figure 1.24 Two stereoisomers of multivicinal fluoroalkanes **1.66** and **1.67**.

1.7.1. All-*cis*-fluorocyclohexanes

Acyclic multi-vicinal fluorinated alkyl chains can easily rotate and therefore adopt conformations which minimise their net molecular dipole moment. In analogous cyclic systems however, conformational flexibility is limited and appropriate stereoselective syntheses can access stable conformations displaying large dipole moments. For example, 1,2,3,4-all-*cis*-tetrafluorocyclohexane **1.68**, the first such structure synthesised by the St Andrews group (Scheme 1.17) can adopt only two isoelectronic conformers (Figure 1.25).[66] Both conformers have a 1,3-diaxial fluorine substitution which accounts for the very high molecular dipole moment (μ = 4.91). The facial polarity of these molecules has led to them being dubbed 'Janus' rings,[67] after the two-faced Ancient Roman deity.

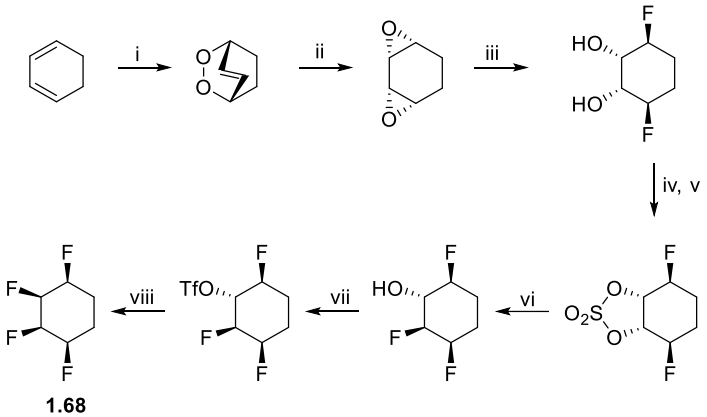

Scheme 1.17. The synthesis of all-*cis*-1,2,3,4-tetrafluorocyclohexane **1.68**; i. $(PhO)_3P$, O_3, CH_2Cl_2, cyclohexa-1,4-diene, -78 °C to -25 °C; ii. $Ru(PPh_3)_3Cl_2$, CH_2Cl_2, 0 °C to r.t., 46% over two steps; iii. $Et_3N.3HF$, 90 °C; iv. thionyl chloride, pyridine, CH_2Cl_2, 0 °C; v. $NaIO_4$, $RuCl_3.xH_2O$, MeCN, H_2O, 35% over three steps; vi. $Et_3N.3HF$, 120 °C, 70%; vii. Tf_2O, pyridine, r.t.; viii. $Et_3N.3HF$, 120 °C, 35% over 2 steps.

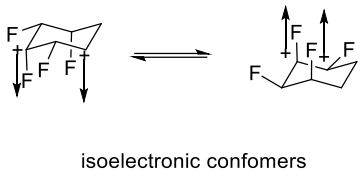

Figure 1.25 The isoelectronic confomers of 1,2,3,4-all-*cis*-tetrafluorocyclohexane **1.68**.

An even greater molecular dipole moment (μ = 5.24) was calculated for the 'Janus' ring, all-*cis*-1,2,4,5-tetrafluorocyclohexane **1.69**.[68] The synthesis was carried out in a two-step process with an overall yield of 12% over two steps, however the second step involved the incorporation of all four fluorine atoms with the *cis* stereochemistry (Scheme 1.18). [68]

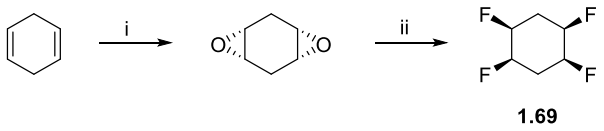

Scheme 1.18 The synthesis of all-*cis*-1,2,4,5-tetrafluorocyclohexane **1.69**; i. mCPBA, CH_2Cl_2, -15°C to -10 °C, 52%; ii. DAST, 70 °C, 24%.

The most polar molecule of this series, all-*cis*-hexafluorocyclohexane **1.70** was synthesised firstly on an analytical scale by the St Andrews group in 2015 in a 12-step, < 1% overall yield process (Scheme 1.19).[69]

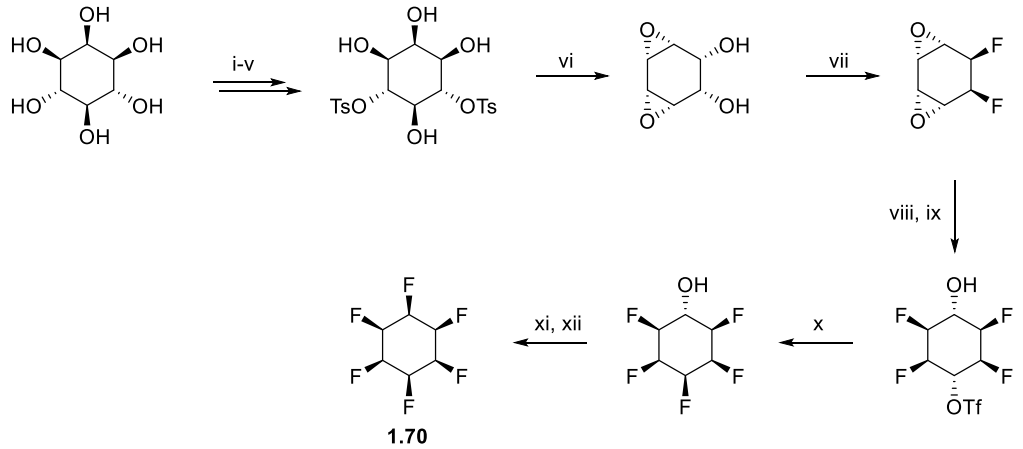

Scheme 1.19 First synthesis of all-*cis*-hexafluorocyclohexane **1.70**; i. $HC(OEt)_3$, *p*TSA, DMF, 5 days, 100 °C, 69%; ii. NaH, BzCl, DMF, 30 min, 55%; iii. TsCl, pyridine, 18 h, 97%; iv. $^{i}BuNH_2$, MeOH, reflux, 4 h, 84%; v. HCl, MeOH, reflux, 4h, 89%; vi. NaOMe, MeOH, $CHCl_3$, 18 h, 85%; vii. Deoxofluor, THF, 60-100 °C, 15 min, MW, 94%; viii. $Et_3N.3HF$, 180 °C, 120 min, MW, 71%; ix. Tf_2O, pyridine, CH_2Cl_2, 88%; x. $Et_3N.3HF$, 120 °C, 2h, MW, 40%; xi. Tf_2O, pyridine, CH_2Cl_2, 71%; xii. $Et_3N.3HF$, 180 °C, 2h, MW, ~10%.[69]

The calculated molecular dipole moment of **1.70** (μ = 6.2) is among the highest known for an aliphatic compound which results in an unexpectedly high melting point (m.p. = 208 °C).[69] The facial polarity (Figure 1.26) arises because of the triaxial alignment of three C-F bonds. This polarisation facilitated the complexation of both chloride anions (to the protic electropositive face) and sodium cations (to the fluorinated electronegative face) in the gas phase (Figure 1.27).[70] These complexes were generated by electrospray ionisation and trapped in a quadrupole ion trap mass spectrometer. They were detected by IR spectroscopy using a free electron laser. The complexes are among the most strongly bound between Na^+ and Cl^- and an organic molecule and similar to that of crown ethers for Na^+.[70]

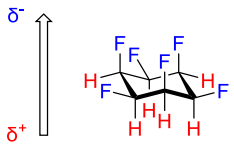

Figure 1.26 The facial polarity of all-*cis*-hexafluorocyclohexane **1.70**.

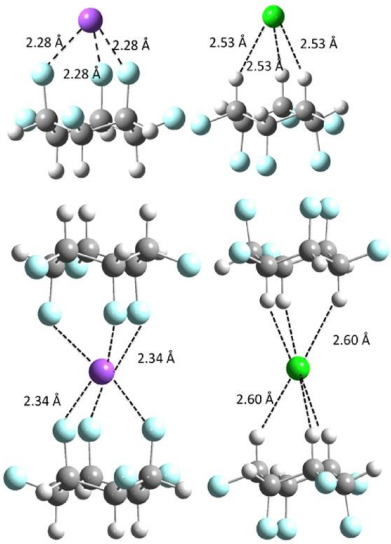

Figure 1.27 Structures of Na^+ (magenta) and Cl^- (green) ions coordinated to ring faces of **1.70**. Reprinted (adapted) with permission from[69] Copyright 2021 American Chemical Society.

Similarly complexes with halides in solution have since been observed with the following affinities (in acetone); F^- (600 ± 400 M^{-1}, causes degradation), Cl^- (400 ± 40 M^{-1}), Br^- (150 ± 7 M^{-1}) and I^- (37 ± 7 M^{-1}).[71] Given the complexation of ions with both positive and negative charges to **1.70**, the use of 'Janus' rings for ion binding applications has become a prospect.

Following the synthesis of the Janus rings **1.68**-**1.70**, the St. Andrews group became interested in exploring the application of such molecules. To this end, efforts were made to synthesise functionalised building blocks for further synthetic manipulation. Initially, this began with the synthesis of 2,3,5,6-all-*cis*-tetrafluorocyclohexylbenzene **1.78** (Scheme 1.20).[72] The five step synthesis to **1.78** begins with the Birch reduction of biphenyl **1.71** to give **1.72**. A familiar epoxidation-fluorination strategy follows to give **1.74** and **1.75**. Triflation, and a final fluorination step generated the desired product **1.78** and a side product **1.79**, which arose from a phenonium ion rearrangement.

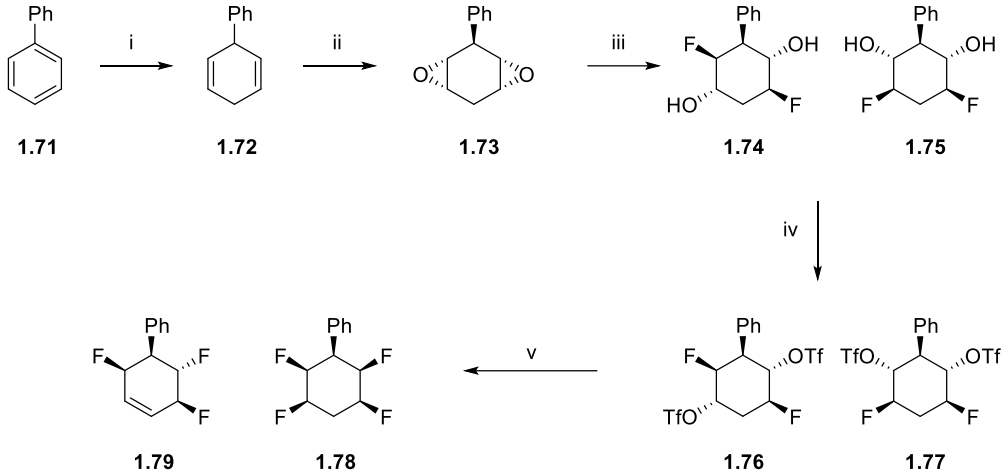

Scheme 1.20 The synthesis of 2,3,5,6-all-*cis*-tetrafluorocyclohexylbenzene **1.78**; i. Li, NH_3, quant.; ii. mCPBA, CH_2Cl_2, 85%; iii. $Et_3N.3HF$, 140 °C; iv. Tf_2O, pyridine CH_2Cl_2 -40 °C to r.t., 90% over 2 steps; v. $Et_3N.3HF$, THF, 100 °C, 31% **1.78** (desired), 42% **1.79** (side product).[72]

Following the isolation of **1.78**, electrophilic aromatic substitution was used to access a variety of building blocks some of which are shown in Figure 1.28.[72–74] Functionalisable handles such as aryl halides **1.80** (for Pd-catalysted cross-coupling reactions), organoazides **1.81** (for Cu-catalysed azide-alkyne cycloaddition (CuAAC) ‘click’ reactions) and amino acids **1.82** (for peptide coupling reactions) could all be accessed through this approach. However, the low yield and somewhat laborious syntheses of these compounds (Scheme 1.20) made exploration of alternative routes to ‘Janus’ ring derivatives attractive and this forms a significant research aim of this thesis.

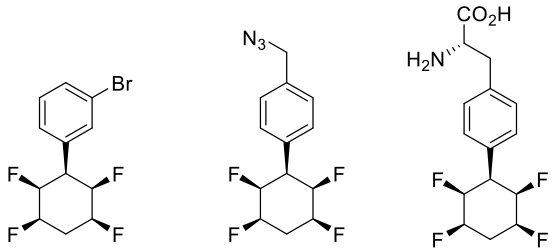

Figure 1.28 Selected building blocks prepared via electrophilic aromatic substitution reactions of 2,3,5,6-tetrafluorocyclohexylbenzene **1.78**.[72–74]

This thesis builds on existing synthetic strategies for the generation of all-*cis*-fluorocyclohexanes. In Chapter 2, a *cis*-selective Rh-catalysed fluoroarene hydrogenation reaction is adapted from the literature and used to generate a library of 'Janus' ring building blocks.[75] Chapter 3 explores elaboration strategies of these building blocks to generate more complex compound libraries and present the utility of the 'Janus' ring for potential applications in drug discovery programs as a proof of concept. Finally, Chapter 4 explores the intermolecular interactions and conformation of 'Janus' rings by preparation of amphiphiles. An examination of X-ray crystal structures is provided, and Langmuir isotherm analysis is conducted to explore phase behaviour at the air-water interface.

1.8. References

[1] M. E. Weeks, *J. Chem. Educ.* **1932**, *9*, 1915-1939

[2] G. B. Kauffman, *J. Chem. Educ.* **1955**, *32*, 301–303.

[3] S. Purser, P. R. Moore, S. Swallow, V. Gouverneur, *Chem. Soc. Rev.* **2008**, *37*, 320–330.

[4] T. Fujiwara, D. O'Hagan, *J. Fluor. Chem.* **2014**, *167*, 16–29.

[5] J. Gardiner, *Aust. J. Chem.* **2015**, *68*, 13–22.

[6] W. R. Dolbier, A. C. Alty, O. P. Phanstiel, *J. Am. Chem. Soc.* **1987**, *109*, 3046–3050.

[7] D. O'Hagan, *Chem. Soc. Rev.* **2008**, *37*, 308–319.

[8] N. A. Senger, B. Bo, Q. Cheng, J. R. Keeffe, S. Gronert, W. Wu, *J. Org. Chem.* **2012**, *77*, 9535–9540.

[9] P. Ryberg, O. Matsson, *J. Org. Chem.* **2002**, *67*, 811–814.

[10] M. L. Trapp, J. K. Watts, N. Weinberg, B. M. Pinto, *Can. J. Chem.* **2006**, *84*, 692–701.

[11] D. Rodrigues Silva, L. de Azevedo Santos, T. A. Hamlin, C. Fonseca Guerra, M. P. Freitas, F. M. Bickelhaupt, *ChemPhysChem* **2021**, *22*, 641–648.

[12] K. B. Wiberg, M. A. Murcko, K. E. Laidig, P. J. MacDougall, *J. Phys. Chem.* **1990**, *94*, 6956–6959.

[13] J. C. R. Thacker, P. L. A. Popelier, *J. Phys. Chem. A* **2018**, *122*, 1439–1450.

[14] D. Wu, A. Tian, H. Sun, *J. Phys. Chem. A* **1998**, *102*, 9901–9905.

[15] R. J. Abraham, A. D. Jones, M. A. Warne, R. Rittner, C. F. Tormena, *J. Chem. Soc. Perkin Trans. 2* **1996**, 533–539.

[16] A. Sun, D. C. Lankin, K. Hardcastle, J. P. Snyder, *Chem. Eur. J.* **2005**, *11*, 1579–1591.

[17] T. Umemoto, K. Tomita, *Tetrahedron Lett.* **1986**, *27*, 3271–3274.

[18] Y. Kobayashi, T. Taguchi, T. Terada, *Tetrahedron Lett.* **1979**, *20*, 2023–2026.

[19] G. Pupo, F. Ibba, D. M. H. Ascough, A. C. Vicini, P. Ricci, K. E. Christensen, L. Pfeifer, J. R. Morphy, J. M. Brown, R. S. Paton, V. Gouverneur, *Science* **2018**, *360*, 638–642.

[20] G. Roagna, D. M. H. Ascough, F. Ibba, A. C. Vicini, A. Fontana, K. E. Christensen, A. Peschiulli, D. Oehlrich, A. Misale, A. A. Trabanco, R. S. Paton, G. Pupo, V. Gouverneur, *J. Am. Chem. Soc.* **2020**, *142*, 14045–14051.

[21] G. Pupo, A. C. Vicini, D. M. H. Ascough, F. Ibba, K. E. Christensen, A. L. Thompson, J. M. Brown, R. S. Paton, V. Gouverneur, *J. Am. Chem. Soc.* **2019**, *141*, 2878–2883.

[22] H. Sun, S. G. DiMagno, *Angew. Chem. Int. Ed.* **2006**, *45*, 2720–2725.

[23] H. Sun, S. G. DiMagno, *J. Am. Chem. Soc.* **2005**, *127*, 2050–2051.

[24] C. G. Bergstrom, R. T. Nicholson, R. M. Dodson, *J. Org. Chem.* **1963**, *28*, 2633–2640.

[25] V. A. Brunet, A. M. Z. Slawin, D. O'Hagan, *Beilstein J. Org. Chem.* **2009**, *5*, 1–9.

[26] W. J. Middleton, *J. Org. Chem.* **1975**, *40*, 574–578.

[27] D. F. Shellhamer, A. A. Briggs, B. M. Miller, J. M. Prince, D. H. Scott, V. L. Heasley, *J. Chem. Soc. Perkin Trans. 2* **1996**, *5*, 973–977.

[28] P. A. Messina, K. C. Mange, W. J. Middleton, *J. Fluor. Chem.* **1989**, *42*, 137–143.

[29] G. S. Lal, G. P. Fez, R. J. Pesaresi, F. M. Prozonic, *Chem. Commun.* **1999**, 215–216.

[30] A. Lheureux, F. Beaulieu, C. Bennett, D. R. Bill, S. Clayton, F. Laflamme, M. Mirmehrabi, S. Tadayon, D. Tovell, M. Couturier, *J. Org. Chem.* **2010**, *75*, 3401–3411.

[31] T. Umemoto, R. P. Singh, Y. Xu, N. Saito, *J. Am. Chem. Soc.* **2010**, *132*, 18199–18205.

[32] N. N. Yarovenko, M. A. Raksha, *Zh. Obshch. Khim.* **1959**, *29*, 2159–2163.

[33] A. Takaoka, H. Iwakiri, N. Ishikawa, *Bull. Chem. Soc. Jpn.* **1979**, *52*, 3377–3380.

[34] V. A. Petrov, S. Swearingen, W. Hong, W. Chris Petersen, *J. Fluor. Chem.* **2001**, *109*, 25–31.

[35] S. Kobayashi, A. Yoneda, T. Fukuhara, S. Hara, *Tetrahedron* **2004**, *60*, 6923–6930.

[36] H. Hayashi, H. Sonoda, K. Fukumura, T. Nagata, *Chem. Commun.* **2002**, *2*, 1618–1619.

[37] P. Tang, W. Wang, T. Ritter, *J. Am. Chem. Soc.* **2011**, *133*, 11482–11484.

[38] F. Sladojevich, S. I. Arlow, P. Tang, T. Ritter, *J. Am. Chem. Soc.* **2013**, *135*, 2470–2473.

[39] T. Fujimoto, T. Ritter, *Org. Lett.* **2015**, *17*, 544–547.

[40] N. W. Goldberg, X. Shen, J. Li, T. Ritter, *Org. Lett.* **2016**, *18*, 6102–6104.

[41] M. K. Nielsen, C. R. Ugaz, W. Li, A. G. Doyle, *J. Am. Chem. Soc.* **2015**, *137*, 9571–9574.

[42] Sigma-Aldrich, 2021 https://www.sigmaaldrich.com/GB/en, (accessed May 2021)

[43] W. K. Hagmann, *J. Med. Chem.* **2008**, *51*, 4359–4369.

[44] C. Heidelberger, N. K. Chaudhuri, P. Danneberg, D. Mooren, L. Griesbach, *Nature* **1957**, *179*, 663–666.

[45] J. Fried, F. Sabo, Emily, *J. Am. Chem. Soc.* **1954**, *76*, 1455–1456.

[46] M. Rowley, D. J. Hallett, S. Goodacre, C. Moyes, J. Crawforth, T. J. Sparey, S. Patel, R. Marwood, S. Patel, S. Thomas, L. Hitzel, D. O'Connor, N. Szeto, J. L. Castro, P. H. Hutson, A. M. Macleod, *J. Med. Chem.* **2001**, *44*, 1603–1614.

[47] Y. Kokuryo, K. Kawata, T. Nakatani, A. Kugimiya, Y. Tamura, K. Kawada, M. Matsumoto, R. Suzuki, K. Kuwabara, Y. Hori, M. Ohtani, *J. Med. Chem.* **1997**, *40*, 3280–3291.

[48] C. A. Lipinski, *Drug Discov. Today Technol.* **2004**, *1*, 337–341.

[49] H. J. Böhm, D. Banner, S. Bendels, M. Kansy, B. Kuhn, K. Müller, U. Obst-Sander, M.

Stahl, *ChemBioChem* **2004**, *5*, 637–643.

[50] S. B. Rosenblum, T. Huynh, A. Afonso, H. R. Davis, N. Yumibe, J. W. Clader, D. A. Burnett, *J. Med. Chem.* **1998**, *41*, 973–980.

[51] Z. Miao, L. Zhu, G. Dong, C. Zhuang, Y. Wu, S. Wang, Z. Guo, Y. Liu, S. Wu, S. Zhu, K. Fang, J. Yao, J. Li, C. Sheng, W. Zhang, *J. Med. Chem.* **2013**, *56*, 7902–7910.

[52] N. A. Meanwell, *J. Med. Chem.* **2018**, *61*, 5822–5880.

[53] J. F. Nadon, K. Rochon, S. Grastilleur, G. Langlois, T. T. H. Dao, V. Blais, B. Guérin, L. Gendron, Y. L. Dory, *ACS Chem. Neurosci.* **2017**, *8*, 40–49.

[54] S. L. Pimlott, A. Sutherland, *Chem. Soc. Rev.* **2011**, *40*, 149–162.

[55] J. Langner, Development of a Parallel Computing Optimized Head Movement Correction Method in Positron Emission Tomography, Master's Thesis, University of Applied Sciences, Dresden, **2003**.

[56] J. W. Fletcher, B. Djulbegovic, H. P. Soares, B. A. Siegel, V. J. Lowe, G. H. Lyman, R. E. Coleman, R. Wahl, J. C. Paschold, N. Avril, L. H. Einhorn, W. W. Suh, D. Samson, D. Delbeke, M. Gorman, A. F. Shields, *J. Nucl. Med.* **2008**, *49*, 480–508.

[57] S. Minoshima, K. Mosci, D. Cross, T. Thientunyakit, *Semin. Nucl. Med.* **2021**, *51*, 230–240.

[58] I. Lawal, M. Sathekge, *Br. Med. Bull.* **2016**, *120*, 55–74.

[59] D. O'Hagan, C. Schaffrath, S. L. Cobb, J. T. G. Hamilton, C. D. Murphy, *Nature* **2002**, *416*, 279.

[60] D. O'Hagan, D. B. Harper, *J. Fluor. Chem.* **1999**, *100*, 127–133.

[61] K. K. J. Chan, D. O'Hagan, in *Methods Enzymol.* **2012**, *516*, 219–235.

[62] S. O. Thomas, V. L. Singleton, J. A. Lowery, R. W. Sharpe, L. M. Pruess, J. N. Porter, J. H. Mowat, N. Bohonos, *Antibiot. Annu.* **1956-1957**, 716-721

[63] X. M. Zhu, S. Hackl, M. N. Thaker, L. Kalan, C. Weber, D. S. Urgast, E. M. Krupp, A. Brewer, S. Vanner, A. Szawiola, G. Yim, J. Feldmann, A. Bechthold, G. D. Wright, D. L. Zechel, *ChemBioChem* **2015**, *16*, 2498–2506.

[64] X. Feng, D. Bello, P. T. Lowe, J. Clark, D. O'Hagan, *Chem. Sci.* **2019**, *10*, 9501–9505.

[65] L. Hunter, P. Kirsch, A. M. Z. Slawin, D. O'Hagan, *Angew. Chem. Int. Ed.* **2009**, *48*, 5457–5460.

[66] A. J. Durie, A. M. Z. Slawin, T. Lebl, P. Kirsch, D. O'Hagan, *Chem. Commun.* **2011**, *47*, 8265.

[67] N. Santschi, R. Gilmour, *Nat. Chem.* **2015**, *7*, 467–468.

[68] A. J. Durie, A. M. Z. Slawin, T. Lebl, P. Kirsch, D. O'Hagan, *Chem. Commun.* **2012**, *48*, 9643.

[69] N. S. Keddie, A. M. Z. Slawin, T. Lebl, D. Philp, D. O'Hagan, *Nat. Chem.* **2015**, *7*, 483–488.

[70] B. E. Ziegler, M. Lecours, R. A. Marta, J. Featherstone, E. Fillion, W. S. Hopkins, V. Steinmetz, N. S. Keddie, D. O'Hagan, T. B. McMahon, *J. Am. Chem. Soc.* **2016**, *138*, 7460–7463.

[71] O. Shyshov, K. A. Siewerth, M. Von Delius, *Chem. Commun.* **2018**, *54*, 4353–4355.

[72] A. J. Durie, T. Fujiwara, R. Cormanich, M. Bühl, A. M. Z. Slawin, D. O'Hagan, *Chem. Eur. J.* **2014**, *20*, 6259–6263.

[73] M. S. Ayoup, D. B. Cordes, A. M. Z. Slawin, D. O'Hagan, *Org. Biomol. Chem.* **2015**, *13*, 5621–5624.

[74] M. S. Ayoup, D. B. Cordes, A. M. Z. Slawin, D. O'Hagan, *Beilstein J. Org. Chem.* **2015**, *11*, 2671–2676.

[75] M. P. Wiesenfeldt, Z. Nairoukh, W. Li, F. Glorius, *Science* **2017**, *357*, 908–912.

2. *Cis*-selective hydrogenation of fluoroarenes

2.1. Background and aims

In 1901, Sabatier and Senderens reported the gas phase hydrogenation of benzene to cyclohexane in the presence of hydrogen and finely divided nickel at 180 °C.[1] Presently, the catalytic hydrogenation of aromatic and heteroaromatic rings such as the hydrogenation of benzene to cyclohexane (Scheme 2.1) is an important industrial reaction.[2,3] Catalysts used for hydrogenation of simple aromatic arenes such as benzene are generally heterogeneous.[4-7] Typically metals such as Ni,[8] Pd,[9] Pt,[10] Rh,[11] and Ru,[12] are dispersed on solid supports such as charcoal, silica or alumina to generate catalytically active nanoparticles.[7,13] Harsh conditions including elevated temperatures and pressure are commonly required to drive the reactions due to the inherent stability of aromaticity and poor functional group tolerance is a common limitation of arene hydrogenation.[5]

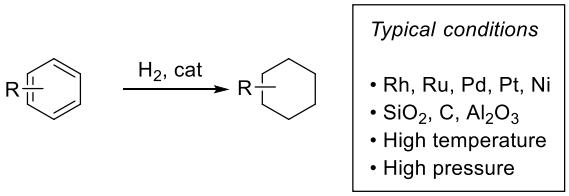

Scheme 2.1 Hydrogenation of benzenes to give cyclohexane derivatives.

Although fluorinated cyclohexane derivatives are high value products, accessing them by one-step hydrogenations of their parent arenes has long proved challenging due to competing hydrodefluorination.[14–16] For example, the hydrogenation of fluorobenzene **2.1** under various conditions has been reported giving cyclohexane **2.2** as the major product.[15–17] Hydrodefluorination can occur by a number of mechanistic pathways including S_NAr, oxidative addition into the C-F bond or β-fluorine elimination and elimination of HF as illustrated in Scheme 2.2.[18]

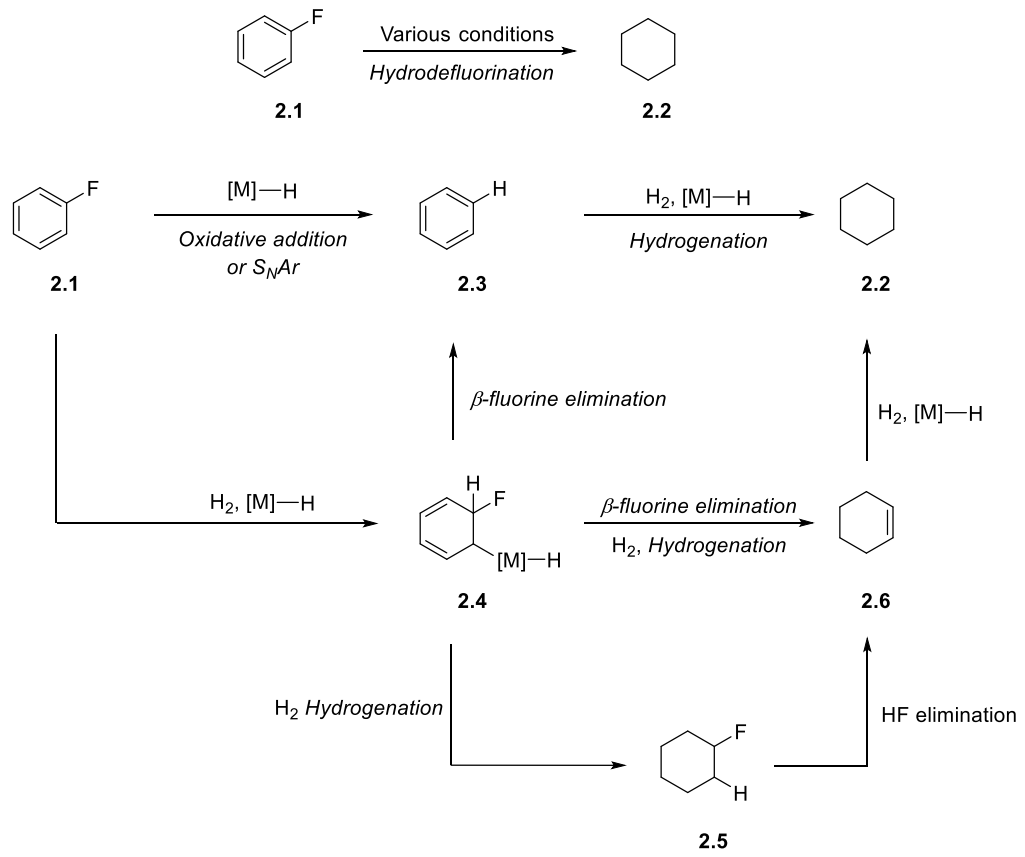

Scheme 2.2 Routes to hydrodefluorination of fluorobenzene **2.1** to give cyclohexane **2.2** (adapted from Ref-[18]).[18]

The challenge of chemoselectivity in arene hydrogenation to cyclohexanes is also notable in the presence of reducible functional groups such as carbonyls, alkenes and nitriles.[19] These groups are often reduced under the conditions required for arene hydrogenation. Chemoselective reduction of aromatic rings can provide access to high value products. For example, the partial reduction of phenol **2.6** to cyclohexanone **2.7** is a high-value transformation as the latter is an important intermediate in the synthesis of nylon 6 and nylon 6:6,[20] and the preparation of **2.7** is complicated by controlling over reaction to cyclohexanol **2.8**. Although high chemoselectivity to **2.7** can be achieved by Pd-catalysed hydrogenation under mild conditions, this is associated with low conversions (Scheme 2.3). A simple modification discovered by Liu *et. al.,* found that addition of 10 mol% of a Lewis acid ($AlCl_3$) greatly enhanced the rate and selectivity of the reaction toward **2.7** (Scheme 2.3).[21]

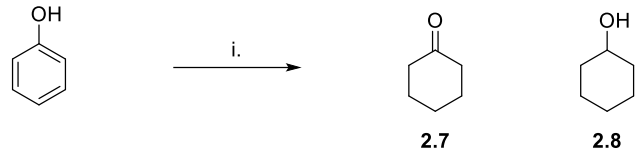

2.7 **2.8**

Lewis acid	Conversion	Selectivity	
No lewis acid	13%	94%	6%
$AlCl_3$ (10 mol%)	>99%	>99%	<1%

Scheme 2.3 The hydrogenation of phenol to give cyclohexanone **2.7** and cyclohexanol **2.8**; i. Pd/C (5 mol%), H_2 (10 bar), CH_2Cl_2, 30 °C, 12 h.[21]

A selective and generally applicable hydrogenation of arenes in the presence of ketones, esters, carboxylic acids and amides was reported in 2015 by Zeng.[22] The hydrogenation of propiophenone **2.9** under mild conditions in the presence of $[RhCODCl]_2$ gave an unselective mixture of reduced products **2.10**-**2.13** (Scheme 2.4). The selectivity towards the desired product 1-cyclohexylpropan-1-one **2.10** was greatly enhanced by the use of a novel Rh catalyst (Rh(CAAC)Cl **2.14**, Figure 2.1) with a strongly σ-donating cyclic(alkyl)(amino)carbene (CAAC) ligand. The hydrogenation of propiophenone **2.9** with the catalyst **2.14** gave a 96% yield of cyclohexyl ketone **2.10** and negligible quantities of other over-reduced hydrogenation products **2.11** and **2.12** (Scheme 2.4).

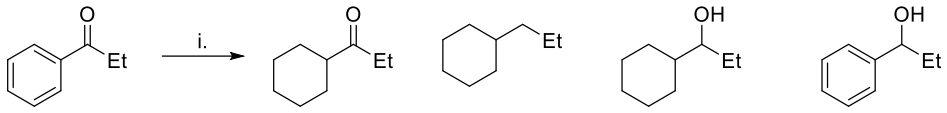

2.9 **2.10** **2.11** **2.12** **2.13**

Catalyst				
$[RhCODCl]_2$	29%	10%	25%	10%
Rh(CAAC)Cl **2.14**	96%	<1%	<1%	none

Scheme 2.4 Selective aryl hydrogenation of aromatic ketone **2.9**; i. Catalyst (3 mol%), H_2 (5 bar), CF_3CH_2OH, 4 Å MS, r.t., 24 h.[22]

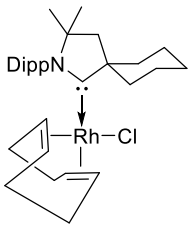

2.14

Figure 2.1 Air-stable rhodium-cyclic(alkyl)(amino)carbene (CAAC) complex **2.14**.[22]

Similarly, the hydrogenation of phenol **2.6** gave cyclohexanone **2.7** in near quantitative yield, and no reduction of the carbonyl was observed, with no formation of cyclohexanol **2.8** (Scheme 2.5). The aryl hydrogenation reactions by Zeng were broadly applicable to a range of aromatic compounds and conditions were tolerant of functional groups including esters and carbamates.

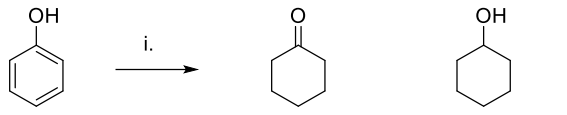

2.6 **2.7**, 99% **2.8**, not detected

Scheme 2.5 The selective hydrogenation of phenol **2.6** to give cyclohexanone **2.7**; i. **2.14** (3 mol%), H_2 (5 bar), 19:1 CF_3CH_2OH:H_2O, 4 Å MS, 70 °C, 24 h.[22]

The strongly electron-donating CAAC ligand **2.15** was first reported by Bertrand and CAACs have been utilised as ligands for various transition-metal catalysts.[23–26] The CAACs are a subset of *N*-heterocyclic carbenes (NHCs) which more commonly have two nitrogen atoms, such as **2.16**.[27] NHCs such as **2.16** are stabilised by the 'push-pull' effect wherein the relatively electronegative nitrogen 'pulls' σ electron density towards itself and orbital overlap facilitates the 'push' of electrons from the filled nitrogen *p*-orbital to the vacant carbene *p*-orbital. This captodative 'push-pull' effect stabilises the carbene and favours the singlet electron configuration.[27] In CAACs (such as **2.15**), one (π-donating, σ-accepting) nitrogen is replaced with a (σ-donating) carbon. The result is that CAACs are both more nucleophilic (σ-donating) and electrophilic (π-accepting) than NHCs such as **2.16**. Computational studies suggest a slightly narrower HOMO-LUMO (and singlet-triplet) gap for CAACs relative to other NHCs.[26]

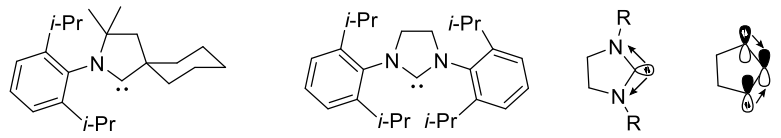

2.15 **2.16**

Figure 2.2 CAAC **2.15**, NHC **2.16** and the stabilisation of NHCs by the 'push-pull' effect.

In 2017, the Glorius group reported the application of the Rh(CAAC)Cl catalyst **2.14** to the *cis*-selective hydrogenation of fluoroarenes.[18] Intriguingly, the hydrogenation products accessed were the high-energy all-*cis*-fluorocyclohexane isomers. Indeed, the methodology was remarkably *cis*-selective and provided scalable access to all-*cis*-fluorocyclohexane derivatives. For example, hexafluorobenzene **2.17** was hydrogenated using the Zeng catalyst **2.14** to give all-*cis*-hexafluorocyclohexane **2.18** in one-step (Scheme 2.6).[18] A modification to the synthesis of **2.18** whereby molecular sieves were replaced by silica gel resulted in a significant improvement in yield (88%).[28]

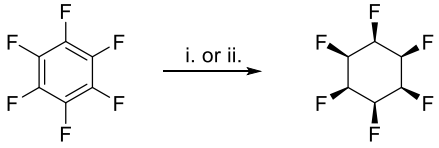

2.17 **2.18**

Scheme 2.6 The *cis*-selective hydrogenation of hexafluorobenzene **2.17** to give all-*cis*-hexafluorocyclohexane **2.18**; i. **2.14** (0.5 mol%), hydrogen (50 bar), 4 Å MS, hexane, r.t., 24 h, 34%;[18] ii. **2.14** (0.5 mol%), hydrogen (50 bar), silica gel, hexane, r.t., 24 h, 88%.[28]

The scope of the hydrogenation reaction is broad, and conditions are tolerant of; silyl ethers, boronic esters, esters, carbamates and ethers. Nitrogen and oxygen containing heterocycles were also tolerated as substrates. Of particular interest are hydrogenation products which incorporated multiple fluorines and at least one other heteroatom which could be used for derivitisation. These products are shown below (Figure 2.3A) and consist of the tetrafluorodisilylether **2.19**, the trifluorosilylethers **2.20** and **2.21** and the difluoroboronic ester **2.22**. Although no nitrogen-containing cyclohexane products were reported with multiple fluorines, three monofluorinated carbamates **2.23**-**2.25** were (Figure 2.3B). Subsequently, the preparation of monofluorinated alkylsilane **2.26** was also reported (Figure 2.3B). Generally, these hydrogenation reactions were high yielding.

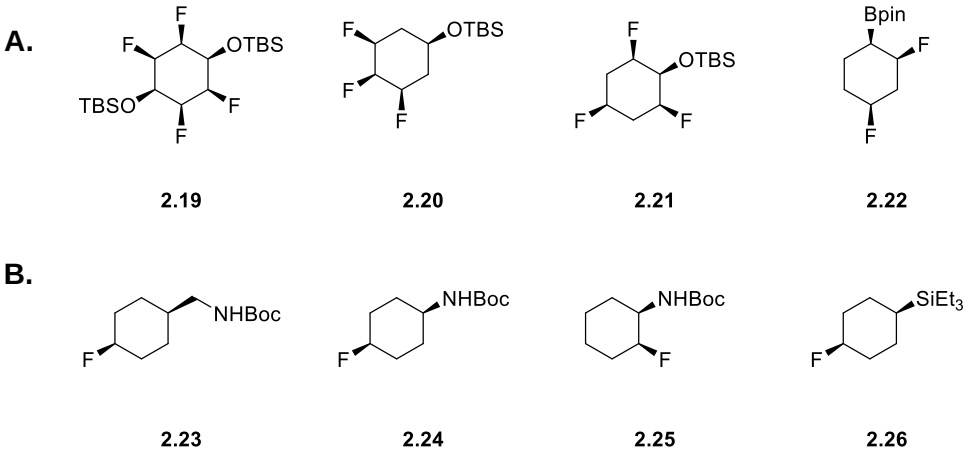

Figure 2.3 A. Hydrogenation products reported by Glorius incorporating more than one fluorine and more than one other heteroatom; **B**. Monofluorinated carbamate and silane hydrogenation products reported by Glorius.[18,28]

A subsequent paper investigating the active catalytic species found that the hydrogenation reaction (Scheme 2.6) is a heterogeneous process.[29] The active catalytic species was found to be Rh(0) nanoparticles supported on silica. The CAAC ligand **2.15** was active in controlling the chemoselectivity of the hydrogenation and the size of the nanoparticles formed.

In 2018, the first *cis*- product bearing five fluorine substituents and a sixth non-fluorine heteroatomic substituent was reported.[30] In that case, the all-*cis*-pentafluorocyclohexylmethyl ether **2.27** was synthesised by the von Delius group using the Rh-hydrogenation method (Figure 2.4A). Interestingly, methyl ether **2.27** demonstrated anion binding in solution of comparable strength (with chloride: K_A = 170±10 M^{-1}) to that observed for **2.18** (with chloride: 400±40 M^{-1}).[30] This observation suggests that the high molecular dipole moment of **2.18** is largely retained for **2.27**, with oxygen replacing a fluorine. A very recent paper has reported the derivatisation of **2.27** to generate five monomers **2.28**-**2.32** which were used as components in supramolecular block copolymers as examples of living supramolecular polymerisation (Figure 2.4B).[31]

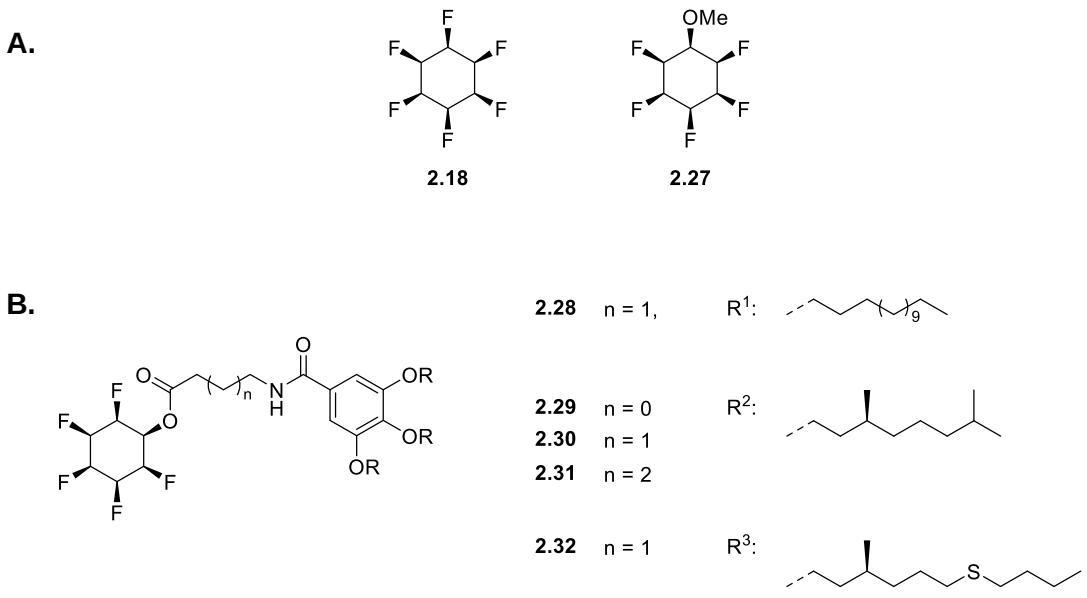

Figure 2.4 A. All-*cis*-hexafluorocyclohexane **2.18** and all-*cis*-pentafluorocyclohexylmethyl ether **2.27**; **B**. Monomers reported in living supramolecular polymerisation derived from **2.27**.[30,31]

In the chair conformation of all-*cis*-hexafluorocyclohexane **2.18**, the 1,3,5-triaxial C-F bond orientation is the major contributor to the elevated molecular dipole moment (Figure 2.5). **2.18** can only adopt a single orientation in the chair conformation. For the methyl ether **2.27** there are two non-equivalent ring flip conformers (Figure 2.5) in which the ether substituent can either arrange to be axial or equatorial. In the axial conformer, the steric clash of the bulky methyl ether with the other axial substituents is destabilising whereas in the equatorial conformer, electrostatic repulsion between the triaxial C-F bonds is destabilising. Acetyl ester **2.33** was prepared by ether cleavage of **2.27** followed by esterification of the resulting alcohol (Scheme 2.7) and its X-ray crystal structure indicates that the triaxial C-F conformation is dominant in the solid state.

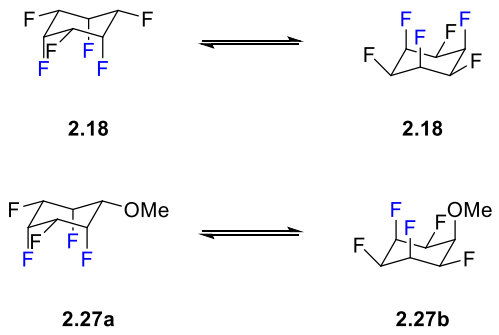

Figure 2.5 Interconverting chair conformation of all-*cis*-hexafluorocyclohexane **2.18** and predicted chair conformation of methyl ether **2.27** showing the axial fluorine substituents in blue.

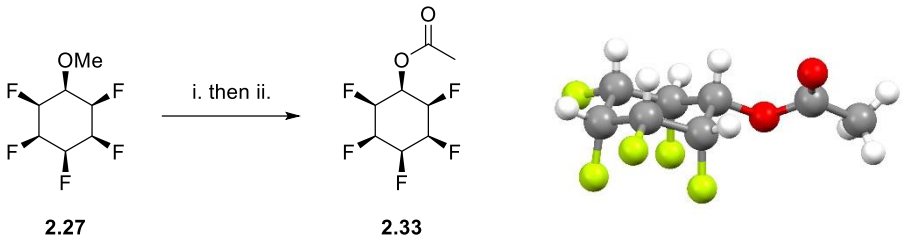

Scheme 2.7 Preparation of acetyl ester **2.33** and its X-ray crystal structure as reported by Von Delius; i. Butane-1-thiol, $AlCl_3$, CH_2Cl_2, r.t., 14 h, 83%; ii. Pentafluorophenyl acetate, Et_3N, DMF, 3 h, 92%.[31]

Given the finding that all-*cis*-pentafluorocyclohexylmethyl ether **2.27** retains a large molecular dipole moment relative to all-*cis*-hexafluorocyclohexane **2.18** and that anion binding is still observed in solution,[30] this project aimed to further explore interactions of the all-*cis*-pentafluorocyclohexyl motif. The potential for this motif in the field of supramolecular chemistry has been demonstrated only very recently and at the end of this thesis work, by its application to living supramolecular polymerisation as previously discussed (Figure 2.4).[31] In this Chapter the scope of the Rh-catalysed hydrogenation reaction will be expanded to broaden the range of pentafluoroarene substrates available. The conformational behaviour of the resulting all-*cis*-pentafluorocyclohexyl building blocks will be examined by X-ray crystallography and NMR spectroscopy and a library of functional derivatives will be generated. Later chapters will explore the utilisation of these building blocks to generate chemically diverse products such as peptidomimetics and further explore their promise for supramolecular assembly.

2.2. Conformation of all-*cis*-pentafluorocyclohexanes

In the first instance, a fundamental exploration of the alkyl substituted all-*cis*-pentafluorocyclohexanes was established. Computational work in collaboration with Professor Rodrigo Cormanich and Bruno Piscelli at the University of Campinas in Brazil revealed a small preference for the more polar Me-equatorial conformer **2.34b** (0.29 kcal mol^{-1}) of all-*cis*-methylpentafluorocyclohexane **2.34** in the gas phase (Figure 2.6). In **2.34**, hyperconjugation interactions were more stabilising for **2.34b** (Me-equatorial) than for **2.34a** (Me-axial) but this was finely balanced against the destabilising electrostatic repulsion between the triaxial C-F bonds. With **2.35**, the equatorial conformer **2.35b**, was more significantly favoured. In this instance electrostatics as well as hyperconjugation favoured the equatorial conformer. The replacement of a hydrogen in **2.34** for a CH_3 in **2.35** results in increased electrostatic repulsion between the axial fluorine and the more electronegative carbon of the CH_3 unit (electronegativity of carbon = 2.55; electronegativity of hydrogen = 2.2).

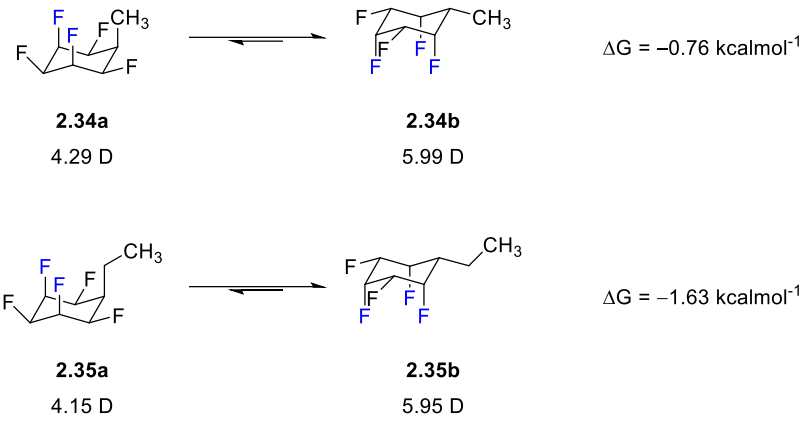

Figure 2.6 Theory evaluation of the magnitude of equatorial preferences in the gas phase for alkyl substituents in all-*cis*-alkylpentafluorocyclohexanes **2.34** and **2.35**, by Rodrigo Cormanich and Bruno Piscelli, University of Campinas, Brazil.[32]

In the first instance, the Zeng/Glorius catalyst **2.14** was prepared by the ligation of the CAAC salt **2.15** to $[RhCODCl]_2$ according to reported procedures and in good yield (Scheme 2.8). Anhydrous conditions were meticulously maintained in an argon atmosphere in a glovebox. The pure catalyst **2.14** was obtained following chromatography and recrystallisation and proved air-stable for up to 3 months.

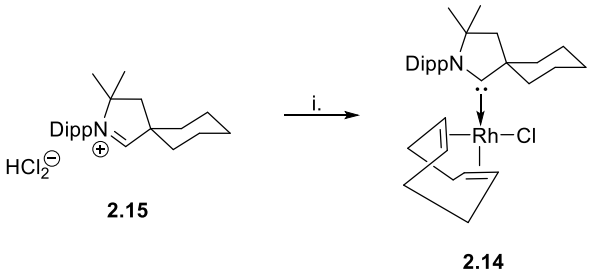

2.15 **2.14**

Scheme 2.8 Preparation of the Zeng/Glorius catalyst **2.14** ; i. $[RhCODCl]_2$, KHMDS, THF, −78 ° C to r.t., 16 h, 53%.[18,33]

In order to explore the conformation of **2.35** in the solid state a hydrogenation of pentafluorostyrene **2.36** to give **2.35** was conducted using the Zeng/Glorius method (Scheme 2.9).[18,22] The X-ray crystal structure of **2.35** has an equatorial preference for the ethyl substituent, consistent with theory. Also notable in the crystal structure of **2.35** are the close intermolecular contacts of 2.45-2.47 Å between hydrogen and fluorine atoms of two rings (Sum of VdW radii = 2.67 Å). This indicates a strong electrostatic attraction between the fluorine and hydrogen of the rings, a feature which further stabilises the Et-equatorial conformer **2.35b** (Figure 2.6) in the solid state, as these interactions would be weakened if the Et group was axial.

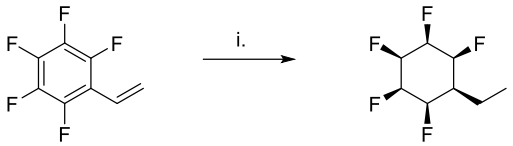

2.36 **2.35**

Scheme 2.9 Hydrogenation of pentafluorostyrene **2.36** to give **2.35**; i. H_2 (50 bar), **2.14** (2 mol%), 4 Å MS, hexane, r.t., 14 h, 76%.[18]

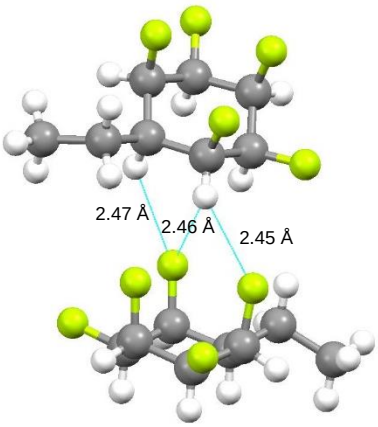

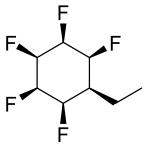

2.35

Figure 2.7 X-ray crystal structure of **2.35**.

A close inspection of the NMR spectra of **2.35** was required to unambiguously assign the dominant conformer in ([$^2H_6$]-acetone) solution. Due to the complex coupling of ring protons to proximal fluorine and hydrogen atoms, and the resultant overlap, only indicative *J* values are shown in Figure 2.8. The $^3J_{HF}$ coupling constant for H4-F3 of 7.6 Hz is consistent with a *gauche* arrangement found in the Et-equatorial conformer. The large and overlapping $^3J_{HF}$ for H3-F2 and H3-F4 of 28.2 Hz indicate antiperiplanar arrangements between H3 and F2 and H3 and F4 consistent with the Et-equatorial conformer. Similarly, the large $^3J_{HF}$ coupling constant for H1-F2 of 34.5 Hz indicates an anti-periplanar arrangement between H1 and the two F2 atoms, an arrangement only possible in the Et-equatorial conformation. The vicinal H-H coupling between H-2, H-3 and H-4 is not well resolved in the $^1H\{^{19}F\}$ NMR spectrum as the peaks are broad due to dynamic conformational exchange. In all such cases $^3J_{HH}$ is approximately 1-2 Hz, consistent with the expected all *gauche* H-H alignment of all of the vicinal hydrogens.

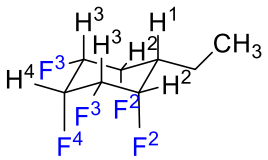

2.35

Vicinal F-H coupling

H4-F3 ($^{3}J_{FH}$) = 7.6 Hz

H3-F2 ($^{3}J_{FH}$) = 28.2 Hz

H3-F4 ($^{3}J_{FH}$) = 28.2 Hz

H1-F2 ($^{3}J_{FH}$) = 34.5 Hz

^{1}H NMR

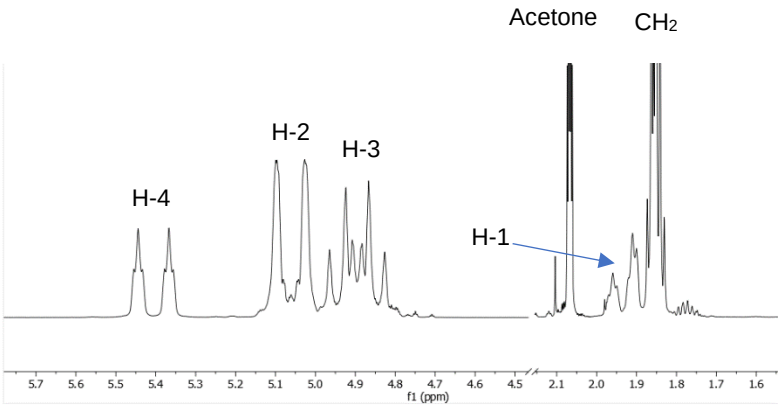

^{1}H {^{19}F} NMR

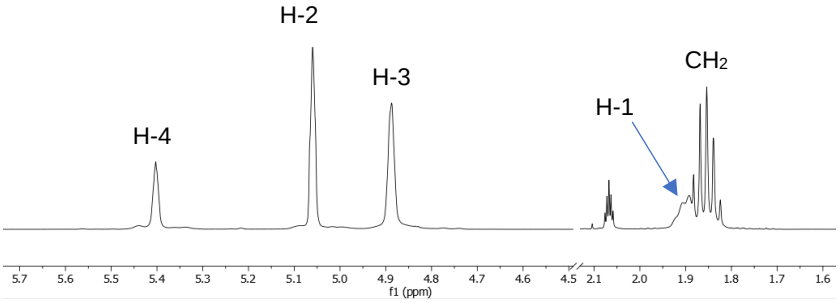

Figure 2.8 The ^{1}H and ^{1}H{^{19}F} NMR spectra of **2.35**.

The ^{19}F{^{1}H} spectrum was assigned by cross peaks in the ^{1}H-^{19}F HMBC spectrum (Figure 2.9). The ^{19}F{^{1}H} spectrum shows an unusually large 'through space' $^{4}J_{FF}$ coupling constant between F2 and F4 of 25 Hz, consistent with the 1,3 triaxial C-F relationship of the Et-equatorial conformer.[34] The 'through space' $^{4}J_{FF}$ coupling constant arises from the rigidity of the ring system which results in an interatomic fluorine distance closer than the sum of the VdW radii. This enables orbital overlap of nonbonding fluorine lone pairs which facilitates spin information exchange though no chemical bond is formed. As the average distance between F2 and F4 in the crystal structure of **2.35** (which occupies the Et-equatorial conformer, Figure 2.7) is 2.76 Å, and this is significantly less than the sum of the VdW radii (2.94 Å), there is

significant orbital overlap in the Et-equatorial conformation. Given the overwhelming evidence from NMR spectra, the dominant conformer in [$^2H_6$]-acetone is assigned as the Et-equatorial conformation.

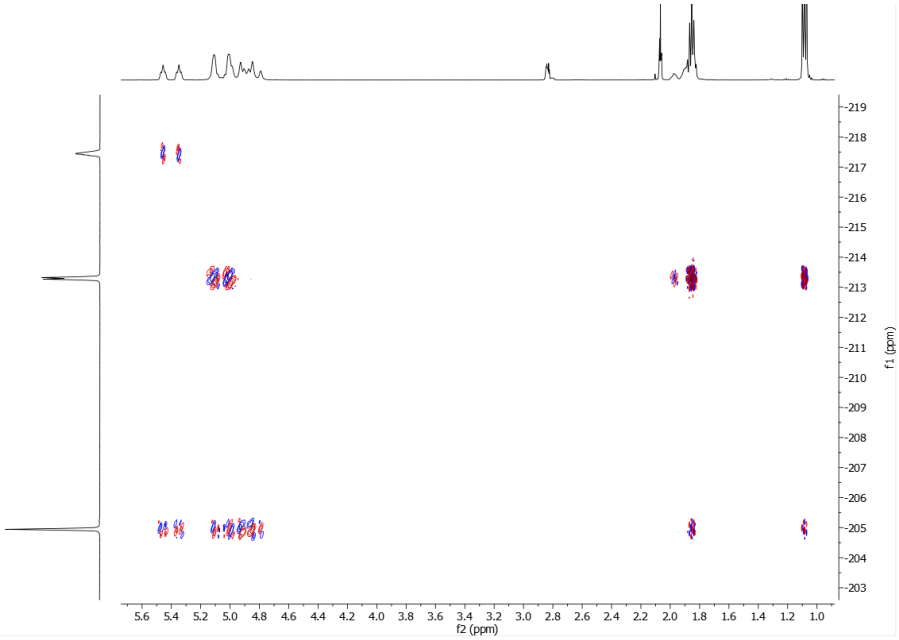

Figure 2.9 ^{19}F-^{1}H HMBC spectrum used to assign $^{19}F\{^{1}H\}$ spectrum of **2.35**.

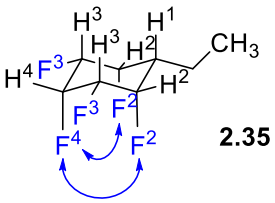

2.35

'Through space' F-F coupling

F2-F4 ($^4J_{FF}$) = 25 Hz

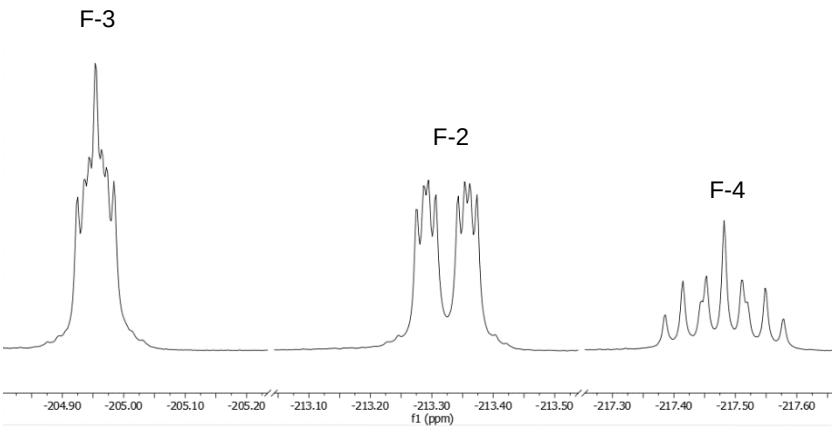

Figure 2.10 The $^{19}F\{^{1}H\}$ spectrum of **2.35**.

2.3. Novel building blocks

2.3.1. Functional group tolerance of the Rh-catalysed hydrogenation of fluoroarenes

Arene hydrogenation is frequently associated with poor chemoselectivity, in particular the tolerance for reducible functional groups is generally low.[5] Preceding reports are encouraging and indicate the tolerance of silyl ethers, esters, boronic esters and alkyl silanes in the Rh-catalysed hydrogenation of fluoroarenes (Figure 2.3).[18,28] To probe further the functional group tolerance of these hydrogenation reactions, several fluoroarenes: benzyl chloride **2.37**, phenol **2.38**, nitrile **2.39** and carboxylic acid **2.40** were used as substrates in the general procedure illustrated in Scheme 2.10. The hydrogenation of these compounds proved elusive and the ^{19}F NMR spectra did not show any evidence of aliphatic C-F bonds.

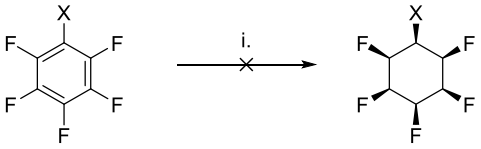

2.37, X = CH_2Cl
2.38, X = OH
2.39, X = CN
2.40, X = CH_2CO_2H

Scheme 2.10 Unsuccessful aryl hydrogenation substrates; i. **2.14** (1 mol%), H_2 (50 bar), 4 Å MS, hexane, r.t., 16 h.

2.3.2. Protecting group strategies towards novel building blocks

Given the challenge of hydrogenating pentafluorophenol **2.38**, presumably due to catalyst poisoning by the substrate, a protecting group strategy was considered. Silyl ethers are often used for the protection of alcohols and are easily cleaved, for example by reaction with a fluoride ion source such as TBAF. The suitability of *tert*-butyldimethylsilyl ether groups for the Rh-catalysed hydrogenation was established by Glorius and selected hydrogenation products reported with this functional group are shown (Figure 2.11).[18]

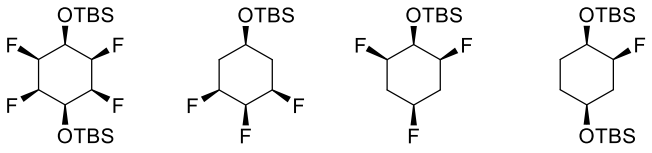

2.19 **2.20** **2.21** **2.41**

Figure 2.11 Selected hydrogenation products with *tert*-butyldimethylsilyl ether groups reported by Glorius.[18]

In practice, pentafluorophenol **2.38** was readily protected as silyl ether **2.42** in near-quantitative yield using a procedure adapted from the literature (Scheme 2.11).[35] The

hydrogenation of **2.42** was first attempted with molecular sieves. No consumption of starting material **2.42** was observed as judged by ^{19}F NMR. The hydrogenation was then reattempted with silica gel and the crude ^{19}F NMR showed a complex mixture of both aromatic and aliphatic defluorinated products, which were not isolated.

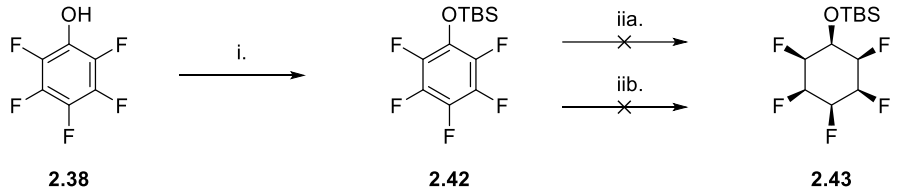

2.38 **2.42** **2.43**

Scheme 2.11 Attempted synthesis of silyl ether **2.43**; i. TBDMSCl, imidazole, CH_2Cl_2, r.t., 98%; iia. **2.14** (2 mol%), hydrogen (50 bar), 4 Å molecular sieves, hexane, r.t., 14 h, no reaction; iib. **2.14** (2 mol%), hydrogen (50 bar), silica gel, hexane, r.t., 14 h, no reaction.

The hydrogenation of the aryl silyl ether **2.42** proved challenging despite the precedent reported by Glorius (Figure 2.11).[18] The fifth fluorine substituent may result in an electron deficient arene that cannot strongly bind the active catalytic species. The steric bulk of the silyl ether may also present a barrier to catalyst-substrate binding. Incorporation of a -CH_2- unit as a spacer to give homologated substrate **2.44** was suggested to improve this binding, thereby reducing the steric clash between the active catalytic species and the alkyl groups of the silyl ether as illustrated in Figure 2.12.

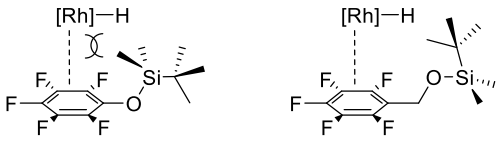

2.42 **2.44**

Figure 2.12 Structures of silyl ether substrates **2.42** and **2.44** indicating reduction of steric clash.

Proceeding with the homologation strategy, pentafluorobenzyl alcohol **2.45** was protected as before, and in good yield.[35] In this case the Rh-catalysed hydrogenation of the resulting silyl ether **2.44** was now successful giving **2.46** in a moderate yield. Contrary to literature reports,[28] the use of 4 Å molecular sieves facilitated the reaction whereas the use of silica gel gave no conversion to the desired product in our hands. In the first instance, deprotection of the silyl ether **2.46** was attempted following an adapted literature procedure by reaction with TBAF,[36] but this resulted in a mixture of defluorinated elimination products.

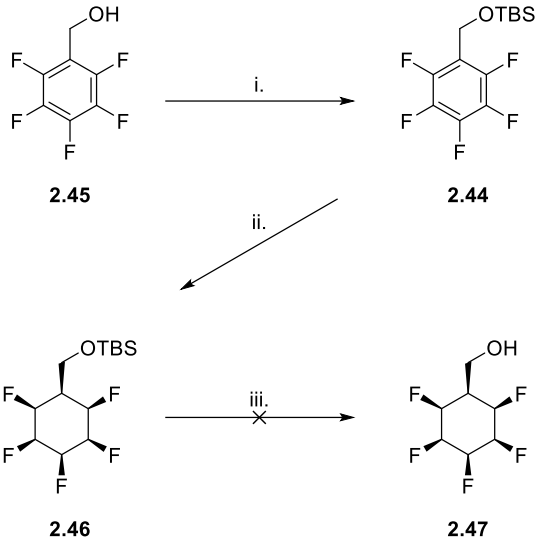

Scheme 2.12 The synthesis of *tert*-butyldimethyl((pentafluorocyclohexyl)methoxy)silane **2.47**; i. TBDMSCl, imidazole, CH_2Cl_2, r.t., 16 h, 71%;[28] ii. **2.14** (2 mol%), H_2 (50 bar), 4 Å molecular sieves, r.t., 14h, 41%;[18] iii. TBAF, THF, r.t., 1h.

The unsuccessful deprotection of **2.46** with TBAF resulted in a complex mixture as was evident from the crude ^{19}F NMR spectrum (Figure 2.13) in which both vinylic and aliphatic fluorine signals can be observed. Because the fluoride anion is basic and because solutions of TBAF are readily hydrated (leading to the formation of hydroxide anions), base-catalysed elimination was implicated in the defluorination of silyl ether **2.46**. The base-promoted elimination of HF in organofluorine compounds generally proceeds by an E1cB mechanism (Scheme 2.13).[37]

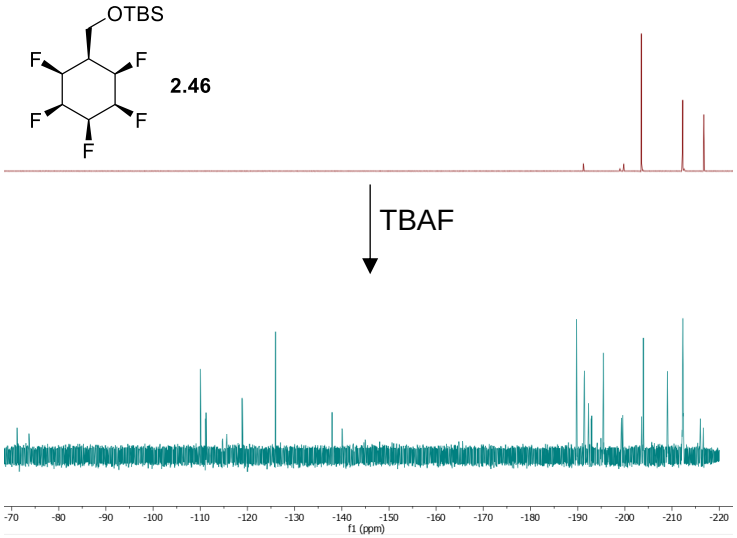

Figure 2.13 Top: The ^{19}F NMR spectra of **2.46**, bottom: the ^{19}F NMR spectra of the crude reaction mixture of **2.46** with TBAF.

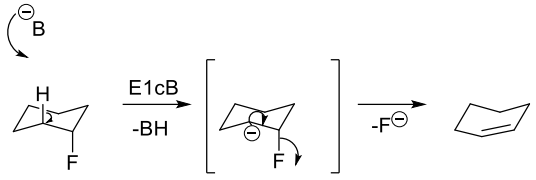

Scheme 2.13 An E1cB hypothesis for base-mediated elimination of HF from alkyl fluorides.[37]

Given the challenging deprotection of silyl ether **2.46** with TBAF due to apparent base-catalysed elimination of HF, an alternative approach was pursued. The deprotection of silyl ethers can also be achieved with TREAT-HF.[38] While both methods for deprotection rely on fluoride attacking the silyl ether, TREAT-HF is less basic as the fluoride is formally protonated (Figure 2.14).

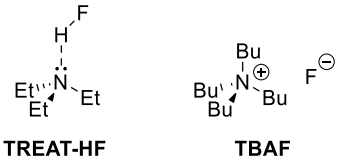

Figure 2.14 TREAT-HF and TBAF.

In practice the deprotection of silyl ether **2.46** with TREAT-HF was conducted according to an adapted literature procedure,[38] in very good (83%) yield and no defluorinated products were detected by ^{19}F NMR (Scheme 2.14).

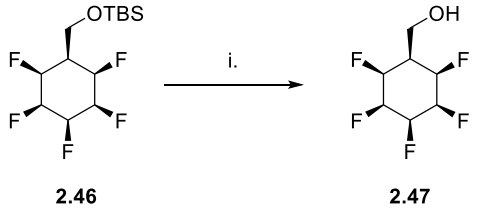

Scheme 2.14 Modified conditions for the deprotection of silyl ether **2.46**; i. TREAT-HF, MeCN, 16 h, r.t., 83%.[38]

The X-ray crystal structure of silyl ether **2.46** shows that the dominant conformer in the solid state has triaxial C-F bonds (Figure 2.15). Close contacts (2.28 Å, 2.47 Å and 2.52 Å) between alternate faces of the ring are also present due to electrostatic attraction (sum of the Van der Waals radii = 2.67 Å).

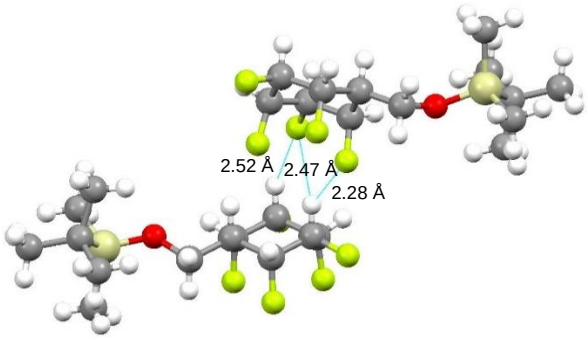

Figure 2.15 X-ray crystal structure of **2.46** with close contacts in blue.

Following the successful synthesis of the alcohol building block **2.47** a route to the analogous primary amine was devised. 'Boc' protected amines were reported by Glorius as compatible with the Rh-catalysed hydrogenation of fluoroarenes (Figure 2.3B) so benzyl carbamate **2.48** was designated as a target substrate for hydrogenation.[18] While a commercial source for the non-protected free amine could not be found, pentafluorobenzonitrile **2.39** was readily available. Carbamate **2.48** could be isolated in quantitative yield using a one-pot reduction-protection procedure adapted from the literature (Scheme 2.15).[39,40] However, the hydrogenation of **2.48** was unsuccessful in our hands.[18] Accordingly, the di-Boc-protected amine **2.50** was explored, by reaction of carbamate **2.48** with a further equivalent of Boc anhydride in moderate yield.[41] However, this hydrogenation was also unsuccessful, and only starting material was recovered.

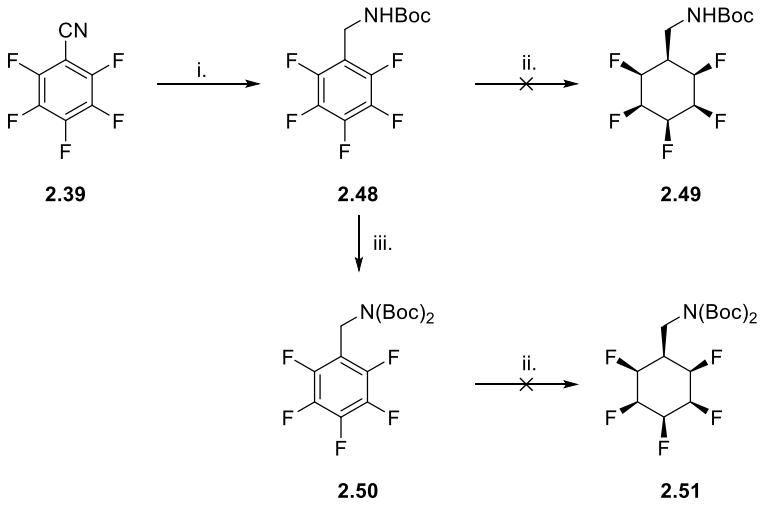

Scheme 2.15 The attempted synthesis of Boc-protected amines **2.49** and **2.51**; i. $NaBH_4$, $NiCl_2$, Boc_2O, MeOH, 0 °C to r.t; 16 h, quantitative;[39,40] ii. **2.14** (2 mol%), hydrogen (50 bar), hexane, 4 Å MS, r.t., 16 h; iii. Boc_2O, DMAP, MeCN, r.t., 24 h, quantitative.[18,41]

Notably, the carbamate-containing cyclohexane hydrogenation products reported by Glorius had only one fluorine on the ring (Figure 2.3B).[18] It is unclear why increased ring fluorination

appears to present a barrier to hydrogenation of some substrates and a greater mechanistic understanding may be required to explain this.

Following this, the next building block that was explored was an all-*cis*-pentafluorocyclohexane compound with a carboxylic acid handle for diverse functionalisation. Turning again to the scope reported by Glorius, two compounds with methyl ester substituents were reported **2.52** and **2.53** (Figure 2.16).[18] Again, both products had only one fluorine substituent and a challenging synthesis of more highly fluorinated analogues was envisioned.

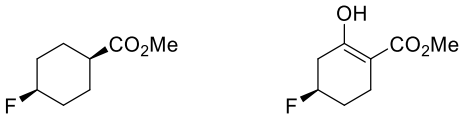

2.52 **2.53**

Figure 2.16 Hydrogenation products reported by Glorius bearing the methyl ester functionality.[18]

Previous work in St Andrews had established that carboxylic acid **2.54** was unstable due to rapid HF elimination from the tetrafluorocyclohexane ring, arising from the acidity of the proton α- to the carboxyl group (Scheme 2.16).[42]

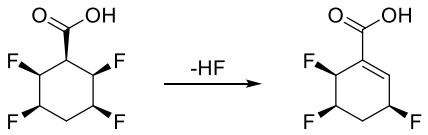

2.54, not isolable **2.55**

Scheme 2.16 Instability of carboxylic acid **2.54** due to elimination of HF.[42]

Given this finding, it was not expected that the aliphatic methyl ester **2.57** would be isolable from the hydrogenation of arene **2.56**, however the reaction was conducted to explore this (Scheme 2.17). In practice the conversion was low < 5% and as anticipated multiple defluorinated products were detected by ^{19}F NMR. This finding was consistent with the previously described incompatibility of carboxyl substitution on 'Janus' rings.[42]

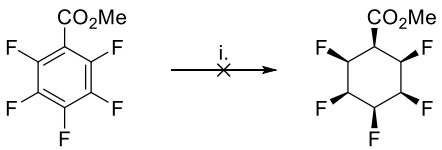

2.56 **2.57**

Scheme 2.17 The attempted hydrogenation of methyl pentafluorobenzoate **2.56**; i. **2.14** (2 mol%), 4 Å MS, hexane, r.t., 16 h.[18]

Given the unsuitability of methyl ester **2.56** as a substrate for hydrogenation, a homologation strategy was again pursued. Homologation had proven effective with the alcohol building block **2.47** following the challenging hydrogenation of the protected aryl silyl ether **2.42**. Thus, all-*cis*-pentafluorocyclohexylacetic acid **2.58** was chosen as the next synthetic target (Figure 2.17).

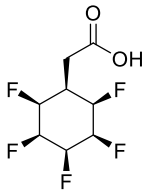

2.58

Figure 2.17 Target building block **2.58**.

Beginning with pentafluorophenylacetic acid **2.40**, esterification was achieved under acidic conditions yielding methyl ester **2.59**.[43] The hydrogenation of **2.59** was successful and progressed with a high yield and both the desired product **2.60** and a minor hydrodefluorinated product **2.61** could be obtained in a 13:1 ratio (Scheme 2.18).[18] Following separation, the structures of both **2.60** and **2.61** were unambiguously assigned by X-ray crystallography.

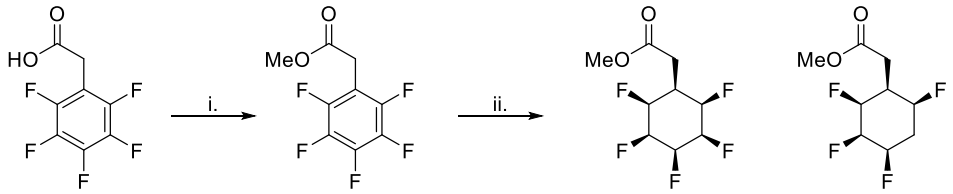

2.40 **2.59** **2.60** (76%) **2.61** (6%)

Scheme 2.18 The synthesis of all-*cis*-pentafluorocyclohexylmethyl acetate **2.60**; i. HCl (1M), MeOH, 65 °C, 94%; ii. **2.14** (1 mol%), Hydrogen (50 bar), 4Å MS, hexane, r.t., 16 h, 76%.[18,43]

The crude ^{19}F NMR spectrum (Figure 2.18) shows the peaks related to the major **2.60** and minor **2.61** products from the hydrogenation of **2.59**. Despite the generation of the minor hydrodefluorinated product **2.61**, the yield for the desired major product **2.60** was high (76%).

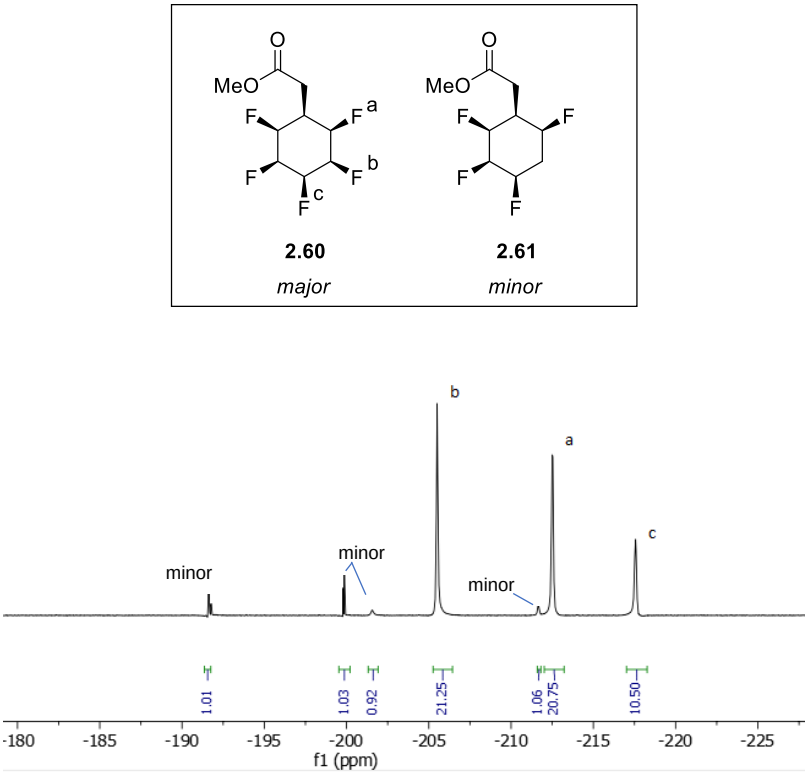

Figure 2.18 ^{19}F NMR spectrum of crude mixture of **2.60** and **2.61**.

The X-ray crystal structure of the major product **2.60** is illustrated in Figure 2.19. The arrangement in the solid state is again the triaxial C-F conformer. Packing occurs with four intermolecular close contacts between axial ring fluorine and hydrogens, these contact distances are 2.39-2.48 Å (Sum of the VdW radii = 2.67 Å). An intermolecular close contact of 2.59 Å is also seen between the carbonyl oxygen and an α-hydrogen (Sum of the VdW radii = 2.72 Å).

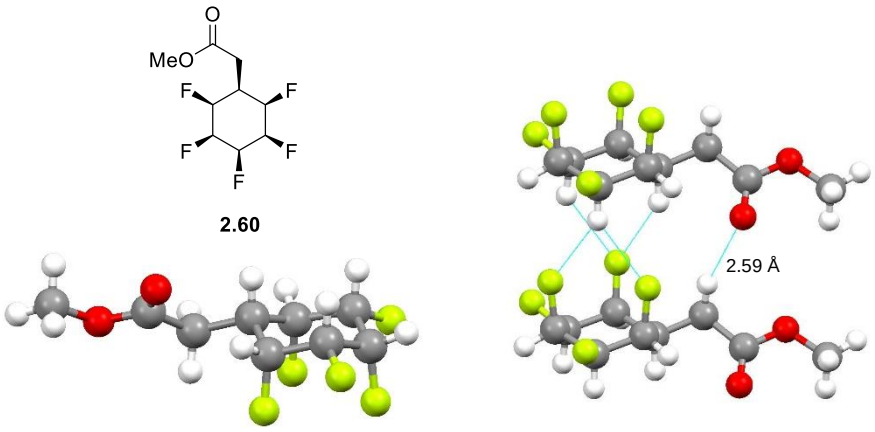

Figure 2.19 Representations of X-ray crystal structure of **2.60** showing close contacts in blue.

Similarly, the X-ray crystal structure of **2.61** (Figure 2.20) shows the dominance of the triaxial C-F arrangement in the solid phase. Intermolecular packing is offset with only two close contacts between stacked axial ring fluorine and hydrogens of 2.40 Å and 2.55 Å. Additional intermolecular hydrogen-fluorine close contacts of 2.50 Å and 2.46 Å are also observed (Sum of the VdW radii = 2.67 Å). The carbonyl oxygen to α-hydrogen close contact from **2.60** (Figure 2.19) is retained in **2.61** (2.52, sum of the VdW radii = 2.72 Å).

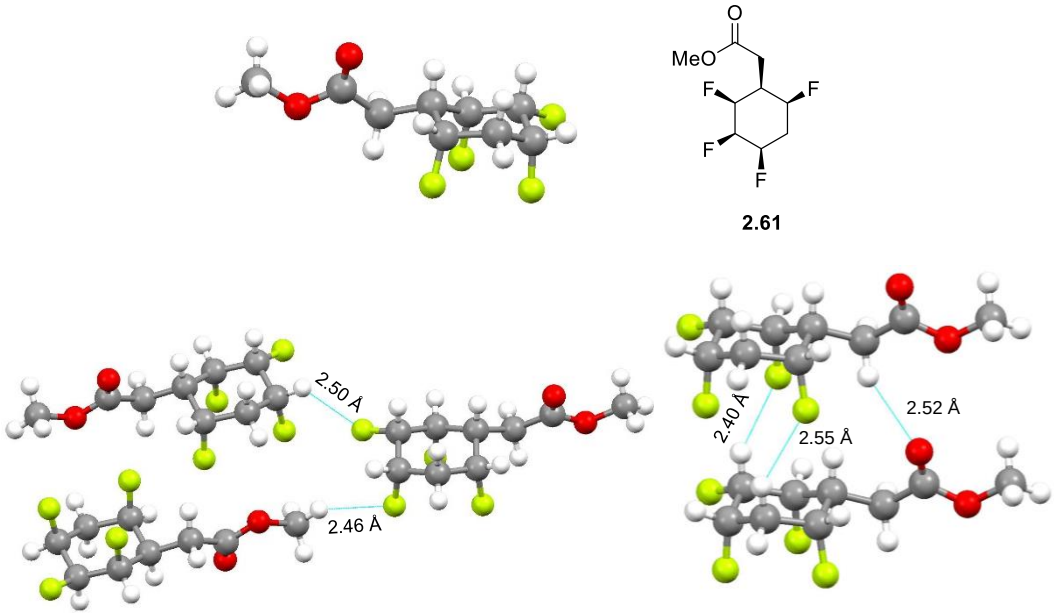

Figure 2.20 Various representations of the X-ray crystal structure of **2.61** with close contacts in blue.

Possible mechanisms for the formation of the hydrodefluorinated side product **2.61** are illustrated in Scheme 2.19. The first pathway consists of oxidative addition of a catalytic rhodium species into an aryl/vinyl C-F bond to give **2.63**, followed by reductive elimination to give **2.64** which could then be hydrogenated as expected to give **2.61**. Alternatively, addition of a rhodium hydride complex into a carbon-carbon double bond would give **2.65** and, following β-fluoride elimination would generate **2.64** which would again result in hydrogenation to the observed product **2.61**.

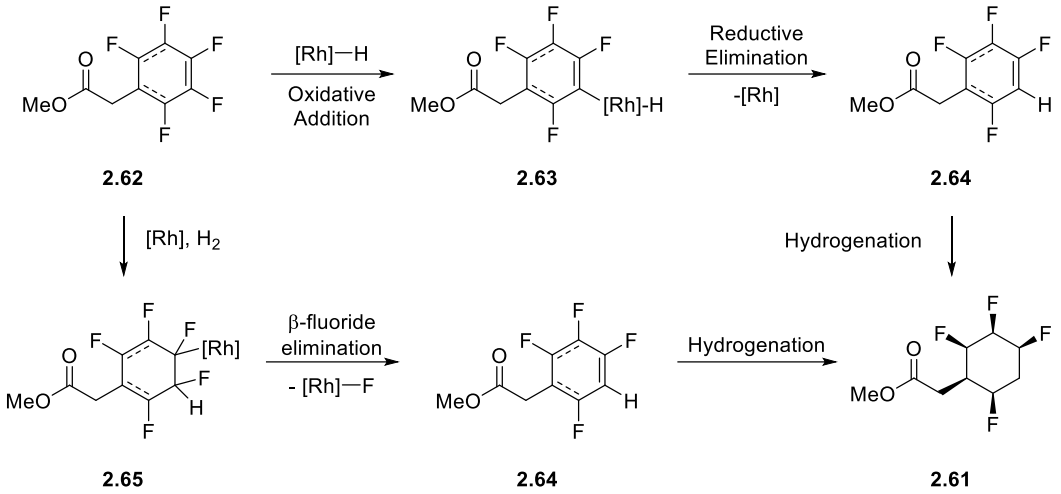

Scheme 2.19 Putative mechanisms for the formation of minor side product **2.61** adapted from ref 18.[18]

Base-catalysed ester hydrolysis of **2.60** was unsuccessful and multiple defluorinated products were detected in the crude ^{19}F NMR spectrum.[44] The base-mediated elimination via the E1cB pathway has been discussed previously (Scheme 2.13). Fortunately, acidic conditions were readily tolerated, and carboxylic acid **2.58** was isolated in high yield after acid-catalysed hydrolysis (Scheme 2.20).[45]

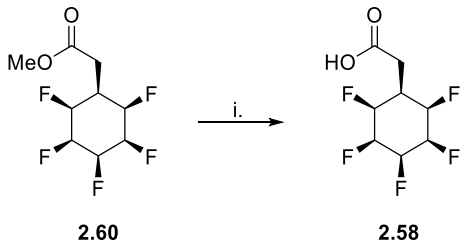

Scheme 2.20 i. HCl (6M), 100 °C, 14 h, 96%.[44,45]

2.4. Extended substrate homologation

Following the challenging hydrogenation of methyl ester **2.56** and silyl ether **2.42**, their direct analogues **2.59** and **2.44** were successfully hydrogenated. Therefore, substrate homologation has proven to be a successful strategy for the generation of all-*cis*-pentafluorocyclohexane building blocks (Figure 2.21).

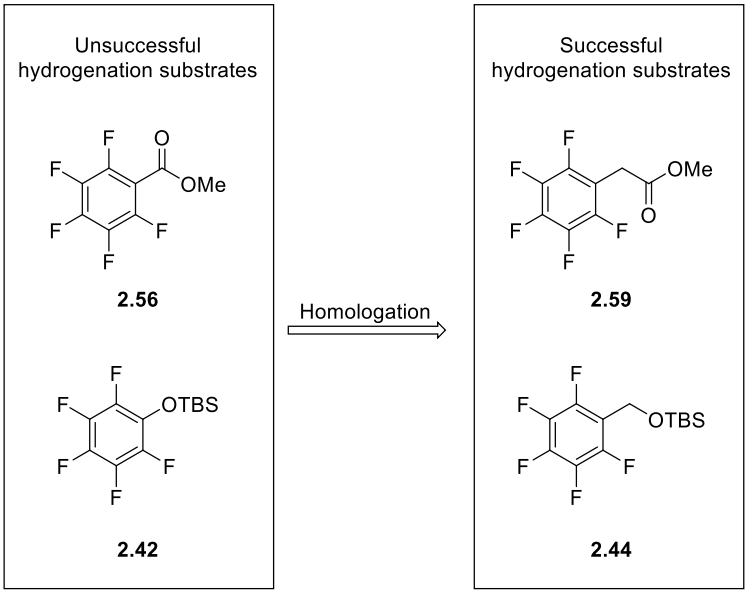

Figure 2.21 Successful homologation strategy for the generation of substrates for *cis*-selective hydrogenation.

Given the success of the homologation approach, it was proposed that longer alkyl spacers might facilitate even more straightforward hydrogenations. To test this hypothesis, a homologated silyl ether hydrogenation was carried out (Scheme 2.21). To access the silyl ether substrate **2.68**, methyl ester **2.59** was reduced to alcohol **2.66** under mild conditions and this was then protected to give silyl ether **2.67**.[35,46] In the event, hydrogenation of **2.67** proceeded in excellent yield (79%) relative to the dehomologated analogue **2.44** (hydrogenation yield 41%).[18]

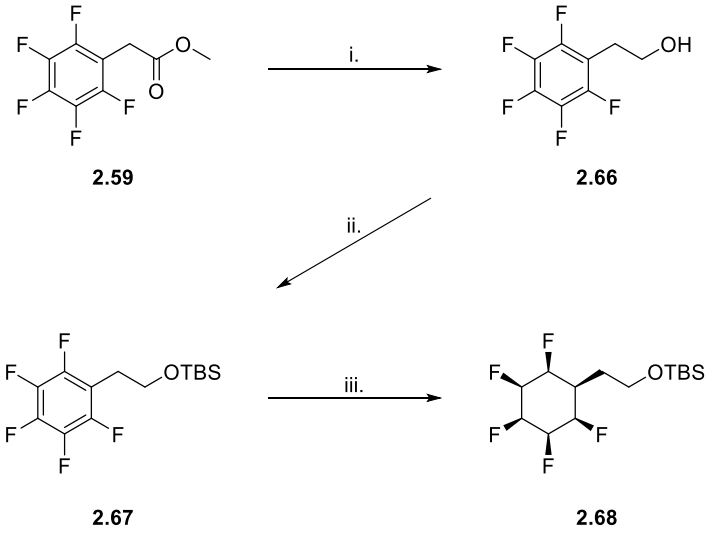

Scheme 2.21 Route to homologated silyl ether **2.68**; i. $LiBH_4$, THF, 0 °C to r.t., 16 h, quantitative; ii. TBDMSCl, imidazole, CH_2Cl_2, r.t., 16 h, 72%; iii. **2.14** (1 mol%), Hydrogen (50 bar), 4 Å molecular sieves, hexane, r.t., 16 h, 79%.[18,35,46]

Given the previous success with extended homologation to improve hydrogenation, the extended chain targets **2.72** and **2.73** were considered each bearing a four-carbon spacer (Scheme 2.22). By utilising a cross metathesis reaction, a modular route to **2.72** and **2.73** was planned from a common starting material, which was the commercially available allylpentafluorobenzene **2.69**. Although the cross-metathesis reaction with **2.70** was expected to be non-selective and therefore low-yielding only modest amounts of material were required to determine the amenability of these candidate substrates to hydrogenation.

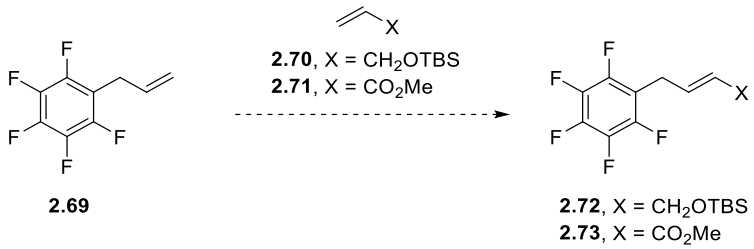

Scheme 2.22 Retrosynthetic analysis of extended chain hydrogenation substrates **2.72** and **2.73**.

The synthesis towards **2.72** began with the protection of allyl alcohol **2.74** as a silyl ether to give **2.70**.[33] The cross-metathesis reaction between **2.69** and **2.70** was indeed unselective, giving only a low yield of the desired hydrogenation substrate **2.72**.[47] However, this product was readily purified and hydrogenation of **2.72** proved to be successful giving **2.75** in a moderate 49% yield.[18] The silyl ether was then deprotected under acidic conditions to give alcohol **2.76**.[48]

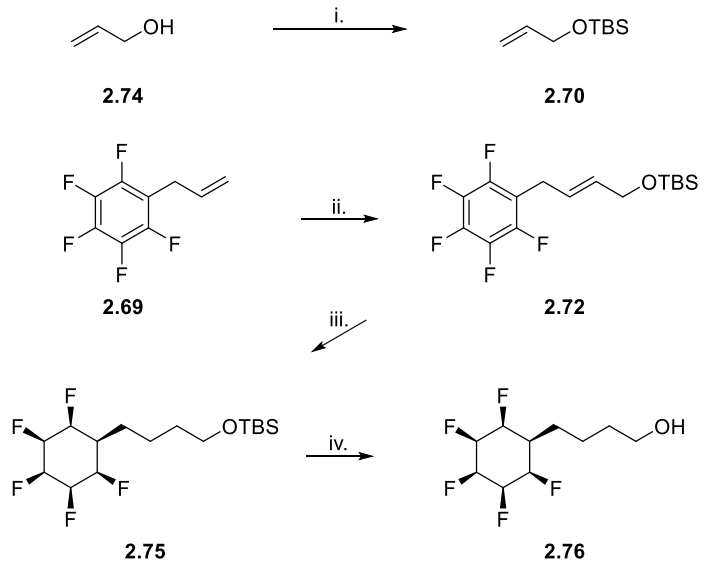

Scheme 2.23 Synthesis of alcohol **2.76**; i. TBDMSCl, imidazole, DMF, r.t., 14 h, 92%; ii. Grubbs I (4 mol%), **2.70**, CH_2Cl_2, r.t., 16 h, 13%; iii. **2.14** (4 mol%), 4 Å MS, hydrogen (50 bar), hexane, r.t., 14 h, 49%; iv. HCl (1M), THF, 66 °C, 14 h, 59 %.[18,35,47,48]

Next, the synthesis of the extended methyl ester **2.77** was undertaken (Scheme 2.24). The cross-metathesis of **2.69** with methyl acrylate proved to be selective due to the inertness of methyl acrylate to homo-coupling.[47] Consequently, the conjugated ether **2.73** was isolated in high yield. The hydrogenation of **2.73** proceeded to give the desired product **2.77** in relatively low 36% yield.[18]

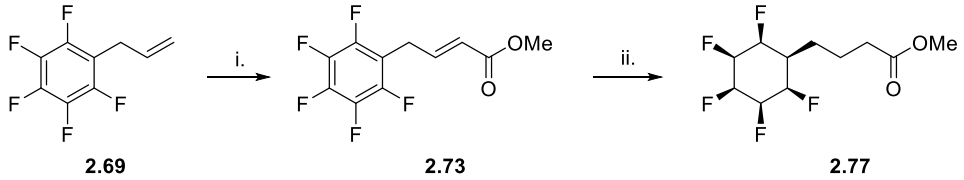

Scheme 2.24 Synthesis of extended methyl ester **2.77**; i. Hoyveda-Grubbs second generation catalyst (2 mol%), methyl acrylate, CH_2Cl_2, 40 °C, 16h, 71%; ii. **2.14** (3 mol%), 4 Å MS, hydrogen (50 bar), hexane, r.t., 14 h, 36%.[18,47]

2.5. Base stability of 'Janus' rings

Following the repeated base-promoted eliminations of HF in the 'Janus' compounds, a screening programme was designed to establish the relative tolerance of the ring system to basic reagents. The use of silyl ether **2.68** as a common substrate avoided any complexity arising from the use of compounds with acidic protons such as **2.60** which has an enolisable α-carbon (pK_a ~ 25) and alcohol **2.76** which can be deprotonated to form the alkoxide (pK_a ~ 16) (Figure 2.22). A standard procedure was utilised in which an excess of a base (4 equiv.) was added to a solution of silyl ether **2.68** and the solution was stirred at r.t.. The stability of **2.68** was determined by direct ^{19}F NMR analysis after 1 h. In each case the results are summarised in Table 2.1. The results of the base-stability assays indicated the compatibility of the 'Janus' ring with weak nitrogen bases but defluorination was observed with stronger bases pK_a > 16. The base test with NaOMe (pK_a = 16) resulted in a partial defluorination with 90% of the starting material **2.68** remaining after 1 h. After repeating the stability test with a large excess of NaOMe (200 eq.) complete defluorination of **2.68** was observed within 1 h.

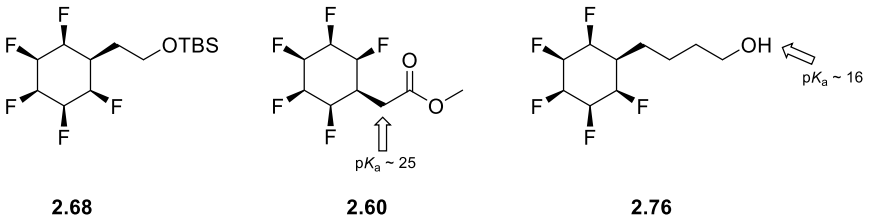

Figure 2.22 Novel 'Janus' ring compounds indicating pK_a of acidic protons.

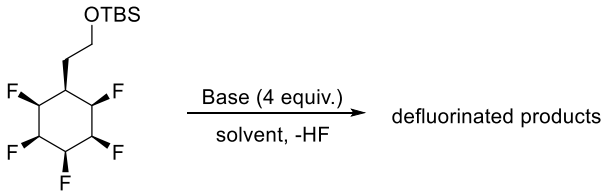

2.68

Base	pK_a	Solvent	Stable (1 h)
Pyridine	5	$CHCl_3$	Yes
Triethylamine	11	$CHCl_3$	Yes
$^{i}Pr_2NEt$	11	$CHCl_3$	Yes
Piperidine	12	$CHCl_3$	Yes
NaOH	14	Water/DMSO	Yes
NaOMe	16	THF	Partially*
^{t}BuONa	17	THF	No
LiHMDS	26	THF	No
NaH	35	THF	No
LDA	36	THF	No
^{n}BuLi	~50	THF	No

Table 2.1 Base stability of silyl ether **2.68** in various bases at r.t.;*90% of starting material **2.68** remains.[49-51]

2.6. Derivatisation of novel hydrogenation products

Having expanded the scope of the Rh-catalysed hydrogenation reaction to obtain a variety of all-*cis*-pentafluorocyclohexane derivatives (Figure 2.23); further derivatisations were considered.

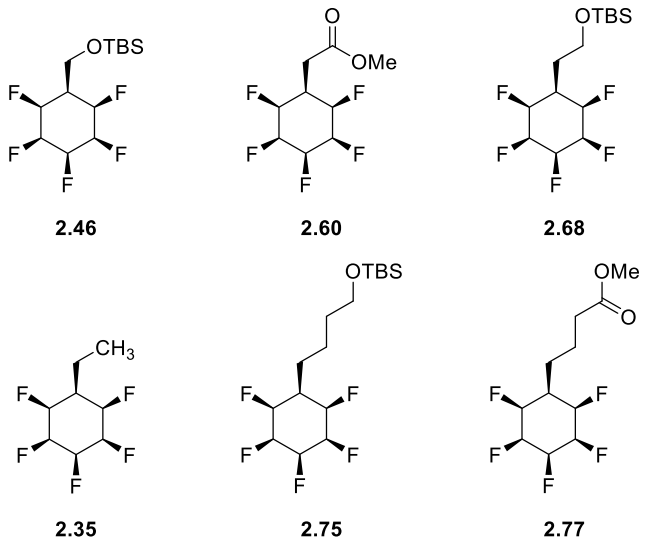

2.46 **2.60** **2.68**

2.35 **2.75** **2.77**

Figure 2.23 Novel all-*cis*-pentafluorocyclohexane hydrogenation products.

One aim was to synthesise a terminal amine building block as this had so far proven to be elusive (Scheme 2.15). A series of proposed functional group interconversions from silyl ether **2.46** are illustrated in Scheme 2.25.

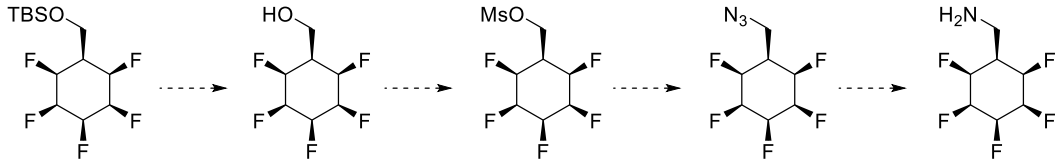

2.46 **2.47** **2.78** **2.79** **2.80**

Scheme 2.25 Functional group interconversions from silyl ether **2.46** to amine **2.80**.

In the first instance, alcohol **2.47** was efficiently converted to mesylate **2.78** (Scheme 2.26).[52] However, the attempted reaction of **2.78** with sodium azide did not give the desired substitution product.[53] In the most probable stable chair conformation **2.78a** (Figure 2.24), the σ* C-O antibonding orbital is inaccessible to incoming nucleophiles. Rotation of the C-O bond to give conformer **2.78b** does result in an accessible σ* orbital, however, the steric clash of the axial fluorine atoms with the mesylate group is likely to result in a high barrier to conformation **2.78b**. Likewise, the ring flip isomers **2.78c** and **2.78d** also have an inaccessible σ* orbital and steric clash respectively, so this system is inherently unreactive.

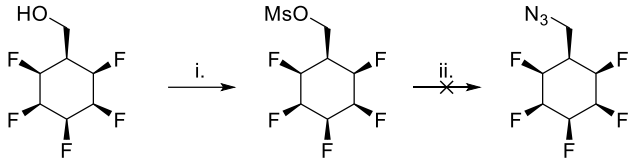

2.47 **2.78** **2.79**

Scheme 2.26 Attempted derivatisation of alcohol **2.47**; i. MsCl, Et_3N, CH_2Cl_2, 0 °C to r.t., 16 h, quantitative; ii. NaN_3, DMF, 70 °C, 14 h.[52,53]

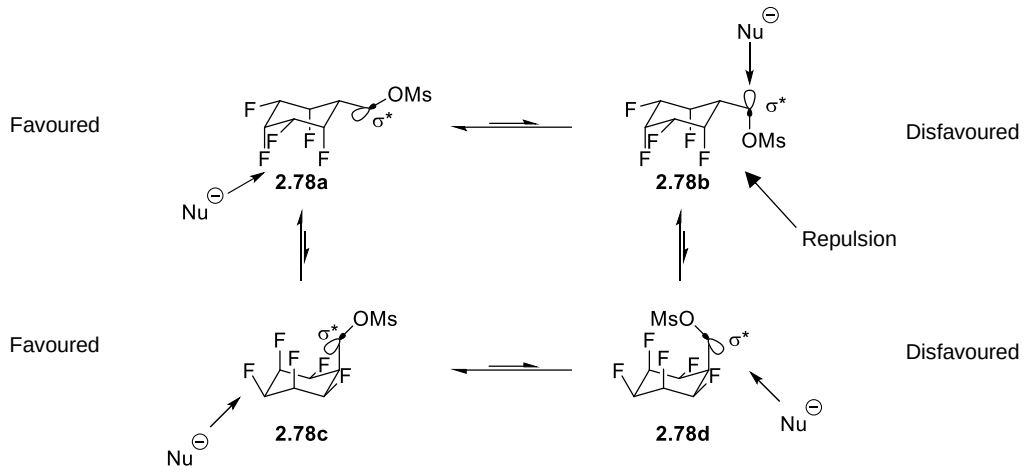

Figure 2.24 Conformers of **2.78** highlighting the challenge for an S_N2 reaction.

An alternative route to an amine building block was envisioned from methyl ester **2.60** (Scheme 2.27). Reduction of this ester would generate alcohol **2.81** and then an Appel reaction of the alcohol would give alkyl bromide **2.82**. This would enable nucleophilic substitution with sodium azide to generate organoazide **2.83**, opening up the possibility of a reduction to give the desired amine **2.84**.

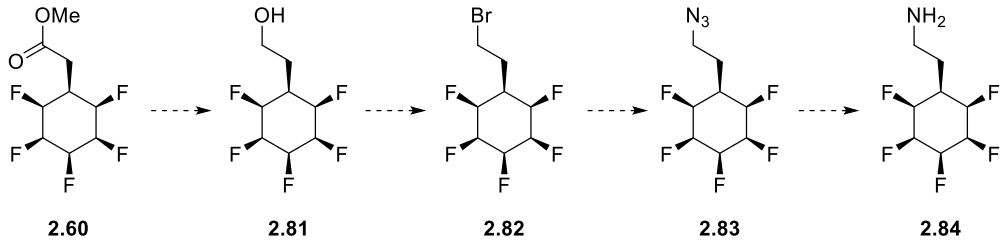

Scheme 2.27 Proposed route to amine **2.84**.

The hydrogenation (Scheme 2.18) proved amenable to scale-up and therefore **2.60** was readily accessible on a gram scale. The synthesis to the desired amine **2.84** began with the reduction of methyl ester **2.60** to primary alcohol **2.81** (Scheme 2.28) with DIBAlH (0 °C to r.t.). This method was found to be more selective than when more reactive hydride reagents such as $LiAlH_4$ were used due to the suppression of competing elimination reactions.[54] With alcohol **2.81** in hand, an Appel reaction was carried out to generate alkyl bromide **2.82** in high yield.[55] Nucleophilic substitution with sodium azide proved to be highly efficient and generated alkyl azide **2.83** also in good yield.[56] Finally, a Staudinger reaction of **2.83** gave the primary amine **2.84** in a very good conversion.[53]

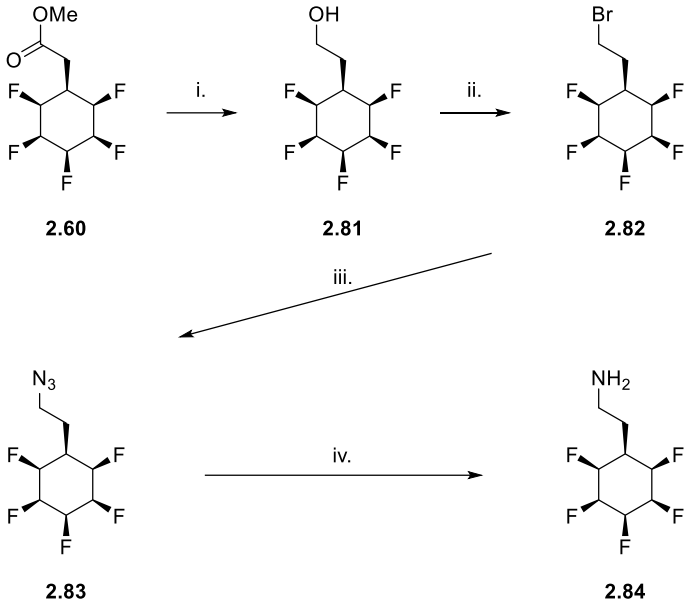

2.60 **2.81** **2.82** **2.83** **2.84**

Scheme 2.28 Route to amine **2.84**; i. DIBAlH 1M, THF, 0 °C to r.t., 16 h, 83%; ii. CBr_4, PPh_3, MeCN, r.t., 16 h, 84% iii. NaN_3, DMF, 70 °C, 6h, quantitative; iv. PPh_3, THF, r.t., 2 h, 64%.[53–56]

Alkyl azide **2.83** was a white crystalline solid material and its X-ray structure shows that the dominant conformer in the solid state is again the triaxial C-F conformer (Figure 2.25B). Close contacts of 2.36 Å-2.47 Å (Sum of the VdW radii = 2.67 Å) between alternate faces of the ring are also present due to electrostatic attraction. The azide group of **2.83** has two zwitterionic resonance forms **2.83a** and **2.83b** (Figure 2.25A). The resonance form **2.83a** confers a partial negative charge to the terminal nitrogen. An intermolecular interaction between the terminal nitrogen of **2.83** and the equatorial 4-H ring hydrogen is evident in a symmetrical tetrameric arrangement in the structure of **2.83** (Figure 2.25B) by the presence of short contacts of 2.60 and 2.63 Å (Sum of the VdW radii = 2.75 Å).

A.

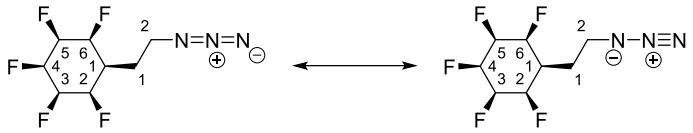

2.83a **2.83b**

B.

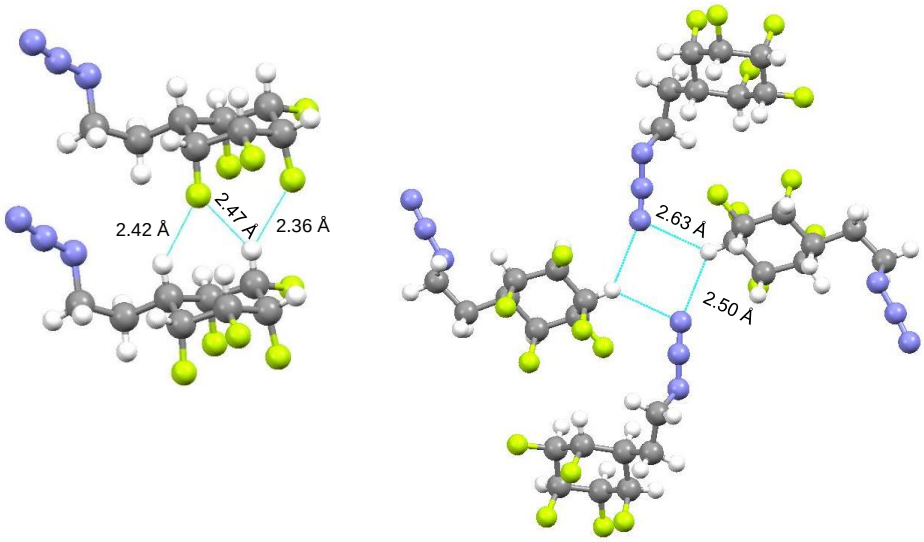

Figure 2.25 A. Resonance forms of organoazide **2.83**; **B**. X-ray crystal structure of **2.83** with short contacts shown in blue.

The hydrochloride salt **2.85** of amine **2.84** was formed by protonation with aqueous HCl (Scheme 2.29). The X-ray crystal structure of **2.85** (Figure 2.26) showed that the dominant conformer in the solid state is the triaxial C-F conformer, with an equatorial alkyl substituent. The X-ray crystal structure show a hydrated ammonium chloride complex but there are no attractive interactions between the cation and the electronegative fluorine atoms. The strong charge-charge electrostatic attraction between the ammonium cation and the chloride anion outcompetes any weaker charge-dipole interactions between the fluorine atoms and the ammonium cation. Attractive interactions were again evident from the short intermolecular contacts between the fluorine and hydrogen atoms (2.36 Å-2.56 Å) of opposite ring faces (Sum of the VdW radii = 2.67 Å).

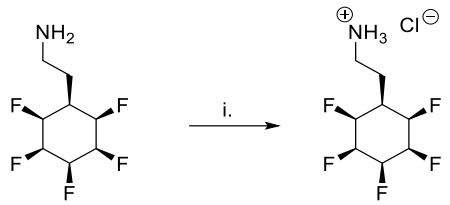

2.84 **2.85**

Scheme 2.29 Preparation of ammonium chloride salt **2.85**; i. HCl (1M), THF, 5 min, quant..

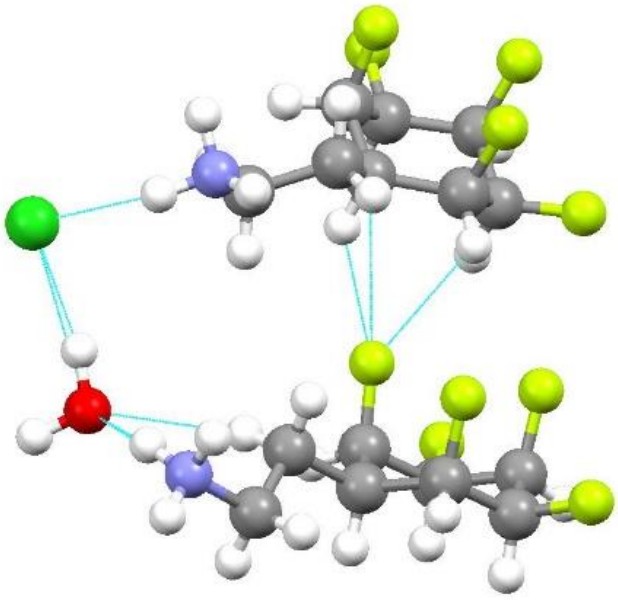

Figure 2.26 X-ray crystal structure of **2.85** with short contacts in blue.

The next synthetic target to be explored was aldehyde **2.87**. The partial reduction of methyl ester **2.60** was attempted at −78 °C using DIBAlH (Scheme 2.30).[57] After 1 hour the reaction mixture was found to contain starting material and alcohol **2.81** but a negligible amount of aldehyde **2.87**. The desired selective reduction of an ester **2.60** to aldehyde **2.87** should proceed via the trapping of **2.86** or a related intermediate consistent with low temperature DIBAlH reductions (Scheme 2.30). The formation of alcohol **2.87** suggests that the tetrahedral intermediate **2.86** is not stable under these conditions and collapses to form aldehyde **2.87** which undergoes further reduction to alcohol **2.81**.

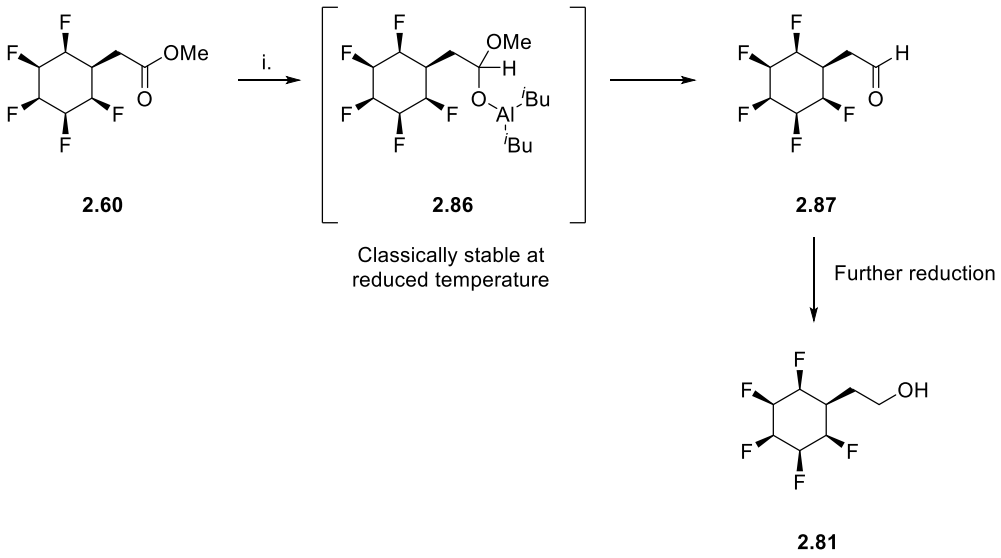

Scheme 2.30 Over-reduction of ester **2.60** to give alcohol **2.81**; i. DIBAlH (1M), THF, −78 °C, 1 h.[57]

However, conversion of ester **2.60** to aldehyde **2.87** was successfully achieved in two steps by reduction to primary alcohol **2.81** and then a Dess-Martin periodinane oxidation at room temperature (Scheme 2.31).[58]

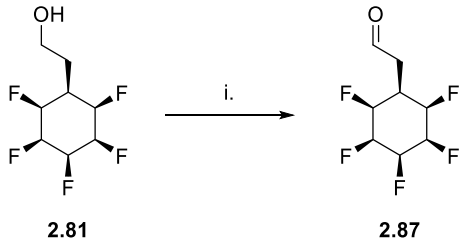

Scheme 2.31 Oxidation of alcohol **2.81** to aldehyde **2.87**; i. Dess-Martin periodinane, THF, r.t., 45 mins, 85%.[58]

Aldehyde **2.87** exists in its expected keto form **2.87a** in [$^2H_6$]-acetone as assigned by its peak at 9.85 ppm consistent with the aldehydic proton (Figure 2.27). In contrast, the ^{1}H NMR spectrum in [$^2H_4$]-methanol (Figure 2.28) shows only a negligible aldehydic peak. The assignment of the ^{1}H NMR spectrum in [$^2H_4$]-methanol was performed by examination of coupling constants and 2D NMR (^{1}H-^{1}H COSY, ^{1}H-^{13}C HSQC and ^{1}H-^{13}C HMBC) which are illustrated in Figure 2.29 and are consistent with the dominance of the hemiacetal form **2.87b**.

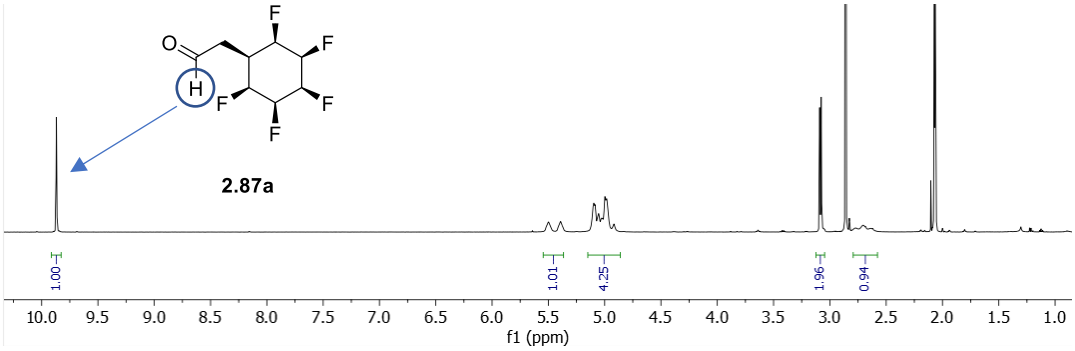

Figure 2.27 ^{1}H NMR spectrum of **2.87** in [$^{2}H_6$]-acetone.

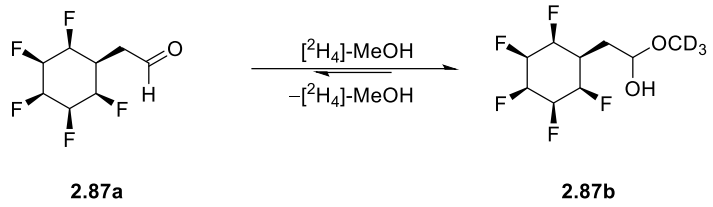

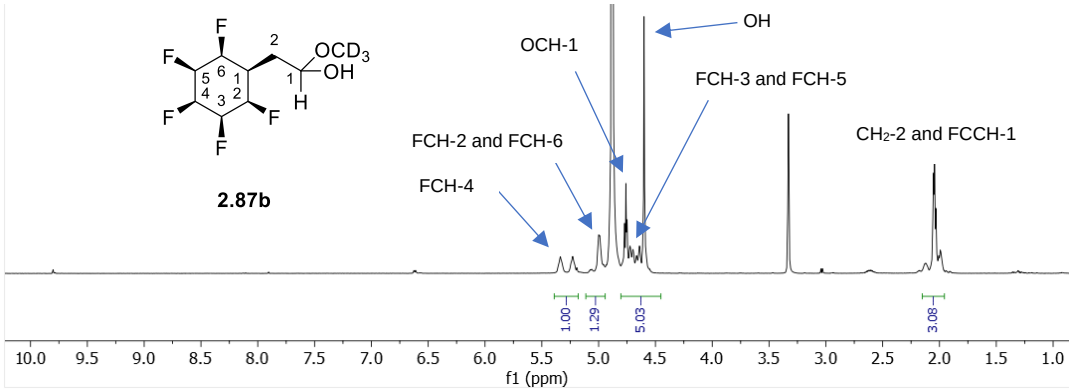

Figure 2.28 ^{1}H NMR spectrum of **2.87** in [$^{2}H_4$]-methanol illustrating the dominance of the hemiacetal form **2.87b**.

^{1}H-^{1}H COSY:

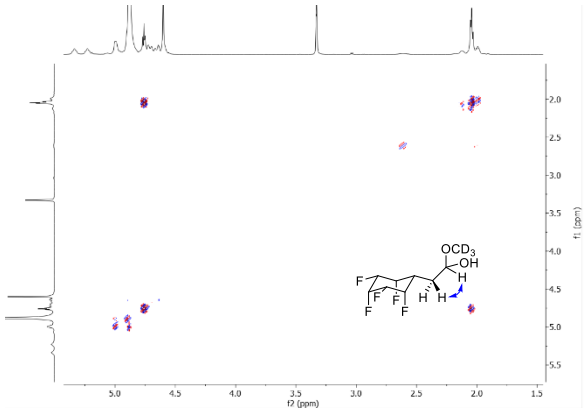

^{1}H-^{13}C HSQC:

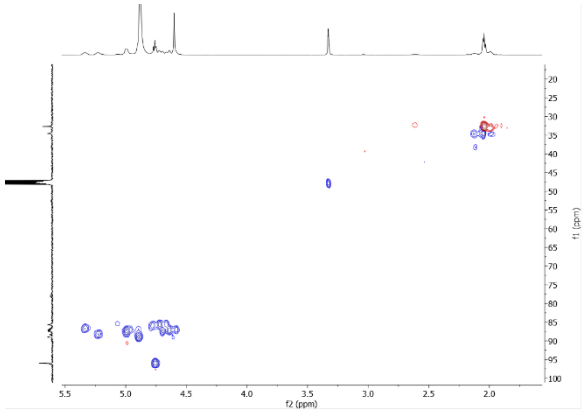

^{1}H-^{13}C HMBC:

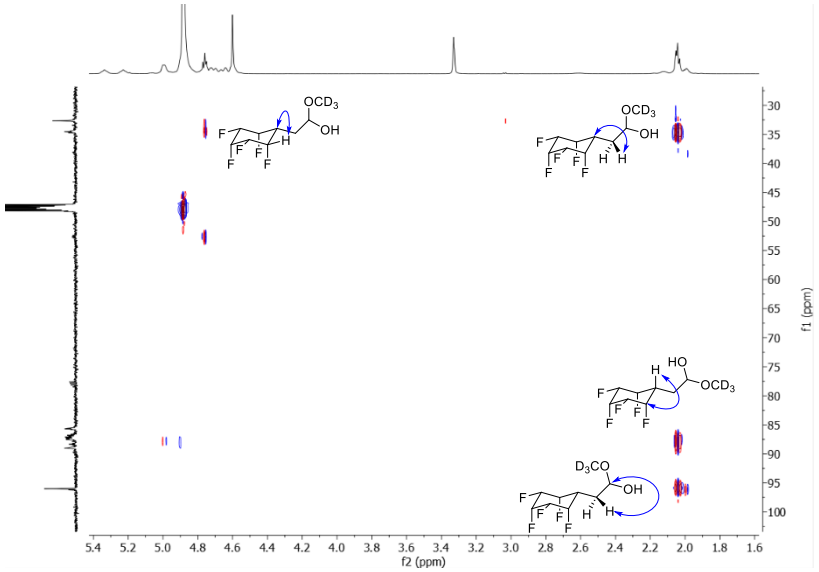

Figure 2.29 2D NMR of **2.87** in [$^{2}H_4$]-methanol indicating dominance of the hemiacetal form **2.87b**.

2.7. Conclusions

The functional group tolerance of the Rh-catalysed hydrogenation has limitations. In this work, hydrogenation of fluoroarenes was not successful for substrates bearing alkyl chloride (**2.37**), alcohol (**2.38**), nitrile (**2.39**), or carboxylic acid (**2.40**) substituents. The functional group tolerance of silyl ethers and methyl esters as reported by Glorius was reproducible and applicable to the hydrogenation of pentafluoroarenes (as for the hydrogenation of **2.44** and **2.59**) but the hydrogenation of *tert*-butyl carbamates proved elusive, such as in the case of **2.48**.[28] Homologation of alkyl substituents proved to be a successful strategy to improve fluoroarene hydrogenation reactions, as summarised in Figure 2.21. The homologation of products also improved their synthetic utility; while mesylate **2.78** was inert to nucleophilic substitution, homologated bromide **2.82** was successfully converted to organoazide **2.83** in quantitative yield.

Synthetic challenges arising from the base-sensitivity of these 'Janus' rings have been observed. Compatibility of the 'Janus' rings with a range of bases was determined (Table 2.1) and this will inform future synthetic manipulation of related compounds. The strong polarisation of 'Janus' rings results in intermolecular attraction between alternate ring faces. This is repeatedly observed by the short contacts between ring fluorines and hydrogens in the X-ray crystal structures. An interaction was observed in the X-ray crystal structure of azide **2.83** (Figure 2.25) between the terminal nitrogen atom and an electropositive ring hydrogen. The electron-withdrawing nature of the 'Janus' ring is evident from the preferred stabilisation of the hemiacetal (**2.87b**) of aldehyde **2.87** in [$^2H_4$]-MeOH.

The elaboration of building blocks prepared in this Chapter form the focus of Chapter 3. First, amide coupling of carboxylic acid **2.58** to protected amino acids is explored. Multicomponent Ugi and Passerini reactions are explored using **2.58** and aldehyde **2.87** to generate a library of peptidic compounds. The experimental determination of the Log P of Ugi products investigates the relevance of the 'Janus' ring moiety to medicinal chemistry. A reductive amination procedure with aldehyde **2.87** is established and the use of **2.87** is also investigated in Wittig reactions. Nucleophilic substitution with the alkyl bromide **2.82** and copper-catalysed alkyne-azide cycloaddition (CuAAC) 'click' reactions with the organoazide **2.83** further show synthetic versatility and provide access to compounds for future study as linkers for metal-organic-frameworks (MOFs) and for supramolecular assembly.

2.8. References

[1] P. Sabatier, J. B. Senderens, *Comptes rendus l'Académie des Sci.* **1901**, *132*, 210.

[2] A. Stanislaus, H. C. Barry, *Catal. Rev.* **1994**, *36*, 75–123.

[3] S. C. Qi, X. Y. Wei, Z. M. Zong, Y. K. Wang, *RSC Adv.* **2013**, *3*, 14219–14232.

[4] P. J. Dyson, *Dalt. Trans.* **2003**, 2964–2974.

[5] H. U. Blaser, C. Malan, B. Pugin, F. Spindler, H. Steiner, M. Studer, *Adv. Synth. Catal.* **2003**, *345*, 103–151.

[6] K. S. Weddle, J. D. Aiken, R. G. Finke, *J. Am. Chem. Soc.* **1998**, *120*, 5653–5666.

[7] J. A. Widegren, R. G. Finke, *J. Mol. Catal. A Chem.* **2003**, *198*, 317–341.

[8] A. A. Philippov, A. M. Chibiryaev, O. N. Martyanov, *Catal. Today* **2020**, DOI 10.1016/j.cattod.2020.06.060.

[9] I. S. Mashkovsky, G. N. Baeva, A. Y. Stakheev, T. V. Voskoboynikov, P. T. Barger, *Mendeleev Commun.* **2009**, *19*, 108–109.

[10] F. Coloma, A. Sepúlveda-Escribano, F. Rodríguez-Reinoso, *J. Catal.* **1995**, *154*, 299–305.

[11] A. Sánchez, M. Fang, A. Ahmed, R. A. Sánchez-Delgado, *Appl. Catal. A Gen.* **2014**, *477*, 117–124.

[12] M. Fang, R. A. Sánchez-Delgado, *J. Catal.* **2014**, *311*, 357–368.

[13] B. L. Tran, J. L. Fulton, J. C. Linehan, J. A. Lercher, R. M. Bullock, *ACS Catal.* **2018**, *8*, 8441–8449.

[14] G. Haufe, S. Pietz, D. Wölker, R. Fröhlich, *European J. Org. Chem.* **2003**, 2166–2175.

[15] R. Baumgartner, K. McNeill, *Environ. Sci. Technol.* **2012**, *46*, 10199–10205.

[16] S. Sabater, J. A. Mata, E. Peris, *Nat. Commun.* **2013**, *4*, 1–7.

[17] S. E. Lyubimov, M. V. Sokolovskaya, A. A. Korlyukov, O. P. Parenago, V. A. Davankov, *J. Iran. Chem. Soc.* **2020**, *17*, 1283–1287.

[18] M. P. Wiesenfeldt, Z. Nairoukh, W. Li, F. Glorius, *Science* **2017**, *357*, 908–912.

[19] J. H. Xie, X. Y. Liu, J. B. Xie, L. X. Wang, Q. L. Zhou, *Angew. Chem. Int. Ed.* **2011**, *50*, 7329–7332.

[20] Y. Wang, J. Zhang, X. Wang, M. Antonietti, H. Li, *Angew. Chem. Int. Ed.* **2010**, *49*, 3356–3359.

[21] H. Liu, T. Jiang, B. Han, S. Liang, Y. Zhou, *Science* **2009**, *326*, 1250–1252.

[22] Y. Wei, B. Rao, X. Cong, X. Zeng, *J. Am. Chem. Soc.* **2015**, *137*, 9250–9253.

[23] V. Lavallo, Y. Canac, C. Präsang, B. Donnadieu, G. Bertrand, *Angew. Chem. Int. Ed.* **2005**, *44*, 5705–9.

[24] M. Soleilhavoup, G. Bertrand, *Acc. Chem. Res.* **2015**, *48*, 256–266.

[25] X. Hu, D. Martin, M. Melaimi, G. Bertrand, *J. Am. Chem. Soc.* **2014**, *136*, 13594–13597.

[26] M. Melaimi, R. Jazzar, M. Soleilhavoup, G. Bertrand, *Angew. Chem. Int. Ed.* **2017**, *56*, 10046–10068.

[27] M. N. Hopkinson, C. Richter, M. Schedler, F. Glorius, *Nature* **2014**, *510*, 485–96.

[28] M. P. Wiesenfeldt, T. Knecht, C. Schlepphorst, F. Glorius, *Angew. Chem. Int. Ed.* **2018**, *57*, 8297–8300.

[29] D. Moock, M. Wiesenfeldt, M. Freitag, S. Muratsugu, S. Ikemoto, R. Knitsch, J. Schneidewind, W. Baumann, A. H. Schäfer, A. Timmer, M. Tada, M. R. Hansen, F. Glorius, *ACS Catal.* **2020**, *10*, 6309–6317

[30] O. Shyshov, K. A. Siewerth, M. Von Delius, *Chem. Commun.* **2018**, *54*, 4353–4355.

[31] O. Shyshov, S. V. Haridas, L. Pesce, H. Qi, A. Gardin, D. Bochicchio, U. Kaiser, G. M. Pavan, M. Von Delius, *Nat. Commun.* **2021**, DOI 10.1038/s41467-021-23370-y.

[32] J. Clark, D. O'Hagan, S. Guldin, A. Slawin, D. B. Cordes, C. Yu, R. A. Cormanich, R. Neyyappadath, A. Geddis, A. Taylor, B. A. Piscelli, *Chem. Sci.* **2021**, *12*, 9712-9719.

[33] Y. Wei, B. Rao, X. Cong, X. Zeng, *J. Am. Chem. Soc.* **2015**, *137*, 9250–9253.

[34] R. A. Cormanich, R. Rittner, D. O'Hagan, M. Bühl, *J. Phys. Chem. A* **2014**, *118*, 7901–7910.

[35] B. D. Dond, S. N. Thore, *Tetrahedron Lett.* **2020**, *61*, 151660.

[36] J. Guo, W. Li, W. Xue, X. S. Ye, *J. Med. Chem.* **2017**, *60*, 2135–2141.

[37] P. Ryberg, O. Matsson, *J. Am. Chem. Soc.* **2001**, *123*, 2712–2718.

[38] J. H. Cho, F. Amblard, S. J. Coats, R. F. Schinazi, *Tetrahedron* **2011**, *67*, 5487–5493.

[39] S. Caddick, D. B. Judd, A. K. d. K. Lewis, M. T. Reich, M. R. Williams, *Tetrahedron* **2003**, *59*, 5417–5423.

[40] S. Caddick, A. K. Alexandra, D. B. Judd, M. R. V. Williams, *Tetrahedron Lett.* **2000**, *41*, 3513–3516.

[41] K. N. Fanning, A. Sutherland, *Tetrahedron Lett.* **2007**, *48*, 8479–8481.

[42] T. Bykova, N. Al-Maharik, A. M. Z. Slawin, D. O'Hagan, *Org. Biomol. Chem.* **2016**, *14*, 1117–1123.

[43] M. Pour, M. Špulák, V. Balšánek, J. Kuneš, P. Kubanová, V. Buchta, *Bioorg. Med. Chem.* **2003**, *11*, 2843–2866.

[44] D. P. Walker, D. G. Wishka, D. W. Piotrowski, S. Jia, S. C. Reitz, K. M. Yates, J. K. Myers, T. N. Vetman, B. J. Margolis, E. J. Jacobsen, B. A. Acker, V. E. Groppi, M. L. Wolfe, B. A. Thornburgh, P. M. Tinholt, L. A. Cortes-Burgos, R. R. Walters, M. R. Hester, E. P. Seest, L. A. Dolak, F. Han, B. A. Olson, L. Fitzgerald, B. A. Staton, T. J.

Raub, M. Hajos, W. E. Hoffmann, K. S. Li, N. R. Higdon, T. M. Wall, R. S. Hurst, E. H. F. Wong, B. N. Rogers, *Bioorg. Med. Chem.* **2006**, *14*, 8219–8248.

[45] S. S. Babu, V. K. Praveen, S. Prasanthkumar, A. Ajayaghosh, *Chem. Eur. J.* **2008**, *14*, 9577–9584.

[46] L. M. V. Tillekeratne, A. Sherette, J. A. Fulmer, L. Hupe, D. Hupe, S. Gabbara, J. A. Peliska, R. A. Hudson, *Bioorg. Med. Chem. Lett.* **2002**, *12*, 525–528.

[47] A. K. Chatterjee, T. L. Choi, D. P. Sanders, R. H. Grubbs, *J. Am. Chem. Soc.* **2003**, *125*, 11360–11370.

[48] E. G. Gioti, T. V. Koftis, E. Neokosmidis, E. Vastardi, S. S. Kotoulas, S. Trakossas, T. Tsatsas, E. E. Anagnostaki, T. D. Panagiotidis, C. Zacharis, E. P. Tolika, A. A. Varvogli, T. Andreou, J. K. Gallos, *Tetrahedron* **2018**, *74*, 519–527.

[49] W. M. Haynes, D. R. Lide, T. J. Bruno, *CRC Handbook of Chemistry and Physics*, Taylor & Francis Group, Boca Raton, **2017**.

[50] D. Gimenez, A. Dose, N. L. Robson, G. Sandford, S. L. Cobb, C. R. Coxon, *Org. Biomol. Chem.* **2017**, *15*, 4081–4085.

[51] S. Tabassum, O. Sereda, P. V. G. Reddy, R. Wilhelm, *Org. Biomol. Chem.* **2009**, *7*, 4009–4016.

[52] P. Gilles, R. S. Kashyap, M. J. Freitas, S. Ceusters, K. Van Asch, A. Janssens, S. De Jonghe, L. Persoons, M. Cobbaut, D. Daelemans, J. Van Lint, A. R. D. Voet, W. M. De Borggraeve, *Eur. J. Med. Chem.* **2020**, *205*, 1–10.

[53] J. X. Qiao, D. L. Cheney, R. S. Alexander, A. M. Smallwood, S. R. King, K. He, A. R. Rendina, J. M. Luettgen, R. M. Knabb, R. R. Wexler, P. Y. S. Lam, *Bioorg. Med. Chem. Lett.* **2008**, *18*, 4118–4123.

[54] J. Louvel, J. F. S. Carvalho, Z. Yu, M. Soethoudt, E. B. Lenselink, E. Klaasse, J. Brussee, A. P. Ijzerman, *J. Med. Chem.* **2013**, *56*, 9427–9440.

[55] D. Sawada, M. Kanai, M. Shibasaki, *J. Am. Chem. Soc.* **2000**, *122*, 10521–10532.

[56] Z. Xu, X. F. Song, M. Qiang, Z. S. Lv, *J. Heterocycl. Chem.* **2017**, *54*, 3735–3741.

[57] L. I. Zakharkin, I. M. Khorlina, *Tetrahedron Lett.* **1962**, *3*, 619–620.

[58] C. L. Moody, D. S. Pugh, R. J. K. Taylor, *Tetrahedron Lett.* **2011**, *52*, 2511–2514.

3. Strategies for the elaboration of 'Janus' ring building blocks

3.1. Aims of derivatisation

Following the successful expansion of the scope of the Rh-catalysed hydrogenation of fluoroarenes reported by Glorius,[1] and subsequent functional group interconversions leading to diverse building blocks (Figure 3.1), attention turned to elaboration strategies of these building blocks to higher molecular architectures. Such elaborations aim to demonstrate synthetic versatility, generate industrially relevant compounds (such as drug-like molecules) and to further probe the influence of the 'Janus' ring on wider molecular structures and properties.

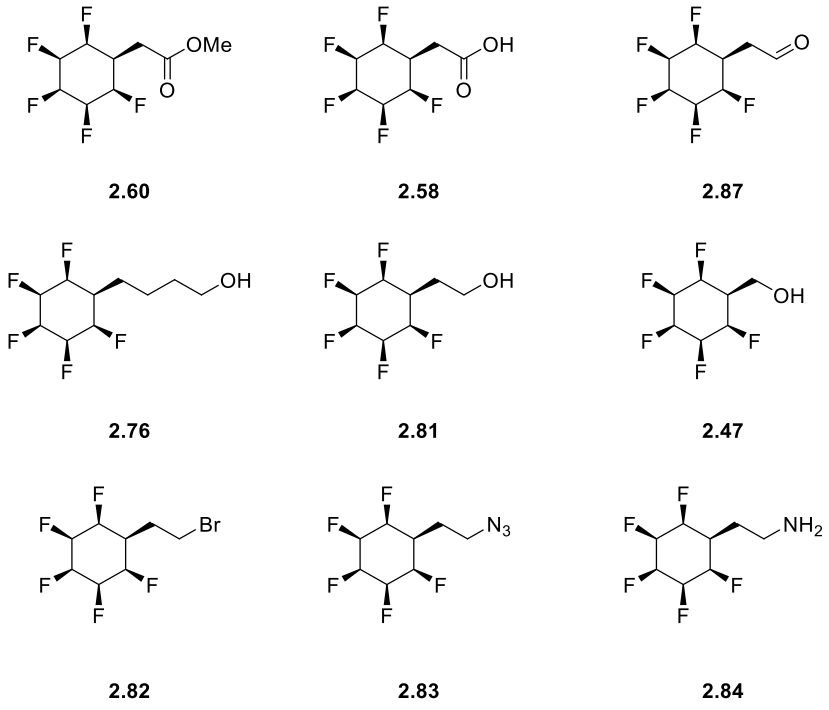

Figure 3.1 Building blocks synthesised in Chapter 2.

3.2. Derivatisation of all-*cis*-pentafluorocyclohexylacetic acid

3.2.1. Amide couplings of 2.58

Carboxylic acid **2.58** presented a versatile building block, particularly for the formation of amides. The coupling of **2.58** to an appropriately protected amino acid was appealing as a route to generate peptidomimetic compounds. If amide coupling proved facile, then higher order peptides could be synthesised and interactions of the 'Janus' ring might be probed. For

example, charge-dipole interactions between the ring substituents and charged amino acid side chains. The proposed general procedure (Scheme 3.1) which was based on previously reported conditions,[2,3] was considered advantageous as the base ($^{i}Pr_2NEt$) had already been shown to be compatible with the base-sensitive 'Janus' rings (Chapter 2, Table 2.1). The mechanism of the peptide coupling reaction with HATU as proposed by Tzakos is illustrated in Scheme 3.2.[4]

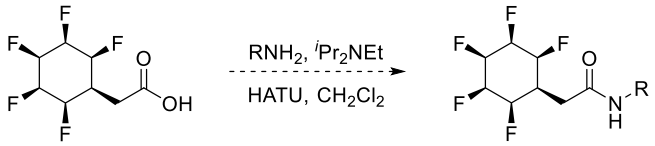

2.58 **3.1**

Scheme 3.1 Proposed synthesis of amides from **2.58**.

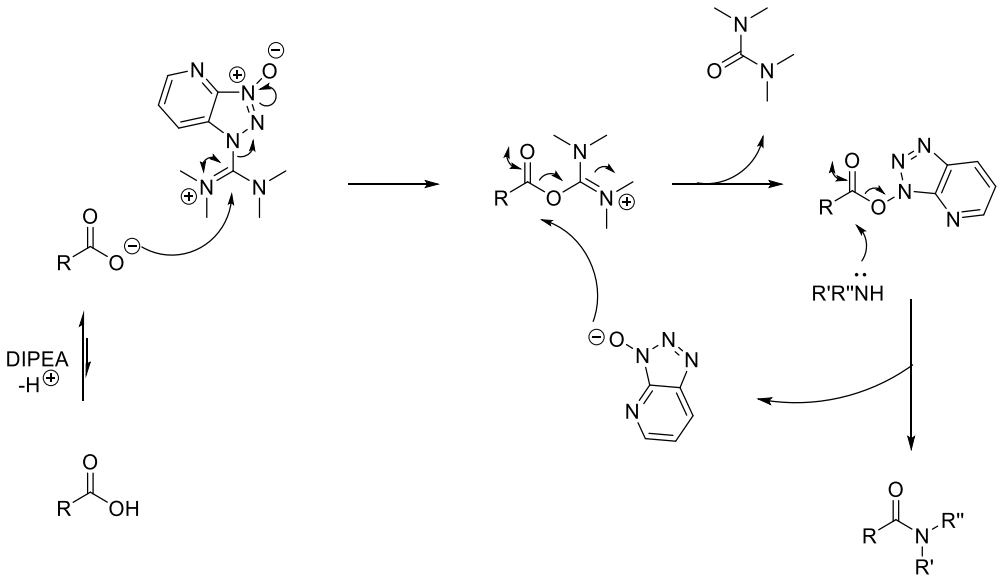

Scheme 3.2 Tzakos' mechanism of peptide coupling with HATU.[4]

In the first instance, amide coupling to an appropriately protected lysine hydrochloride was attempted under standard conditions (Scheme 3.3).[2,3,5] However, the reaction was unsuccessful and only starting material was recovered. Carboxylic acid **2.58** was poorly soluble in the non-polar reaction solvent, CH_2Cl_2. The reaction was explored in the more polar DMF and the product amide **3.2** was isolated albeit in low yield (Scheme 3.3). The low yield is most probably due to the low solubility of **2.58** in DMF which although better than in CH_2Cl_2, was still limited. The poor solubility profile of **2.58** arises because of strong intermolecular interactions between the rings which are apparent from its extremely high melting point of 235 °C. Carboxylic acid **2.58** has an additional H-bond donor which facilitates strong

interactions between two carboxylic acid groups (Figure 3.2A). By comparison, the melting point of the related methyl ester **2.60** is only 151 °C and the solubility of **2.60** was qualitatively better in organic solvents.

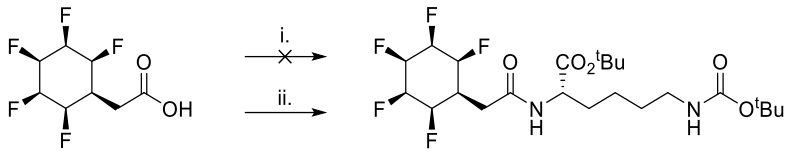

Scheme 3.3 Synthesis of peptide **3.2**; i. H-Lys(Boc)-OtBu.HCl, HATU, $^{i}Pr_2EtN$, CH_2Cl_2, 0 °C to r.t., 16 h; ii. H-Lys(Boc)-OtBu.HCl, HATU, $^{i}Pr_2EtN$, DMF, 0 °C to r.t., 16 h, 20%.[2,3,5]

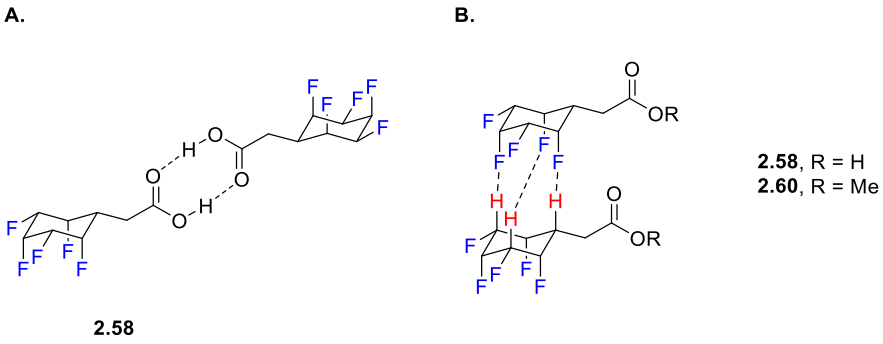

Figure 3.2 A. Intermolecular hydrogen bonding interactions in carboxylic acid **2.58**; **B**. Electrostatic attraction between rings of carboxylic acid **2.58** and methyl ester **2.60**.

The removal of both the N-Boc and O-^{t}Bu groups of **3.2** was achieved using TFA and the fully deprotected amino acid was isolated as its TFA salt **3.3** (Scheme 3.4).

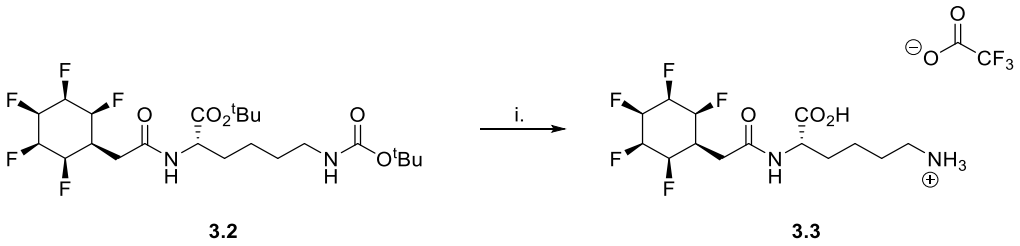

Scheme 3.4 Deprotection of **3.2** to give **3.3**; i. TFA, CH_2Cl_2, r.t., 16 h, 91%.

Using these optimised conditions, the amide coupling was repeated with the protected glutamic acid to give **3.4**, which was also fully deprotected under acidic conditions which in turn gave dicarboxylic acid **3.5** (Scheme 3.5). Similarly, amide coupling with the protected arginine gave **3.6** (Scheme 3.6).

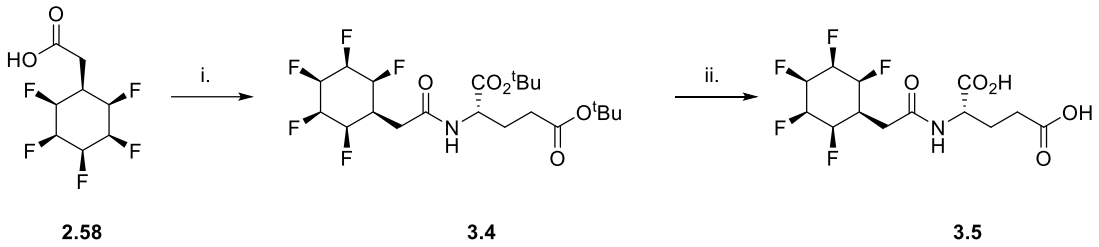

Scheme 3.5 Synthesis of glutamate dipeptide **3.5**; i. H-Glu(OtBu)-O^{t}Bu.HCl, HATU, ^{i}Pr$_2$EtN, DMF, 0 °C to r.t., 16 h; ii. TFA, CH_2Cl_2, r.t., 16 h, 43% over two steps.

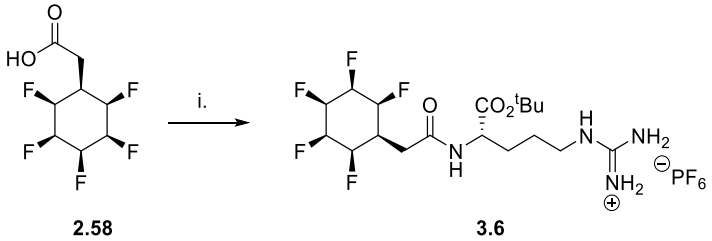

Scheme 3.6 Synthesis of arginine dipeptide **3.6**; i. L-Arginine-*tert*-butyl ester dihydrochloride, HATU, ^{i}Pr$_2$EtN, DMF, 0 °C to r.t., 16 h, 23%.

3.2.2. Isocyanide multicomponent reactions (IMCRs)

Multicomponent reactions (MCRs) have three or more reagents and aim to generate molecular complexity in one-step. Moreover, the modular nature of MCRs allows diverse libraries of compounds to be generated from just a few starting materials. The application of MCRs to combinatorial chemistry now has a long history as it presents an appealing method to access libraries of, 'drug-like' peptidomimetics for bioactivity screening.[6,7] Isocyanide multicomponent reactions (IMCRs) involve the use of a reactive isocyanide component. Isocyanides are unique functional groups which can be considered to exist between a pair of resonance forms, the zwitterionic **3.7a** and the carbene **3.7b** (Scheme 3.7). Isocyanides are unusual, being stable organic compounds with a formally divalent carbon and this provides their unique chemistry. The carbenic nature of isocyanides has long been apparent from their insertion into acyl chlorides as was reported by Nef as far back as 1892 (Scheme 3.7).[8,9]

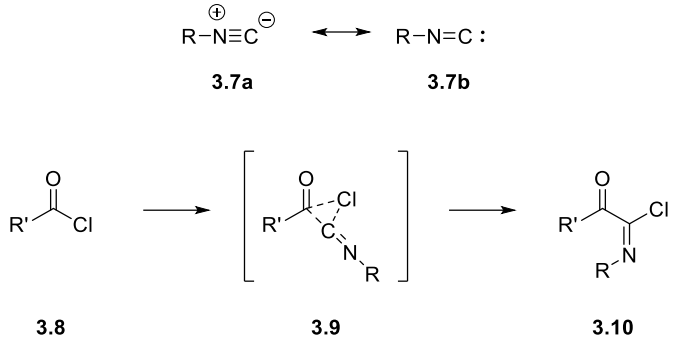

Scheme 3.7 The resonance forms of isocyanides and the Nef reaction.[5]

A curious consequence of the isocyanide electronic structure is that the terminal carbon is both electrophilic and nucleophilic in character; this is observed in the three-component Passerini reaction (Scheme 3.8).[7] By considering a concerted mechanism, the terminal carbon of the isocyanide acts as a nucleophile – attacking the carbonyl of the aldehyde component, and as an electrophile – attacked by the carboxylate oxygen resulting in the unstable α-adduct **3.11** which undergoes acyl transfer and amide tautomerism to give the α-acyloxy amide product **3.12**. The rate of the reaction is first order in each of the components which is consistent with this mechanism.[7]

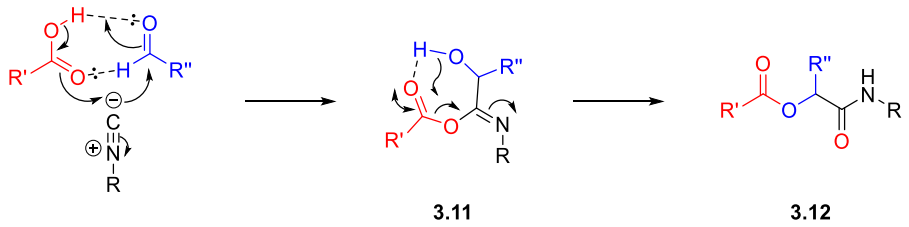

Scheme 3.8 Representation of the concerted mechanism of the three-component Passerini reaction as proposed by Ugi.[7]

α-Acyloxy amide **3.13** could be prepared using carboxylic acid **2.58**, benzaldehyde and *tert*-butyl isocyanide (Scheme 3.9). The concerted mechanism proposed by Ugi (Scheme 3.10),[7] is thought to be favoured at high concentrations, as the rate is dependent on the concentration of all three components. Although **2.58** was reasonably soluble in acetonitrile, at high concentrations it did not form a homogeneous solution and this likely compromised the yield of the reaction.[10] The assigned ^{1}H NMR of **3.13** is illustrated in Figure 3.3.

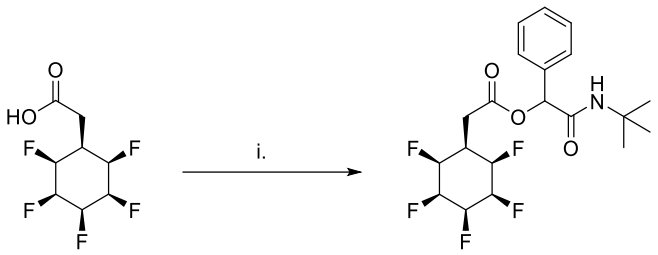

2.58 **3.13**

Scheme 3.9 Passerini reaction to generate α-acyloxy amide **3.13**; i. benzaldehyde, *tert*-butyl isocyanide, acetonitrile 70 °C, 14 h, 44%.[10]

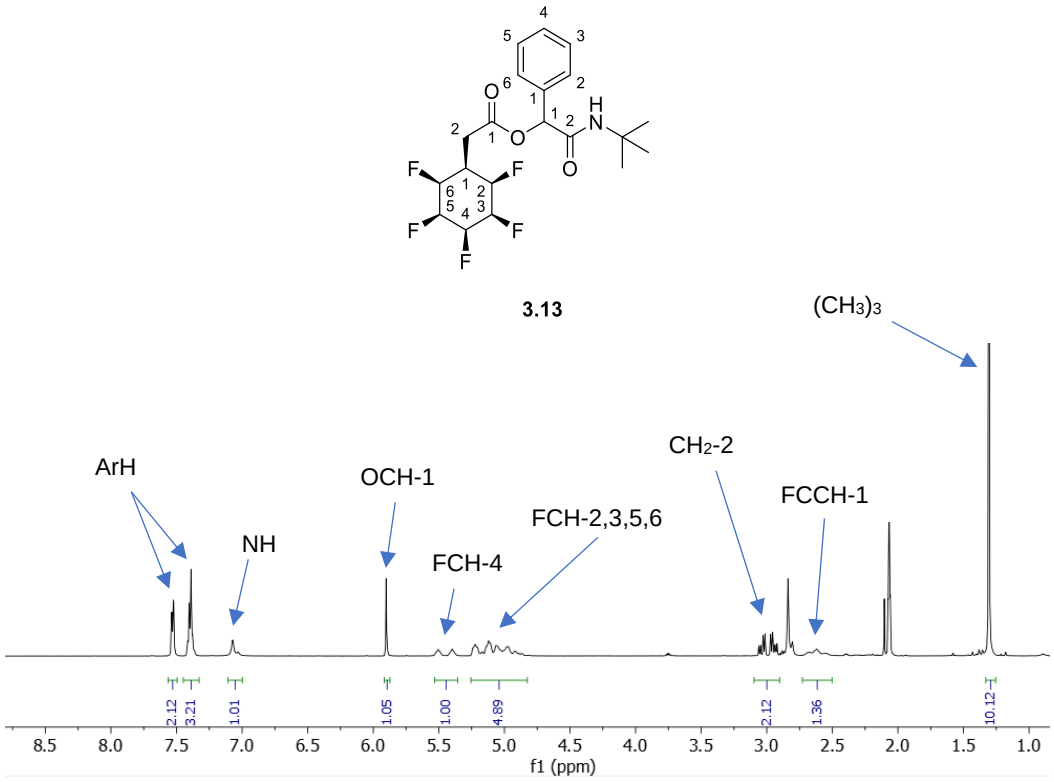

Figure 3.3 ^{1}H NMR of α-acyloxy amide **3.13**.

Given the poor conversion of the Passerini reaction at high concentrations, consideration was given to the reported rate acceleration of Passerini reactions with water (up to 300 fold acceleration) which were carried out in concentrations as low as 0.1 M.[11,12] The rate enhancement arises due to the entropic 'cost' (negative activation volume) in the formation of intermediate **3.11**. The components are non-polar, and the hydrophobic effect drives their aggregation.[7] An alternative and complimentary explanation suggests a change of mechanism to the proposed stepwise/ionic mechanism (Scheme 3.10). Following reversible protonation of the aldehyde by the carboxylic acid, the isocyanide acts as a nucleophile to form a new carbon-carbon bond to generate nitrilium intermediate **3.14**. Attack of the carboxylate to the

nitrilium ion gives a second adduct **3.11** which undergoes acyl transfer to the final product **3.12**.[8]

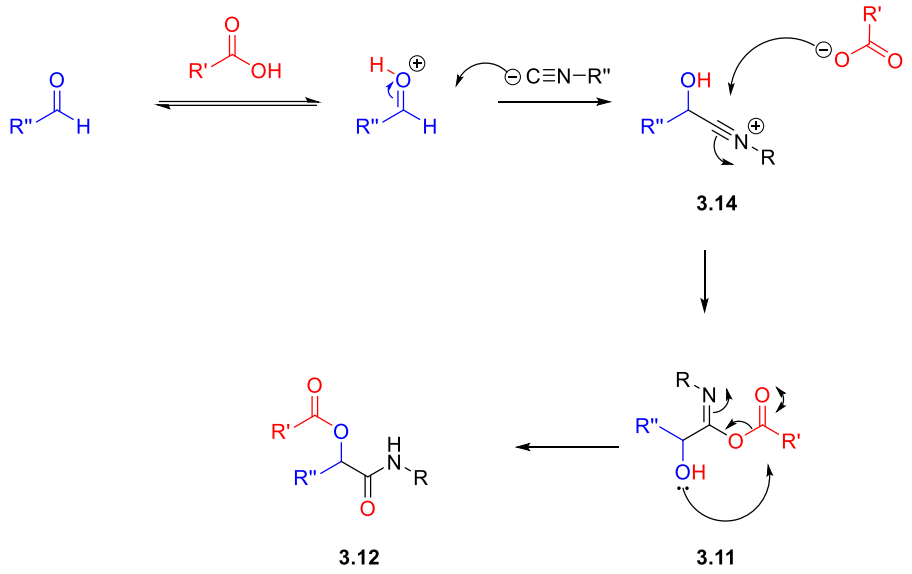

Scheme 3.10 Proposed ionic/stepwise mechanism of Passerini reaction.[8]

Applying the aqueous methodology to the Passerini reaction shown in Scheme 3.11 had mixed results. Firstly, in water alone, the carboxylic acid **2.58** was completely insoluble and there was no reaction (Step i., Scheme 3.11). Although low solubility was expected, heterogeneity is considered necessary to the aqueous rate-enhancement effect because it promotes the hydrophobic effect which drives the aggregation of components. Evidently, some solubility is required for reaction, therefore when the reaction was conducted with methanol as a cosolvent in a ratio of 5:1 water:methanol (Step ii., Scheme 3.11), then the reaction did proceed reasonably well.[11,12]

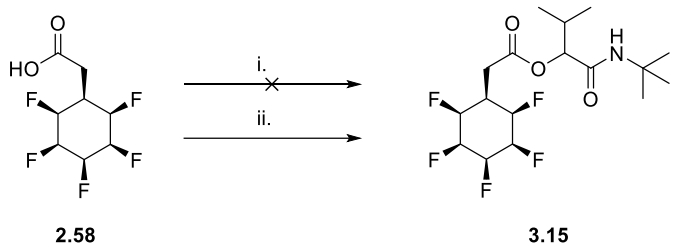

Scheme 3.11 Aqueous Passerini reaction to form α-acyloxy amide **3.15**; i. Isobutyraldehyde, *tert*-butyl isocyanide, water, no reaction; ii. isobutyraldehyde, *tert*-butyl isocyanide, 5:1 water, MeOH, 16 h, 52%.[11,12]

The Ugi multicomponent reaction (Ugi-MCR), which was reported by Ivar Ugi in 1959, consists of four components. These are a carboxylic acid, a primary amine, an aldehyde or ketone and an isocyanide.[13,14] The Ugi reaction is illustrated Scheme 3.12 proceeds through multiple

steps. Even after decades the subtleties of the mechanism remain the subject of debate with recent publications challenging the classically proposed mechanism.[15,16] It is generally agreed that the process starts with the formation of an imine by condensation of the amine and an aldehyde/ketone. Protonation by the carboxylic acid generates an iminium ion which reacts with the other components in the disputed pathway to give an imidate. The classically proposed mechanism for conversion of the iminium ion to the imidate (Scheme 3.12B) proceeds by nucleophilic attack through the terminal isocyanide carbon to give the nitrilium ion which is trapped by the carboxylate anion to generate the imidate.[7] Recent studies using theory calculations have resulted in the proposal of an alternative mechanism for the conversion of the iminium ion to the imidate (Scheme 3.12C).[15] This proceeds by the formation of a hemiaminal intermediate to which the isocyanide undergoes insertion to give the imidate. The alternative pathway (Scheme 3.12C) remains a working hypothesis as the existence of the hemiaminal intermediate has not been shown despite attempts to identify intermediates using mass spectrometry.[16,17] The final step of both mechanisms involves the Mumm rearrangement of the imidate to give the α-aminoacyl amide product.[7,15]

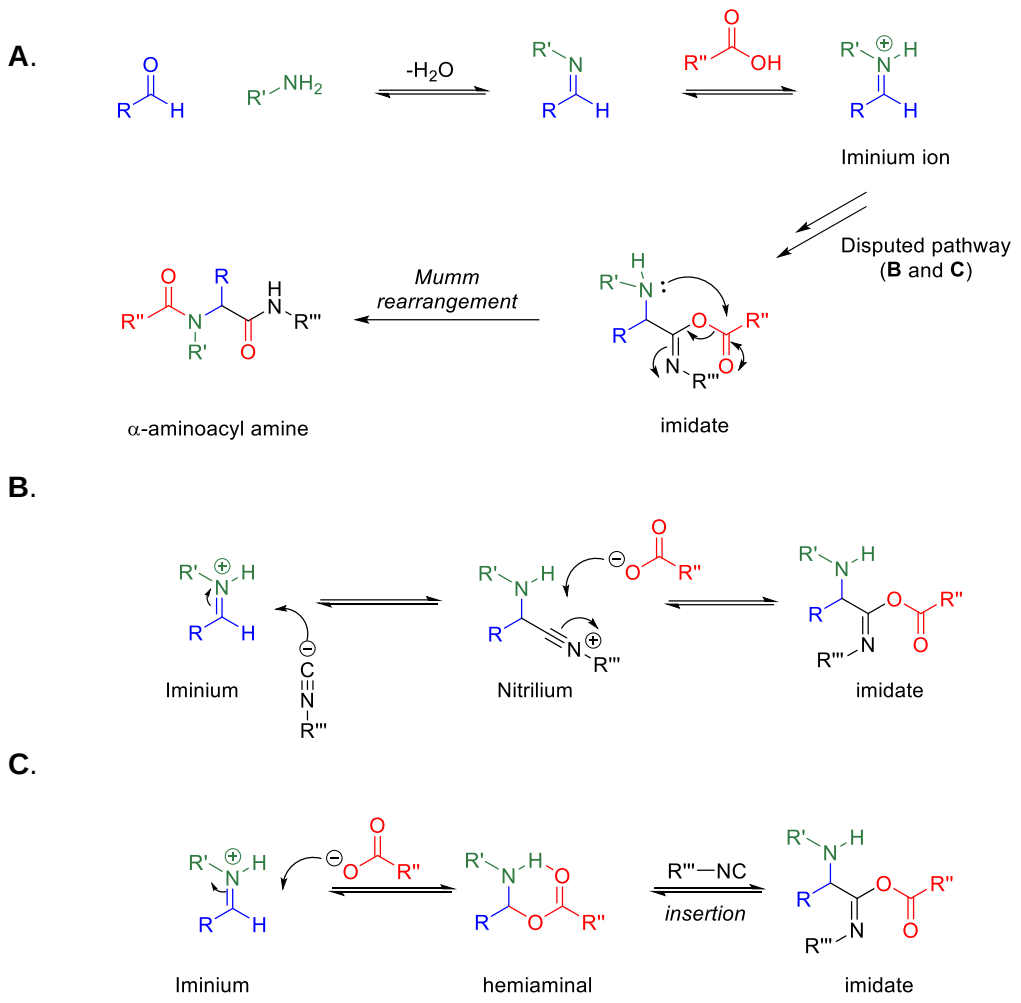

Scheme 3.12 A. Agreed mechanistic steps of the Ugi MCR; **B**. Classically proposed mechanism proceeding through a nitrilium intermediate; **C**. Recently reported hemiaminal pathway.[15,16]

At the outset, the Ugi reaction was carried out in two steps (Scheme 3.13). Firstly, allylamine and 4-fluorobenzaldehyde were combined in a solution of dichloromethane to form imine **3.16**. As imine formation proceeds with the loss of water, anhydrous $MgSO_4$ was added to the reaction mixture to move the equilibrium in favour of product **3.16**. It was considered prudent to pre-form the imine as this has been reported to improve the yield of the reaction.[7] Furthermore, driving the imine condensation disfavours the undesired generation of Passerini products which have been observed under similar reaction conditions.[18] The formation of the imine was monitored by TLC and ^{1}H NMR, and in particular the disappearance of the aldehyde peak at 9.96 ppm was indicative. After complete condensation had occurred, then *tert*-butyl isocyanide and carboxylic acid **2.58** were added. This second step was performed in methanol as **2.58** had already proved poorly soluble in CH_2Cl_2. The desired product **3.17** was isolated in low yield, however no undesired Passerini product was detected. The challenge of obtaining a homogeneous solution of **2.58** even in methanol required high dilution (concentration = 0.1 M) which is known to disfavour Ugi reactions.

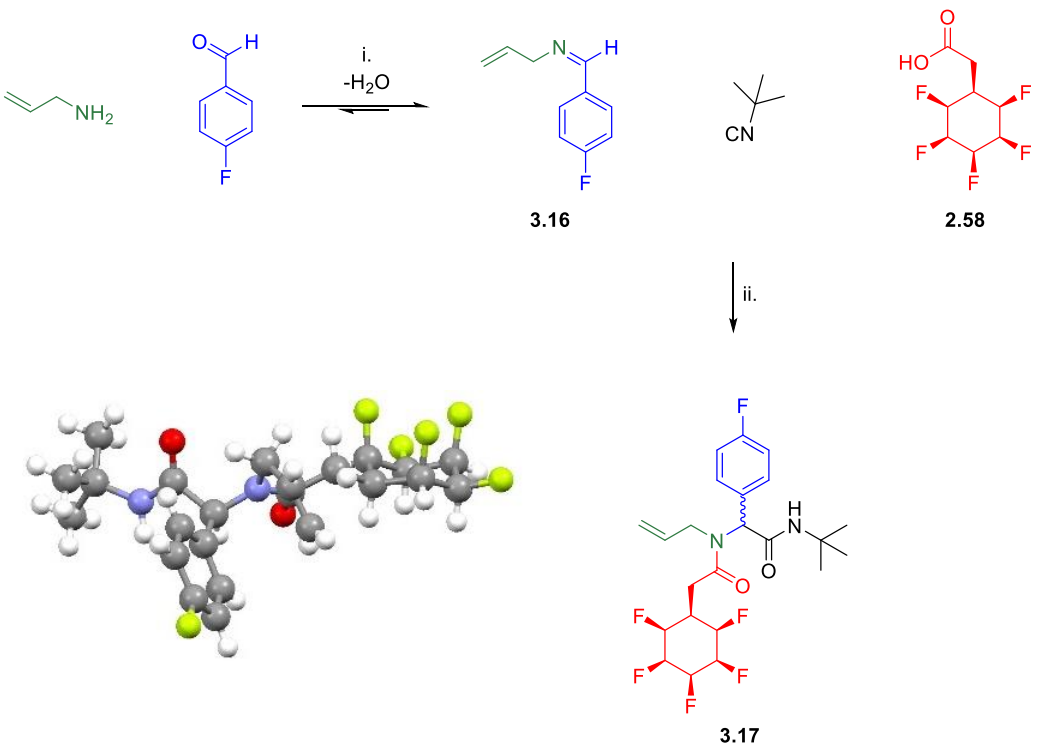

Scheme 3.13 Ugi reaction to produce *bis*-amide **3.17**; i. $MgSO_4$, CH_2Cl_2; ii. MeOH, r.t., 14 h, 20%.

In order to improve the Ugi reaction and to generate products with the all-*cis*-pentafluorocyclohexyl motif, other components bearing the all-*cis*-pentafluorocyclohexane ring were considered for reaction, in place of carboxylic acid **2.58**. Particular consideration was given to the use of aldehyde building block **2.87**. The aldehyde **2.87** had already demonstrated a good solubility profile in polar solvents such as MeOH. However, concerns were raised about its suitability as a component for the Ugi reaction in MeOH as it exists in an equilibrium dominated by the hemiacetal form **2.87b** (Figure 2.28). Therefore, in the first instance, CH_2Cl_2 was used as the reaction solvent. Although **2.87** was poorly soluble in CH_2Cl_2, complete conversion to imine **3.18** could be observed in ^{1}H NMR after stirring for 16 h (Scheme 3.14).

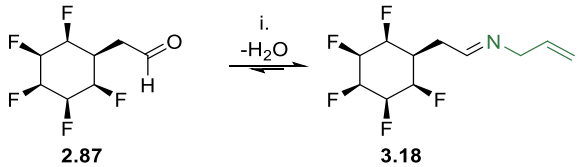

Scheme 3.14 Reaction of aldehyde **2.87** to form imine **3.18**; i. allylamine, $MgSO_4$, CH_2Cl_2, r.t., 16 h.

A general Ugi procedure was developed (Scheme 3.15) and used to generate a small library of peptidomimetics from aldehyde **2.87**. Product yields ranged from fair to good and the lowest

yielding reaction (to give **3.23**, Table 3.1) was optimised by changing the solvent from CH_2Cl_2 to MeOH resulting in an increase from 18% to 60% yield. The presence of hemiacetal **2.87b** did not significantly hinder imine formation.

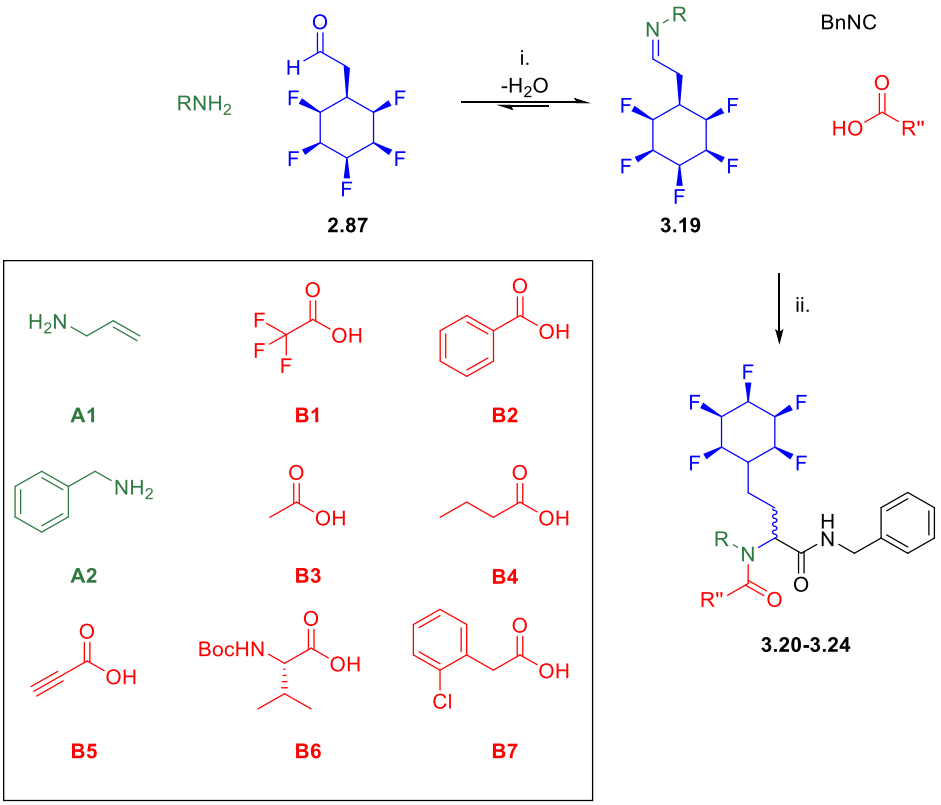

Scheme 3.15 General Ugi reaction; i. $MgSO_4$, 16 h; ii. $MgSO_4$, 16 h.

Product	RNH_2	RCO_2H	Solvent	Temperature	Yield
3.20	A1	B2	CH_2Cl_2	r.t.	85%
3.21	A1	B4	CH_2Cl_2	r.t.	43%
3.22	A2	B5	CH_2Cl_2	r.t.	67%
3.23	A1	B3	CH_2Cl_2	r.t.	18%
3.23	A1	B3	MeOH	r.t.	60%
3.24	A1	B1	MeOH	50 °C	24%

Table 3.1 Conditions used to generate Ugi products **3.20**-**3.24**.

In order to optimise the Ugi reaction, consideration was given to the multiple literature reports suggesting that microwave-assistance facilitates the reaction.[19–23] Microwave heating is often more efficient than conventional methods of heating. When a solvent with a significant dipole moment is used, heating is transferred due to the alignment of the dipoles to the applied oscillating electric field. The ability of a solvent to transfer microwave energy into heat is quantified by the loss tangent, $\tan\delta = \frac{\varepsilon''}{\varepsilon'}$,where ε'' is the dielectric loss constant (the

efficiency with which microwave energy is transferred as heat) and ε′ is the dielectric constant which quantifies the polarizability of the solvent in an electric field. Loss tangents of some are summarised in Table 3.2.

Solvent	ε'	tan δ
Ethylene glycol	41.4	1.350
Methanol	33.0	0.659
DMF	38.3	0.161
Dichloromethane	8.93	0.042
Hexane	1.89	0.020

Table 3.2 The loss tangent (tan δ) at 2.45 GHz for given solvents.[24,25]

Methanol was chosen for its high tan δ as the reaction solvent in test reactions. The Ugi product **3.24** was obtained by conventional heating in 24% yield in 17 h (Table 3.1). However, under microwave-assisted conditions (2.45 GHz, 45 °C, 45 mins) using an adapted literature procedure **3.24** was isolated in 68% yield despite the reduced reaction time (Table 3.3). Similarly, the yield of **3.23** was increased to 72% higher than either the 18% or 60% (Table 3.1) achieved through conventional heating. Conversely the microwave-assisted synthesis of **3.22** gave a slightly reduced yield compared with conventional heating (Table 3.1). More investigation is needed to determine the general effect of the microwave-assisted conditions on these yields. In general, the microwave-assisted procedure substantially reduced the reaction time of the reactions an observation that is relevant to the high-throughput requirements of combinatorial and modular chemistry.

Product	RNH_2	RCO_2H	Yield
3.24	A1	B1	68%
3.23	A1	B3	72%
3.22	A2	B5	46%
3.25	A2	B3	41%
3.26	A2	B6	58%
3.27	A1	B7	79%

Table 3.3 Outcomes of Ugi multicomponent reaction using microwave-assisted conditions (2.45 GHz, 45 °C, 45 mins).

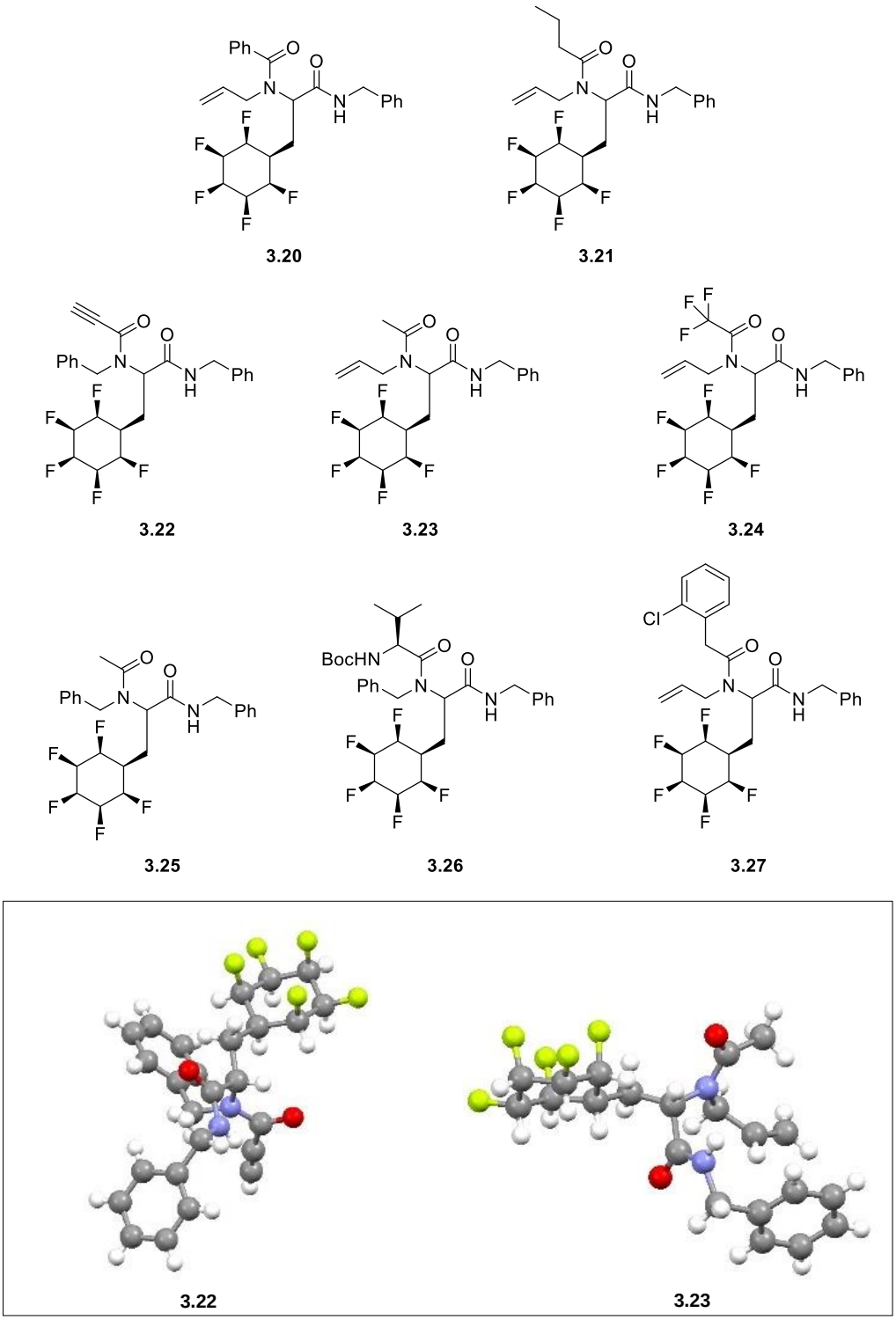

Figure 3.4 α-Acylamides synthesised by Ugi multicomponent reactions **3.20**-**3.27** and X-ray crystal structures of **3.22** and **3.23**.

3.2.3. Influence of the all-*cis*-pentafluorocyclohexane ring on molecular lipophilicity

In drug discovery programs, the Lipinski's rule of five has gained unparalleled recognition as a guiding principle for candidate design. The rule states that poor absorption and poor

membrane permeability are more likely when there are more than 5 H-bond donors or 10 H-bond acceptors, the molecular weight is greater than 500 Da or the Log P is more than 5.[26,27] Log P, which is a function of lipophilicity is a measure of the partition of a compound between octanol and water. Alternatively, Log P can be approximated by the use of HPLC due to the proportionality between Log P and retention time using a given stationary and mobile phase.[28] Previous studies from the St Andrews group using an HPLC method for Log P determination demonstrated that increasing fluorination of a cyclohexane ring results in a reduction in Log P.[29] The electronegativity of fluorine induces an increased electropositivity of the ring hydrogens, and this facilitates electrostatic attraction (non-classical hydrogen bonding) between ring hydrogens and water molecules.[29] The experimental set up reported was a reverse-phase Shimadzu Prominence HPLC, a Phenomenex Luna C_{18} 100 Å (250 mm x 4.60 mm) 5 µm column, 5-10 µL of 0.5 mg/mL solution of analyte in MeCN. The mobile phase was 60:40 MeCN:H_2O with 0.05% TFA and a flow rate of 1 ml/min. Capacity factor (k) was calculated from the retention times and the column dead time (1.97 min) according to the following equation.

$$Capacity\ factor\ (k) = \frac{Retention\ time - Dead\ time\ of\ the\ column}{Dead\ time\ of\ the\ column}$$

A calibration process wherein Log k was plotted against Log P of known compounds led to the derivation of the following equation for the experimental apparatus used.[29]

$$Log\ k = 0.3693 \times LogP - 0.4835$$

The measurement of Log P promised to quantify the influence of the all-*cis*-pentafluorocyclohexane ring on molecular lipophilicity in the 'drug-like' Ugi products **3.23**, **3.25** and **3.27** synthesised previously. The clear increase in polarity of the all-*cis*-pentafluorocyclohexane ring suggests a potential moderating effect on lipophilicity relative to non-polar groups. Therefore, the suitability of all-*cis*-pentafluorocyclohexyl motif as an isostere for aromatic rings was envisioned. Aromatic rings are found in over 80% of approved drugs but high lipophilicity prevents many candidate drugs from progressing to the clinic.[30] Aromatic analogues **3.28**-**3.30** of each of three Ugi products (**3.23**, **3.25** and **3.27**) and one cyclohexane analogue **3.31** were synthesised using the optimised microwave-assisted conditions. An example HPLC trace of **3.28** is shown in Figure 3.6. The Log P of the fluorinated cyclohexyl motifs **3.23**, **3.25** and **3.27** were significantly less than their aromatic (**3.28**-**3.30**) and cyclohexyl (**3.31**) analogues owing to the high molecular dipole moment of the all-*cis*-pentafluorocyclohexane (Figure 3.5). This finding demonstrates the potential of the 'Janus'

rings in drug discovery and related programmes, as the motif can occupy space but is significantly less hydrophobic than an aromatic or cyclohexyl ring.

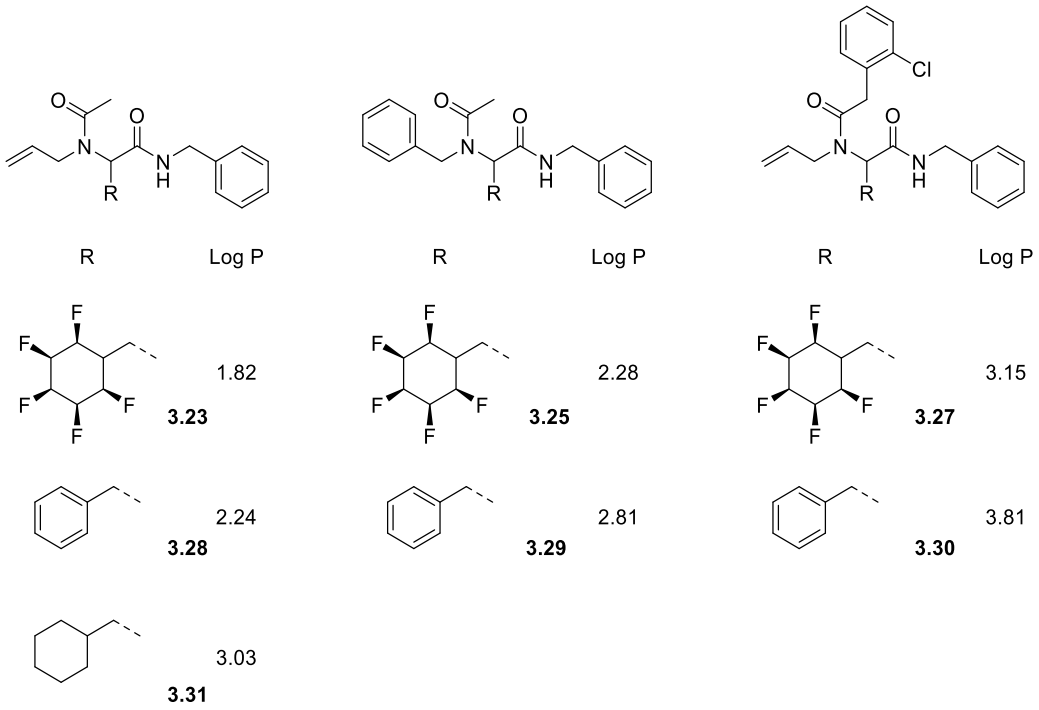

Figure 3.5 Log P comparison of all-*cis*-pentafluorocyclohexyl, benzyl and cyclohexyl motifs.

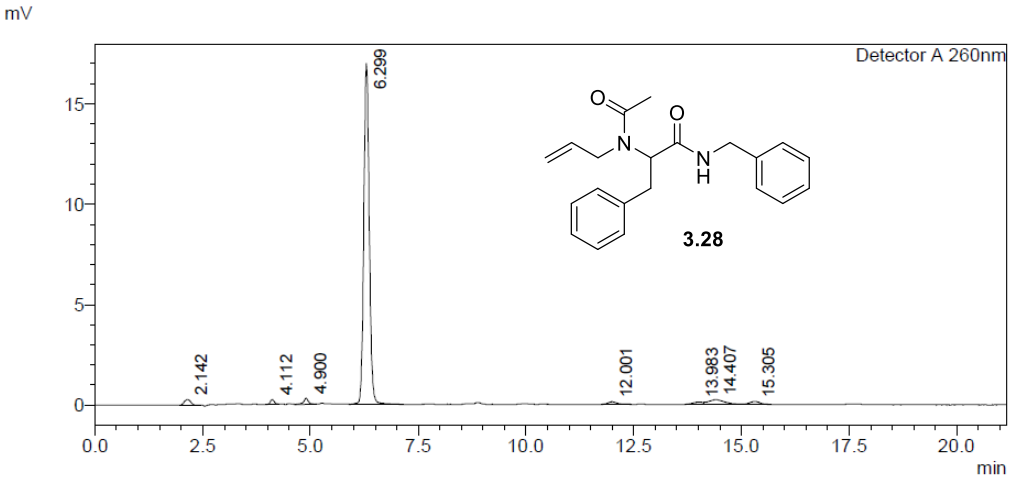

Figure 3.6 Example HPLC trace of **3.28**.

3.3. Reactions with aldehyde 2.87

Aldehyde **2.87** proved robust as a component in Ugi multicomponent reactions to generate a variety of products. Next alternative methods of elaboration were considered. Dibenzylamine was chosen as the amine component for a reductive amination with **2.87**. It was foreseen that

the product would be easily isolable due to a strong UV chromophore and that it would provide an alternative route to the amine building block **2.84** by subsequent hydrogenolysis of the C-N bonds (Scheme 3.16).

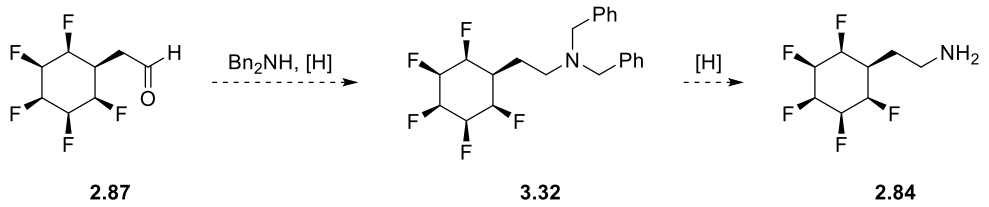

2.87 **3.32** **2.84**

Scheme 3.16 Proposed reductive amination to tertiary amine **3.32** and hydrogenolysis to amine building block **2.84**.

A method described by Hernández was explored for the reductive amination with dibenzylamine.[31] In the event the tertiary amine was obtained but in a modest 32% yield (Scheme 3.17). This low yield may be a consequence of having to overcome two reversible steps which are disfavoured under basic conditions (Scheme 3.18). An equivalent of water must be lost during formation of the enamine intermediate **3.33**, and after **3.33** has formed it needs to tautomerise to the iminium **3.34**, a process that requires protonation, and therefore is disfavoured under basic conditions.

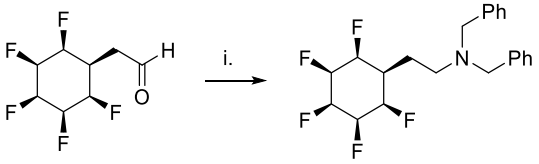

2.87 **3.32**

Scheme 3.17 Reductive amination of **2.87** with dibenzylamine to give amine **3.32**; i. Dibenzylamine, THF, r.t. 16 h, then $Na(OAc)_3BH$, Et_3N, r.t., 1h, 32%.[31]

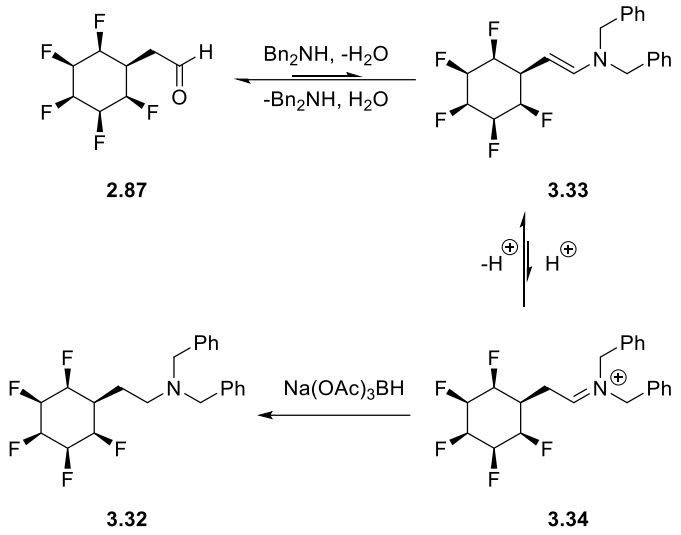

Scheme 3.18 The mechanism of reductive amination of **2.87** to give **3.32**.

In order to optimise the reductive amination reaction, triethylamine was substituted for acetic acid and consistent with the above discussion,[32] the reaction yield was significantly improved to 62% (Scheme 3.19). Because of the reversible dehydration step in the reaction mechanism (Scheme 3.18), the reaction was also run with 4 Å molecular sieves, although this only resulted in a modest increase in yield (to 65%) and did not noticeably accelerate the reaction.

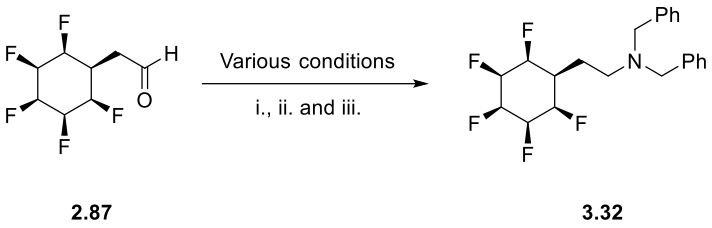

Scheme 3.19. Reductive amination of **2.87** with dibenzylamine to give amine **3.32**; i. Dibenzylamine, THF, r.t. 16 h, then $Na(OAc)_3BH$, Et_3N, r.t., 1h, 32%; ii. Dibenzylamine, CH_2Cl_2, r.t., 16 h then $Na(OAc)_3BH$, AcOH, r.t., 16 h, 62%; iii. Dibenzylamine, 4 Å MS, CH_2Cl_2, r.t., 16 h then $Na(OAc)_3BH$, AcOH, r.t., 1 h, 65%.

The Pd-catalysed hydrogenolysis of **3.32** was successful although the isolated yield was moderate (Scheme 3.20).[33] TLC showed a complete conversion of the starting material to product however, isolation of the amine **2.84** proved laborious. In particular, the removal of residual palladium catalyst required acid-base extraction and multiple filtrations through celite, and the high polarity of the amine product made it unsuitable for chromatographic purification.

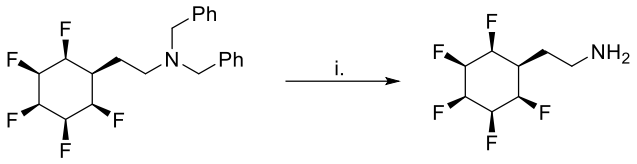

3.32 **2.84**

Scheme 3.20. Hydrogenolysis of tertiary amine **3.32** to give amine building block **2.84**; i. Pd (10%) on carbon, EtOAc, H_2 (1 atm), r.t., 32 h, 42%.

The overall yield over three steps from alcohol **2.81** to amine **2.84** was 20%. By comparison the synthetic route to **2.84** described in Chapter 2 had an overall yield of 55% over three steps and is the preferable route to this building block (Scheme 3.21).

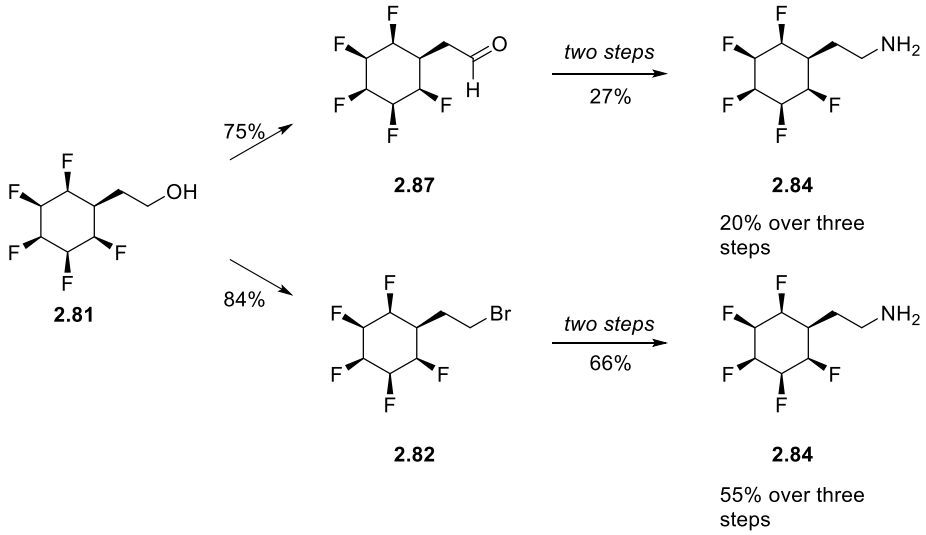

Scheme 3.21 Two synthetic routes to amine building block **2.84**.

Two heterocyclic amine products **3.35** and **3.36** were also synthesised using the acetic acid/reductive amination reaction (Scheme 3.22).

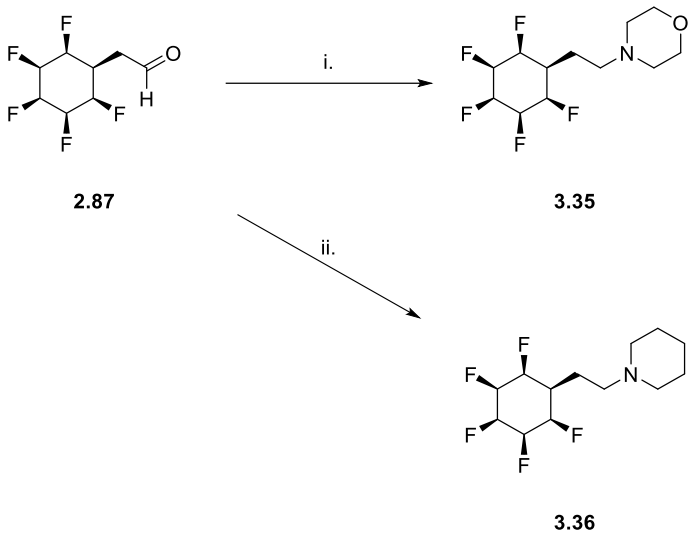

Scheme 3.22 Reductive amination reactions to generate heterocyclic amines **3.35** and **3.36**; i. Morpholine, CH_2Cl_2, 16 h, then $Na(OAc)_3BH$, AcOH, r.t., 16h, 63%; ii. Piperidine, 1,2-DCE, 16 h, then $Na(OAc)_3BH$, AcOH, r.t., 16 h 29%.

The Wittig reaction, was considered as another method for the elaboration of the aldehyde building block **2.87**. The mechanism proceeds through either a [2+2] cycloaddition of the ylene to an aldehyde or a similar 'two-stage one-step' mechanism with the ylide and an aldehyde[34,35] Previous assertions of a betaine intermediate have been disproven and the only intermediates are the *cis* and *trans* oxaphosphetanes (OPAs).[34–36] The OPA irreversibly rearranges to give triphenylphosphine oxide and the *E*- and *Z*- alkene products. The diastereoselectivity of the reaction is predictable with unstabilised ylides giving predominantly *Z*-alkenes (via the *cis*-OPA) and stabilised ylides giving predominantly *E*-alkene products (via the *trans*-OPA).

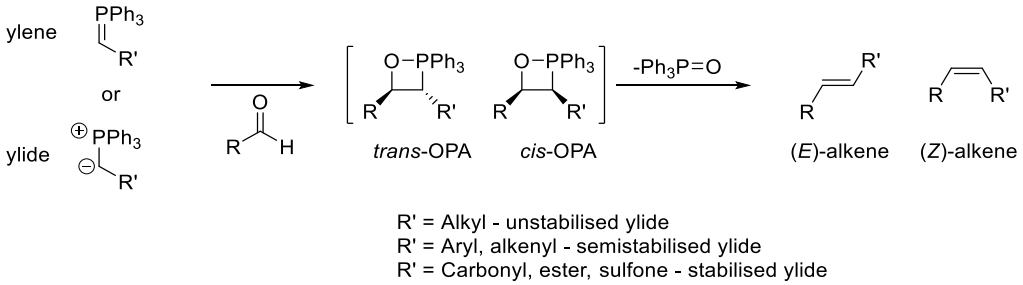

Scheme 3.23 The Wittig reaction *via* formation of oxaphosphetane (OPA) intermediates.

In the first Wittig trials (Scheme 3.24), methyltriphenylphosphonium bromide was deprotonated *in-situ* to generate an unstabilised ylide to which **2.87** was added, however no product was observed.

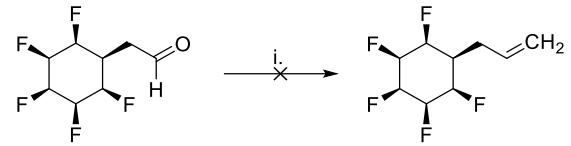

2.87 **3.37**

Scheme 3.24 Wittig reaction of **2.87** with unstabilised ylide; i. Ph_3PCH_3Br, n-BuLi, THF, r.t., 16h.

Reactions with a stabilised ylide, $Ph_3P{=}CO_2Et$ were then explored (Scheme 3.25). In this case the Wittig reaction proved successful, and the product olefin **3.38** was obtained in good yield. As expected for a stabilised ylide the product was predominantly the *E*- isomer and was isolated in a diastereomeric ratio of 9:1 *E*:*Z*.

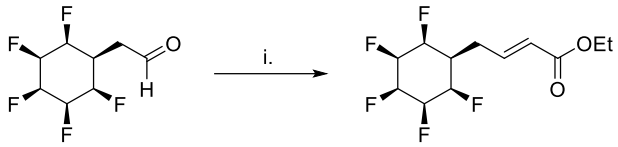

2.87 **3.38**

Scheme 3.25. Wittig reaction of **2.87** with a stabilised ylide; i. $Ph_3P{=}CO_2Et$, CH_2Cl_2, r.t., 4 h, 68%.

Given the fickle reactivity of aldehyde **2.87** to Wittig reactions, an alternative Wittig reagent was considered with the 'Janus ring' attached to the phosphonium ylide. Beginning with the alkyl bromide building block **2.82**, the triphenylphosphonium bromide salt was obtained after a reflux with triphenylphosphine in toluene (Scheme 3.26).

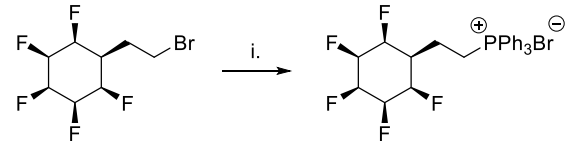

2.82 **3.39**

Scheme 3.26. Synthesis of triphenylphosphonium bromide salt **3.39**; PhMe, 111 °C, 16 h, 93%.

The Wittig reaction was attempted with three aldehydes, isobutyraldehyde **3.40**, benzaldehyde **3.41** and *n*-decanal **3.42** (Scheme 3.27). TLC indicated that the ylide was formed *in-situ* by the deprotonation of phosphonium bromide **3.39** with KO^{t}Bu but in each case the ylide proved inert to reaction with any of the aldehydes, and none of the desired products could be recovered.

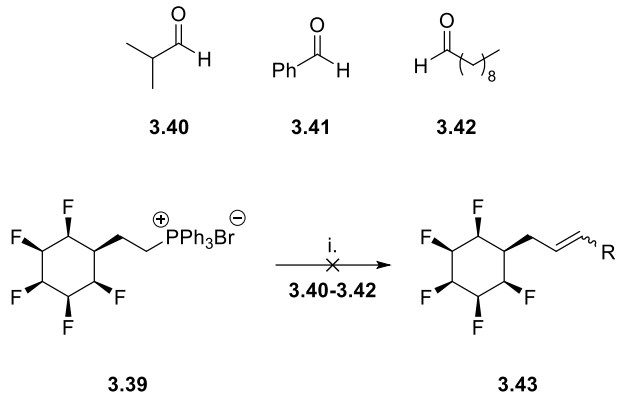

Scheme 3.27 Attempted Wittig reactions with **3.39**; i. KO^{t}Bu, THF, 0 °C to r.t., 5 h.

3.4. Etherification of alkyl bromide 2.82

Given the successful S_N2 reaction of alkyl bromide **2.82** and triphenylphosphine, an etherification reaction of **2.82** with a suitable alcohol was considered. However, the base stability analysis (Table 2.1) indicated the challenges of this reaction due to the vulnerability of 'Janus' rings to HF elimination. Following incubation of silyl ether **2.68** with NaOMe (pK_a 16), moderate conversion (10%) to defluorinated products occurred. With NaO^{t}Bu (pK_a 17), complete conversion of **2.68** to defluorinated products was observed (Scheme 3.28).

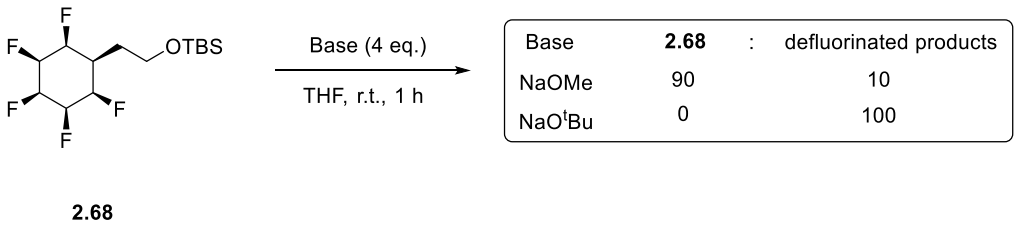

Base	**2.68**	:	defluorinated products
NaOMe	90		10
NaO^{t}Bu	0		100

Scheme 3.28 Results of the base stability test of **2.68** with alkoxide bases.

Given the base instability with an alkoxide, a phenolic nucleophile (with a lower pK_a) was considered. In particular, the phenols **3.44** and **3.45** were envisioned due to the electron withdrawing nature of the ester groups (to lower the pK_a). Additionally, it was foreseen that hydrolysis of the methyl esters following etherification could furnish candidate metal-organic-framework (MOF) linkers as a proof of concept. Structurally related compounds **3.46** and **3.47** have previously been reported as MOF linkers in MIL-53 (Sc) (for CO_2 adsorption) and STAM-17-OEt (Cu) (For NH_3 adsorption) (Figure 3.7).[37,38]

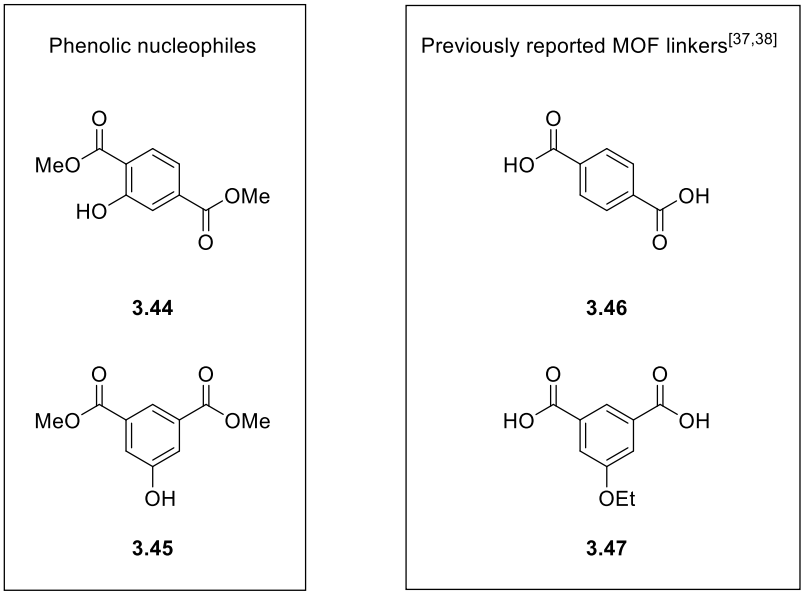

Figure 3.7 Left: Phenolic nucleophiles **3.44** and **3.45** for etherification of alkyl bromide **2.82**. Right: Previously reported MOF linkers.[37,38]

The synthesis of **3.49** was successfully achieved in two steps in a procedure adapted from the literature (Scheme 3.29).[39] Using potassium carbonate as a mild base, deprotonation of the phenol **3.44** was effected without competing elimination of HF from **2.82**. The resulting S_N2 reaction gave the diester **3.48** in good yield. The hydrolysis of **3.48** was achieved under acidic conditions to give the 1,4,-diacid product **3.49** which was isolated by acidification and then extraction into EtOAc. Similarly, the S_N2 reaction of alkyl bromide **2.82** with phenol **3.45** (Scheme 3.30) was also achieved under similar conditions to generate the diester **3.50**.

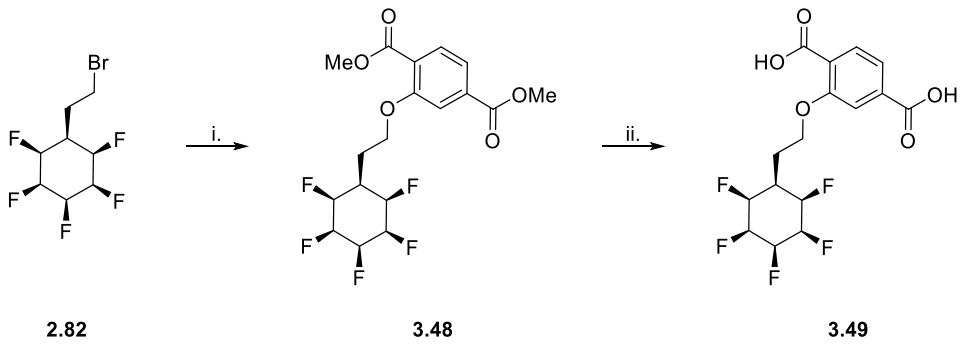

2.82 **3.48** **3.49**

Scheme 3.29 Preparation of dicarboxylic acid **3.49**; i. **3.44**, K_2CO_3, DMF, 90 °C, 14 h, 69%; ii. 6N HCl, 100 °C, 14 h, 96%.

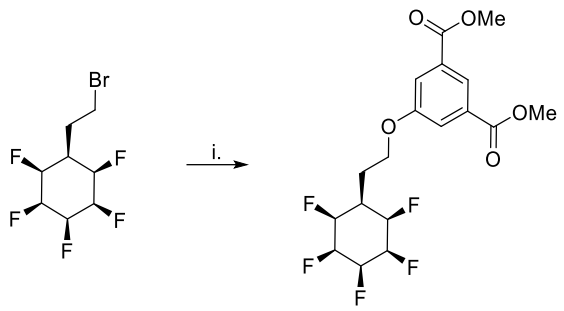

2.82 **3.50**

Scheme 3.30 Preparation of diester **3.50**; i. **3.45**, K_2CO_3, DMF, 90 °C, 14 h, 62%.

3.5. Copper-catalysed azide-alkyne cycloadditions of 2.83

The copper-catalysed azide-alkyne cycloaddition (CuAAC) reaction which was reported independently by the groups of Sharpless and Meldal,[40,41] is the most prominent example of a 'click' reaction. 'Click' reactions are described as easy to perform, high yielding, giving little or no byproducts, being wide in scope, using benign solvents and being easy to purify.[42] The mechanism of the 'click' reaction as described by Hein is shown in Scheme 3.31.[42]

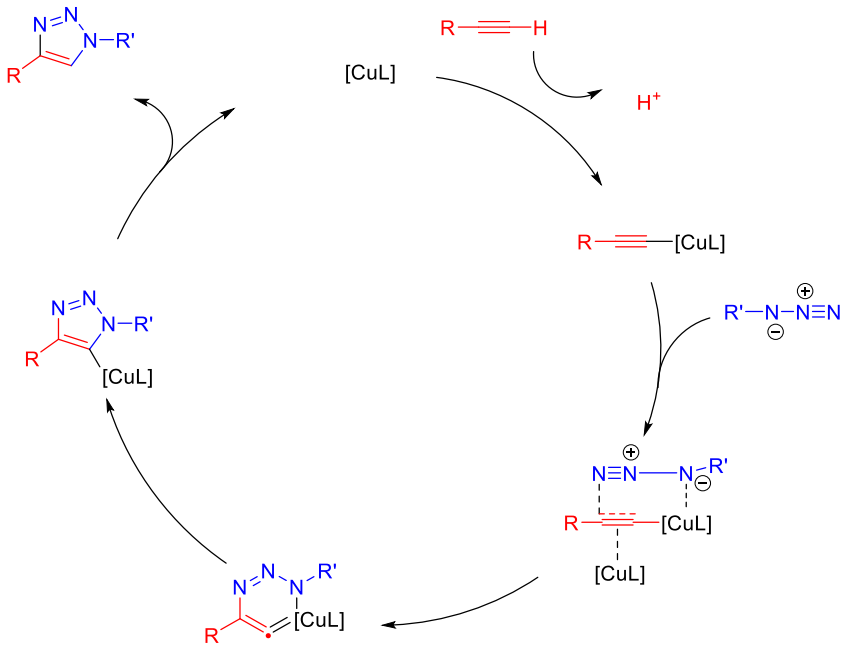

Scheme 3.31 The catalytic mechanism of the CuAAC 'click' reaction adapted from Ref-42.[42]

The CuAAC is considered an excellent modular reaction compatible with the needs of combinatorial chemistry. For these reasons, the CuAAC reaction was chosen as a method of derivatisation of the organoazide building block **2.83**. In the first instance propiolic acid was used as the alkyne reagent in a CuAAC reaction with **2.83** (Scheme 3.32). Stirring at r.t. for

16 h did not give any reaction and both starting materials could be reisolated. The reaction was therefore conducted at an increased temperature of 65 °C, with stirring for 16 h. The starting materials were now completely consumed. In the event, the product **3.51** was not suitable for purification by silica gel chromatography due to its high polarity but it was successfully isolated by acidification and extraction into EtOAc.

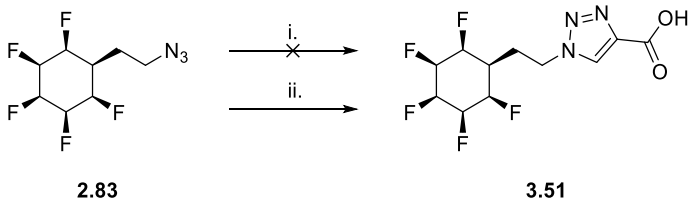

Scheme 3.32 CuAAC reaction of **2.83** with propiolic acid; i. $CuSO_4.6H_2O$, sodium ascorbate, water, ^{t}BuOH, r.t., 16 h; ii. $CuSO_4.6H_2O$, sodium ascorbate, water, ^{t}BuOH, 65 °C, 16 h, 79%.

A CuAAC reaction was carried out with the alkyne **3.52** using the elevated temperature conditions (Scheme 3.33). The isolated yield of **3.53** (23%) was low perhaps due to coordination of the unprotected alcohol to the Cu catalyst. Alternatively, the bulk of the alkyne reagent **3.52** may have presented a steric barrier to cycloaddition as the approach of the organoazide **2.83** is highly hindered by the trisubtituted carbon in **3.52** (Figure 3.8).

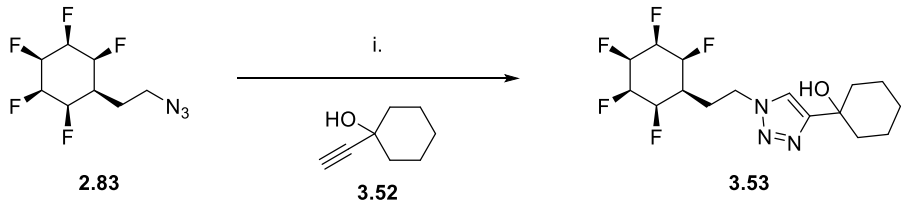

Scheme 3.33 CuAAC reaction with hindered alkyne **3.52**; i. $CuSO_4.6H_2O$, sodium ascorbate, water, EtOH, 65 °C, 16 h, 23%.

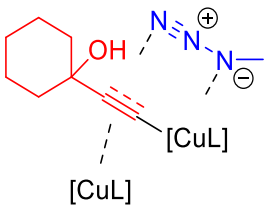

Figure 3.8 Illustration of the steric clash hindering cycloaddition in the reaction shown in Scheme 3.33.

Following the challenging preparation of **3.53**, three more CuAAC reactions were conducted under similar conditions (Scheme 3.34). Firstly 4-ethynyl toluene was chosen as an alkyne for the CuAAC reaction. This also facilitated purification as the product **3.54** has a strong

chromophore for UV visualisation by TLC. Also, the non-polar ring improved mobility in silica gel column chromatography. The reaction with 4-ethynylbenzoic acid was also successful and triazole **3.56** was isolated in high yield. This was achieved by acidification and extraction into EtOAc. Similarly, triazole **3.55** was also prepared in good yield. The X-ray crystal structure of **3.55** shows short intermolecular contacts of 2.52-2.56 Å (Sum of the VdW radii = 2.67 Å) between opposite faces of the pentafluorocyclohexane rings (Figure 3.9).

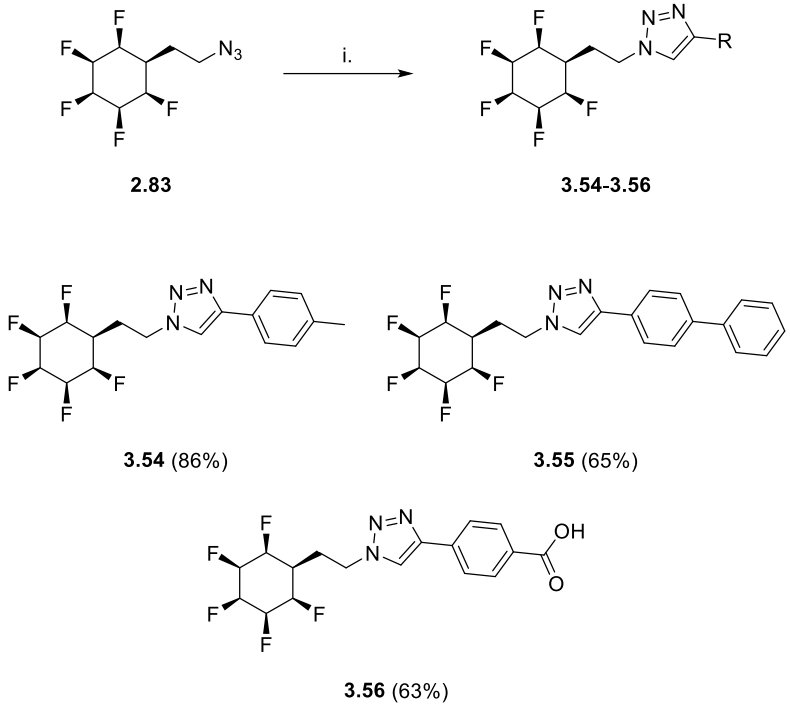

Scheme 3.34 Further 'click' reactions; i. $CuSO_4.6H_2O$, sodium ascorbate, water, MeOH/EtOH/^{t}BuOH, 65 °C, 16 h.

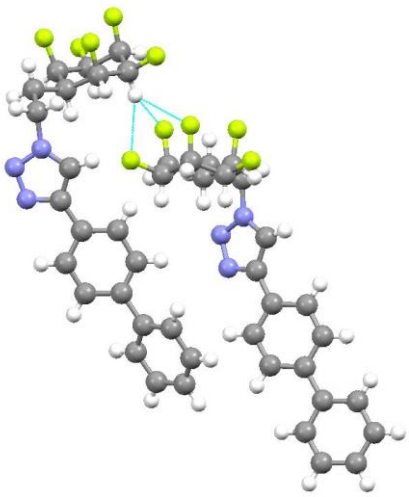

Figure 3.9 X-ray crystal structure of **3.55**.

A further area of exploration involved the use of the CuAAC reaction to generate compounds bearing multiple 'Janus' rings. Such compounds could have a clear role in exploring the 'Janus' ring in supramolecular chemistry. In the first instance the *bis*-ring compound **3.57** was synthesised from 1,4-diethynylbenzene (Scheme 3.35). As found previously, elevated temperature were required to drive the formation of product **3.57**. The polarity of **3.57** resulted in its precipitation from the reaction solvent and it was easily isolated in high purity by filtration. The high polarity was immediately apparent by its inability to move with MeOH by TLC (R_f = 0.0 in MeOH) and once isolated it showed no melt transition at temperatures in excess of 300 °C.

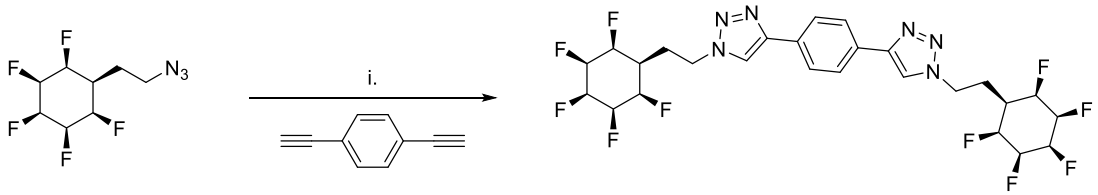

2.83 **3.57**

Scheme 3.35 CuAAC synthesis of *bis*-ring product **3.57**; i. $CuSO_4.6H_2O$, sodium ascorbate, water, ^{t}BuOH, 80 °C, 3 h, 83%.

The extremely high polarity of *bis*-ring compound **3.57** may have implications for the use of related structures in supramolecular chemistry. The only solvent found capable of forming a homogeneous solution of **3.57** was DMSO and the product was not isolable by silica gel chromatography. The 1,2,3-triazole motif has a high dipole moment (4.8-5.6 D) of comparable magnitude to the 'Janus' ring (~ 5.9 D).[42,43] Future investigations into solution phase supramolecular applications should seek to incorporate solubilising groups, like ether linkages, alongside 'Janus' rings in the molecular structure.

3.6. Conclusions

In Chapter 3 a range of elaboration strategies have been employed showing the synthetic versatility of the 'Janus' ring building blocks made in Chapter 2. Here, strategies to generate molecular diversity have been developed and optimised utilising amide couplings, multi-component reactions (MCRs), reductive aminations, Wittig reactions and CuAAC 'click' reactions. Many of these products are 'drug-like', indeed the promise of the 'Janus' ring to medicinal chemistry was demonstrated by its moderation (lowering) of Log P across a series of Ugi products relative to arene and cyclohexane bearing derivatives. The CuAAC 'click' reaction has shown promise as a route to highly polarised 'Janus' *bis*-ring systems of interest in the field of supramolecular chemistry.

3.7. References

[1] M. P. Wiesenfeldt, Z. Nairoukh, W. Li, F. Glorius, *Science,* **2017**, *357*, 908–912.

[2] J. T. Van Herpt, M. C. A. Stuart, W. R. Browne, B. L. Feringa, *Chem. Eur. J.* **2014**, *20*, 3077–3083.

[3] L. A. Carpino, H. Imazumi, B. M. Foxman, M. J. Vela, P. Henklein, A. El-Faham, J. Klose, M. Bienert, *Org. Lett.* **2000**, *2*, 2253–2256.

[4] E. I. Vrettos, N. Sayyad, E. M. Mavrogiannaki, E. Stylos, A. D. Kostagianni, S. Papas, T. Mavromoustakos, V. Theodorou, A. G. Tzakos, *RSC Adv.* **2017**, *7*, 50519–50526.

[5] L. A. Carpino, *J. Am. Chem. Soc.* **1993**, *115*, 4397–4398.

[6] S. Gedey, J. Van Der Eycken, F. Fülöp, *Org. Lett.* **2002**, *4*, 1967–1969.

[7] A. Dömling, I. Ugi, *Angew. Chem. Int. Ed.* **2000**, *39*, 3168–3210.

[8] J. U. Nef, *Justus Liebigs Ann. Chem.* **1892**, *270*, 267.

[9] F. La Spisa, G. C. Tron, L. El Kaïm, *Synthesis* **2014**, *46*, 829–841.

[10] A. A. Esmaeili, S. Amini Ghalandarabad, S. Jannati, *Tetrahedron Lett.* **2013**, *54*, 406–408.

[11] M. C. Pirrung, K. Das Sarma, *J. Am. Chem. Soc.* **2004**, 444–445.

[12] M. C. Pirrung, K. Das Sarma, *Tetrahedron* **2005**, *61*, 11456–11472.

[13] I. Ugi, *Angew. Chem.* **1959**, *71*, 386.

[14] I. Ugi, *Angew. Chem. Int. Ed.* **1962**, *I*, 8–21.

[15] N. Chéron, R. Ramozzi, L. El Kaïm, L. Grimaud, P. Fleurat-Lessard, *J. Org. Chem.* **2012**, *77*, 1361–1366.

[16] R. O. Rocha, M. O. Rodrigues, B. A. D. Neto, *ACS Omega* **2020**, *5*, 972–979.

[17] G. A. Medeiros, W. A. da Silva, G. A. Bataglion, D. A. C. Ferreira, H. C. B. de Oliveira, M. N. Eberlin, B. A. D. Neto, *Chem. Commun.* **2014**, *50*, 338–340.

[18] T. Bykova, N. Al-Maharik, A. M. Z. Slawin, D. O'Hagan, *Org. Biomol. Chem.* **2016**, *14*, 1117–1123.

[19] R. Ovadia, C. Mondielli, J. J. Vasseur, C. Baraguey, K. Alvarez, *Eur. J. Org. Chem.* **2017**, *2017*, 469–475.

[20] C. Y. Hsiao, S. Q. Huang, W. H. Lien, C. Y. Hsu, K. lin Hsieh, M. H. Lin, M. J. Wu, C. C. Fu, H. C. Chen, H. P. Fang, C. J. Li, P. S. Pan, *Res. Chem. Intermed.* **2017**, *43*, 3585–3597.

[21] A. Liu, H. Zhou, G. Su, W. Zhang, B. Yan, *J. Comb. Chem.* **2009**, *11*, 1083–1093.

[22] H. Tye, M. Whittaker, *Org. Biomol. Chem.* **2004**, *2*, 813–815.

[23] M. Nikulnikov, S. Tsirulnikov, V. Kysil, A. Ivachtchenko, M. Krasavin, *Synlett* **2009**, 260–262.

[24] C. O. Kappe, *Chem. Soc. Rev.* **2008**, *37*, 1127–1139.

[25] W. M. Haynes, D. R. Lide, T. J. Bruno, *CRC Handbook of Chemistry and Physics*, Taylor & Francis Group, Boca Raton, **2017**.

[26] C. A. Lipinski, F. Lombardo, B. W. Dominy, P. J. Feeney, *Adv. Drug Deliv. Rev.* **1997**, *23*, 3–25.

[27] C. A. Lipinski, *Drug Discov. Today Technol.* **2004**, *1*, 337–341.

[28] C. Giaginis, A. Tsantili-Kakoulidou, *J. Liq. Chromatogr. Relat. Technol.* **2008**, *31*, 79–96.

[29] A. Rodil, S. Bosisio, M. S. Ayoup, L. Quinn, D. B. Cordes, A. M. Z. Slawin, C. D. Murphy, J. Michel, D. O'Hagan, *Chem. Sci.* **2018**, *9*, 3023–3028.

[30] F. Mao, W. Ni, X. Xu, H. Wang, J. Wang, M. Ji, J. Li, *Molecules* **2016**, *21*, 1–18.

[31] D. Hernández, C. Carro, A. Boto, *J. Org. Chem.* **2021**, *86*, 2796–2809.

[32] T. Hanke, F. Rörsch, T. M. Thieme, N. Ferreiros, G. Schneider, G. Geisslinger, E. Proschak, S. Grösch, M. Schubert-Zsilavecz, *Bioorg. Med. Chem.* **2013**, *21*, 7874–7883

[33] J. Magano, B. G. Conway, D. Farrand, M. Lovdahl, M. T. Maloney, M. J. Pozzo, J. J. Teixeira, J. Rizzo, D. Tumelty, *Synthesis* **2014**, *46*, 1399–1406.

[34] E. Chamorro, M. Duque-Noreña, N. Gutierrez-Sánchez, E. Rincón, L. R. Domingo, *J. Org. Chem.* **2020**, *85*, 6675–6686.

[35] P. A. Byrne, D. G. Gilheany, *Chem. Soc. Rev.* **2013**, *42*, 6670–6696.

[36] P. Farfán, S. Gómez, A. Restrepo, *J. Org. Chem.* **2019**, *84*, 14644–14658.

[37] L. N. McHugh, M. J. McPherson, L. J. McCormick, S. A. Morris, P. S. Wheatley, S. J. Teat, D. McKay, D. M. Dawson, C. E. F. Sansome, S. E. Ashbrook, C. A. Stone, M. W. Smith, R. E. Morris, *Nat. Chem.* **2018**, *10*, 1096–1102.

[38] L. Chen, J. P. S. Mowat, D. Fairen-Jimenez, C. A. Morrison, S. P. Thompson, P. A. Wright, T. Düren, *J. Am. Chem. Soc.* **2013**, *135*, 15763–15773.

[39] S. M. Hawxwell, G. M. Espallargas, D. Bradshaw, M. J. Rosseinsky, T. J. Prior, A. J. Florence, J. Van De Streek, L. Brammer, *Chem. Commun.* **2007**, 1532–1534.

[40] V. V. Rostovtsev, L. G. Green, V. V. Fokin, K. B. Sharpless, *Angew. Chem. Int. Ed.* **2002**, *41*, 2596–2599.

[41] C. W. Tornøe, C. Christensen, M. Meldal, *J. Org. Chem.* **2002**, *67*, 3057–3064.

[42] J. E. Hein, V. V. Fokin, *Chem. Soc. Rev.* **2010**, *39*, 1302–1315.

[43] J. Clark, D. O'Hagan, S. Guldin, A. Slawin, D. B. Cordes, C. Yu, R. A. Cormanich, R. Neyyappadath, A. Geddis, A. Taylor, B. A. Piscelli, *Chem. Sci.* **2021**, *12*, 9712-9719.

4. Intermolecular interactions and phase behaviour of 'Janus rings'

4.1. Background and Aims

Highly fluorinated compounds such as perfluorinated alkanes (where all hydrogens in a parent compound are replaced by fluorine) have unique chemical properties. Perfluoroalkane solvents such as perfluorohexane are immiscible with both water and common organic solvents (although miscibility with the latter is temperature dependent). They form a third 'fluorous' phase which has been widely utilised in synthesis and purification strategies particularly in the field of bi- and tri-phasic catalysis.[1,2] Most famously, Teflon™ (PTFE, (poly(tetrafluoroethylene))) has gained wide application as a 'non-stick' coating for cookware owing to its high heat stability, hydrophobicity and oleophobicity.[3] On the other hand, partially fluorinated materials such as the structurally related polymer PVDF (poly(vinylidene fluoride) (Figure 4.1) differ in properties as the electronegative fluorine atoms induce an electropositivity in the proximal -CH_2- groups and thus a molecular dipole moment is established. This high polarity is evidenced by the piezoelectricity of PVDF.[4]

Figure 4.1 Poly(tetrafluoroethylene) (PTFE) and poly(vinylidene fluoride) (PVDF).

Like PVDF, all-*cis*-hexafluorocyclohexane **1.70** is a highly polarised compound. The *cis*-substitution of the fluorines results in a 'Janus' phase character with faces of opposite polarisation. The X-ray crystal structure of all-*cis*-hexafluorocyclohexane reveals the preferential stacking of fluorine to hydrogen faces with close intermolecular contacts (as low as 2.43 Å) between the fluorine and hydrogen atoms (Figure 4.2),[5] rather than fluorous, fluorine to fluorine packing.

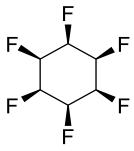

1.70

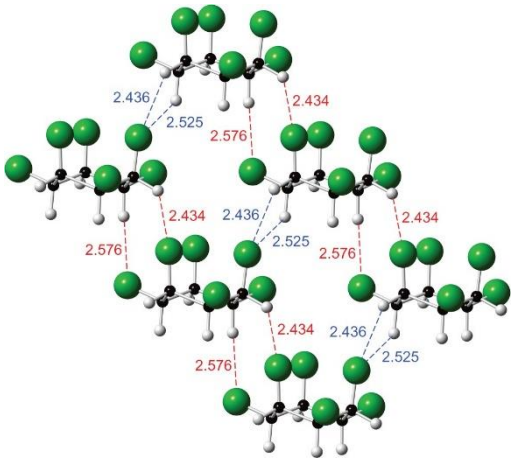

Figure 4.2 Representation of packing in the X-ray crystal structure of all-*cis*-hexafluorocyclohexane **1.70** indicating close intermolecular contacts (distances in angstrom) between hydrogens and fluorines.[5]

This ring orientation of the fluorinated faces to protic faces is very different to that in fluorous-fluorous associations of perfluorinated compounds. The contact distances are shorter than the combined Van der Waals radii of hydrogen and fluorine (2.67 Å),[6] and the strength of the interaction between two 'Janus' rings of **1.70** has been calculated at ~ 8.2 kcal mol^{-1} similar to the strength of a good hydrogen bond. The strength of these intermolecular interactions suggests a propensity for supramolecular assembly. Additionally, the macroscopic polarisation arising from the net dipole moment in the aggregated phase suggests potential applications in ferroelectric and non-linear optical (NLO) materials.[7]

This Chapter explores the nature of the intermolecular interactions between 'Janus' all-*cis*-fluorocyclohexane rings in amphiphilic compounds and their potential role in organising supramolecular assembly. Close examination of X-ray crystal structures informs understanding of intermolecular interactions in the solid state. Further, the propensity for molecular self-assembly of the amphiphiles is explored through Langmuir isotherms.[8] When an amphiphilic molecule such as stearic acid (Figure 4.3) is deposited on a water subphase, the attractive hydrogen bonding interactions between the hydrophilic head group and the water molecules are balanced by the hydrophobicity of the tail which prevents dissolution in the aqueous subphase.

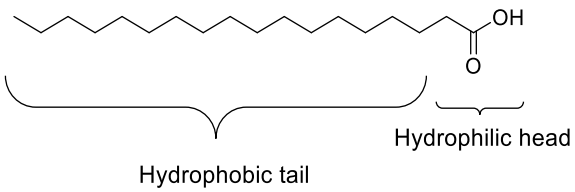

Figure 4.3 Amphiphilicity of stearic acid.

The Langmuir trough apparatus (Figure 4.4) is comprised of movable barriers placed on the water subphase which compress the deposited amphiphile film. A sensitive Wilhelmy plate and electrobalance measures the surface pressure with the changing surface area, and thus a pressure/area isotherm is obtained. The Langmuir trough experiments are sensitive, and efforts must be made to ensure; the purity of the water subphase, accurate measurement of the amount of amphiphile deposited and the preservation of a vibration-free environment.

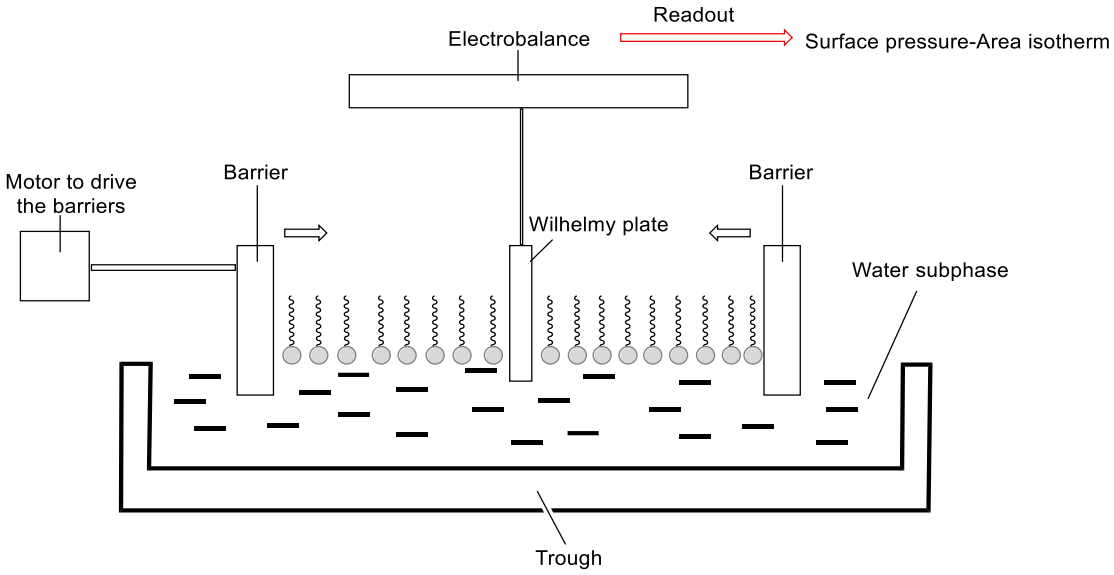

Figure 4.4 Schematic of a Langmuir trough.

Upon deposition at the air-water interface the amphiphile occupies a 2D 'gaseous' phase, where molecules are disordered and not in contact (Figure 4.5A). The first phase transition occurs during barrier compression at the liquid-expanded phase, where molecules remain disordered but come into contact (Figure 4.5B). On further compression a transition to a condensed monolayer occurs (Figure 4.5C) which eventually collapses to form higher order phases such as bilayers or more disordered arrangements (Figure 4.5D).[9,10] Some or all of the phase transitions may be identified by a discontinuity in the gradient of the isotherm. The annotated Langmuir isotherm for stearic acid is shown in Figure 4.6 to illustrate this principle.[11]

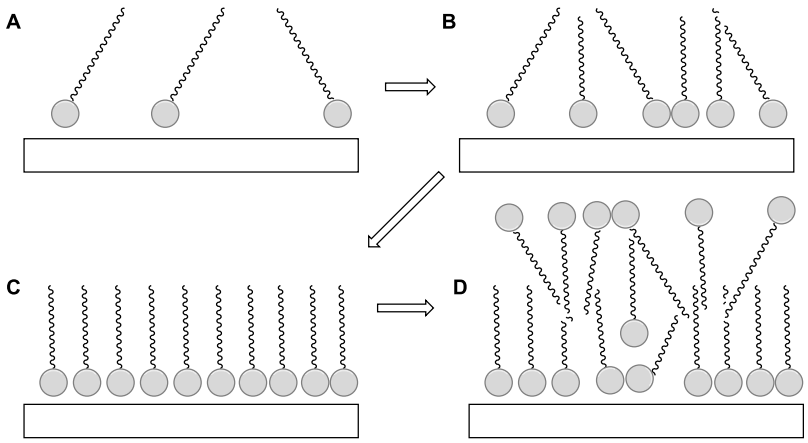

Figure 4.5 Various phases of an amphiphile during Langmuir barrier compression; A. gaseous; B. liquid-expanded; C. condensed monolayer; D. collapse and higher order phases.

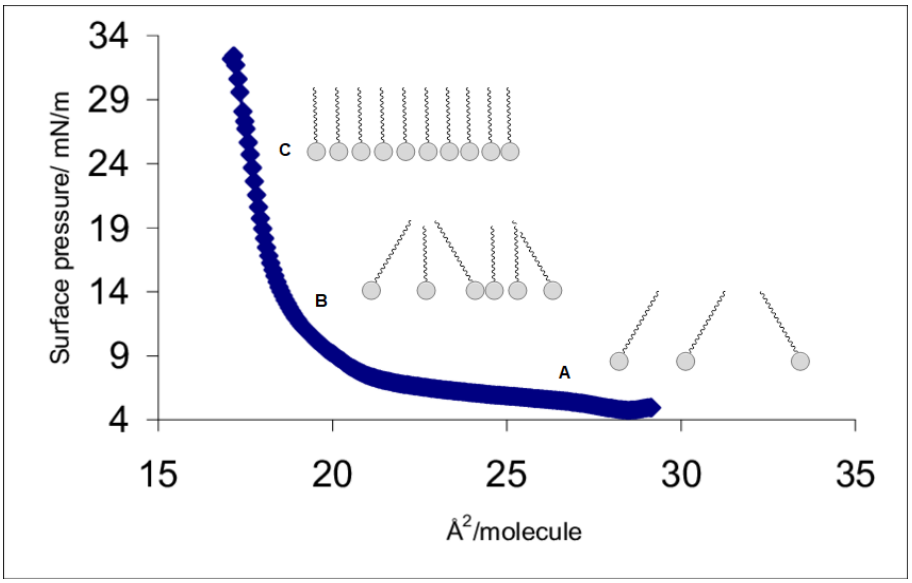

Figure 4.6 Langmuir isotherm of stearic acid with annotated phase behaviour adapted from El Hefian *et al*..[11]

The amphiphilic synthetic targets that were selected to probe the surface behaviour of the 'Janus' ring were carboxylic acid **4.1** and alcohol **4.2** (Figure 4.7). The non-fluorinated carboxylic acid **4.4** and alcohol **4.5** were also prepared as reference compounds. It was anticipated that the pentafluorocyclohexyl containing amphiphiles **4.1** and **4.2** may undergo phase transitions more rapidly and with less compression due to the attractive interactions between the 'Janus' rings than for the unfluorinated analogues **4.4** and **4.5**. Another synthetic target was alkylcyclohexane **4.3**, although not bearing a classical hydrogen-bonding head group, it was anticipated that monolayer formation of **4.3** could occur during Langmuir isotherm experiments if the polar water molecules could form electrostatic interactions/non-classical hydrogen bonds to the polar ring faces of **4.3**.

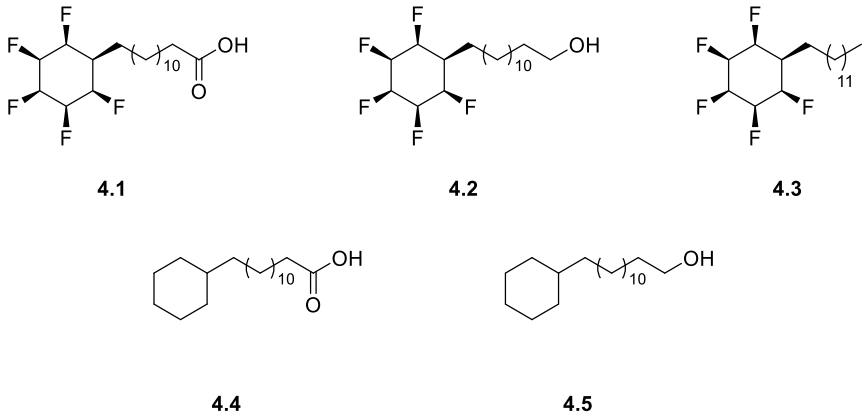

Figure 4.7 Amphiphilic synthetic targets for Langmuir analysis.

4.2. Synthesis of 'Janus' ring containing amphiphiles

The proposed synthesis of two of the fluorinated amphiphiles **4.1** and **4.2** is illustrated in Scheme 4.1. Phosphonium bromide **4.7** could be accessed from 12-bromododecanoic acid **4.6** by substitution with PPh_3. The ylide formed when **4.7** is deprotonated (*in-situ*) has been reported as a suitable Wittig reagent.[12] Therefore, a Wittig reaction with pentafluorophenyl acetaldehyde followed by esterification of the product would give the unsaturated methyl ester **4.8**. Hydrogenation under the Glorius/Zeng conditions could then give the 'Janus ring' containing ester **4.9**.[13] Reduction and hydrolysis of **4.9** should lead to alcohol **4.1** and carboxylic acid **4.2** respectively (Scheme 4.1).

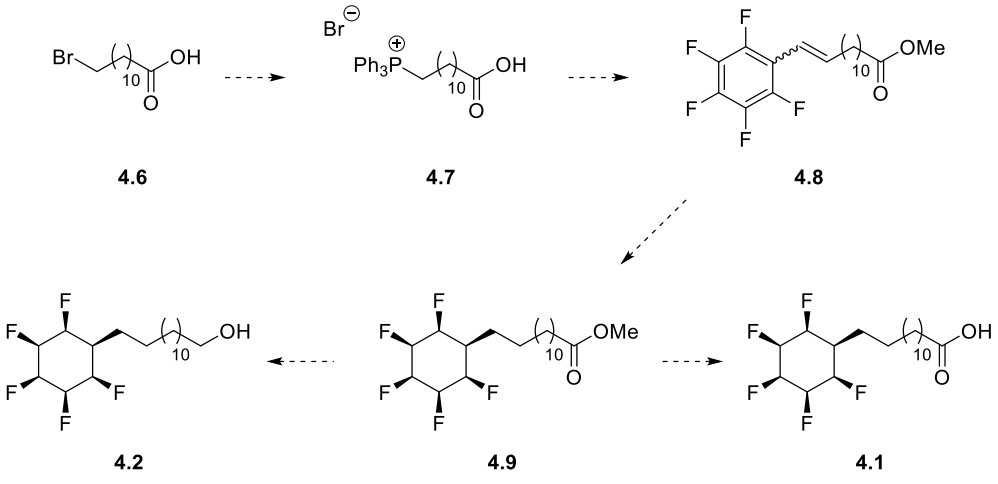

Scheme 4.1 Proposed synthetic route to amphiphiles **4.1** and **4.2**.

In the event, the phosphonium bromide salt **4.7** was prepared from 12-bromododecanoic acid **4.6** and triphenylphosphine in high yield (Scheme 4.2).[14] It was isolated as viscous oil and proved insoluble in most organic solvents. However, a Wittig reaction of **4.7** with freshly

distilled benzaldehyde was attempted but this gave no reaction and no evidence for the formation of the phosphonium ylide was observed by NMR, when using sodium *bis*(trimethylsilyl)amide or potassium *tert*-butoxide as the base.[15]

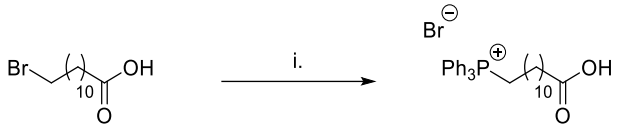

4.6 **4.7**

Scheme 4.2 Synthesis of **4.7**; i. PPh_3, $PhCH_3$, 111 °C, 16 h, 80%.[14]

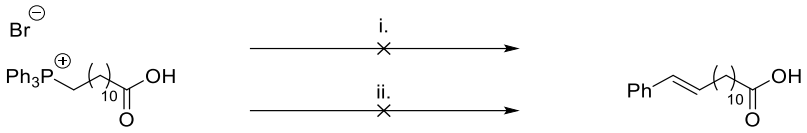

4.7 **4.8**

Scheme 4.3 Unsuccessful synthesis of **4.8**; i. PhCHO, NaHMDS, THF, -60 °C to r.t., 0%; ii. PhCHO, KO^{t}Bu, THF, 0 °C to r.t.[15]

As the Wittig reaction with phosphonium bromide **4.7** had proven challenging, an alternative approach was envisaged (Scheme 4.4). A report by Wang *et al*., indicated that phosphonate **4.11** was a suitable substrate for Horner-Wadsworth-Emmons (HWE) reactions.[16] A HWE reaction with methyl-12-oxododecanoate **4.12** should give the desired hydrogenation substrate **4.8**.

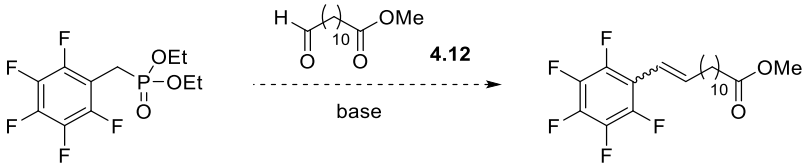

4.11 **4.8**

Scheme 4.4 Alternative route to **4.8**.

At the outset, the preparation of phosphonate **4.11** by an Arbuzov reaction proved to be problematic, where the reaction was sluggish under neat refluxing conditions. However, the reaction proved to be remarkably efficient under microwave-assisted conditions, an approach adapted from a literature procedure (Scheme 4.5).[17]

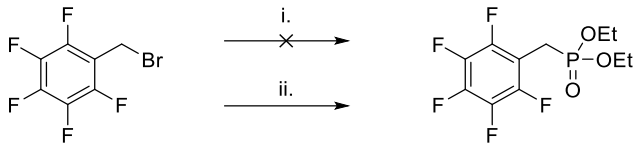

4.13 **4.11**

Scheme 4.5 Arbuzov reaction to give phosphonate **4.11**; i. $P(OEt)_3$, 156 °C, 48 h; ii. $P(OEt)_3$, 140 °C (microwave), 5 mins, 99%.

With the required phosphonate in hand, aldehyde **4.12** was next prepared by functional group interconversions from 12-hydroxydodecanoic acid **4.14** (Scheme 4.6). First, esterification under acidic conditions gave methyl ester **4.15**, a compound which was isolated in high yield.[18] A Swern oxidation was then utilised to introduce the terminal aldehyde in product **4.12**.[19]

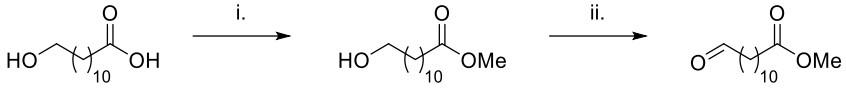

4.14 **4.15** **4.12**

Scheme 4.6 Synthesis of aldehyde **4.12**; i. MeOH, HCl (1M), 65 °C, 14 h, 95%; ii. $(COCl)_2$, Et_3N, DMSO, THF, −78 °C to r.t., 1h, 74%.[18,19]

The HWE reaction with aldehyde **4.12** and phosphonate **4.11** (Scheme 4.7) proved to be successful, generating olefin **4.8** as a mixture of *E*- and *Z*- isomers (*E*:*Z* 5:1), and in an overall moderate yield.[20] This isomeric mixture was used in the next hydrogenation step without further purification.

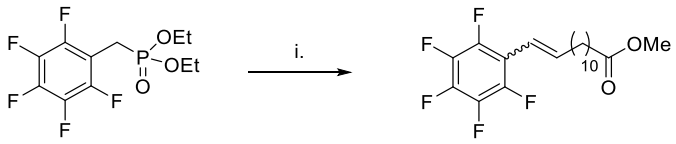

4.11 **4.8**

Scheme 4.7 Horner-Wadsworth-Emmons reaction to unsaturated methyl ester **4.8**; i. NaH, THF, **4.12**, 0 °C to 50 °C, 14 h, 58%.

The isomeric mixture of **4.8** was subject to a global hydrogenation under the conditions reported by Glorius.[13] The all-*cis*-pentafluorocyclohexyl ester **4.9** was obtained from this reaction but in the event the yield was low after purification by flash column chromatography (Scheme 4.8).

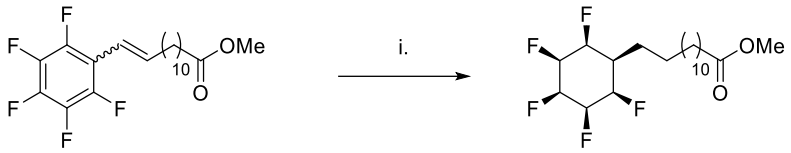

4.8 **4.9**

Scheme 4.8 Hydrogenation of **4.8** to give 'Janus' derivative **4.9**; i. **2.14** (3 mol%), H_2 (50 bar), silica gel, hexane, r.t., 14 h, 22%.

Fatty acid **4.1** was now obtained after a hydrolysis reaction. As conventional hydrolysis under basic conditions risked E1cB elimination of HF from the cyclohexane ring, the fatty acid was prepared under acid-catalysed hydrolysis (Scheme 4.9).[21] The reaction proceeded efficiently, and the fatty acid **4.1** could be isolated in high yield (95%).

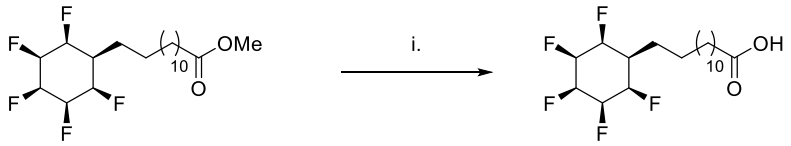

4.9 **4.1**

Scheme 4.9 Acid catalysed hydrolysis of methyl ester **4.9** to give fatty acid **4.1**; i. HCl (6M), H_2O, 100 °C, 14 h, 95%.

The long chain alcohol **4.2** was prepared by reduction of methyl ester **4.9** under mild conditions using DIBAlH, a reaction that occurred in good yield and without any deterioration of the pentafluorocyclohexane ring system (Scheme 4.10).[22]

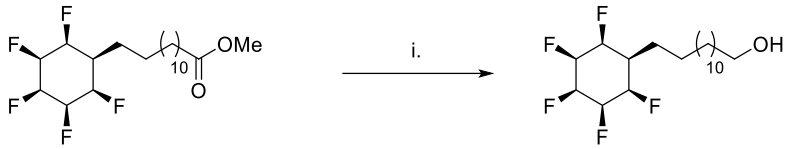

4.9 **4.2**

Scheme 4.10 Reduction of methyl ester **4.9** to alcohol **4.2**; i. DIBAlH, CH_2Cl_2, -78 °C to r.t., 14 h, 64%.[22]

The synthesis of **4.3** was approached by cross-metathesis of allylpentafluorobenzene **2.69** and 1-dodecene (Scheme 4.11).[23] This gave a statistical mixture of the desired cross-metathesis product **4.16** but also homodimers of the starting materials **4.17** and **4.18** (Figure 4.8). Silica gel chromatography was used to purify the mixture, but the desired product **4.16** was not easily separated from the hydrocarbon homodimer **4.18** as both had similar polarities (Rf > 0.9 (hexane)) on TLC. The global hydrogenation reaction was successful but again in a low overall yield. The long chain aliphatic **4.3** was isolated and could be easily separated from

other contaminants due to the increased polarity from the 'Janus ring', which increased its retention on silica gel relative to the fluoroarene **4.16**.[13]

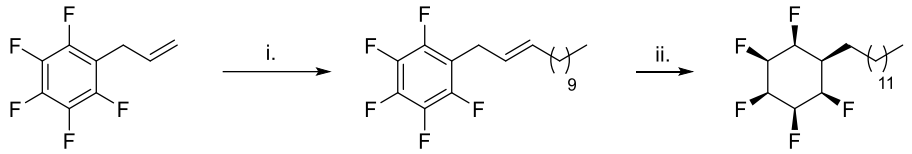

2.69 **4.16** **4.3**

Scheme 4.11 Synthesis of **4.3**; i. Grubbs I catalyst ®, 1-dodecene, CH_2Cl_2, 40 °C, 14 h; ii. H_2 (50 bar), **2.14** (3 mol%), 4 Å MS, hexane, r.t., 24 h, 32% over two steps.[13,23]

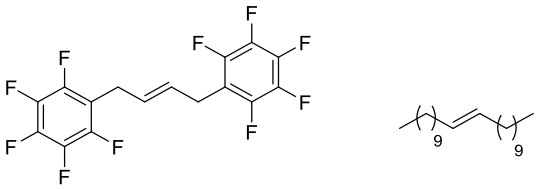

4.17 **4.18**

Figure 4.8 Homodimer side products from Step i. Scheme 4.11.

4.3. Towards a *bis*-ring system with an alkyl spacer

Although the use of 'click' reactions had already provided access to *bis*-ring system **3.57** (Chapter 3), the solubility of **3.57** was poor in a range of organic solvents owing to the combined high polarity of the triazole and 'Janus' rings. It was envisioned that the use of an alkyl spacer in **4.19** would improve the solubility of the *bis*-ring system by increasing its lipophilicity. With a longer alkyl spacer (as n increases), the more lipophilic and therefore more soluble the *bis*-ring system is anticipated to be (Figure 4.9).

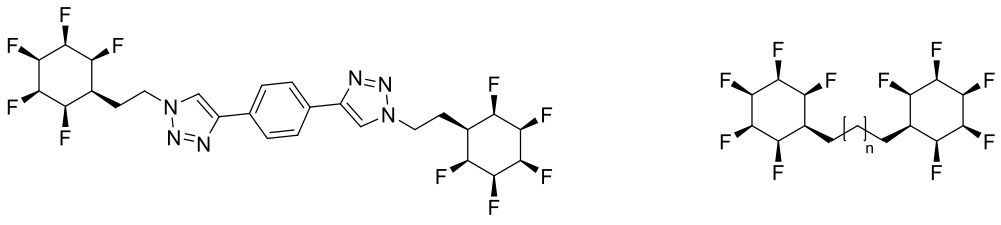

3.57 **4.19**

Figure 4.9 Left: 'Click' product **3.57** isolated by CuAAC reaction (Chapter 3); Right: *Bis*-ring system **4.19** with tunable lipophilicity based on the length of the alkyl spacer.

In the first instance the homodimer side product **4.17** from the metathesis reaction in Scheme 4.11 was isolated and global hydrogenation was attempted (Scheme 4.12).[13] After stirring for

16 h, ^{19}F NMR indicated a negligible conversion to the desired product. It was foreseen that a preliminary hydrogenation of the alkene bond could furnish **4.21** which may hydrogenate more easily to give the desired product **4.20**. In practice, Pd-catalysed hydrogenation of the alkene efficiently furnished the *bis*-arene **4.21**,[24] which was then amenable to aryl hydrogenation. In the event only a singly aryl hydrogenated product **4.22** could be isolated. It is suggested that following the hydrogenation of one of the arene rings to an all-*cis*-pentafluorocyclohexyl ring, that the increased polarity associated with the 'Janus' ring causes the product to precipitate out of the hexane solution, thus precluding the second hydrogenation to the desired product **4.20**.

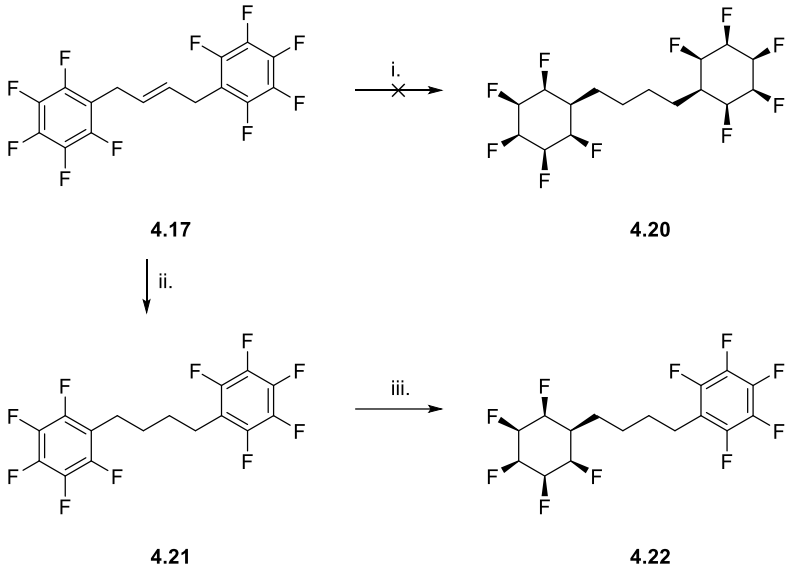

Scheme 4.12 The attempted preparation of *bis*-'Janus' ring system **4.20**; i. **2.14** (4 mol%), H_2 (50 bar), 4 Å MS, hexane, r.t., 16 h; ii. Pd/C 10% w/w, H_2 (1 bar), MeOH, r.t., 16 h; iii. **2.14** (4 mol%), H_2 (50 bar), 4 Å MS, hexane, r.t., 16 h, 41% over two steps.[13,24]

Given the challenges of isolating the desired *bis*-ring system **4.20** with a four carbon alkyl spacer, a target with a longer spacer was chosen to promote solubility of partially hydrogenated intermediates in hexane. In the first instance a metathesis-HWE route to symmetrical diene **4.26** was envisaged (Scheme 4.13). Hydrogenation of **4.26** under the Zeng/Glorius conditions could give the desired *bis*-ring compound **4.27**.

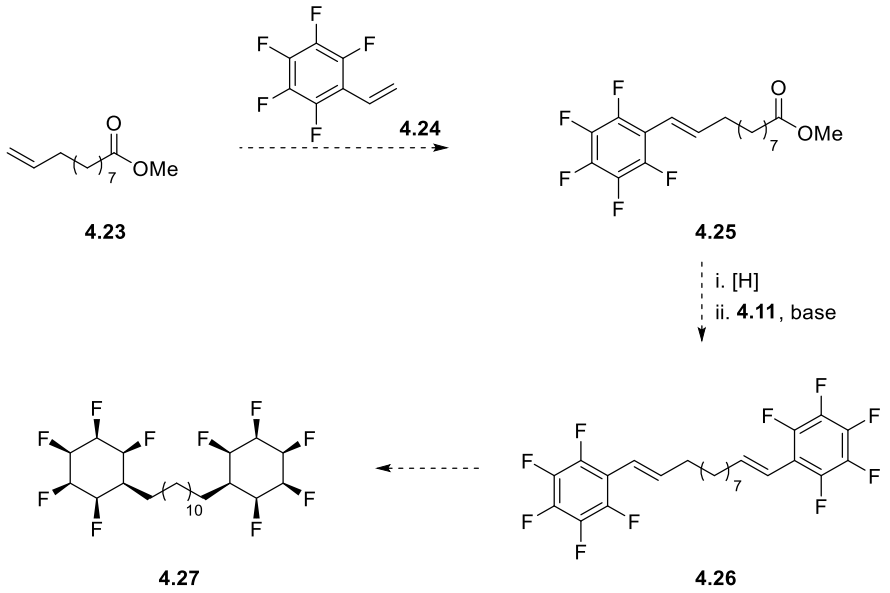

Scheme 4.13 Proposed synthesis of extended *bis*- 'Janus' ring compound **4.27**.

In the first instance, a metathesis reaction was chosen with selectivity in mind. Methyl-10-undecenoate **4.23** is a reactive Type I olefin meaning that homodimerisation is rapid and the dimer is consumed in the metathesis, whereas styrenes such as **4.24** are less reactive Type II olefins, meaning that homodimerisation is slow and the dimer is sparingly consumed in metathesis. The comparison of selectivity in Type I–Type II metathesis with the statistical outcomes are illustrated in Scheme 4.14.[23] Furthermore, the reaction was biased with a 2:1 stoichometry of **4.24**:**4.23**. In the reaction the desired *E*- product **4.25** was isolated in good yield (54%) (Scheme 4.15).[25] Although the yield was good it was lower than expected based on the reported selectivity of cross-metathesis between Type I and Type II olefins. Indeed, the homodimer of **4.28** was isolated in 37% yield. In future the yield of the desired product may be improved by using a higher stoichometric excess of **4.24**.[23]

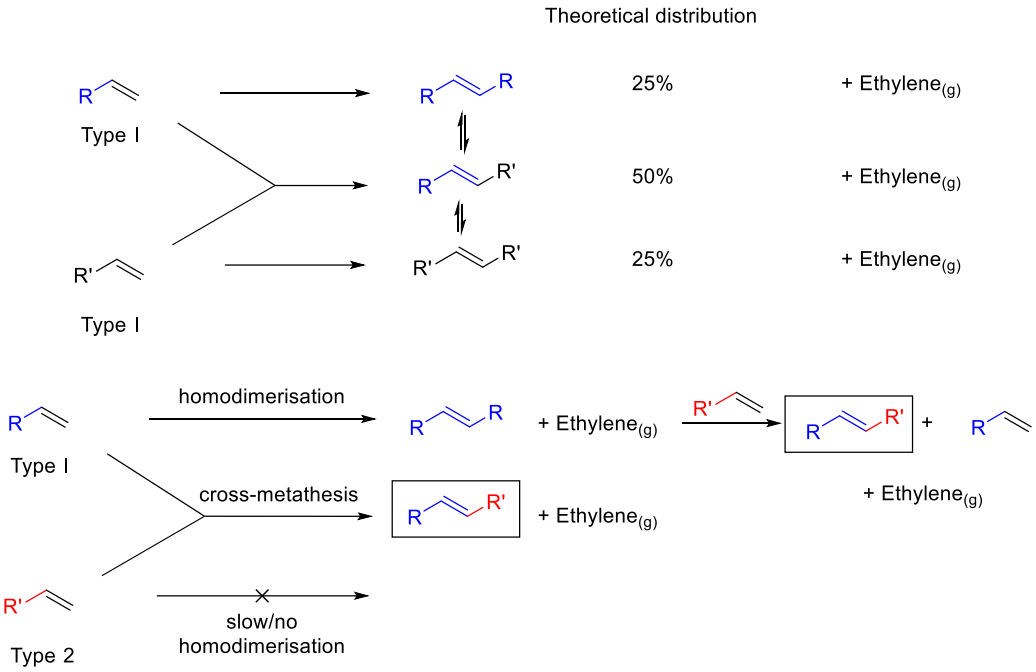

Scheme 4.14 Top: non-selective cross metathesis between two Type I olefins resulting in a statistical mixture of products; Bottom: selective cross metathesis between Type I and Type II olefins.[23]

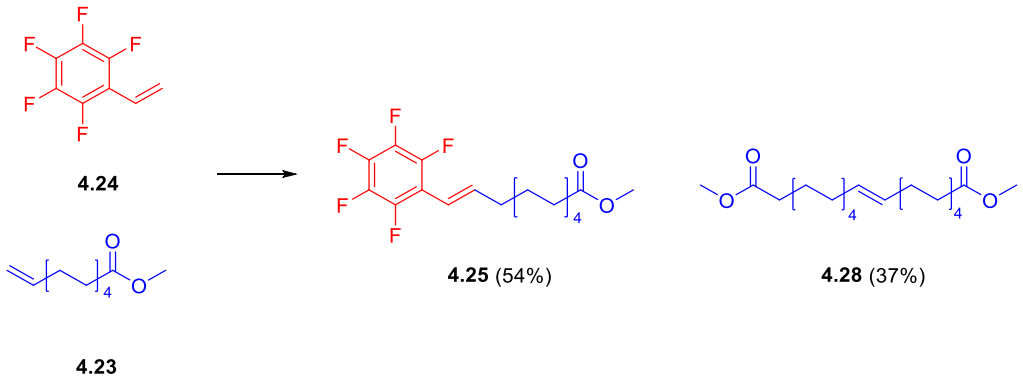

Scheme 4.15 The outcome of the cross-methathesis reaction; i. Hoveyda-Grubbs 2nd generation catalyst ®, CH_2Cl_2, 40 °C, 14 h.[25]

With unsaturated methyl ester **4.25** in hand, reduction using DIBAL at -78 °C gave aldehyde **4.29** directly following work-up (Scheme 4.16).[26] There was no evidence of over-reaction to the alcohol. The aldehyde **4.29** was used in the Horner-Wadsworth-Emmons reaction with phosphonate **4.11** under mild conditions, and this gave predominantly the *E*- alkene **4.26** (*E*:*Z* 6:1) as expected, as the carbanion formed from the deprotonation of phosphonate **4.11** at the α-position is stabilised.[27] The global hydrogenation of the unsaturated *bis*-arene was successfully carried out albeit in low yield.[13] Due to the demands of reducing two aromatic rings and two carbon-carbon double bonds a higher than usual (5 mol%) catalyst loading was

employed. In future an even higher catalyst loading could be used to attempt to improve the yield of the reaction.

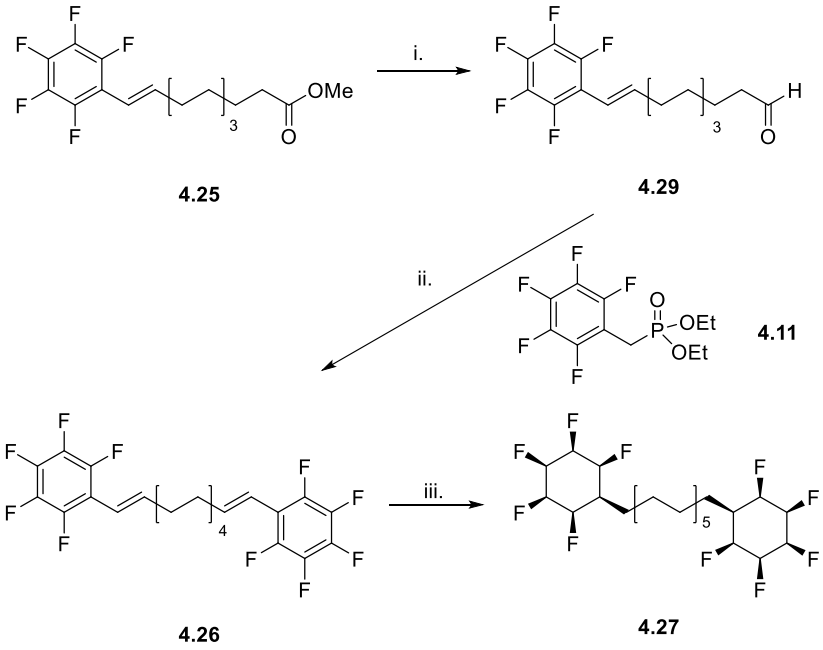

Scheme 4.16 Synthesis of **4.27**; i. DIBAlH, CH_2Cl_2, -78 °C, 40 min, quant.; ii. NaH, THF, 0 °C to 66 °C, 53%; iii. H_2 (50 bar), **2.14** (5 mol%), 4 Å MS, hexane, r.t., 33%.[13,26,27]

4.4. X-ray crystal structures of 'Janus' ring containing amphiphiles

X-ray crystal structures of some of the amphiphiles synthesised were obtained and examined for an insight into their packing in the solid phase. The crystal structure of the long chain alcohol **4.2** is presented in Figure 4.11. In the solid state the cyclohexyl ring of alcohol **4.2** adopts a chair conformer in which a triaxial C-F bond orientation is preserved. This maximises the molecular dipole moment of the ring system. The alkyl spacer sits in an equatorial orientation at an angle of 130° to the plane of the ring reducing any steric clash with axial ring substituents. Torsional strain arising both from the steric clash of the adjacent fluorine atoms (Average intramolecular F_{ax}-F_{ax} distance = 2.82 Å; Sum of the VdW radii = 2.94 Å) and electrostatic repulsion is evident from an examination of the dihedral angles (Average dihedral F_{ax}-C2/6-C1-C13 = 49.0°; F_{ax}-C2/6-C1-C2/6 = 73.6°). The intermolecular packing of **4.2** follows the predicted hydrogen to fluorine face orientation although the rings are offset with close axial to equatorial close contacts (F_{ax}-H_{eq} = 2.33 Å, 2.57 Å; F_{eq}-H_{ax} = 2.40 Å; sum of the VdW radii = 2.67 Å). The wider packing network shows an edge-to-edge association between adjacent rings leading to a bilayer structure in which the alkyl chains are pointed in opposite directions. The bilayer facilitates a hydrogen bonding network (hydrogen bonding distance = 2.16 Å) with the alcohol groups interacting at the termini. The alkyl chains of **4.2**, which run

parallel to each other, are separated by 4.1-4.2 Å (carbon-carbon separation) at their closest contacts. This results in contacts close to the Van der Waals radii between hydrogen atoms (2.7-2.8 Å, sum of the VdW radii – 2.4 Å) of adjacent chains.

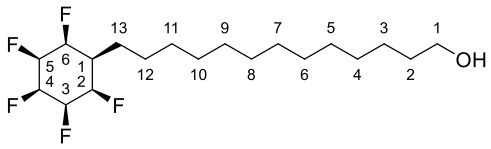

4.2

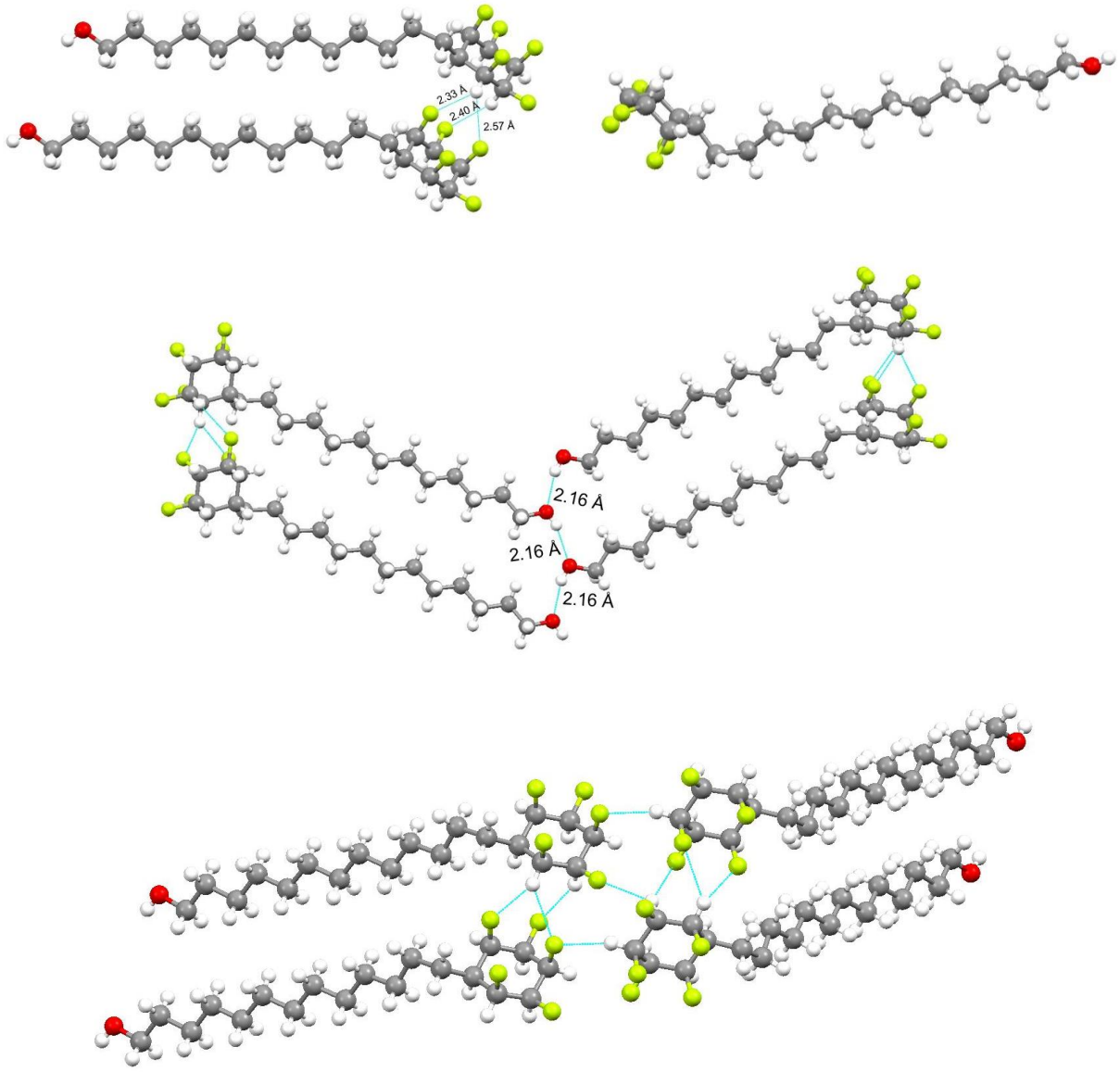

Figure 4.10 Various representations of the X-ray crystal structure of **4.2**.

The X-ray crystal structure of the all-*cis*-pentafluorocyclohexylalkane **4.3** is illustrated in Figure 4.11. In the solid state the cyclohexyl ring again adopts a chair conformer in which a triaxial

C-F bond orientation is preserved as previously observed in alcohol **4.2**. Likewise, the alkyl chain sits equatorial from the cyclohexane ring at an angle of 130° to the ring plane. The intermolecular F_{ax}-F_{ax} distance of 2.82 Å is identical to that of **4.3** but ring strain appears less significant than for alcohol **4.2** as the dihedral angles are closer to the 60° expected for *gauche* substituents (Average dihedral F_{ax}-C1/5-C6-$C1_{Alkyl}$ = 52.9°; F_{ax}-C1/5-C6-C1/5 = 70.8°). Intermolecular packing of **4.3** is similar to that of the alcohol **4.2** with offset stacking of hydrogen to fluorine faces and with axial to equatorial close contacts (F_{ax}-H_{eq} = 2.38 Å; F_{eq}-H_{ax} = 2.50 Å; sum of the VdW radii = 2.67 Å). The alkyl chains are separated by 4.0-4.2 Å (carbon-carbon separation) and intermolecular contacts between chain hydrogen atoms are just above the sum of the VdW radii (2.7-2.8 Å, sum of the VdW radii – 2.4 Å).

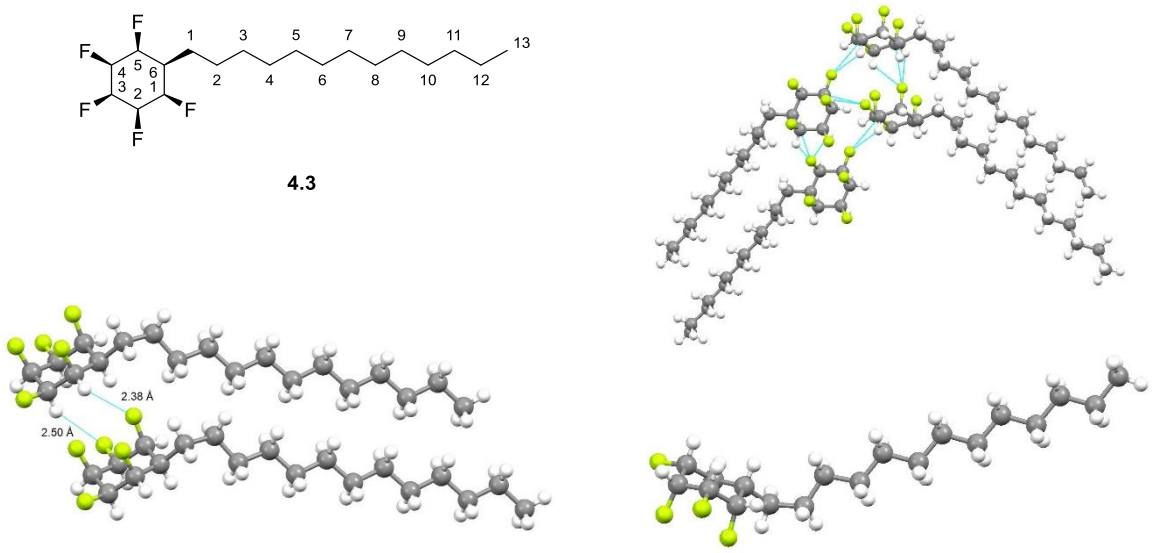

4.3

Figure 4.11 Various representations of the X-ray crystal structure of **4.3**.

The partially hydrogenated *bis*-ring compound **4.22** provides an opportunity to examine the packing in a crystal structure of a compound with both 'Janus' and pentafluoroaryl rings (Figure 4.12). Notably, the 'Janus' rings self-associate and the aryl rings self-associate but the different rings do not interact with each other. The 'Janus' ring again adopts a chair conformer with triaxial C-F bonds. Strain is present in the ring as before as seen in the average intramolecular F_{ax}-F_{ax} distance = 2.81 Å (Sum of the VdW radii = 2.94 Å) and the dihedral angles (Average F_{ax}-C2/6-C1-$C4_{Alkyl}$ = 54.5°; F_{ax}-C2/6-C1-C2/6 = 73.0°). The alkyl spacer sits equatorial to minimise steric clash and extends in a zig-zag conformation parallel to the plane of the ring. Intermolecular packing shows aligned 'Janus' ring stacking with four close contacts between F_{ax}-H_{ax} (2.56 Å, 2.41 Å, 2.37 Å, 2.50 Å; Sum of the VdW radii = 2.67 Å). Edge to edge packing is also apparent with close contacts between F_{ax} and H_{eq} (2.50 Å; Sum of the VdW radii = 2.67 Å). Stacking of the pentafluorophenyl rings is offset with the electronegative 3-fluorine substituent directly above the electropositive centre of another aryl ring.

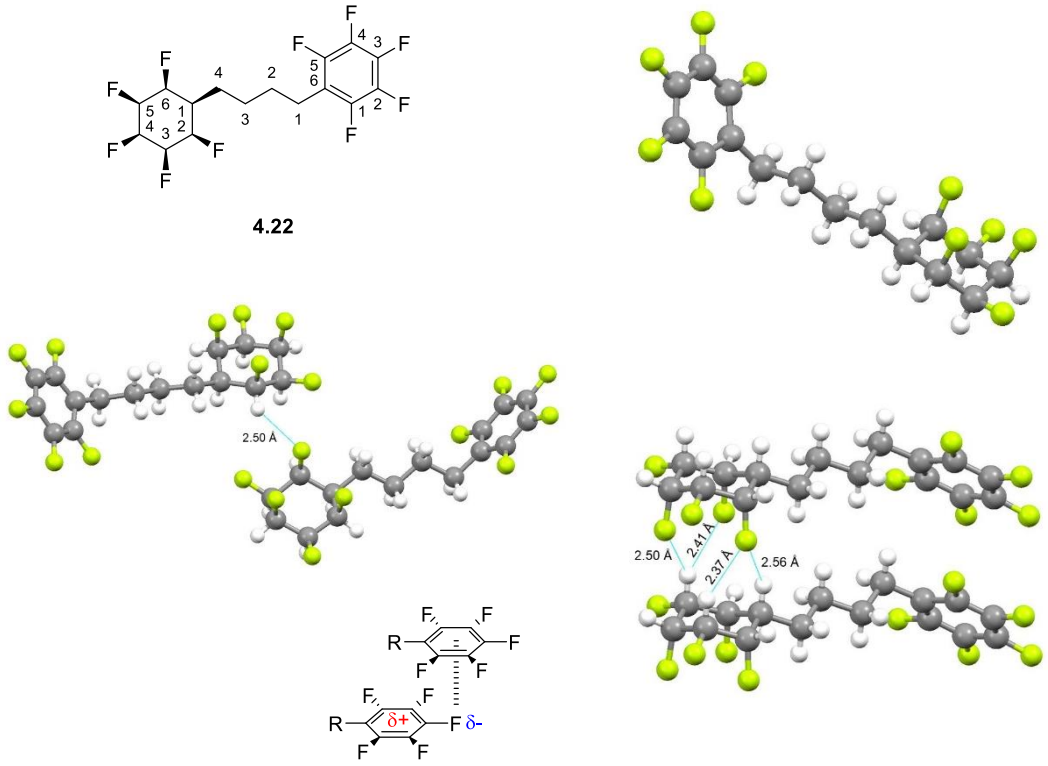

Figure 4.12 Various representations of the X-ray crystal structure of **4.22**.

The X-ray structure of the C_{12} alkyl spaced *bis*-ring system **4.27** in the solid state is illustrated in Figure 4.13. As expected, each ring adopts a chair conformer with triaxial C-F bonds. Strain is present in the ring evident from the average intramolecular F_{ax}-F_{ax} distance = 2.75 Å (Sum of the VdW radii = 2.94 Å). The dihedral angles show less strain than that in compounds **4.2**, **4.3** and **4.22** with values closer to the expected 60° for *gauche* alignment (Average F_{ax}-C2/6-C1-C1/12$_{Alkyl}$ = 58.1°; F_{ax}-C2/6-C1-C2/6 = 68.4°). The alkyl spacer sits in an equatorial orientation to minimise steric clashes and extends in a zig-zag conformation parallel to the plane of the ring. Intermolecular packing features aligned stacking of the 'Janus' rings with three close contacts between F_{ax}-H_{ax} (2.27 Å, 2.38 Å, 2.46 Å; Sum of the VdW radii = 2.67 Å). Edge to edge packing is also apparent with close contacts between F_{ax} and H_{eq} (2.48 Å; Sum of the VdW radii = 2.67 Å). The 2.27 Å H-F contact in **4.27** is among the closest CF-HC contacts found in the Cambridge Structural Database.[28–30]

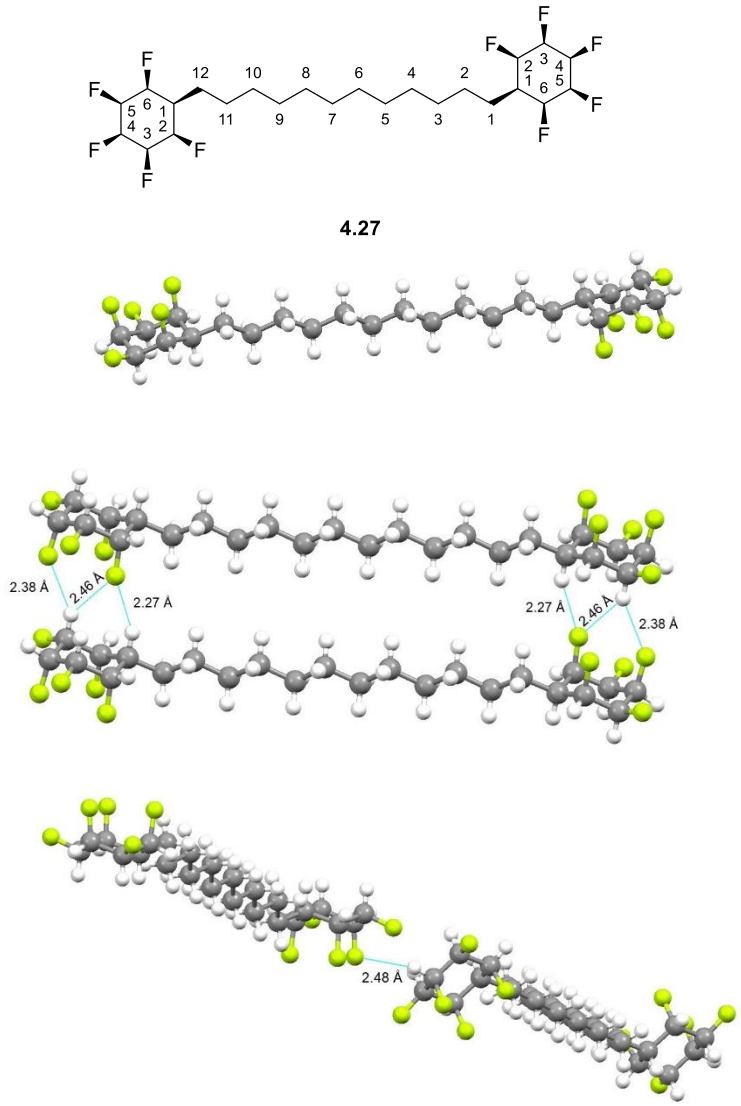

4.27

Figure 4.13 Various representations of the X-ray crystal structure of *bis*-'Janus' ring compound **4.27**.

4.5. Synthesis of non-fluorinated amphiphile reference compounds

With both fluorinated amphiphile targets **4.1** and **4.2** in hand a synthesis of the unfluorinated analogues **4.4** and **4.5** was required to provide reference compounds. It was envisaged that the cross metathesis of two commercially available alkenes **4.30** and **4.23** could give unsaturated methyl ester **4.31** suitable for hydrogenation (Scheme 4.17). From the hydrogenation product **4.32**, hydrolysis and reduction could give the carboxylic acid **4.4** and alcohol **4.5** respectively.

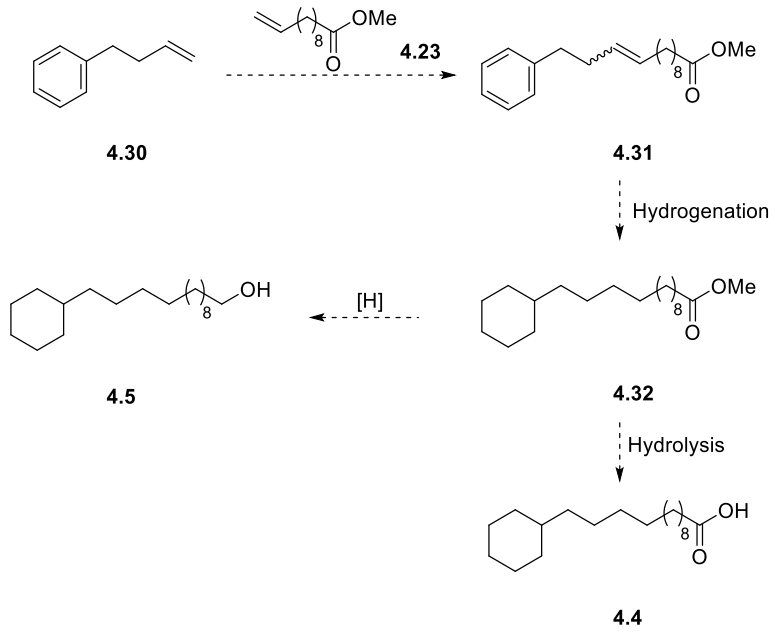

Scheme 4.17 Proposed route to amphiphile reference compounds **4.4** and **4.5**.

The synthesis began with a cross-metathesis reaction between 4-phenyl-1-butene **4.30** and methyl 10-undecenoate **4.23** (Scheme 4.18). Both alkenes **4.30** and **4.23** are of Type I, therefore they can homocouple rapidly as well as undergo cross metathesis.[23] Equilibration of the homodimers with the desired cross-metathesis product was expected to result in a statistical mixture with a maximum theoretical yield of 50% (Scheme 4.19). This anticipated yield was not considered prohibitive due to the low cost and availability of the reagents. In the event, the desired cross-metathesis product **4.31** could be separated from the homocoupled side products **4.33** and **4.34** by silica gel column chromatography and was recovered in a 39% yield.

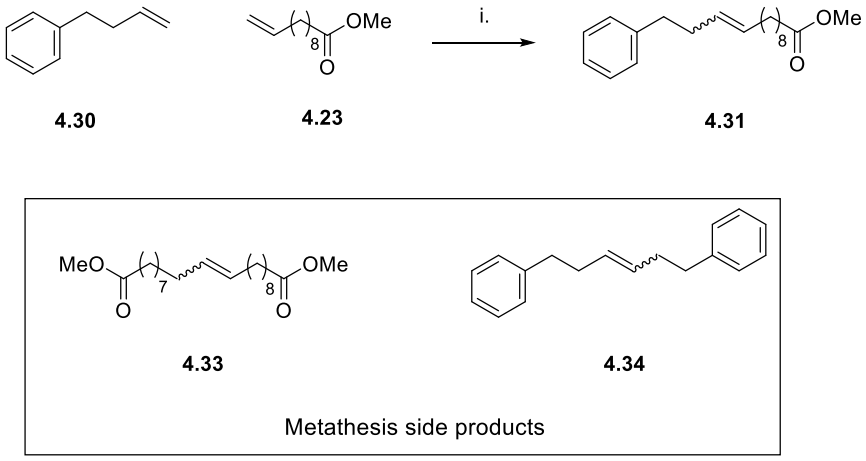

Scheme 4.18 Cross-metathesis reaction of **4.30** and **4.23** to give **4.31** and homocoupled products **4.33** and **4.34**; i. Grubbs I (5 mol%), CH_2Cl_2, 40 °C, 14 h, 39%.[23]

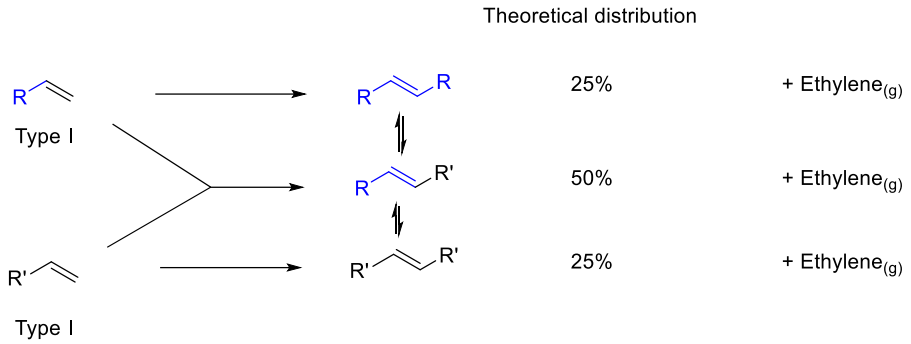

Scheme 4.19 Schematic of cross-metathesis between two Type I alkenes.[23]

Following the isolation of the desired cross-metathesis product **4.31**, a global hydrogenation reaction using Zeng's Rh catalyst was carried out to give the fully saturated ester **4.32** (Scheme 4.20).[13] This proved to be a straightforward reaction and methyl ester **4.32** was isolated in 74% yield. Ester **4.32** was then readily reduced to generate terminal alcohol **4.5** in a reaction with an excess of DIBAlH.[22] The ester **4.32** was also hydrolysed under basic conditions. An acid work up and then extraction into EtOAc gave carboxylic acid **4.4** in quantitative yield.[31]

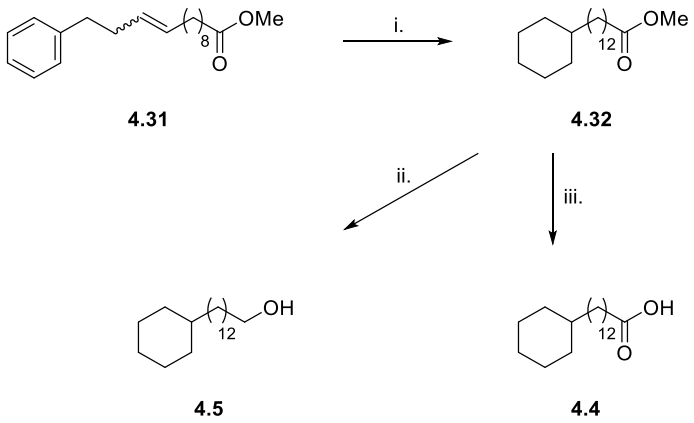

Scheme 4.20 Final steps towards hydrocarbon amphiphiles **4.4** and **4.5**; i. **2.14** (8 mol%), 4 Å MS, hexane, r.t., 14 h 74%; ii. DIBAlH, CH_2Cl_2, -78 °C to r.t., 1h, 81%; iii. NaOH, H_2O, MeOH, 65 °C, 14 h, quant.[22,31]

4.6. Langmuir isotherm analysis

With the five target compounds **4.1**-**4.5** in hand (Figure 4.14), attention then turned to Langmuir trough experiments. These were carried out during visits to the laboratory of Dr Stefan Guldin at University College London. Stock solutions of the amphiphilic compounds (**4.1**-**4.5**) were prepared in $CHCl_3$. Fatty acid **4.1** was not soluble in $CHCl_3$ therefore in that case stock solutions was prepared in a mixture of 1:1 $CHCl_3$:acetone or 9:1 $CHCl_3$:acetone. The amphiphiles were then applied to the water surface in a Langmuir trough and pressure-area isotherms where recorded.

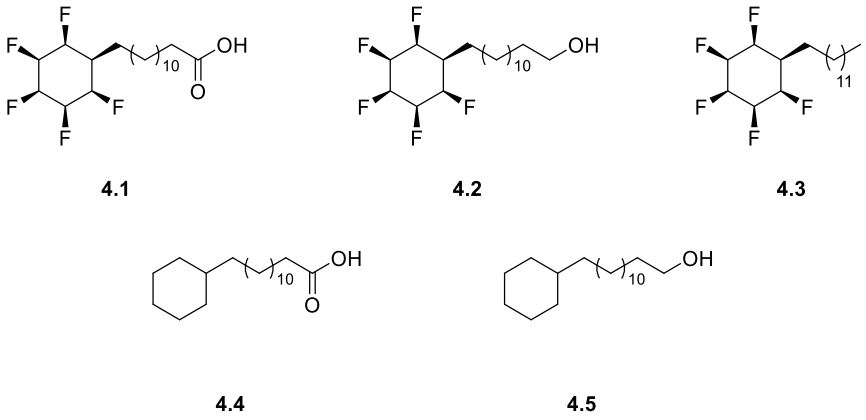

Figure 4.14 Amphiphiles prepared for Langmuir analysis.

4.6.1. Isotherms of hydrocarbon reference compounds

In the first instance, the hydrocarbon alcohol **4.5** and fatty acid **4.4** were explored. Using a microsyringe, 20 µL of a stock solution (0.89 mg/mL) of alcohol **4.5** in $CHCl_3$ was deposited at the water subphase and an isotherm was recorded. The isotherm (Figure 4.15A) shows a phase transition at a limiting area of 22 $Å^2$ per molecule (estimated by extrapolation of the constant slope region to a surface pressure of zero). Surface pressure continues to increase on further compression until a plateau at ~ 10 $Å^2$ at a surface pressure of 35 mNm^{-1}. The experiment was repeated with 30 µL of stock solution (0.89 mg/mL) and the resultant isotherm (Figure 4.15B) showed an increase in surface pressure and again a tangent to the constant slope region bisects the x-axis, this time at an area per molecule of 26 $Å^2$. The surface pressure continues to rise until a plateau at ~ 15 $Å^2$ at a surface pressure of 36 mNm^{-1}. The increases in surface pressure in these isotherms indicate a phase transition at a molecular area of 22-26 $Å^2$ which is consistent with the formation of a monolayer. By comparison, the phase transition associated with monolayer formation in stearic acid (octadecanoic acid) has been experimentally reported at an area per molecule of 19-24 $Å^2$.[32–34]

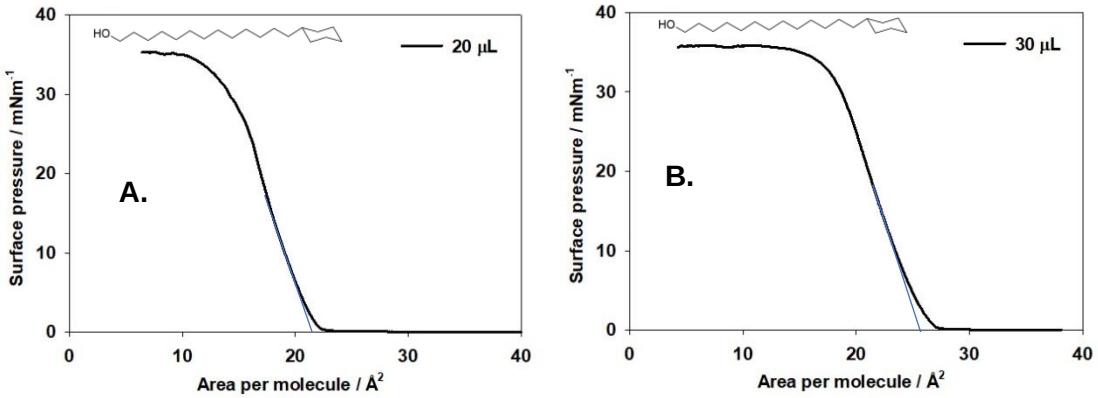

Figure 4.15 A. Langmuir isotherm obtained for 20 µL of alcohol **4.5**; **B.** Langmuir isotherm obtained for 30 µL of alcohol **4.5**.

By modelling stearic acid as a cylinder (Figure 4.16A) in the manner described by Petty,[10] the reported area per molecule at monolayer formation (19-24 Å^2)[32–34] can be used to estimate the cross sectional radius r = 2.5-2.8 Å (by $A_{monolayer} = \pi r^2$) . This is half the centre-centre distance between molecules in a compressed monolayer (5.0-5.6 Å, Figure 4.16B). A similar analysis of the phase transition for alcohol **4.5** (at 22-26 Å^2 per molecule) indicates a similar molecular radius (2.7-2.9 Å, Figure 4.16C) and a centre-centre distance of molecules also consistent with a monolayer (5.4-5.8 Å, Figure 4.16D).

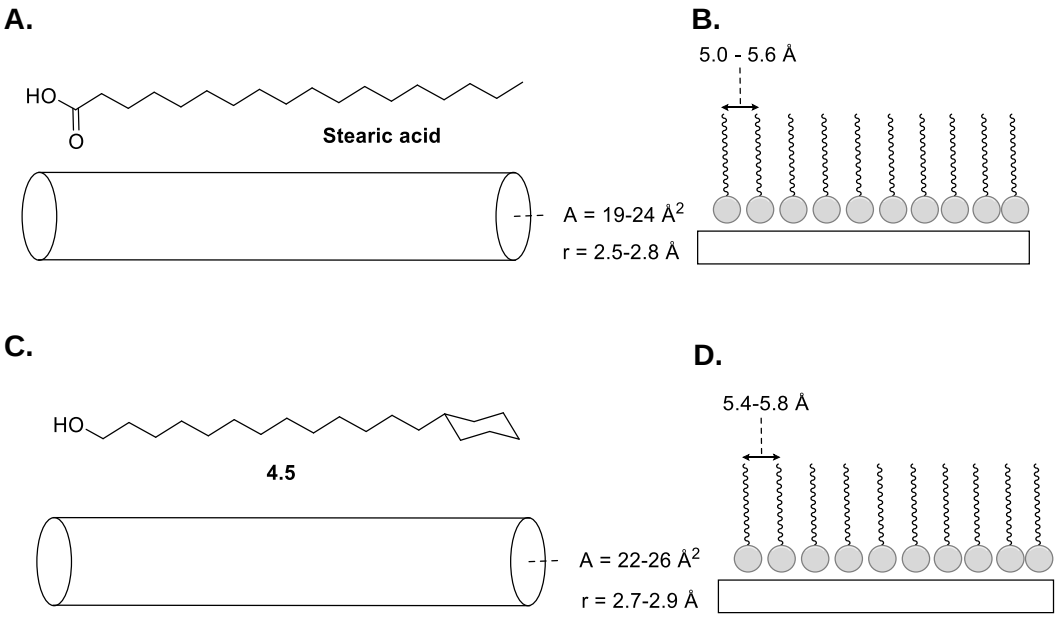

Figure 4.16. **A**. Approximation of 2D molecular area of stearic acid by modelling molecular geometry as a cylinder. **B**. Illustration of a monolayer formation of stearic acid. **C**. Approximation of 2D molecular area of **4.5** by modelling molecular geometry as a cylinder. **D**. Illustration of monolayer formation of **4.5**.

Following the finding of monolayer formation for reference compound **4.5**, a similar pair of experiments was conducted for the reference fatty acid **4.4.** In the first instance, 30 µL of a

stock solution (0.32 mg/mL) of acid **4.4** in $CHCl_3$ was deposited on the water subphase using a microsyringe. The isotherm (Figure 4.17A) shows a more gradual increase in surface pressure beginning at 35 $Å^2$ (indicating the formation of a liquid-expanded phase) and a tangent to the constant slope region bisects the x-axis at an area per molecule = 31 $Å^2$ (at the condensed monolayer phase). The surface pressure continues to increase on further compression until a decline, indicating that a structural collapse occurs, from the peak surface pressure of 16 mNm^{-1} at an area per molecule of 26 $Å^2$. The surface pressure plateaus until a second phase transition is observed with an increase in pressure at a limiting area per molecule = 11 $Å^2$. The surface pressure continues to increase until it begins to plateau around 30 mNm^{-1}. The experiment was repeated was 100 µL of stock solution (0.32 mg/mL) and the resultant isotherm (Figure 4.17B) also showed a gradual increase in surface pressure beginning at 34 $Å^2$ (indicating the formation of a liquid-expanded phase) but with a tangent to the constant slope region which bisects the x-axis at an area per molecule of 29 $Å^2$. This indicated the formation of the condensed monolayer phase. The surface pressure continues to increase on further compression until a decline occurs from the peak at 21 mNm^{-1} and at an area per molecule of 23 $Å^2$. The surface pressure plateaus until a second phase transition is observed through an increase in surface pressure where a tangent to the constant slope region bisects the x-axis at an area per molecule = 14 $Å^2$, consistent with bi- or multi-layer formation.

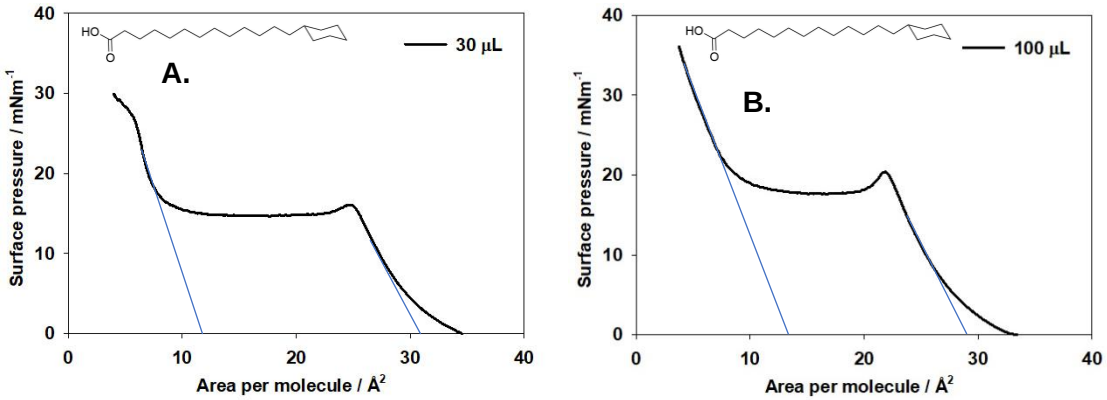

Figure 4.17 A. Langmuir isotherm of unfluorinated carboxylic acid **4.4** (30 µL); **B**. Langmuir isotherm of unfluorinated carboxylic acid **4.4** (100 µL).

Modelling acid **4.4** as a cylinder (Figure 4.18A), the molecular radius calculated from the first phase transition (3.0-3.1 Å) gives a molecule-molecule distance of 6.0-6.2 Å consistent with a monolayer. The second phase transition which occurs at an area per molecule of 11-14 $Å^2$ is less than half but more than a third of the area per molecule at monolayer transition and corresponds to a less well defined multilayer phase as illustrated in Figure 4.18C.

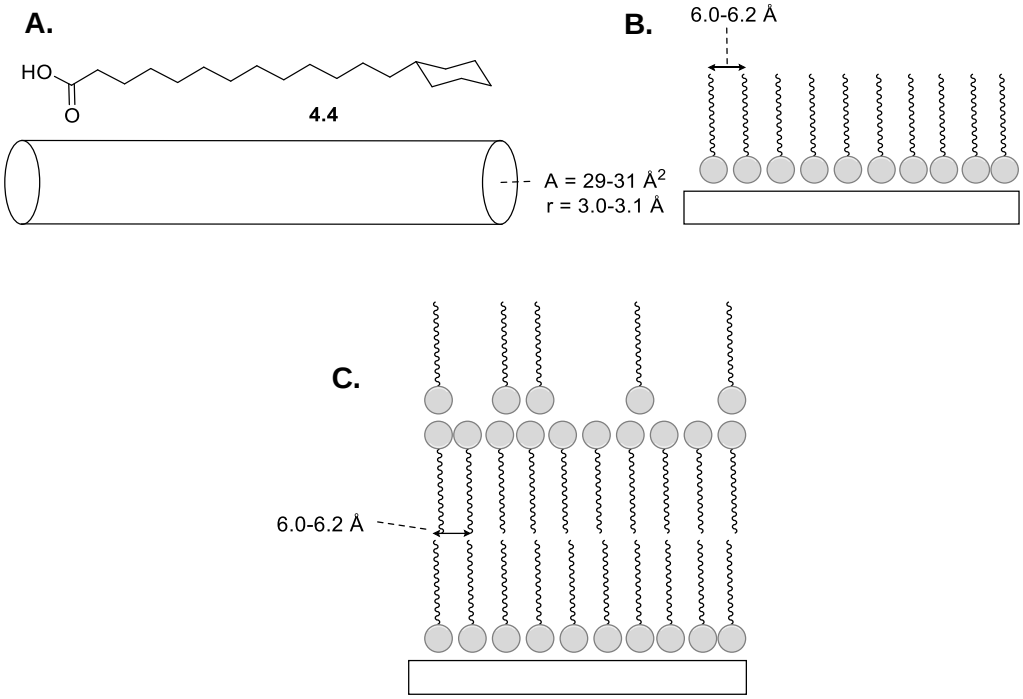

Figure 4.18 A. Approximation of 2D molecular area of **4.4** by modelling molecular geometry as a cylinder. **B**. Illustration of monolayer formation of **4.4**. **C**. Putative multilayer structure formed at second phase transition.

4.6.2. Langmuir isotherms of the 'Janus' ring containing amphiphiles

Langmuir analysis of the fluorinated alcohol **4.2** was explored. Isotherms were generated following the deposition of a stock solution of **4.2** (1.25 mg/mL) in $CHCl_3$ to the water subphase, applied manually by microsyringe. The first isotherm (analyte volume = 20 µL, Figure 4.19A) showed a gradual increase in surface pressure beginning at 25 $Å^2$, with the formation of a liquid-expanded phase. As the pressure increased a tangent to the constant slope region bisects the x-axis at an area per molecule of 13 $Å^2$, the surface pressure then continues to increase to 16 mNm^{-1}. This phase transition was observed again in three more isotherms of analyte volume = 25, 35 and 40 µL and in each case similar areas per molecule of 14-16 $Å^2$ (Figure 4.19B, 4.19C and 4.19D) were observed. For the two isotherms with analyte volume = 35 and 40 µL (Figure 4.19C and 4.19D) a second phase transition was observed both at 7 $Å^2$ with surface pressure reaching a maximum 32 mNm^{-1} and 38 mNm^{-1} respectively.

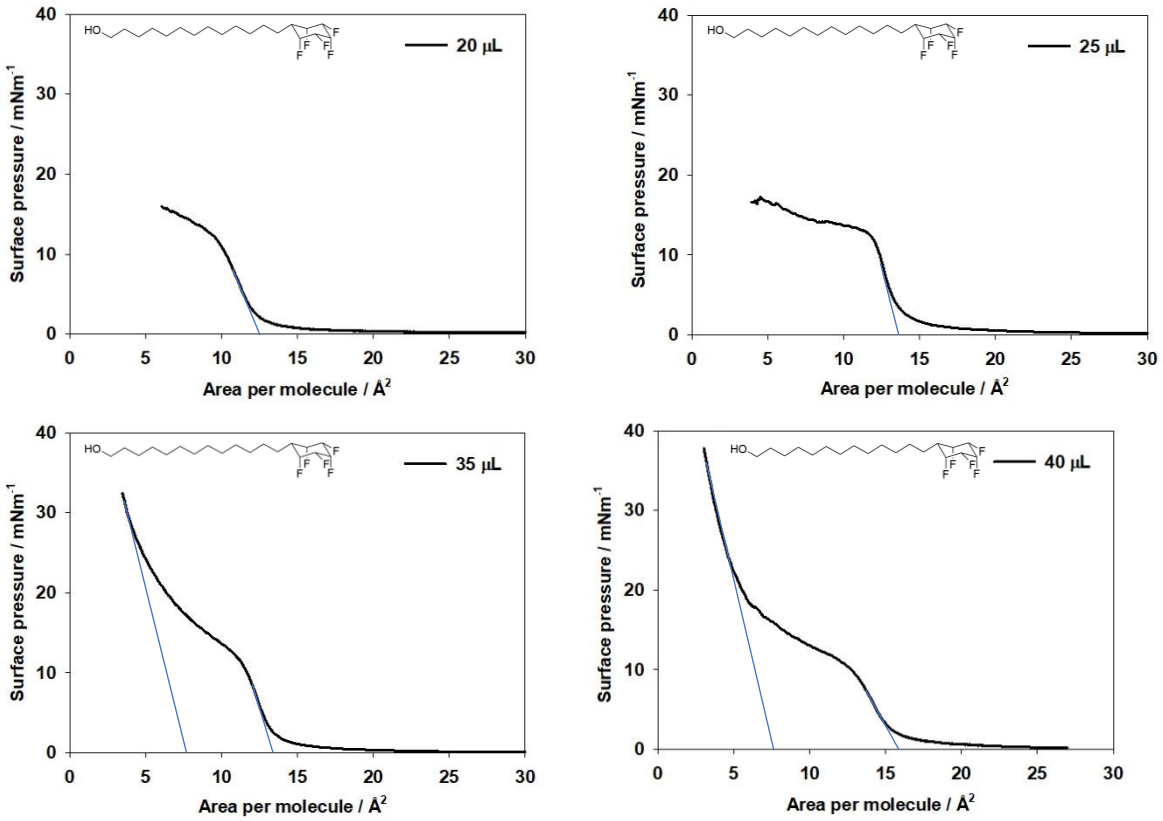

Figure 4.19 Langmuir isotherms obtained for fluorinated alcohol **4.2 A.** Analyte volume = 20 µL; **B**. Analyte volume = 25 µL; **C**. Analyte volume = 35 µL; **D**. Analyte volume = 40 µL.

The first phase transition of **4.2** which occurs at 13-16 Å^2 is too condensed to represent a monolayer at about half the value of the first phase transition for the hydrocarbon reference compounds **4.2** and **4.2**. The area is much more consistent with formation of a bilayer (Figure 4.20A). This is presumably a consequence of the attraction between 'Janus' rings and evidence of pre-aggregation assembly.

Again, modelling the geometry of **4.2** as a cylinder (Figure 4.20B) and assuming bilayer formation, the cross-sectional radius that is obtained (from $A_{per\ molecule\ at\ bilayer} = \frac{\pi r^2}{2}$) is r = 2.9-3.2 Å. A re-examination the X-ray crystal structure (Figure 4.20C) indicates that the intermolecular distance between chemically equivalent atoms in **4.2** is 5.5-5.6 Å, and this is consistent with bilayer formation at 13-16 Å^2 per molecule. The second phase transition of **4.2** which occurs at an area per molecule at 7 Å^2 may be indicative of more compressed higher order multilayer phases.

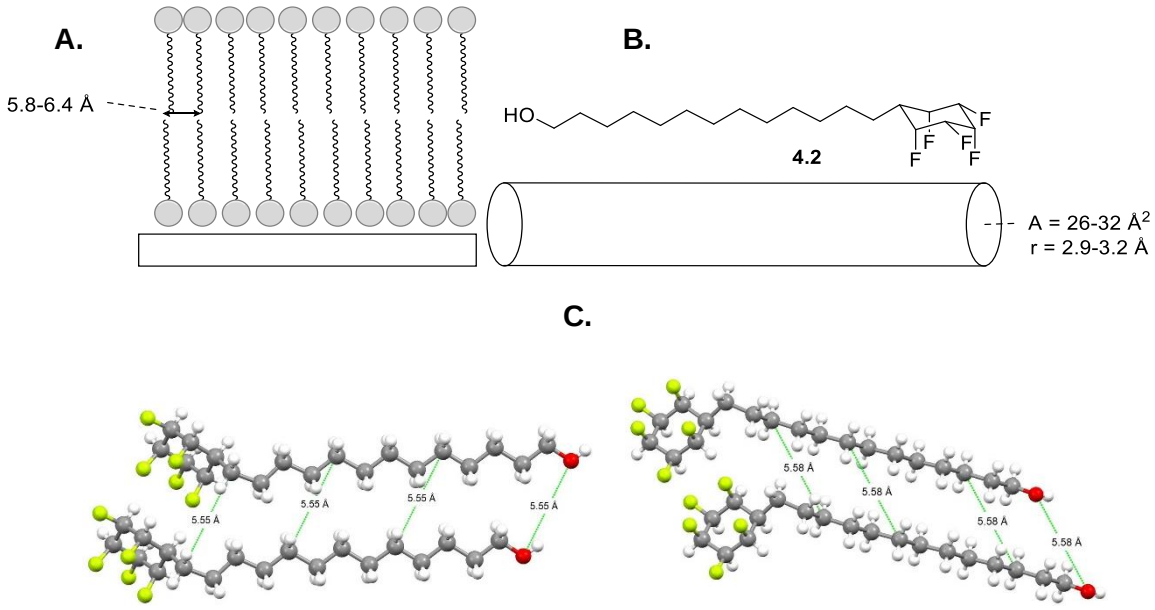

Figure 4.20 **A**. Representation of bilayer structure of **4.2** at area per molecule = 13-16 Å^2; **B**. Approximation of 2D molecular area of **4.2** by modelling molecular geometry as a cylinder; **C**. Separation in the solid state packing of **4.2** between chemically equivalent atoms of 5.5-5.6 Å.

The alcohol **4.2**, self-assembled into a bilayer structure immediately after deposition from a solution in $CHCl_3$. This is presumably due to the attractive electrostatic interactions between 'Janus' rings. To further probe this self-assembly behaviour, the Langmuir isotherm experiment with **4.2** was repeated, but with acetone as a co-solvent (10% by volume). The resultant isotherm (Figure 4.21) showed a new phase transition at an area per molecule of 24 Å^2, twice that observed previously and representative of an initial monolayer. On further compression the monolayer collapsed and the now familiar transition to a bilayer occurred at 11 Å^2. Evidently, the polar acetone molecules interrupt the attractive interactions between the 'Janus' rings and disperse pre-aggregated assemblies after deposition at the water subphase.

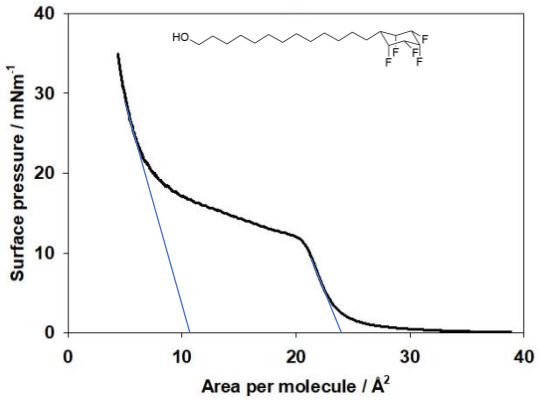

Figure 4.21 Langmuir isotherm of **4.2** with 10% acetone additive.

Having observed the formation of a monolayer after the deposition of **4.2** in a solution containing acetone, the stability of the monolayer was probed by a cycle of repeated compressions and expansions (Figure 4.22). Unstable monolayers are known to display hysteresis during cycles due to molecular reorganisation to more stable phases.[35,36] The expansion and compression cycles showed no recurrence of the monolayer phase indicating that its stability is low and that reorganisation to multilayer phases had occurred.

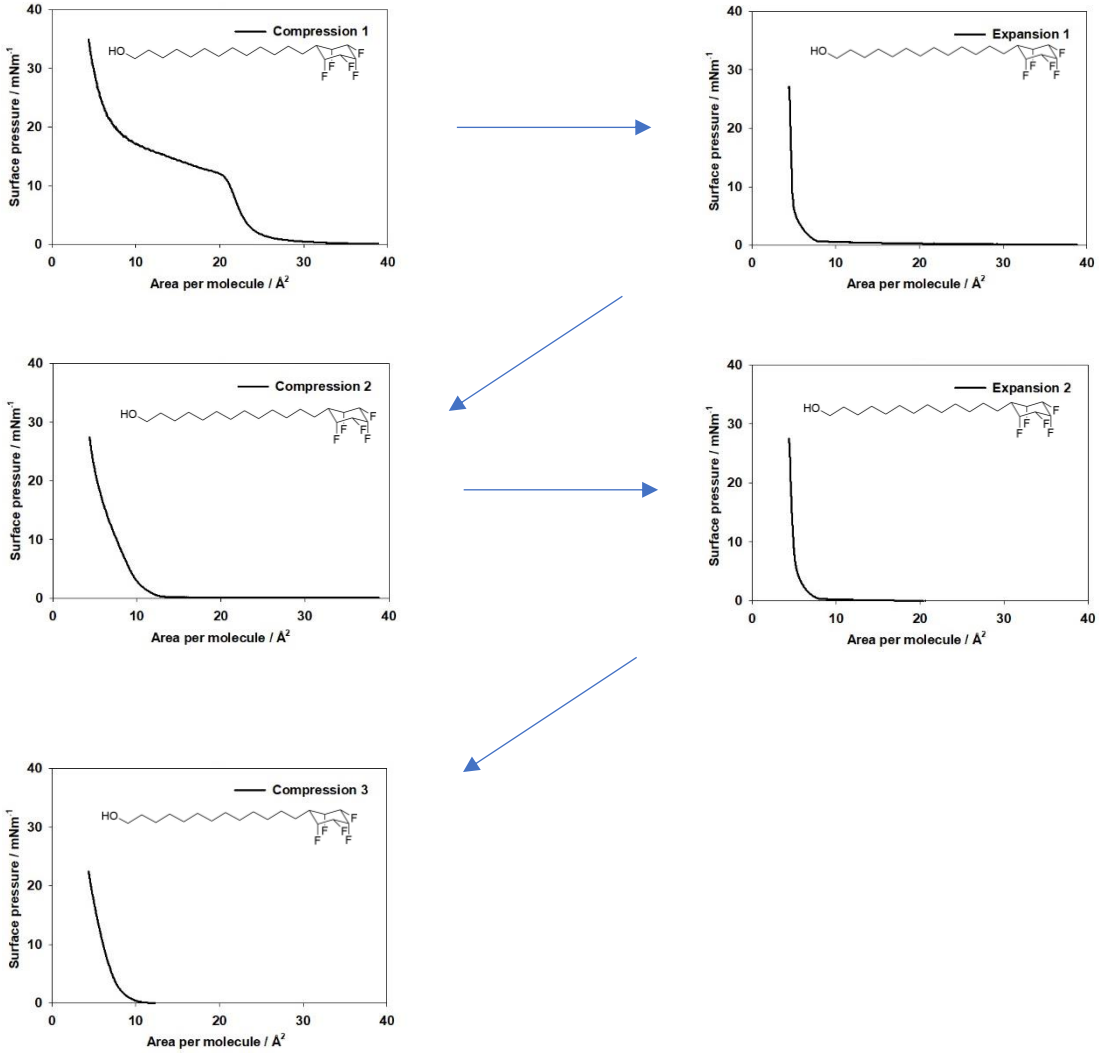

Figure 4.22 Langmuir isotherms of fluorinated alcohol **4.2** with 10% acetone added showing hysteresis on repeated compression/expansion cycles.

The phase behaviour of the fluorinated carboxylic acid **4.1** was now explored. This proved immediately problematic because **4.1** was poorly soluble in $CHCl_3$. In Langmuir isotherm experiments, the analyte is typically dissolved in water immiscible solvents such as $CHCl_3$ or benzene.[37] This ensures that the amphiphile spreads across the water surface without being lost into the bulk of the subphase via dissolution. While **4.1** was soluble in polar solvents such

as acetone and methanol, no solvent could be found that was both immiscible with water and capable of dissolving carboxylic acid **4.1**. Therefore, in the first instance a homogeneous solution of **4.1** in a 1:1 acetone:$CHCl_3$ mixture was prepared. It was envisioned that the high $CHCl_3$ content of the solution would preserve enough immiscibility to achieve deposition without substantial loss to the bulk. Even so, care was taken to deposit **4.1** at the subphase by controlled addition with the use of a syringe pump to minimise losses. The langmuir isotherm of carboxylic acid **4.1** (Figure 4.23) was recorded following the deposition of 50 µL of solution (0.65 mg/mL). This showed a sharp increase in the surface pressure beginning at 10 $Å^2$ per molecule. A tangent to the constant slope region bisects the x-axis at an area per molecule of 7 $Å^2$. This value indicates a significant level of pre-aggregation and multilayer formation, just as observed for alcohol **4.2**. The area per molecule at the phase transition is too compressed to result from a coherent bilayer and indicates higher order multilayer formation. Alternatively, despite careful application of the analyte to the subphase, the acetone content may have resulted in some material dissolution into the bulk, which would also lower the average value for the area per molecule.

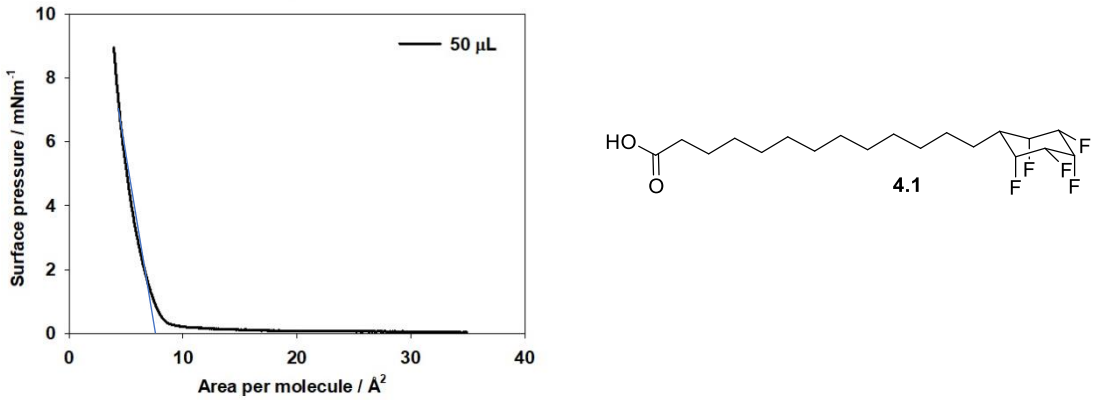

Figure 4.23 Langmuir isotherm of fluorinated carboxylic acid **4.1** (50 µL, 1:1 acetone:$CHCl_3$).

To investigate the effect of a lower acetone content on the isotherm of carboxylic acid **4.1**, a second solution of **4.1** was prepared in 9:1 $CHCl_3$:acetone. It was expected that a reduced acetone content might result in a more expanded isotherm if miscibility with the aqueous bulk was a factor with higher acetone content. However, the preparation of this solution was also challenging and required extensive sonication to achieve homogeneity due to the poor solubility of **4.1** in $CHCl_3$. Two isotherms of similar shape were obtained (Figure 4.24). In both isotherms a gradual increase in the surface pressure was observed indicating a liquid-expanded phase. Tangents drawn from the constant slope region bisect the x-axis at areas per molecule of 13 and 19 $Å^2$ respectively. In both cases phase transition occurred at a higher area per molecule than was recorded for the solution in 1:1 acetone:$CHCl_3$ but, the transitions remain significantly lower than an area per molecule that would be expected for a monolayer.

Across the three isotherms obtained for **4.1**, a large range of area per molecule values at phase transition was observed (7-19 Å^2). This range is attributed to the poor solubility of **4.1** in $CHCl_3$ and the tendency for acetone to cause analyte loss into the bulk subphase through dissolution. Furthermore, the solvent dependence on phase behaviour was demonstrated previously from the perturbation of self-assembly observed for the isotherm of alcohol **4.2** when acetone was used as an additive (Figure 4.21). Nonetheless, there was no evidence for monolayer formation in the isotherms of carboxylic acid **4.1** and further evidence for pre-aggregation due to the attractive interactions between 'Janus' rings is consistent with these isotherms (Figure 4.23 and 4.24).

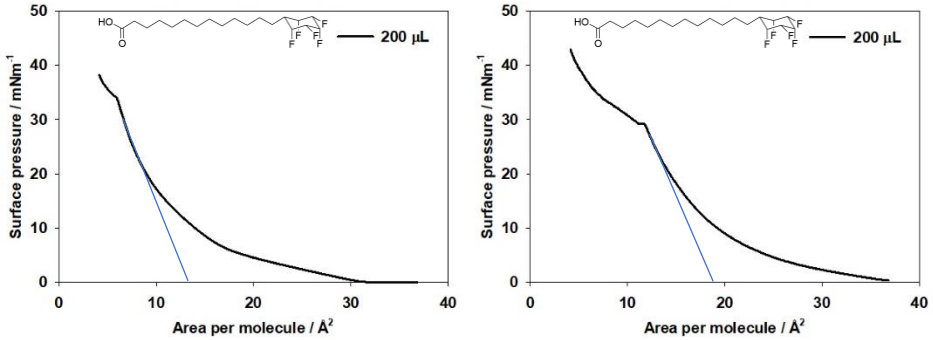

Figure 4.24 Langmuir isotherms of carboxylic acid **4.1** from a solution of 9:1 $CHCl_3$:acetone.

In order to assess the strength of any possible interaction between 'Janus' rings and water molecules, surface pressure-area isotherms were also recorded for the methyl terminated alkane **4.3**. It was anticipated that **4.3** may interact with the water subphase through electrostatic interactions and non-classical hydrogen bonds to the 'Janus' ring (Figure 4.25). Amphiphiles capable of forming monolayers and related structures in Langmuir experiments have both a hydrophobic region which prevents dissolution and a hydrophilic region which promotes dissolution. The balance of the properties leads to the phase behaviours already explored.

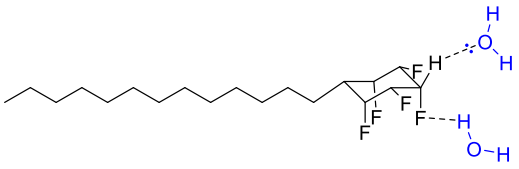

4.3

Figure 4.25 Predicted interactions between 'Janus' ring of **4.3** and water molecules.

Isotherms were obtained by deposition of 25, 30, 35 and 40 µL of a stock solution of **4.3** (1.34 mg/mL) in $CHCl_3$ at the water subphase by microsyringe and these are illustrated in Figure 4.26. Three of these isotherms (v = 25, 30 and 35 µL; Figure 4.26A, 4.26B and 4.26C)

show phase transition at areas per molecule with values in the range of 26-30 Å^2. These are clearly associated with monolayer formation. However, the isotherm at v = 40 µL (Figure 4.26D showed a slightly more compressed phase transition at an area per molecule of 21 Å^2 which is less than expected for a monolayer. Though monolayer formation was observed for **4.3** in three of the isotherms, the deviation from this behaviour in one isotherm raises questions regarding reproducibility of the experiments and the nature of the proposed interactions of the 'Janus' ring with water (Figure 4.26). If the attraction between the 'Janus' ring and water molecules is significantly weaker than between a typical hydrogen bond donor and acceptor, **4.3** may be more weakly bound to the water subphase which would explain the variation in phase behaviour. Nonetheless, evidence for an interaction between the 'Janus' ring and water has been established from these results although further characterisation of the nature of this interaction is required.

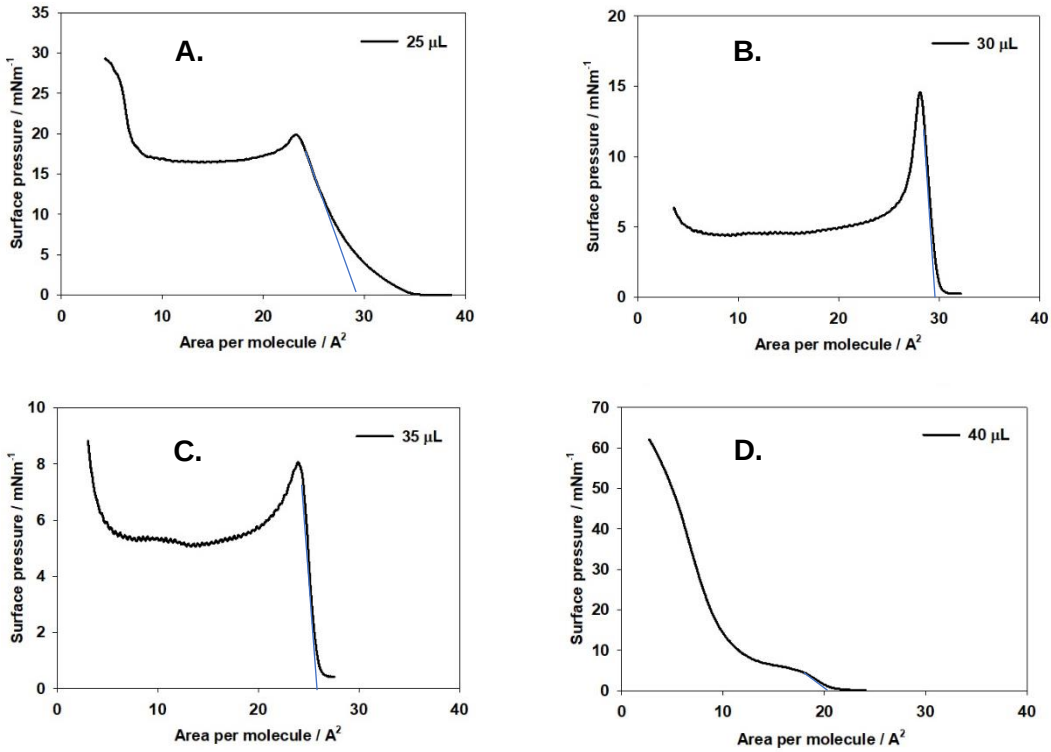

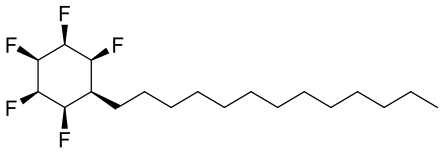

4.3

Figure 4.26 Langmuir isotherms of fluoroalkane **4.3** for various volumes of analyte **A.** Analyte volume = 25 µL; **B**. Analyte volume = 30 µL; **C**. Analyte volume = 35 µL; **D**. Analyte volume = 40 µL.

4.7. Conclusions

In this Chapter, a series of 'Janus' ring containing amphiphiles were prepared as well as their non-fluorinated reference compounds. Evaluation of several of the X-ray crystal structures of these compounds has provided an insight into their packing in the solid phase. The electrostatic interactions between opposite faces of 'Janus' rings was evident in the examination of all of these crystal structures by close intermolecular fluorine-hydrogen contacts (< sum of the VdW radii). A series of surface pressure-area (Langmuir) isotherms were recorded on a water subphase for these amphiphiles, and for hydrocarbon reference compounds. The rare occurrence of monolayer behaviour and repeated observation of spontaneous aggregations to bilayer and multilayer phases is attributed to the attraction between the 'Janus' rings. No spontaneous pre-aggregation to these phases was ever observed for the non-fluorinated reference compounds. The influence of solvent choice to phase behaviour was probed using different $CHCl_3$ to acetone ratios. Although further study could be carried out to explore the nature of these interactions it is clear that the 'Janus' rings are very significantly prone to pre-aggregation.

4.8. References

[1] A. P. Dobbs, M. R. Kimberley, *J. Fluor. Chem.* **2002**, *118*, 3–17.

[2] E. De Wolf, G. Van Koten, B. J. Deelman, *Chem. Soc. Rev.* **1999**, *28*, 37–41.

[3] G. J. Puts, P. Crouse, B. M. Ameduri, *Chem. Rev.* **2019**, *119*, 1763–1805.

[4] Z. He, F. Rault, M. Lewandowski, E. Mohsenzadeh, F. Salaün, *Polymers*, **2021**, *13*, 174.

[5] N. S. Keddie, A. M. Z. Slawin, T. Lebl, D. Philp, D. O'Hagan, *Nat. Chem.* **2015**, *7*, 483–488.

[6] D. O'Hagan, *Chem. Soc. Rev.* **2008**, *37*, 308–319.

[7] S. M. Pratik, A. Nijamudheen, A. Datta, *ChemPhysChem* **2016**, 2373–2381.

[8] P. Dynarowicz-Łątka, A. Dhanabalan, O. N. Oliveira, *Adv. Colloid Interface Sci.* **2001**, *91*, 221–293.

[9] C. M. Knobler, R. C. Desai, *Annu. Rev. Phys. Chem.* **1992**, *43*, 207–236.

[10] M. C. Petty, *Langmuir-Blodgett Films An Introduction*, Cambridge University Press, Cambridge, **1996**.

[11] E. A. El-Hefian, M. Misran, A. H. Yahaya, *Maejo Int. J. Sci. Technol.* **2009**, *3*, 277–286.

[12] A. R. Lewis, K. P. Reber, *Tetrahedron Lett.* **2016**, *57*, 1083–1086.

[13] M. P. Wiesenfeldt, Z. Nairoukh, W. Li, F. Glorius, *Science*, **2017**, *357*, 908–912.

[14] J. R. Al Dulayymi, M. S. Baird, E. Roberts, *Tetrahedron* **2005**, *61*, 11939–11951.

[15] T. Fortunati, M. D'Acunto, T. Caruso, A. Spinella, *Tetrahedron* **2015**, *71*, 2357–2362.

[16] W. Wang, A. Clay, R. Krishnan, N. J. Lajkiewicz, L. E. Brown, J. Sivaguru, J. A. Porco, *Angew. Chem. Int. Ed.* **2017**, *56*, 14479–14482.

[17] D. Villemin, F. Simeon, H. Decreus, P. A. Jaffres, *Phosphorus, Sulfur Silicon Relat. Elem.* **1998**, *133*, 209–213.

[18] X. Qiu, S. Ong, C. Bernal, D. Rhee, C. Pidgeon, *J. Org. Chem.* **1994**, *59*, 537–543.

[19] J. E. Baldwin, R. M. Adlington, S. H. Ramcharitar, *J. Chem. Soc. Chem. Commun.* **1991**, *48*, 940–942.

[20] S. S. Babu, V. K. Praveen, S. Prasanthkumar, A. Ajayaghosh, *Chem. Eur. J.* **2008**, *14*, 9577–9584.

[21] Z. Fei, D. Zhao, T. J. Geldbach, R. Scopelliti, P. J. Dyson, *Chem. Eur. J.* **2004**, *10*, 4886–4893.

[22] J. Louvel, J. F. S. Carvalho, Z. Yu, M. Soethoudt, E. B. Lenselink, E. Klaasse, J. Brussee, A. P. Ijzerman, *J. Med. Chem.* **2013**, *56*, 9427–9440.

[23] A. K. Chatterjee, T. L. Choi, D. P. Sanders, R. H. Grubbs, *J. Am. Chem. Soc.* **2003**, *125*, 11360–11370.

[24] T. W. Johnson, E. J. Corey, *J. Am. Chem. Soc.* **2001**, *123*, 4475–4479.

[25] P. Korinkova, V. Bazgier, J. Oklestkova, L. Rarova, M. Strnad, M. Kvasnica, *Steroids* **2017**, *127*, 46–55.

[26] L. I. Zakharkin, I. M. Khorlina, *Tetrahedron Lett.* **1962**, *3*, 619–620.

[27] J. A. Bisceglia, L. R. Orelli, *Curr. Org. Chem.*, **2015**, 19, 744–775

[28] J. A. K. Howard, V. J. Hoy, D. O'Hagan, G. T. Smith, *Tetrahedron* **1996**, *52*, 12613–12622.

[29] J. D. Dunitz, R. Taylor, *Chem. Eur. J.* **1997**, *3*, 89–98.

[30] C. R. Groom, I. J. Bruno, M. P. Lightfoot, S. C. Ward, *Acta Crystallogr. Sect. B Struct. Sci. Cryst. Eng. Mater.* **2016**, *72*, 171–179.

[31] R. J. DeVita, R. Bochis, A. J. Frontier, A. Kotliar, M. H. Fisher, W. R. Schoen, M. J. Wyvratt, K. Cheng, W. W. S. Chan, B. Butler, T. M. Jacks, G. J. Hickey, K. D. Schleim, K. Leung, Z. Chen, S. H. Lee Chiu, W. P. Feeney, P. K. Cunningham, R. G. Smith, *J. Med. Chem.* **1998**, *41*, 1716–1728.

[32] C. McFate, D. Ward, J. Olmsted, *Langmuir* **1993**, *9*, 1036–1039.

[33] K. Ray, D. Bhattacharjee, T. N. Misra, *J. Chem. Soc. Faraday Trans.* **1997**, *93*, 4041–4045.

[34] A. Ulman, *An Introduction to Ultrathin Organic Films: From Langmuir-Blodgett to Self-Assembly*, Academic Press Inc., San Diego, **2013**.

[35] P. Dynarowicz-Łątka, A. Dhanabalan, O. N. Oliveira, *J. Phys. Chem. B* **1999**, *103*, 5992–6000.

[36] A. M. Barros, A. Dhanabalan, C. J. L. Constantino, D. T. Balogh, O. N. Oliveira, *Thin Solid Films* **1999**, *354*, 215–221.

[37] K. Ariga, Y. Yamauchi, T. Mori, J. P. Hill, *Adv. Mater.* **2013**, *25*, 6477–6512.

5. Conclusions and future work

5.1. Conclusions

In this work a library of ‘Janus’ ring building blocks were prepared (Chapter 2). The utility of these has been demonstrated by their elaboration to higher order molecular structures in Chapter 3. The potential for ‘Janus’ rings to be used as arene isosteres has been established with an accompanying reduction in Log P observed. Evidence for molecular self-assembly has been observed through the Langmuir isotherms presented in Chapter 4 and this presents an exciting avenue for future work in supramolecular chemistry.

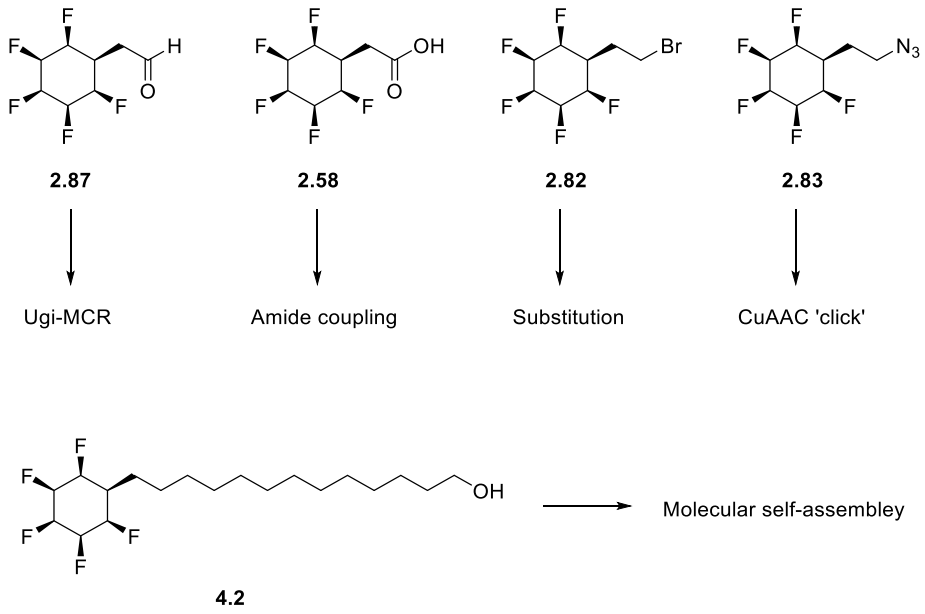

Figure 5.1 Synthetic utility of novel ‘Janus’ ring building blocks.

5.2. Future work

5.2.1. Further investigation of the applications of the ‘Janus’ ring to Medicinal Chemistry

The polar ‘Janus’ ring has a reducing effect on molecular Log P relative to aryl analogues as established in Chapter 3. Preliminary investigations conducted by Prof. Cormac Murphy and Dr Mohd Khan have indicated that the ‘Janus’ ring system is inert to metabolism by P450 monooxygenases. In these experiments, carboxylic acid **2.58**, methyl ester **2.60** and alcohol **2.81** were incubated with cultures of *Cunninghamella elegans* which has been reported as a fungal model of mammalian drug metabolism.[1] Likewise, incubations of **2.58**, **2.60** and **2.81** in the related organism *Cunninghamella echinulata* did not result in observed metabolism of

the ‘Janus’ ring. The apparent metabolic stability of the ‘Janus’ ring may facilitate its incorporation into candidate drug molecules as an isostere of other ring systems.

To further investigate the use of the ‘Janus’ ring as an isostere, future work will seek to replace ring systems in known drugs and drug candidates with the ‘Janus’ rings. For example, the advanced antituburcular agent lead **5.1** has an MIC (minimum inhibitory concentration) of 0.06 μgmL^{-1} for its target protein *Mtb*-FtsZ.[2] As **5.1** bears a cyclohexane group, it is an obvious target for isosteric replacement with a Janus ring. The pentafluorocyclohexyl analogue **5.2** could be readily prepared from the previously synthesised ‘Janus’ ring alcohol **2.47** according to the retrosynthetic analysis illustrated in Figure 5.2.

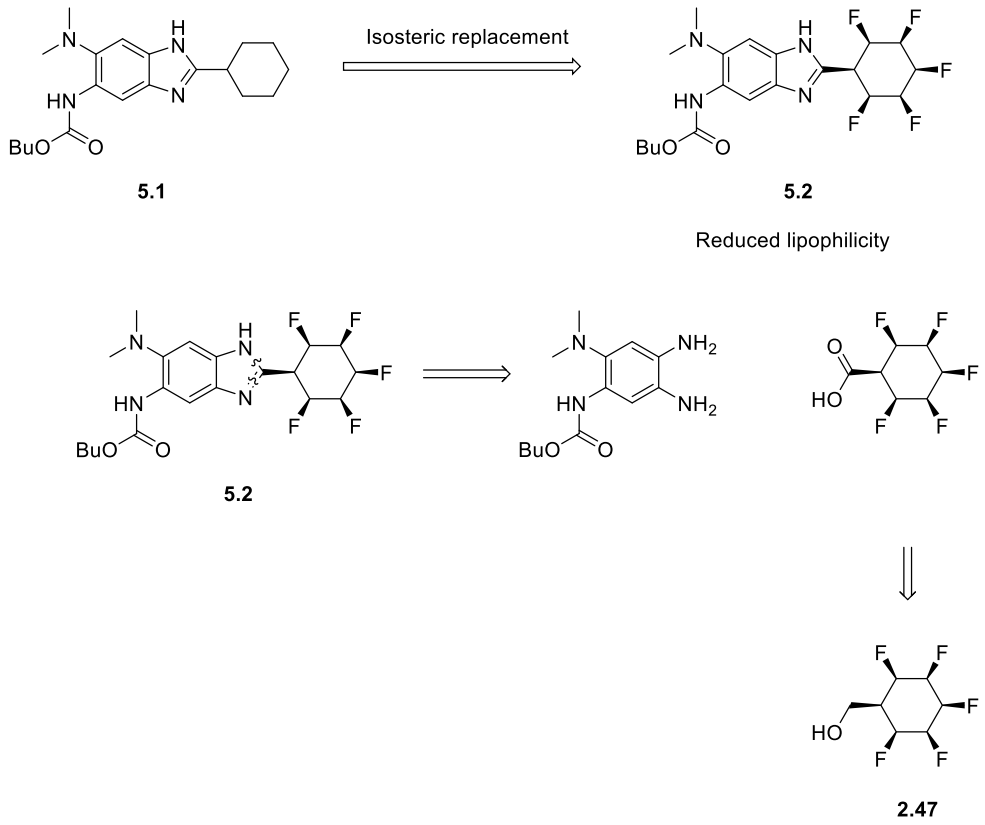

Figure 5.2 Proposed retrosynthesis of antituburcular agent analogue **5.2**.

Following the preparation of **5.2**, binding affinity to *Mtb*-FtsZ could be measured by the FtsZ polymerisation inhibitory assay study reported previously. The facial polarisation of the ‘Janus’ ring system is unlike motifs found in nature and ‘Janus’ rings may have unique binding interactions to amino acids particularly those with charged side chain residues. These may be expected to increase binding affinity to certain targets. To understand the nature of these interactions a better understanding of the interactions between the polar ‘Janus’ ring and proteins is required to establish the value of the motif for medicinal chemistry. This could be

achieved by examination of the X-ray crystal structure of a protein and a bound 'Janus' ring-bearing substrate such as **5.2**.

5.2.2. Metal-organic frameworks (MOFs)

Metal organic frameworks are porous, crystalline materials composed of metal ions and organic linkers. Their potential applications are extensive and include gas storage for clean energy and medical uses. For example, MIL-53 (Sc) is a MOF composed of ScO_6 nodes and 1,4-benzodicarboxylic acid **3.46** and is capable of adsorbing CO_2. Carbon capture and storage is of great research interest due to the potential mitigating effects for global warming. The 'Janus' ring bearing 1,4-benzodicarboxylic acid derivative **3.49** which was synthesised in Chapter 3 will be investigated as an organic linker for analogous MOFs to MIL-53 (Sc) for gas adsorption. Similarly, Stam-17-OEt (Cu) is a MOF composed of 5-ethoxyisophthalic acid **3.47** and Cu (II) paddlewheel dimers and is known for its ability to adsorb the toxic gas ammonia. The diacid **5.3** could be prepared by the hydrolysis of its parent diester **3.50** which has been reported in Chapter 3. The polarised 'Janus' ring may display an additional binding strength to ammonia due to the electrostatic attraction between the electronegative Nitrogen atom and the electropositive protic face of the ring as illustrated in Figure 5.3.[3,4]

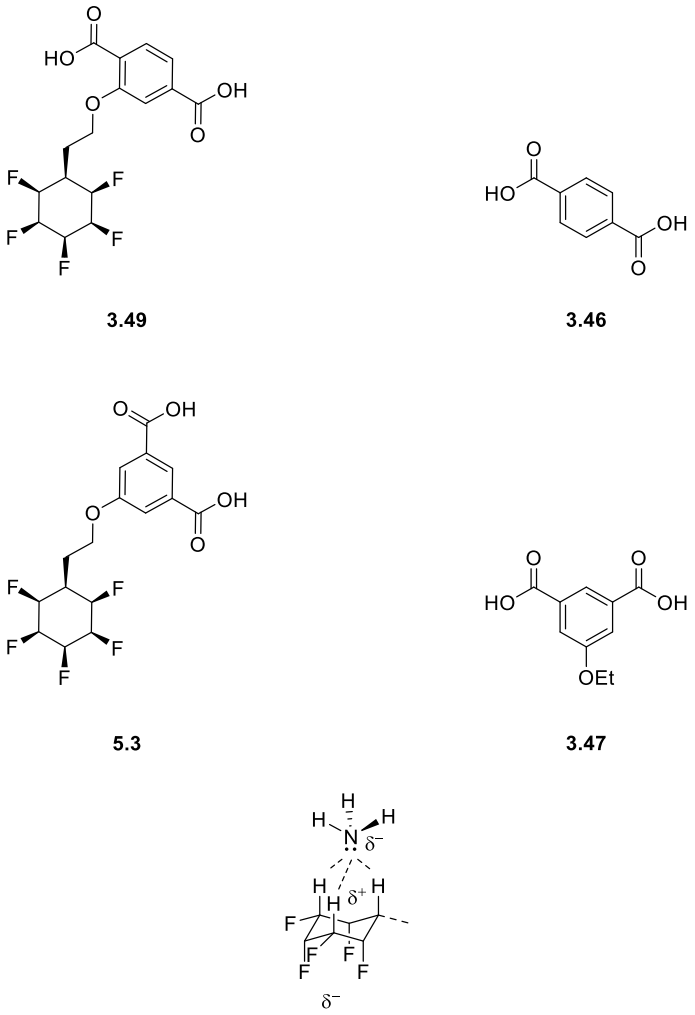

Figure 5.3 Proposed candidate MOF linkers and proposed interactions between the electropositive 'Janus' ring face and ammonia.

5.2.3. Liquid crystals

Modern vertical alignment (VA) liquid crystal displays (LCDs) require materials with a net molecular dipole moment perpendicular to the long molecular axis which results in a negative dipolar anisotropy ($\Delta\varepsilon < 0$). The use of the carbon-fluorine bond to induce such dipole moments in liquid crystals has generated significant research interest. Examples of previously reported candidate fluorinated liquid crystals are given in Figure 5.4.[5-7] The selective axial monofluorination of cyclohexane rings resulted in the negative dipolar anisotropy in **5.4**-**5.6**. Multi-fluorinated 'Janus' ring analogues of **5.6** (**5.7**-**5.9**) were previously synthesised by the St Andrews group but $\Delta\varepsilon$ values could not be recorded as poor solubility in the test host mixture was observed. The poor solubility of **5.7**-**5.9** was attributed partly to electrostatic interactions between the 'Janus' rings and the aryl groups (observed by X-ray crystallography) and also to insufficient alkyl solubilising groups.

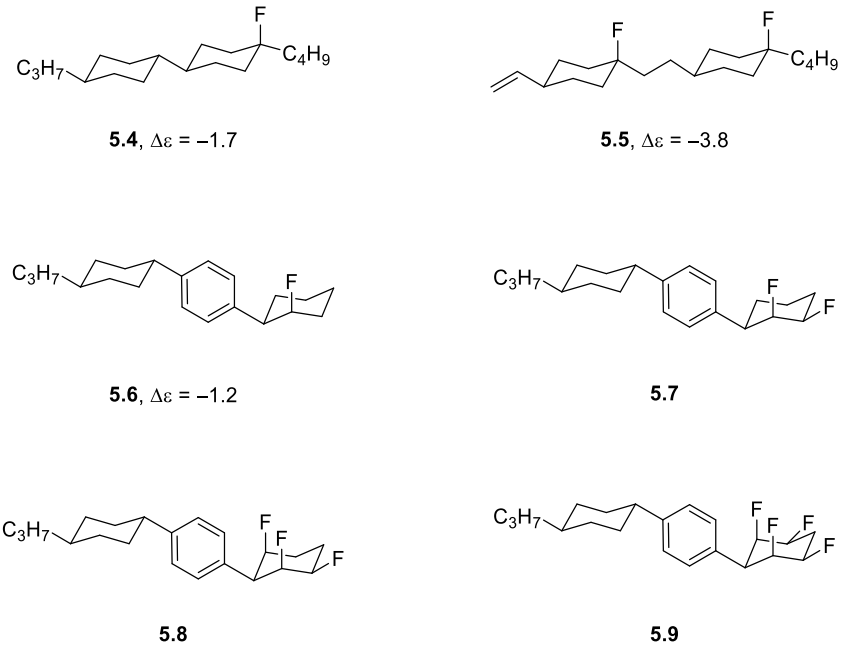

Figure 5.4 Previously reported fluorinated liquid crystal candidates with given dipolar anisotropy values.

The 'Janus' ring candidates **5.7**-**5.9** were not found to be suitable materials for liquid crystal applications.[5] Their synthetic preparation was challenging and accessing analogues with more favourable properties was therefore problematic. The subsequent publication of the Zeng/Glorius hydrogenation method for the preparation of 'Janus' ring facilitates scope for further exploration of the 'Janus' ring for liquid crystal applications. For example, the proposed candidate liquid crystals **5.10** and **5.11** would be readily accessible by the hydrogenation of their parent arenes. A future project will work towards the synthesis of **5.10** and **5.11** and an evaluation of their molecular anisotropy (Δε) and liquid crystal properties. Subsequently, optimisation of these properties and/or solubility may be undertaken by the variation of the alkyl chain lengths and the number of fluorine atoms incorporated in the molecules.

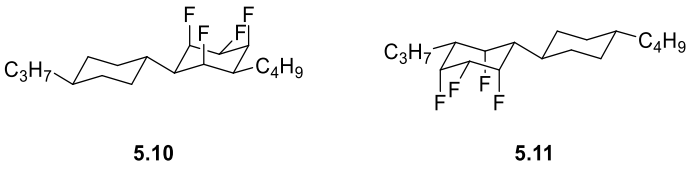

Figure 5.5 Proposed candidate liquid crystals

5.3. References

[1] M. Hezari, P. J. Davis, *Drug Metab. Dispos*. **1993**, *21*, 259-267.

[2] D. Awasthi, K. Kumar, S. E. Knudson, R. A. Slayden, I. Ojima, *J. Med. Chem.* **2013**, *56*, 9756–9770

[3] L. Chen, J. P. S. Mowat, D. Fairen-Jimenez, C. A. Morrison, S. P. Thompson, P. A.Wright, T. Düren, *J. Am. Chem. Soc.* **2013**, *135*, 15763–15773.

[4] L. N. McHugh, M. J. McPherson, L. J. McCormick, S. A. Morris, P. S. Wheatley, S. J. Teat, D. McKay, D. M. Dawson, C. E. F. Sansome, S. E. Ashbrook, C. A. Stone, M. W. Smith, R. E. Morris, *Nat. Chem.* **2018**, *10*, 1096–1102.

[5] N. Al-Maharik, P. Kirsch, A. M. Z. Slawin, D. B. Cordes, D. O'Hagan, *Org. Biomol. Chem.* **2016**, *14*, 9974–9980.

[6] P. Kirsch, K. Tarumi, *Angew. Chem. Int. Ed.* **1998**, *37*, 484–489.

[7] P. Kirsch, M. Heckmeier, K. Tarumi, *Liq. Cryst.* **1999**, *26*, 449–452.

6. Experimental

6.1. General experimental

Air and moisture sensitive reactions were carried out under a nitrogen or argon atmosphere in flame or oven-dried glassware. Room temperature (r.t.) was 18-25 °C. Flash column chromatography was performed using Merck Geduran silica gel 60 (250-400 mesh) under a positive pressure of compressed air eluting with solvents as reported. Commercial reagents were supplied by; Acros, Alfa Aesar, Apollo, Fisher Scientific, Fluorochem, Merck, Sigma-Aldrich, TCI and Strem. Anhydrous solvents (CH_2Cl_2, Et_2O, THF, toluene, hexane) were dispensed from an MBraun MB SPS-800 solvent purification system by filtration through two drying columns under an argon atmosphere. Oxalyl chloride was freshly distilled before use.
NMR spectra were recorded at 298 K using a Bruker Avance III-HD 500, Bruker Avance II 400, Bruker Avance 400, Bruker Avance 300, Bruker Avance III 500 or Bruker Avance III-HD 700. For ^{1}H and ^{13}C NMR the deuterated solvent was used for an internal deuterium lock and chemical shifts were referenced to the residual protic solvent. The ^{1}H NMR were recorded at 300, 400, 500 or 700 MHz and chemical shifts are reported to two decimal places. The ^{13}C NMR were recorded at 75, 100, 126 or 176 MHz and chemical shifts are reported to one decimal place. Chemical shifts, δ are reported in parts per million (ppm) relative to a standard. In ^{1}H and ^{13}C NMR chemical shifts are stated relative to TMS (0.00 ppm). In ^{19}F NMR chemical shifts are stated relative to CCl_3F (0.00 ppm). Coupling constants (*J*) are reported in Hz. Data processing was completed using MestReNova 12.0.0. The abbreviations for the multiplicity of signals are as follows: s singlet, d double, dd doublet of doublets, ddd doublet of doublet of doublets, t triplet, dt doublet of triplets, q quartet, m multiplet, br s broad singlet. Two-dimensional experiments (HSQC, COSY, HMBC, NOESY) were used where applicable to unambiguously assign resonances.
Melting points were determined using either an Electrothermal 9100 or a Griffin MPA350 melting point apparatus. Mass spectra were obtained by electrospray (ESI), electron impact (EI) ionisation modes. These spectra were obtained by Caroline Horsburgh (University of St Andrews) and Alan Taylor (University of Edinburgh). Electrospray ionisation was achieved using a Micromass LCT spectrometer. Electron impact ionisation was achieved using a Micromass GCT spectrometer, a Finnigan MAT 95 XP and a ThermoElectron MAT 900. Reported m/z values have units of Daltons.
Infrared spectra were acquired on a Shimadzu IRAffinity-1S spectrometer with a diamond ATR attachment. Signals are reported in units of wavenumbers (cm^{-1}). Single Crystal X-Ray analysis was carried out by Prof. Alexandra Slawin or Dr David Cordes (University of St Andrews) using a molybdenum or copper X-Ray source. The copper X-Ray source utilised an

MM-007 high-brilliance generator with an AFC10/Saturn 92 detector. The molybdenum source utilised an MM-007 high-brilliance generator with VariMax optics and either an AFC7/Mercury or AFC8/Saturn 70 detector.

6.2. Langmuir isotherm analysis

Langmuir isotherm analysis was conducted using a Biolin Scientific KSV Nima KN-2002 (“medium”) Langmuir Trough. Subphase temperature was controlled with a Grant GR150 water and digital probe. Surface tension measurements were obtained with a maximum measuring range of 300 mN/m and a resolution of 0.03 µN/m. The trough and barrier were cleaned using an Alconox solution (10g/L) and rinsed with deionised water.

The Wilhelmy probe was calibrated with a precisely measured washer (273.2 mg). The paper Wilhelmy plates were soaked in deionised water for 15 mins prior to use. Movement of the barriers was between the ‘fully open’ and ‘fully closed’ positions at 0mm and 130 mm respectively. The open area of the trough was 23,650 mm^2 and the closed area was 2,410 mm^2. The maximum area compression ratio was approximately 10.

The subphase was prepared with the barriers at the ‘fully closed’ position by the addition of deionised water. A ‘blank’ compression isotherm measurement was performed at constant compression speed to assess the cleanliness of the water surface. Where surface pressure increases of < 0.3 mN/m were observed, the surface was treated as clean. Otherwise, decontamination was performed by negative pressure aspiration of the surface and/or a rinsing and repreparation of the subphase.

Samples were prepared as either solutions in chloroform, acetone, or a mixture of the two. Solutions were deposited at the air-water interface either manually from a microsyringe or by continuous injection through a needle via a syringe pump. Following deposition an equilibration period of 30 mins was allocated prior to compression. The rate of barrier compression was constant relative to the remaining area of 5% per minute.

6.3. Synthetic procedure and characterisation of compounds

6.3.1. Chapter 2

Chloro[2-(2,6-diisopropylphenyl)-3,3-dimethyl-2-azaspiro[4.5]dec-1-ylidene][1,2,5,6-η-1,5-cyclooctadiene]rhodium 2.14[1]

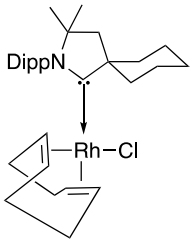

$[RhCODCl]_2$ (77 mg, 0.16 mmol), 2-(2,6-Diisopropylphenyl)-3,3-dimethyl-2-azaspiro[4.5]dec-1-en-2-ium hydrogen dichloride (131 mg, 0.329 mmol) and KHMDS (150 mg, 0.750 mmol) were added to a Schlenk tube inside an argon-filled glovebox. THF (10 mL) was added dropwise over 10 min at -78 °C. The resulting suspension was stirred for 10 min at -78 °C, and then warmed to room temperature and stirred for 16 h. The mixture was filtered and concentrated *in vacuo* to give the crude product, which was purified by flash column chromatography (19:1 pentane:Et_2O). The pure fractions were combined and concentrated *in vacuo* to give an oily residue. The residue was redissolved in CH_2Cl_2 (1 mL) and **2.14** was precipitated by dropwise addition of pentane. The excess solvent was decanted giving **2.14** as a yellow powder (97 mg, 0.170 mmol, 53%): ^1H NMR ($CDCl_3$, 500 MHz) δ_H 7.46-7.38 (2H, m, ArH), 7.14 (1H, dd *J* = 7.5, 1,5, ArH), 5.24 (1H, t, *J* = 7.6), 4.60 (1H, q, *J* = 7.8), 3.94-3.85 (1H, m), 3.48-3.42 (1H, m), 2.92-2.84 (2H, m), 2.64-2.45 (3H, m), 2.31-2.24 (1H, m), 2.20-2.09 (1H, m), 2.04-1.91 (3H, m), 1.79-1.72 (7H, m), 1.60-1.52 (2H, m), 1.50 (s, 3H), 1.46-1.30 (3H, m), 1.27-1.22 (9H, m), 1.20 (3H, s), 0.95 (3H, d, J = 6.7); ^{13}C NMR ($CDCl_3$, 125 MHz) δ_C 148.2, 146.4, 137.0, 129.0, 126.5, 124.1, 101.3 (d, J = 6.1 Hz), 98.2 (d, J = 5.8 Hz), 78.2, 71.9 (d, J = 15.0 Hz), 64.8, 64.6 (d, J = 13.9 Hz), 45.6, 41.8, 38.1, 35.0, 33.7, 30.9, 30.3, 28.9, 28.3, 28.0, 26.6, 26.4, 26.1, 25.9, 25.5, 24.6, 24.0, 22.6; data are in agreement with literature.[1]

(*1r,2R,3R,4s,5S,6S*)-1-Ethyl-2,3,4,5,6-pentafluorocyclohexane 2.35[2]

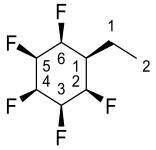

Activated 4 Å molecular sieves (5 g), pentafluorostyrene (0.50 g, 2.58 mmol) and **2.14** (0.02 g, 0.035 mmol, 1 mol%) were suspended in hexane (30 mL) in a vial and the vial placed inside an autoclave. The autoclave was pressurised with hydrogen to 50 Bar and the reaction mixture

stirred at room temperature for 14 h. After depressurising and removing the vial, the suspension was filtered and concentrated in vacuo to give the crude product, which was purified by flash column chromatography (SiO_2, 10% EtOAc in hexane to 50% EtOAc in hexane) to give **2.35** as a white crystalline solid, (396 mg, 1.96 mmol, 76%); m.p. (acetone): 148 °C; ^{1}H NMR (400 MHz, Acetone-D_6) δ_H 5.41 (1H, app dt *J* = 54.1, 8.1 Hz, FCH-4), 5.16-4.99 (2H, m, FCH-2 and FCH-6), 4.90 (2H, app dtt *J* = 39.7, 28.4, 2.8 Hz, FCH-3 and FCH-5) 1.92-1.77 (3H, overlapping m, FCCH-1, CH_2-1), 1.07 (3H, t *J* = 7.4 Hz, CH_3-2); ^{19}F NMR (377 MHz, Acetone-D_6) δ_F −204.9, −213.4, −217.5; ^{13}C NMR (176 MHz, Acetone-D_6) δ_C 89.1 (FC-4), 88.1 (FC-2, FC-6), 87.1 (FC-3, FC-5), 40.3 (FCC-1), 19.95 (*C*H_2-1), 11.4 (*C*H_3-2); HRMS m/z (ESI$^+$) (calculated $C_8H_{11}F_5Na^+$ = 225.0673) found 225.0669 $[M+Na]^+$; ν_{max}/cm^{-1} 1123 (C-F).

tert-Butyldimethyl(perfluorophenoxy)silane 2.42

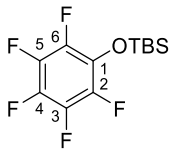

TBDMSCl (482 mg, 0.318 mmol) was added to a solution of pentafluorophenol (368 mg, 2.00 mmol) and imidazole (408 mg, 5.99 mmol) in CH_2Cl_2 (20 mL). The solution was stirred at r.t. for 14 h and then quenched by the addition of H_2O (20 mL). The phases were separated, and the aqueous phase was extracted into CH_2Cl_2 (2 x 20 mL). The combined organic phase was washed with brine, dried over $MgSO_4$, filtered and concentrated *in vacuo* to give the crude product which was purified by flash column chromatography (SiO_2, hexane) to give **2.42** as a colourless oil (587 mg, 1.97 mmol, 98%): ^{1}H NMR (500 MHz, $CDCl_3$) δ_H 1.01 (9H, s, $(CH_3)_3$), 0.21 (6H, s, $(CH_3)_2$); ^{19}F NMR (471 MHz, $CDCl_3$) δ_F −158.0, −164.4, −167.0; ^{13}C NMR (126 MHz, $CDCl_3$) δ_C 141.1 (CF), 138.0 (CF), 136.9 (CF), 130.9 (ArC-1) 25.5 ((*C*H_3)$_3$), −4.8 ((*C*H_3)$_2$); HRMS m/z (ESI$^-$) (Calculated $C_6F_5O^-$ = 182.9875) found 182.9869 $[M-Si(CH_3)_2(C(CH_3)_3)]$; ν_{max}/cm^{-1} 1258, 1171 (C-F).

tert-Butyldimethyl((perfluorophenyl)methoxy)silane 2.44

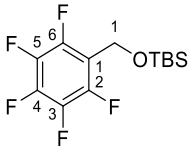

TBDMSCl (167 mg, 1.11 mmol) was added to a solution of pentafluorobenzylalcohol (200 mg, 1.01 mmol), 4-dimethylaminopyridine (12 mg, 0.10 mmol) and imidazole (110 mg, 1.62 mmol) in CH_2Cl_2 (3 mL) at 0 °C. The resulting solution was warmed to r.t. and stirred for 16 h. The mixture was filtered to remove solids, and the filtrate was concentrated *in vacuo*. The residual

oil was redissolved in Et_2O (5 mL) and acidified to pH 1 with HCl (1M). The solution was diluted with EtOAc (20 mL) and the combined organic phase washed with brine (3 x 20 mL), dried over MgSO4, filtered and concentrated *in vacuo* to give the crude product, which was purified by flash column chromatography (SiO_2, 5% EtOAc in hexane) to give **2.44** as a colourless solution (225 mg, 0.720 mmol, 71%): ^{1}H NMR ($CDCl_3$, 500 MHz) δ_H 4.77 (2H, s, CH_2-1), 0.90 (9H, s, $(CH_3)_3$), 0.12 (6H, s, $(CH_3)_2$); ^{19}F NMR ($CDCl_3$, 470 MHz) δ_F −143.9, −155.0, −162.4 (2F, m); ^{13}C NMR (CDCl3, 125 MHz): δ_C 146.6-144.3 (m, ArCF), 142.4-139.9 (m, ArCF), 138.8-136.4 (m, ArCF), 114.1 (ArC), 53.1 (CH_2), 25.9 ($C(CH_3)_3$), 18.5 ($(CH_3)_3$), −5.4 ($(CH_3)_2$); HRMS m/z (ESI$^+$) (Calculated $C_{13}H_{17}OF_5SiNa^+$ = 335.0861) found 335.0874 $(M+Na)^+$; ν_{max}/cm^{-1} 2932br (C-H), 2954br (C-H), 1256 and 1126 (C-O).

tert-Butyldimethyl(((1r,2R,3R,4s,5S,6S)-2,3,4,5,6-pentafluorocyclohexyl)methoxy)silane 2.46

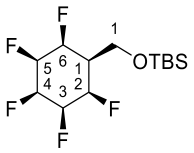

Activated 4 Å molecular sieves (500 mg), **2.44** (50 mg, 0.16 mmol) and **2.14** (1 mg, 0.002 mmol, 1 mol%) were suspended in hexane (2 mL) in a vial and the vial placed inside an autoclave. The autoclave was pressurised with hydrogen to 50 Bar and the reaction mixture stirred at room temperature for 14 h. After depressurising and removing the vial, the suspension was filtered and concentrated *in vacuo* to give the crude product, which was purified by flash column chromatography (SiO_2, 25% EtOAc in hexane) to give **2.46** as a white crystalline solid (21 mg, 41%); m.p. (MeOH): 120-121 °C; ^{1}H NMR ($CDCl_3$, 400 MHz): δ_H 5.37 (1H, app dt *J* = 52.7, 7.4 Hz, H-4), 5.21-5.01 (2H, m, H-2, H-6), 4.60-4.34 (2H, m, H-3, H-5), 4.06 (2H, d, *J* = 7.4, CH_2-1), 1.95-1.72 (1H, m, FCCH-1), 0.93 (9H, s, $((CH_3)_3)$, 0.12 (6H, s, $(CH_3)_2$); ^{19}F NMR ($CDCl_3$, 376 MHz): δ_F −203.6, −212.3, −216.8; ^{13}C NMR (CD_3OD, 125 MHz): δ_C 89.4 (CF), 87.9 (CF), 87.4 (CF), 60.1 (CH_2-1), 42.4 (FCC-1), 26.3 ($(CH_3)_3$), -5.5 ($(CH_3)_2$); HRMS m/z (ESI$^+$) (calculated $C_{13}H_{23}F_5NaOSi^+$ = 341.1331) found 341.1325 $[M+Na]^+$; ν_{max}/cm^{-1} 2930br (C-H), 1105 and 1049 (C-F).

((*1r,2R,3R,4s,5S,6S*)-2,3,4,5,6-Pentafluorocyclohexyl)methanol 2.47

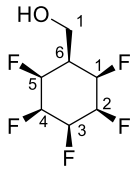

To a solution of **2.46** (77 mg, 0.24 mmol) in acetonitrile (5 mL) in a teflon round bottom flask was added triethylamine trihydrofluoride (0.1 mL, 0.6 mmol). The solution was stirred at r.t. for 16 h and quenched with saturated sodium bicarbonate (10 mL). The mixture was extracted into EtOAc (3 x 10 mL). The organic layers were dried over MgSO4, filtered and concentrated *in vacuo*. The residue was purified by flash column chromatography (SiO_2, 9:1 EtOAc:Hexane) to give **2.47** as a crystalline white solid, (40 mg, 0.20 mmol, 83%): m.p. (MeOH): 176-177 °C; ^{1}H NMR (500 MHz, CD_3OD) δ_H 5.30 (1H, app dt *J* = 53.7, 7.3 Hz, FCH-3), 5.13-5.03 (2H, m, FCH-1, FCH-5), 4.79-4.60 (2H, m, FCH-2, FCH-4), 3.95 (2H, d *J* = 7.5 Hz, CH_2-1), 2.04-1.87 (1H, m, H-6); ^{19}F NMR (376 MHz, CD_3OD) δ_F −206.1, −213.9, −218.2; ^{13}C NMR (126 MHz, CD_3OD) δ_C 87.8 (FC-3), 86.5 (FC-2, FC-4), 86.1 (FC-1, FC-5), 57.3 (H_2C-1), 40.9 (C-6); HRMS m/z (ESI$^+$) (calculated $C_7H_9F_5ONa^+$ = 227.0466) found 227.0461 $[M+Na]^+$; ν_{max}/cm^{-1} 3248br (O-H), 2920 (C-H), 1121 (C-F).

***tert*-Butyl ((perfluorophenyl)methyl)carbamate 2.48**

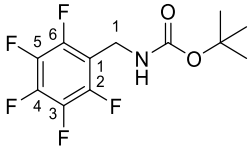

$NaBH_4$ (3.16 g, 83.5 mmol) was slowly added to a solution of $NiCl_2.6H_2O$ (2.85 g, 12.0 mmol), Boc_2O (5.24 g, 24.0 mmol) and pentafluorobenzonitrile (1.52 mL, 12.1 mmol) in MeOH (100 mL) at 0 °C. The reaction mixture was warmed to room temperature and stirred for 24 h. The resulting suspension was filtered to remove solids and the filtrate concentrated *in vacuo*. The residue was then dissolved in EtOAc (50 mL) and washed with aqueous saturated sodium bicarbonate solution (50 mL). The aqueous phase was extracted into EtOAc (2 x 50 mL). The combined organic phase was dried over MgSO4, filtered and concentrated in vacuo to give **2.48** (3.57 g, quant.), which was used without further purification: ^{1}H NMR (CD_3OD, 500 MHz): δ_H 4.41 (2H, s, CH_2-1), 1.43 (9H, s, CH_3); ^{19}F NMR (CD_3OD, 470 MHz) δ_F −143.1, −154.9, −161.8; ^{13}C NMR (CD_3OD, 125 MHz) δ_C 157.1 (C=O), 156.4 (ArCF), 144.4 (ArCF), 136.3 (ArCF), 112.8 (ArC), 79.2 ($C(CH_3)_3$), 31.6 (H_2C-1), 27.3 (($CH_3)_3$); HRMS m/z (ESI$^+$) (calculated $C_{12}H_{12}F_5NO_2Na^+$ = 320.0680) found 320.0676 [M+Na]; ν_{max}/cm^{-1} 3393 (N-H), 1692 (C=O).

tert-Butyl (*tert*-butoxycarbonyl)((perfluorophenyl)methyl)carbamate 2.50

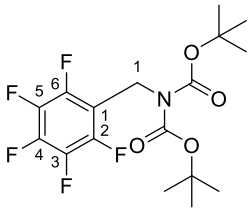

Boc_2O (79 mg, 0.36 mmol), **2.48** (72 mg, 0.24 mmol), and 4-dimethylaminopyridine (30 mg, 0.24 mmol) were dissolved in MeCN (0.2 mL) and stirred at room temperature for 24 h. Water (1 mL) was added, and the mixture was extracted into EtOAc (3 x 3 mL). The combined organic phase was washed with 1 M HCl (3 mL) and brine (3 x 3 mL), dried over $MgSO_4$, filtered and concentrated in vacuo to give **2.50** as a colourless oil (95 mg, 0.24 mmol, quant.) which was used without further purification: ^{1}H NMR ($CDCl_3$, 500 MHz) δ_H 4.92 (2H, s, CH_2-1), 1.48 (18H, s, $(CH_3)_3$); ^{19}F NMR ($CDCl_3$, 470 MHz) δ_F −142.9, −155.7, −162.6; ^{13}C NMR ($CDCl_3$, 125 MHz) δ_C 152.1 (C=O), 145.3 (ArF), 140.5 (ArF), 137.5 (ArF), 112.1 (ArC), 83.5 ($C(CH_3)_3$), 38.6 (H_2C-1), 28.1 ((CH_3)$_3$); HRMS m/z (ESI$^+$) (calculated $C_{17}H_{20}F_5NNaO_4^+$ = 420.1205) found 420.1196 $(M+Na)^+$.

Methyl 2-(perfluorophenyl)acetate 2.59

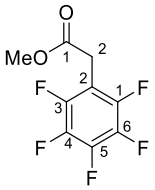

To a solution of pentafluorophenylacetic acid (5.13 g, 22.6 mmol) in MeOH (10 mL) was added HCl (1M, 0.5 mL). The solution was heated to reflux for 14 h before being concentrated *in vacuo*. The residue was basified to pH 8 with saturated $NaHCO_3$ solution and extracted into EtOAc (3x 10 mL). The combined organic layer was washed with brine (30 mL), dried over $MgSO_4$, filtered and concentrated *in vacuo* to give **2.59** as a colourless oil (5.11 g, 21.3 mmol, 94%): ^{1}H NMR (500 MHz, $CDCl_3$) δ_H 3.75 (3H, s, OCH_3), 3.74 (2H, s, CH_2-2); ^{19}F NMR (471 MHz, $CDCl_3$) δ_F −142.3, −155.1, −162.2; ^{13}C NMR (126 MHz, CD_3OD) δ_C 170.6 (C=O), 146.7 (Ar*C*F), 141.7 (Ar*C*F), 138.7 (Ar*C*F), 110.15 (ArC-2), 53.1 (H_2C-2), 28.1 (OCH_3); HRMS m/z (ESI$^-$) (calculated $C_9H_4F_5O_2^-$ = 239.0137) found 239.0134 $(M-H)^-$; ν_{max}/cm^{-1} 1746 (C=O).

Methyl 2-((*1r,2R,3R,4s,5S,6S*)-2,3,4,5,6-pentafluorocyclohexyl)acetate 2.60

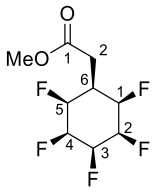

Activated 4 Å molecular sieves (7 g), **2.59** (0.850 g, 3.54 mmol) and **2.14** (16 mg, 0.028 mmol, 1 mol%) were suspended in hexane (40 mL) in a vial and the vial placed inside an autoclave. The autoclave was pressurised with hydrogen to 50 Bar and the reaction mixture stirred at room temperature for 16 h. After depressurising and removing the vial, the suspension was filtered and concentrated *in vacuo* to give the crude product, which was purified by flash column chromatography (SiO_2, 50% EtOAc in hexane) to give **2.60** as a white crystalline solid (0.662 g, 2.69 mmol, 76%); m.p. (acetone): 151 °C; ^{1}H NMR (700 MHz, Acetone-D_6) δ_H 5.50-5.38 (1H, m, FCH-3), 5.12-4.83 (overlapping m, FCH-1, FCH-2, FCH-4, FCH-5), 3.70 (3H, s, OCH_3), 2.85 (2H, d *J* = 7.2 Hz, CH_2-2) , 2.64-2.47 (1H, m, FCCH-6); ^{13}C NMR (126 MHz, Acetone-D_6) δ_C 172.4 (C=O), 89.5 (C-F), 88.0 (C-F), 86.6 (C-F), 52.2 (OCH_3), 36.0 (C-6), 31.0 (H_2C-2); ^{19}F NMR (659 MHz, Acetone-D_6) δ_F −205.5, −212.5, −217.6; HRMS m/z (ESI$^+$) (calculated $C_9H_{12}F_5O_2^+$ = 247.0752) found 247.0750 $(M+H)^+$; v_{max}/cm^{-1} 1728 (C=O).

Methyl 2-((*1S,2S,3R,4R,6S*)-2,3,4,6-tetrafluorocyclohexyl)acetate 2.61

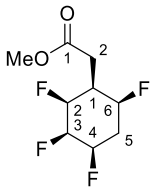

Activated 4 Å molecular sieves (7 g), **2.59** (0.850 g, 3.54 mmol) and **2.14** (16 mg, 0.028 mmol, 1 mol%) were suspended in hexane (40 mL) in a vial and the vial placed inside an autoclave. The autoclave was pressurised with hydrogen to 50 Bar and the reaction mixture stirred at room temperature for 16 h. After depressurising and removing the vial, the suspension was filtered and concentrated *in vacuo* to give the crude product, which was purified by flash column chromatography (SiO_2, 50% EtOAc in hexane) to give **2.61** as a white crystalline solid (0.049 g, 0.21 mmol, 6%); m.p. (acetone): 129-130 °C; ^{1}H NMR (500 MHz, Acetone-D_6) δ_H 5.17-4.78 (4H, overlapping m, FCH-2, FCH-3 FCH-4 and FCH-6), 3.68 (3H, s, OCH_3), 2.76 (2H, d *J* = 6.9 Hz, CH_2-2), 2.67-2.48 (2H, overlapping m, FCCH-1 and CH-5a), 2.19 (1H, app dtt *J* = 39.9, 16.3, 3.3 Hz, CH-5b); ^{19}F NMR (470 MHz, Acetone-D_6) δ_F −191.65, −199.85, −201.6, −211.6; ^{13}C NMR (126 MHz, Acetone-D_6) δ_C 172.7 (*C*=O), 89.3 (*C*F), 87.55 (*C*F), 86.7 (*C*F), 52.1 (OCH_3), 39.35 (FCC-1), 33.35 (C-5), 31.65 (CH_2-2); HRMS m/z ESI$^+$ (Calculated

$C_9H_{12}F_4O_2Na^+$ = 251.0666) found 251.0664 $[M+Na]^+$; ν_{max}/cm^{-1} 1726 (C=O), 1094 and 1045 (C-F).

2-((*1r,2R,3R,4s,5S,6S*)-2,3,4,5,6-Pentafluorocyclohexyl)acetic acid 2.58

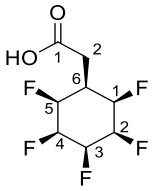

Ester **2.60** (20 mg, 0.081 mmol) was suspended in HCl (6M, 10 mL) and heated to reflux for 14 h. The resulting solution was basified to pH 8 with saturated $NaHCO_3$ solution and residual starting material was extracted into EtOAc (3 x 50 mL). The aqueous phase was re-acidified by addition of HCl (1M) and extracted into EtOAc (3 x 100 mL). The organic phase was dried over $MgSO_4$, filtered and concentrated *in vacuo* to give **2.58** as a white crystalline solid (18 mg, 0.078 mmol, 96%): m.p. (MeOH): 235-236 °C; ^{1}H NMR (500 MHz, CD_3OD) δ_H 5.33-5.22 (1H, m, FCH-3), 5.05-4.94 (2H, m, FCH-1 and CH-5), 4.84-4.60 (2H, m, FCH-2 and FCH-4), 2.80 (2H, d *J* = 7.2 Hz, CH_2-2), 2.44-2.25 (1H, m, FCCH-6); ^{19}F NMR (471 MHz, CD_3OD) δ_F −206.35, −213.3, −218.3; ^{13}C NMR (126 MHz, CD_3CN) δ_C 172.8 (C=O), 89.6 (CF), 87.85 (CF), 86.3 (CF), 35.5 (C-6), 30.7 (H_2C-2); HRMS m/z (ESI$^-$) (calculated $C_8H_8F_5O_2^-$ = 231.0450) found 231.0447 $(M-H)^-$; ν_{max}/cm^{-1} 2967 br (O-H), 1709 (C=O), 1431 (O-H).

2-(Perfluorophenyl)ethan-1-ol 2.66

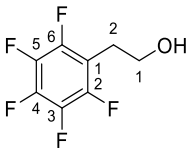

$LiBH_4$ (9 mL, 2M in THF, 18 mmol) was added to a solution of **2.59** (1.00 g, 4.00 mmol) in THF (20 mL) at 0 °C. The solution was warmed to r.t. and stirred for 16 h, before being poured into saturated $NaHCO_3$ (50 mL), extracted into EtOAc (50 mL) and the organic phase washed with water (2 x 50 mL) and brine (50 mL). The organic phase was then dried over $MgSO_4$, filtered and concentrated *in vacuo* to give **2.66** as a colourless oil (0.85 g, 4.00 mmol, quantitative) which was used in the next step without further purification: ^{1}H NMR (500 MHz, $CDCl_3$) δ_H 3.85 (2H, t *J* = 6.5 Hz, CH_2-1), 2.97 (2H, tt *J* = 6.5, 1.5 Hz, CH_2-2); ^{19}F NMR (470 MHz, $CDCl_3$) δ_F −143.5, −156.95, −162.7; ^{13}C NMR (126 MHz, $CDCl_3$) δ_C 145.35 (ArCF), 139.7 (ArCF), 137.5 (ArCF), 111.85 (ArC-1), 61.2 (H_2C-1), 25.9 (H_2C-2); data are in agreement with literature.[3]

tert-Butyldimethyl(2-(perfluorophenyl)ethoxy)silane 2.67

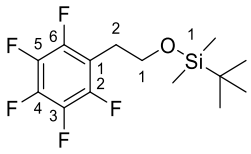

TBDMSCl (1.80 g, 11.9 mmol) was added to a solution of **2.66** (1.68 g, 7.92 mmol) and imidazole (1.56 g, 23.8 mmol) in CH_2Cl_2 (120 mL) at 0 °C. The resulting solution was warmed to r.t. and stirred for 16 h. The mixture was filtered to remove solids, and the filtrate was concentrated *in vacuo*. The residual oil was in EtOAc (60 mL) and the organic phase washed with water (2 x 60 mL) and brine (60 mL), dried over MgSO4, filtered and concentrated *in vacuo* to give the crude product, which was purified by flash column chromatography (SiO_2, 20% EtOAc in hexane) to give **2.67** as a colourless oil (1.85 g, 5.67 mmol, 72%): ^{1}H NMR (500 MHz, $CDCl_3$) δ_H 3.81 (2H, t *J* = 6.5 Hz, CH_2-1), 2.94 (2H, tt *J* = 6.5, 1.5 Hz, CH_2-2), 0.86 (9H, s, (CH_3)$_3$), 0.00 (6H, s, (CH_3)); ^{19}F NMR (470 MHz, $CDCl_3$) δ_F −143.4, −157.7, −163.5; ^{13}C NMR (126 MHz, $CDCl_3$) δ_C 145.6 (Ar*C*F), 139.8 (Ar*C*F), 137.4 (Ar*C*F), 112.6 (ArC), 61.5 (H_2C-1), 26.2 (H_2C-2), 25.8 ((H_3C)$_3$) , −5.5 (H_3C); HRMS m/z (EI$^+$) (Calculated $C_{14}H_{19}F_5OSi^-$ = 326.1131) found 326.1126 [M+e]$^-$; ν_{max}/cm^{-1} 2932 (C-H), 1501 (C=C Ar), 1103 and 1076 (C-F).

tert-Butyldimethyl(2-((*1r,2R,3R,4s,5S,6S*)-2,3,4,5,6-pentafluorocyclohexyl)ethoxy)silane 2.68

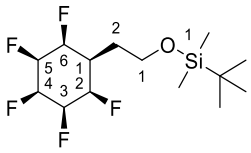

Activated 4 Å molecular sieves (5 g), **2.67** (0.500 g, 1.53 mmol) and **2.14** (0.012 g, 0.021 mmol, 1 mol%) were suspended in hexane (30 mL) in a vial and the vial placed inside an autoclave. The autoclave was pressurised with hydrogen to 50 Bar and the reaction mixture stirred at room temperature for 16 h. After depressurising and removing the vial, the suspension was filtered and concentrated in vacuo to give the crude product, which was purified by flash column chromatography (SiO_2, 40% EtOAc in hexane to 60% EtOAc in hexane) to give **2.68** as a white crystalline solid (0.402 g, 1.21 mmol, 79%): m.p. (Acetone): 83-84 °C; ^{1}H NMR (500 MHz, Acetone-D_6) δ_H 5.40 (1H, app dt *J* = 53.8, 8.0 Hz, FCH-4), 5.13-4.82 (4H, overlapping m, FCH-2, FCH-3, FCH-5, FCH-6), 3.87 (2H, t *J* = 6.2 Hz, CH_2-1), 2.33-2.14 (1H, m, FCCH-1), 2.05-2.00 (2H, m, CH_2-2), 0.89 (9H, s, (CH_3)$_3$), 0.08 (6H, s, CH_3); ^{19}F NMR (471 MHz, Acetone-D_6) δ_F −204.9, −212.2, −217.4; ^{13}C NMR (126 MHz, Acetone-D_6) δ_C 89.0 (*C*F), 88.7 (*C*F), 87.5 (*C*F), 60.7 (H_2C-1), 35.9 (FCC-1), 29.8 (H_2C-2), 26.3 ((CH_3)$_3$), 18.8 (*C*((CH_3)$_3$)), −5.2 (H_3C); HRMS m/z (ESI$^+$) (Calculated $C_{14}H_{25}F_5OSiNa^+$ = 355.1487) found 355.1481 [M+Na]$^+$; ν_{max}/cm^{-1} 2932 (C-H), 1252 (C-O), 1088 and 1045 (C-F).

(Allyloxy)(*tert*-butyl)dimethylsilane 2.70

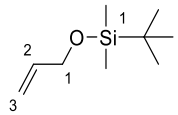

Allyl alcohol (0.541 g, 9.32 mmol) was added to a solution of TBDMSCl (1.50 g, 9.95 mmol) and imidazole (0.680, 9.99 mmol) in CH_2Cl_2 (30 mL) at 0 °C. The solution was warmed to r.t. and stirred for 14 h before being concentrated *in vacuo*. The residue was redissolved in Et_2O (30 mL) and washed with saturated ammonium chloride (3 x 30 mL) and brine (2 x 30 mL). The organic phase was dried over $MgSO_4$, filtered and concentrated *in vacuo* to give **2.70** as a colourless oil (1.48 g, 8.57 mmol, 92%) that was used without further purification: ^{1}H NMR (400 MHz, $CDCl_3$) δ 5.95 (1H, ddt *J* = 17.1, 10.4, 4.6 Hz, H-2), 5.29 (1H, dq *J* = 17.1, 1.9 Hz, H-3a), 5.11 (1H, dq *J* = 10.4, 1.8 Hz, H-3b), 4.19-4.17 (2H, dt *J* = 4.6, 1.8 Hz, CH_2-1), 0.92 (9H, s, $((CH_3)_3)$), 0.07 (6H, s, (CH_3)); data are in accordance with the literature.[4]

(*E*)-*tert*-Butyldimethyl((4-(perfluorophenyl)but-2-en-1-yl)oxy)silane 2.72

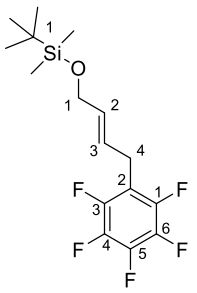

Silyl ether **2.70** (0.94 g, 5.45 mmol) was added to a solution of Grubbs Catalyst™ First generation (200 mg, 0.24 mmol, 4 mol%) and 1-allyl-2,3,4,5,6-pentafluorobenzene (1.63 g, 7.83 mmol) in CH_2Cl_2 (30 mL) and the solution was stirred at r.t., for 16 h. The solution was concentrated *in vacuo* and purified directly by flash column chromatography (SiO_2, hexane to 20% EtOAc in hexane) to give **2.72** as a colourless oil (250 mg, 0.709 mmol, 13%): ^{1}H NMR (500 MHz, $CDCl_3$) δ_H 5.75-5.68 (1H, m, CH), 5.64-5.58 (1H, m, CH), 4.14-4.10 (2H, m, CH_2), 3.44-3.40 (2H, m, CH_2), 0.89 (9H, s, $(CH_3)_3$) , 0.04 (6H, s, CH_3); ^{19}F NMR (470 MHz, $CDCl_3$) δ_F −144.0, −157.6, −162.8; ^{13}C NMR (126 MHz, $CDCl_3$) δ_C 145.0 (Ar*C*F), 137.65 (Ar*C*F), 132.3 (C=C), 129.7 (ArCF), 124.71 (C=C), 113.55 (ArC-2), 63.3 (O*C*H_2-1), 26.0 ($(CH_3)_3$), 25.0, 18.5, −3.5 ($(CH_3)_2$); HRMS m/z EI$^+$ (Calculated $C_{16}H_{21}F_5O^{28}Si^+$ = 352.1276) found 352.1252 [M−e]$^+$; ν_{max}/cm^{-1} 1657 (C=C), 1522 and 1504 (C=C Ar).

tert-Butyldimethyl(4-((*1r,2R,3R,4s,5S,6S*)-2,3,4,5,6-pentafluorocyclohexyl)butoxy)silane 2.75

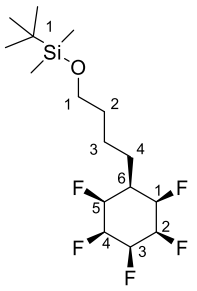

Activated 4 Å molecular sieves (1.2 g), **2.72** (0.100 g, 0.284 mmol) and **2.14** (0.006 g, 0.01 mmol, 4 mol%) were suspended in hexane (6 mL) in a vial and the vial placed inside an autoclave. The autoclave was pressurised with hydrogen to 50 Bar and the reaction mixture stirred at room temperature for 14 h. After depressurising and removing the vial, the suspension was filtered and concentrated in vacuo to give the crude product, which was purified by flash column chromatography (SiO_2, 10% EtOAc in hexane to 50% EtOAc in hexane) to give **2.75** as a white crystalline solid (0.050 g, 0.139 mmol, 49%): m.p. (MeOH): 62-63 °C; ^1H {^{19}F} NMR (400 MHz, CD_3OD) δ_H 5.27 (1H, s, FCH-3), 4.92 (2H, s, FCH-1 and FCH-5) 4.65 (2H, t *J* = 2.6 Hz, FCH-2 and FCH-4), 3.70 (2H, t *J* = 6.0 Hz, CH_2-1), 1.83-1.79 (3H, overlapping m, FCCH-6 and CH_2), 1.62-1.50 (4H, overlapping m, 2 x CH_2), 0.92 (9H, s, $(CH_3)_3$), 0.09 (6H, s, CH_3); ^{19}F NMR (376 MHz, CD_3OD) δ_F −205.8, −213.6, −218.1; ^{13}C NMR (101 MHz, CD_3OD) δ_C 88.1 (*C*F-3), 87.9 (*C*F-1 and *C*F-5), 86.6 (*C*F-2 and *C*F-4), 62.5 (H_2C-1), 37.8 (C-6), 32.3 (H_2C), 25.4 (H_2C), 25.0 ((CH_3)$_3$) 22.4 (H_2C), 17.8 ($C(CH_3)_3$), −6.6 (H_3C); HRMS m/z ESI$^+$ (Calculated $C_{16}H_{30}F_5OSi^+$ = 361.1981) found 361.1979 $[M+H]^+$; ν_{max}/cm^{-1} 2930 (C-H), 1123 and 1045 (C-F).

4-((*1r,2R,3R,4s,5S,6S*)-2,3,4,5,6-Pentafluorocyclohexyl)butan-1-ol 2.76

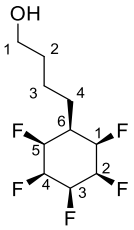

HCl (0.5 mL, 1 M) was added to a solution of **2.75** (25 mg, 0.069 mmol) in THF (2 mL). The solution was heated to 66 °C and stirred for 14 h before saturated $NaHCO_3$ (5 mL) and EtOAc (5 mL) were added. The aqueous layer was extracted with EtOAc (2 x 5 mL) and the combined organic phase was washed with brine (3 x 15 ml), dried over $MgSO_4$, filtered and concentrated *in vacuo* to give the crude product which was purified by flash column chromatography (SiO_2, EtOAc) to give **2.76** as a white crystalline solid (10 mg, 0.041 mmol, 59%): m.p. (Acetone): 138-139 °C; ^1H NMR (500 MHz, Acetone-D_6) δ_H 5.41 (1H, dt *J* = 54.1, 8.1 Hz, FCH-4), 5.11-

4.78 (4H overlapping m, FCH-1, FCH-2, FCH-4 and FCH-5), 3.57 (2H, t J = 5.9 Hz, CH_2-1), 2.09-1.91 (1H, m, FCCH-6), 1.84 (2H, q J = 7.4 Hz, CH_2-4), 1.59-1.53 (4H, overlapping m, CH_2-2 and CH_2-3); ^{19}F NMR (471 MHz, Acetone-D_6) δ_F −204.9, −213.1, −217.35; ^{13}C NMR (126 MHz, Acetone-D_6) δ_C 88.25 (FC-3), 88.1 (FC-1 and FC-5), 86.8 (FC-2 and FC-4), 61.7 (H_2C-1) , 38.0 (C-6), 32.7 (H_2C), 25.9 (H_2C-4), 22.9 (H_2C); HRMS m/z ESI$^+$ (Calculated $C_{10}H_{15}F_5ONa^+$ = 269.0935) found 269.0931 $[M+Na]^+$; ν_{max}/cm^{-1} 3337br (O-H), 2940 (C-H), 1051 (O-H).

Methyl (*E*)-4-(perfluorophenyl)but-2-enoate 2.73

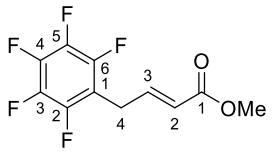

Methyl acrylate (0.172 g, 2.00 mmol) and allyl-2,3,4,5,6-pentafluorobenzene (0.208 g, 1.00 mmol) were added to a solution of Hoveyda-Grubbs Catalyst® M720 (0.012 g, 0.019 mmol, 2 mol%) in CH_2Cl_2 (5 mL). The solution was heated to 40 °C and stirred for 16 h before being concentrated *in vacuo* and purified directly by flash column chromatography (SiO_2, hexane to 30% EtOAc) to give **2.73** as a colourless oil (0.190 g, 0.714 mmol, 71%) as a mixture of stereoisomers in the ratio *E*:*Z* 95:5, only signals of the major isomer are assigned: ^{1}H NMR (500 MHz, $CDCl_3$) δ_H 6.95 (1H, dt J = 15.6, 6.4 Hz, H-3), 5.80 (1H, d J = 15.6 Hz, H-2), 3.72 (3H, s, OCH_3), 3.60-3.57 (2H, m, CH_2-4); ^{19}F NMR (471 MHz, $CDCl_3$) δ_F −143.25, −155.65, −161.8; ^{13}C NMR (126 MHz, $CDCl_3$) δ_C 166.3 (C=O), 144.9 (ArCF), 142.4 (HC-3), 140.3 (ArCF), 137.7 (ArCF), 123.15 (HC-2), 110.9 (ArC-1), 51.7 (O*C*H$_3$) , 24.7 (H_2C-4); HRMS m/z ESI$^+$ (Calculated $C_{11}H_8F_5O_2^+$ = 267.0439) found 267.0439; ν_{max}/cm^{-1} 1724 (C=O), 1501 (C=C Ar), 1273 (C-F).

Methyl 4-((1r,2R,3R,4s,5S,6S)-2,3,4,5,6-pentafluorocyclohexyl)butanoate 2.77

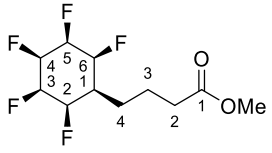

Activated 4 Å molecular sieves (0.5 g), **2.73** (0.050 g, 0.19 mmol) and **2.14** (0.003 g, 0.005 mmol, 3 mol%) were suspended in hexane (2 mL) in a vial and the vial placed inside an autoclave. The autoclave was pressurised with hydrogen to 50 Bar and the reaction mixture stirred at room temperature for 14 h. After depressurising and removing the vial, the suspension was filtered and concentrated in vacuo to give the crude product, which was purified by flash column chromatography (SiO_2, 40% EtOAc in hexane to 60% EtOAc in hexane) to give **2.77** as a white crystalline solid (0.019 g, 0.069 mmol, 36%): m.p. ($CHCl_3$):

99-100 C; ^{1}H NMR (500 MHz, $CDCl_3$) δ_H 5.42-5.25 (1H, m, FCH-4), 4.95 (2H, app d *J* = 49.3 Hz, FCH-2 and FCH-6), 4.43 (2H, app dt *J* = 40.6, 26.6 Hz, FCH-3 and FCH-5), 3.69 (3H, s, OCH_3), 2.41 (2H, t *J* = 7.2 Hz, CH_2-2), 1.92-1.75 (4H, overlapping m, CH_2-3 and CH_2-4), 1.68-1.51 (1H, m, FCCH-1); ^{19}F NMR (471 MHz, $CDCl_3$) δ_F −203.3, −212.1, −216.7; ^{13}C NMR (176 MHz, Acetone-D_6) δ_C 173.9 (C=O), 89.3 (*C*F), 88.2 (*C*F), 87.15 (*C*F), 51.7 (O*C*H_3), 38.5 (FCC-1), 34.1 (H_2C-2), 26.3 (H_2C), 22.6 (H_2C); HRMS m/z ESI$^+$ (Calculated $C_{11}H_{15}F_5O_2Na^+$ = 297.0884) found 297.0874 $[M+Na]^+$; ν_{max}/cm^{-1} 1730 (C=O), 1130 and 1047 (C-F).

((*1r,2R,3R,4s,5S,6S*)-2,3,4,5,6-Pentafluorocyclohexyl)methyl methanesulfonate 2.78

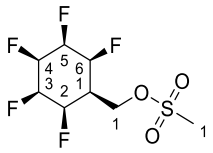

Methanesulfonyl chloride (48 mg, 0.42 mmol) was added to a solution of **2.47** (33 mg, 0.16 mmol) and Et_3N (0.064 mL, 0.48 mmol) in CH_2Cl_2 (5 mL) at 0 °C. The solution was warmed to r.t. and stirred for 16 h. The solution was washed with 1M HCl and the aqueous phase extracted into EtOAc (3 x 5 mL). The combined organic phase was dried over $MgSO_4$, filtered and concentrated *in vacuo*. The residue was purified by flash column chromatography (SiO_2, 30% EtOAc in hexane to 70% EtOAc in hexane) to give **2.78** as a white crystalline solid (45 mg, 0.16 mmol, quantitative): m.p. (Acetone): 175 °C; ^{1}H NMR (500 MHz, Acetone-D_6) δ_H 5.55-5.39 (1H, m, FCH-4), 5.32-5.18 (2H, m, FCH-2 and FCH-6), 5.12-4.91 (2H, m, FCH-3 and FCH-5), 4.63 (2H, d *J* = 7.5 Hz, CH_2-1), 3.20 (3H, s, CH_3), 2.71-2.54 (1H, m, FCCH-1); ^{19}F NMR (470 MHz, CD_3CN) δ_F −206.0, −213.4, −218.05; ^{13}C NMR (126 MHz, CD_3CN) δ_C 88.7 (*C*F), 87.3 (*C*F), 86.8 (*C*F), 66.1 (O*C*H_2-1), 38.9 (FCC-1), 37.2 (H_3C); HRMS m/z (ESI$^+$) (Calculated $C_8H_{11}F_5O_3SNa^+$ = 305.0241) found 305.0236; ν_{max}/cm^{-1} 2922br (C-H), 1356 and 1327 (S=O), 1175 (C-F).

2-((*1r,2R,3R,4s,5S,6S*)-2,3,4,5,6-Pentafluorocyclohexyl)ethan-1-ol 2.81

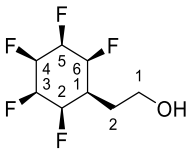

DIBAlH (1M in hexane, 9.7 mL, 9.7 mmol) was added dropwise to a solution of **2.60** (0.588 g, 2.39 mmol) in THF (20 mL) at 0 °C. The solution was slowly warmed to r.t. and stirred for 16 h. The reaction was then diluted with Et_2O (50 mL) cooled to 0 °C and quenched by the slow subsequent addition of water (0.4 mL), aqueous sodium hydroxide (15% w/w, 0.4 mL) and water (1 mL). The mixture was warmed to r.t. and stirred for 15 mins before $MgSO_4$ was added and the resulting suspension stirred for 15 mins. The suspension was then filtered to remove

aluminium salts and the filtrate concentrated *in vacuo*. The crude product was purified by flash column chromatography (SiO_2, 60% EtOAc in hexane to 100% EtOAc) to give **2.81** as a white crystalline solid (0.433 g, 1.98 mmol, 83%) as a crystalline white solid: m.p. (MeOH): 126-127 °C; ^{1}H NMR (500 MHz, CD_3OD) δ_H 5.34-5.18 (1H, m, FCH-4), 5.01-4.87 (2H, m, FCH-2 and FCH-6), 4.77-4.52 (2H, m, FCH-3 and FCH-5), 3.73 (2H, d *J* = 6.0 Hz, CH_2-1), 2.11-1.85 (3H, overlapping m, CH_2-2 and FCCH-1); ^{19}F NMR (659 MHz, CD_3OD) δ_F -205.8, -213.2, -218.2; ^{13}C NMR (CD_3OD, 126 MHz): δ_C 89.9 (FC-4), 88.4 (FC-2 and FC-6), 87.1 (FC-3 and FC-5), 59.3 (H_2C-1), 36.0 (FCC-1), 29.8 (H_2C-2); HRMS m/z (ESI+) (calculated $C_8H_{11}F_5ONa^+$ = 241.0622) found 241.0618 $[M+Na]^+$; v_{max}/cm^{-1} 3400 br (O-H), 2940 (C-H), 1364 (O-H), 1045 (C-O).

(*1r,2R,3R,4s,5S,6S*)-1-(2-Bromoethyl)-2,3,4,5,6-pentafluorocyclohexane 2.82

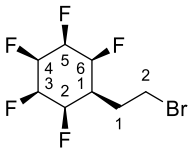

Ph_3P (0.278 g, 1.06 mmol) and CBr_4 (0.352 g, 1.06 mmol) were added to a solution of **2.81** (0.1155 g, 0.5294 mmol) in CH_3CN (5 mL) at r.t. for 16 h. The reaction mixture was concentrated *in vacuo* and purified directly by flash column chromatography (SiO_2, hexane to 40% EtOAc in hexane) to give **2.82** as a white crystalline solid (0.125 g, 0.445 mmol, 84%): m.p. (MeOH): 154-155 °C; ^{1}H NMR (400 MHz, CD_3OD) δ_H 5.37-5.17 (1H, m, FCH-4), 5.06-4.88 (2H, m, FCH-2 and FCH-6), 4.83-4.54 (2H, m, FCH-3 and FCH-5), 3.65 (2H, t *J* = 6.7 Hz, CH_2-2), 2.32 (2H, m, CH_2-1), 2.13 (1H, m, FCCH-1); ^{19}F NMR (377 MHz, CD_3OD) δ_F -206.1, -213.0, -218.3; ^{13}C NMR (101 MHz, CD_3OD) δ_C 89.7 (FC-4), 88.5 (FC-2 and FC-6), 87.6 (FC-3 and FC-5), 37.9 (FCC-1), 31.0 (H_2C-2), 30.2 (H_2C-1); HRMS m/z (ESI$^+$) (calculated $C_8H_{10}F_5{}^{79}BrNa^+$ = 302.9778) found 302.9782 $[M+Na]^+$; v_{max}/cm^{-1} 2900 br (C-H).

(*1r,2R,3R,4s,5S,6S*)-1-(2-Azidoethyl)-2,3,4,5,6-pentafluorocyclohexane 2.83

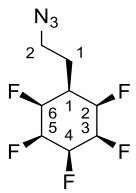

To a solution of **2.82** (0.441 g, 1.57 mmol) in DMF (10 mL) was added sodium azide (0.201 g, 3.09 mmol). The solution was warmed to 70 °C and stirred for for 6 h until TLC showed complete consumption of the starting material. Water (5 mL) was added, and the mixture extracted into EtOAc (3 x 20 mL). The combined organic phase was washed with brine, dried over $MgSO_4$, filtered and concentrated *in vacuo* to give the crude product which was purified

by flash column chromatography (SiO_2, 40% EtOAc in hexane) to give **2.83** as a white crystalline solid (0.381 g, 1.57 mmol, quantitative): m.p. (MeOH): 102-103 °C; ^{1}H NMR (500 MHz, CD_3OD) δ_H 5.36-5.17 (1H, m, H-4), 5.00-4.88 (2H, m, H-2 and H-6), 4.78-4.55 (2H, m, H-3 and H-5), 3.54 (2H, t *J* = 6.5, CH_2-2), 2.08-1.88 (3H, overlapping m, CH_2-1 and FCCH-1); ^{19}F NMR (471 MHz, CD_3OD) δ_F -205.9, -213.1, -218.2; ^{13}C NMR (126 MHz, CD_3OD) δ_C 89.8 (FC-4), 88.4 (FC-2 and FC-6), 87.1 (FC-3 and FC-5), 49.4 (H_2C-2), 36.8 (FCC-1), 26.4 (H_2C-1); HRMS m/z (ESI$^+$) (Calculated $C_8H_{10}F_5N_3Na$ = 266.0693) found 266.0682 $[M+Na]^+$; v_{max}/cm^{-1} 2976 and 2951 (C-H), 2102 (N=N=N).

2-((*1r,2R,3R,4s,5S,6S*)-2,3,4,5,6-Pentafluorocyclohexyl)ethan-1-amine 2.84

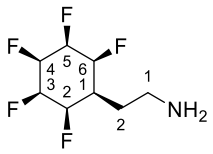

Ph_3P (147 mg, 0.560 mmol) was added to a solution of **2.83** (0.068 g, 0.28 mmol) in THF (1 mL). The solution was stirred at r.t. for 2h and then water (0.1 mL) was added. The mixture was stirred for a further 22 h before being quenched by addition of HCl (2M, 0.25 mL). The aqueous layer was washed with EtOAc (3 x 1 mL) before being basified with NaOH (2M) to pH 2. The basic aqueous phase was extracted into EtOAc (3 x 5 mL) and this organic phase was washed with brine (2 x 5 mL), dried over $MgSO_4$, filtered and concentrated *in vacuo* to give **2.84** (40 mg, 0.18 mmol, 64%) as a crystalline white solid: m.p. (EtOAc) 141-142 °C; ^{1}H NMR (500 MHz, CD_3OD) δ_H 5.37-5.19 (1H, m, FCH-4), 4.98-4.87 (2H, m, FCH-2 and FCH-6), 4.75-4.55 (2H, m, FCH-3 and FCH-5), 2.81 (2H, t *J* = 6.9 Hz, CH_2-1), 1.99-1.82 (3H, overlapping m, FCCH-1 and CH_2-2); ^{19}F NMR (471 MHz, CD_3OD) δ_F -205.8, -213.5, -218.2; ^{13}C NMR (126 MHz, CD_3OD) δ_C 89.9 (FC), 88.5 (FC), 87.1 (FC-3 and FC-5), 39.2 (H_2C-1), 36.6 (FCC-1), 29.9 (H_2C-2); HRMS m/z (ESI$^+$) (Calculated $C_8H_{13}F_5N^+$ = 218.0963) found 218.0958 $[M+H]^+$; v_{max}/cm^{-1} 3354 br (N-H), 2955 (C-H), 1576 (N-H), 1124 and 1047 (C-N).

2-((*1r,2R,3R,4s,5S,6S*)-2,3,4,5,6-Pentafluorocyclohexyl)acetaldehyde 2.87

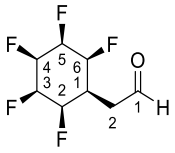

To a solution of **2.81** (0.346 g, 1.41 mmol) in THF (21 mL) was added dess-martin periodinane (0.88 g, 2.1 mmol) at 0 °C. The suspension was warmed to r.t. and stirred for 45 mins until complete consumption of starting material was observed by thin layer chromatography. The reaction was quenched by the addition of sodium thiosulfate solution (25% w/w, 9.7 mL) and saturated $NaHCO_3$ solution (9.7 mL). The mixture was stirred for 30 mins before being

extracted into EtOAc (3 x 50 mL). The combined organic phase was dried over $MgSO_4$, filtered and concentrated *in vacuo*. The residue was purified by flash column chromatography (SiO_2, 40% EtOAc in hexane to 60% EtOAc in hexane) to give **2.87** as a white crystalline solid, (0.259 g, 1.20 mmol, 85%), only peaks for the keto form are assigned: m.p. (acetone) 205-206 °C; ^{1}H NMR (500 MHz, Acetone-D_6) δ_H 9.85 (1H, s, C(O)H-1), 5.42 (1H, app d *J* = 54.3 Hz, FCH-4), 5.10-4.88 (4H, overlapping m, FCH-2, FCH-3, FCH-5 and FCH-6), 3.07 (2H, d *J* = 6.7 Hz, CH_2-2), 2.79-2.59 (1H, m, FCCH-1); ^{19}F NMR (471 MHz, Acetone-D_6) δ_F −205.3, −212.1, −217.6; ^{13}C NMR (126 MHz, Acetone-D_6) δ_C 200.6 (*C*=O), 89.7 (*C*F), 88.1 (*C*F), 86.5 (*C*F), 40.6 (H_2C-2), 33.3 (FCC-1); HRMS m/z ESI$^+$ (Calculated $C_8H_9F_5ONa^+$ = 239.0466) found 239.0463 $[M+Na]^+$; ν_{max}/cm^{-1} 2820 (C-H), 1721 (C=O), 1398 (C-H).

6.3.2. Chapter 3

tert-Butyl N^6-(_tert_-butoxycarbonyl)-N^2-(2-((1r,2R,3R,4R,5S,6S)-2,3,4,5,6-pentafluorocyclohexyl)acetyl)-L-lysinate 3.2

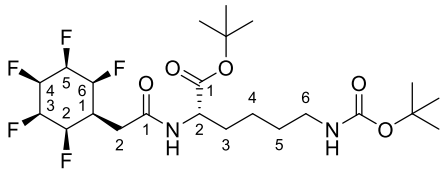

HATU (383 mg, 1.01 mmol), H-Lys(Boc)-O^{t}Bu.HCl (188 mg, 0.554 mmol) and ^{i}Pr$_2$NEt (0.263 mL, 1.51 mmol) were added to a solution of **2.58** (117 mg, 0.504 mmol) in DMF (7 mL) at 0 °C. The solution was warmed to r.t. and stirred for 16 h before being concentrated *in vacuo*. The residue was redissolved in EtOAc (20 mL) and washed with water (2 x 20 mL) and brine (2 x 20 mL). The organic phase was dried over $MgSO_4$, filtered and concentrated *in vacuo* to give the crude product which was purified by flash column chromatography (SiO_2, 30% EtOAc in hexane to 60% EtOAc in hexane) to give **3.2** (53 mg, 0.103 mmol, 20%) as a white crystalline solid: m.p. (Acetone): 92-93 °C; ^{1}H NMR (700 MHz, Acetone-D$_6$) δ_H 7.55 (1H, app d *J* = 7.3 Hz, NH), 5.95 (1H, br s, NH), 5.42 (1H, app dt *J* = 7.4, 53.8 Hz, FCH-4), 5.09-4.85 (4H, overlapping m, FCH-2, FCH-4, FCH-5 and FCH-6), 4.31-4.28 (1H, m, NCH-2), 3.08-3.01 (2H, m, NCH-6), 2.76 (2H, app t *J* = 7.1 Hz, CH_2-2), 2.52 (1H, app t *J* = 34.6 Hz, FCCH-1), 1.84-1.65 (2H, m, CH_2-3), 1.53-1.46 (2H, m, CH_2-5), 1.45-1.41 (2H, m, CH_2-4), 1.44 (9H, s, CH_3), 1.39 (9H, s, CH_3); ^{19}F NMR (376 MHz, Acetone-D$_6$) δ_F −205.2, −211.9, −217.4; ^{13}C NMR (176 MHz, Acetone-D$_6$) δ_C 172.1 (*C*=O), 170.6 (*C*=O), 156.7 (*C*=O), 89.1 (FC), 87.9 (FC), 86.9 (FC), 81.4 (*C*(CH$_3$)$_3$), 78.4 (*C*(CH$_3$)$_3$), 54.05 (NC-2), 40.7 (NC-6), 36.1 (FCC-1), 32.5 (H_2C-2), 32.05 (H_2C-3), 30.45 (H_2C-5), 28.65 (H_3C), 28.1 (H_3C), 23.6 (H_2C-4); HRMS m/z ESI$^+$ (Calculated $C_{23}H_{38}F_5N_2O_5^+$ = 517.2705) found 517.2695 [M+H]$^+$; v_{max}/cm^{-1} 3329br (N-H), 1684 and 1639 (C=O), 1665 and 1130 (C-F); $[\alpha]_D^{20}$ = −17 (*c* 0.80, MeOH).

(*S*)-5-carboxy-5-(2-((*1r,2R,3R,4R,5S,6S*)-2,3,4,5,6-Pentafluorocyclohexyl)acetamido)pentan-1-aminium 3.3

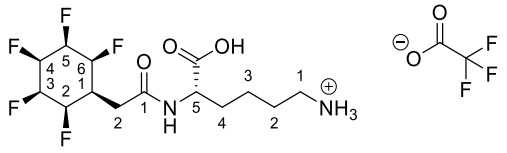

Trifluoroacetic acid (1.0 mL, 13 mmol).To a solution of **3.2** (0.045 g, 0.095 mmol) in CH_2Cl_2 (1 mL) was added The reaction was stirred at r.t. for 15 h before being concentrated *in vacuo* to give **3.3** (0.041 g, 0.086 mmol, 91%) as a white crystalline solid: m.p. (MeOH): 230-231 °C; ^{1}H NMR (400 MHz, CD_3OD) δ_H 5.24 (1H, app d *J* = 53.7 Hz, FCH-4), 5.00-4.85 (2H, m, FCH-2 and FCH-6), 4.68 (2H, app dt *J* = 41.2, 28.9 Hz, FCH-3 and FCH-5), 4.40-4.32 (1H, dd *J* =

9.2, 4.9 Hz, NCH-5), 2.89 (2H, t J = 7.6, NCH_2-1), 2.74 (2H, d, *J* = 7.4 Hz, $OCCH_2$-2), 2.46-2.20 (1H, m, FCCH-1), 1.94-1.86 (1H, m, NCHC*H*$_2$-4a), 1.77-1.62 (3H, overlapping m, NCHC*H*$_2$-4b and NCH_2C*H*$_2$-2), 1.51-1.41 (2H, m, NCH_2CH_2C*H*$_2$-3); ^{19}F NMR (377 MHz, CD_3OD) δ_F -77.1 (C*F*$_3$COOH), -206.3, -212.6, -218.3; ^{13}C NMR (126 MHz, CD_3OD) δ_C 175.1 (*C*OOH), 173.1 (OC-1), 89.95 (CF), 88.5 (CF), 86.9 (CF), 53.5 (NC-5), 40.5 (NC-1), 36.8 (FCC-1), 33.0 (OCC-2), 31.8 (NCC-4), 28.0 (NCC-2), 23.93 (NCCC-3); HRMS m/z (ESI^+) (Calculated $C_{14}H_{22}F_5N_2O_3^+$ = 361.1545) Found 361.1536 [M+H]; ν_{max}/cm^{-1} 2953br (C-H and N-H), 1717 and 1674 (C=O), 1634 (N-H), 1198 and 1132 (C-N); $[\alpha]_D^{20}$ = −7.3 (*c* 1.46, MeOH).

(2-((*1r,2R,3R,4R,5S,6S*)-2,3,4,5,6-Pentafluorocyclohexyl)acetyl)-L-glutamic acid 3.5

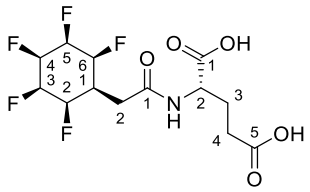

HATU (2 eq, 1.48 mmol, 0.564 g), ^{i}Pr$_2$NEt (3eq, 2.22 mmol, 0.287 g) and L-glutamic acid di-*tert*-butyl ester hydrochloride (207 mg, 0.815 mmol) were added to a solution of **2.58** (0.172 g, 0.741 mmol) in DMF (10mL) at 0 °C. The solution was warmed to r.t. and stirred for 16 h. Water (30 mL) was then added and the mixture extracted into EtOAc (3 x 30 mL). The combined organic phase was dried over $MgSO_4$, filtered and concentrated *in vacuo*. The residue was redissolved in CH_2Cl_2 (5 mL) and trifluoroacetic acid (0.10 mL, 1.3 mmol) was added dropwise. The solution was stirred for 1 h at r.t. before being basified with saturated $NaHCO_3$ solution. Residual starting material was extracted with EtOAc (3 x 20 mL) and the aqueous phase was then reacidified by addition of HCl (1M). The product was extracted into EtOAc (3 x 50 mL), dried over $MgSO_4$, filtered and concentrated *in vacuo* to give **3.5** as a white crystalline solid (0.116 g, 0.321 mmol, 43%): m.p. (MeOH): 251-252 °C; ^{1}H NMR (500 MHz, CD_3OD) δ_H 5.37-5.21 (1H, app d *J* = 54.1 Hz, FCH-4), 5.05-4.88 (2H, m, FCH-2 and FCH-6), 4.78-4.61 (FCH-3 and FCH-5), 4.46 (1H, dd *J* = 9.2, 5.1 Hz, NCH-2), 2.79 (1H, dd *J* = 7.5, 4.9 Hz, CH_2-2), 2.48-2.30 (3H, overlapping m, FCCH-1 and CH_2-4), 2.27-2.19 (1H, m, CH_2-3a), 2.02-1.95 (1H, m, CH_2-3b); ^{13}C NMR (126 MHz, CD_3OD) δ_C 176.3 (C=O), 174.95 (C=O), 173.1 (C=O), 89.9 (*C*F), 88.5 (*C*F), 86.6 (*C*F), 53.3 (N*C*-2), 36.9 (FCC-1), 33.05 (H_2C-2), 31.3 (H_2C-4), 27.7 (H_2C-3); ^{19}F NMR (471 MHz, CD_3OD) δ_F -206.3, -212.7, -218.3; HRMS m/z ESI^+ (Calculated $C_{13}H_{17}F_5O_5N^+$ = 362.1021) found 362.1027 $[M+H]^+$; ν_{max}/cm^{-1} 2918 (C-H), 1715 and 1645 (C=O), 1088 (C-F); $[\alpha]_D^{20}$ = −11.2 (*c* 0.60, MeOH).

Amino(((*S*)-5-(*tert*-butoxy)-5-oxo-4-(2-((*1r,2R,3R,4R,5S,6S*)-2,3,4,5,6-pentafluorocyclohexyl)acetamido)pentyl)amino)methaniminium hexafluorophosphate 3.6

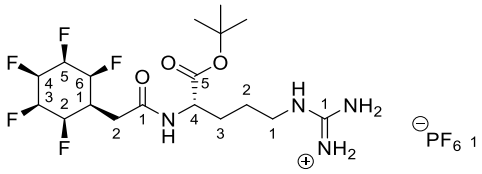

HATU (0.622 g, 1.64 mmol), $^{i}Pr_2NEt$ (0.48 mL, 2.74 mmol) and L-arginine-tert-butyl ester dihydrochloride (0.250 g, 0.821 mmol) to a solution of **2.58** (0.127 g, 0.547 mmol) in DMF (7 mL) at 0 °C was added. The solution was warmed to r.t. and stirred for 16 h. The solution was concentrated *in vacuo* and then redissolved in n-butanol (10 mL). The solution was washed with brine (3 x 10 mL). The organic phase was dried over $MgSO_4$, filtered, and concentrated *in vacuo* to give **3.6** (0.073 g, 0.124 mmol, 23%) as a yellow oil: ^{1}H NMR (500 MHz, CD_3OD) δ_H 5.37-5.19 (1H, m, FCH-4), 5.04-4.89 (2H, m, FCH-2 and FCH-6), 4.84-4.60 (2H, m, FCH-3 and FCH-5), 4.30 (1H, dd *J* = 8.9, 5.1 Hz, NCH-4), 3.23 (2H, tdh J = 6.9, 2.8, NCH-1) 2.84-2.73 (2H, m, OCCH-2) 2.52-2.30 (1H, m, FCCH-1), 1.94-1.85 (1H, m, NCCH-3a), 1.78-1.64 (3H, overlapping m, NCCH-3b and NCCH-2), 1.47 (9H, s, $C(CH_3)_3$); ^{19}F NMR (470 MHz, CD_3OD) δ_F −74.4, −206.2, −212.5, −218.2; ^{13}C NMR (126 MHz, CD_3OD) δ_C 173.0 (1-C=O), 172.5 (5-C=O), 158.6 (1-C=N), 89.8 (CF), 88.5 (CF), 86.9 (CF), 83.0 ($C(CH)_3$), 54.3 (NC-4), 40.3 (NC-1), 36.8 (FC-1), 33.0 (OCC-2), 29.5 (NCC-3), 28.2 ($C(CH_3)_3$), 26.42 (NCC-2); HRMS m/z (ESI$^+$) (Calculated $C_{18}H_{30}F_5N_4O_3^+$ = 445.2233) found 445.2226 (M^+); 3242br (N-H), 3026 (C-H), 1732 (C=O), 1645 (C=N), 1157 (C-O); $[\alpha]_D^{20}$ = −16.0 (*c* 6.02, MeOH).

2-(*tert*-Butylamino)-2-oxo-1-phenylethyl 2-((*1r,2R,3R,4s,5S,6S*)-2,3,4,5,6-pentafluorocyclohexyl)acetate 3.13

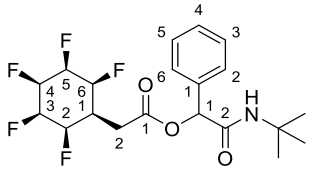

Benzaldehyde (18 µL, 0.18 mmol) and *tert*-Butyl isocyanide (45 µL, 0.40 mmol) were added to **2.58** (50 mg, 0.22 mmol) in acetonitrile (0.4 mL). The solution was heated to 70 °C for 14 h and then concentrated *in vacuo*. The residue was redissolved in EtOAc (3 mL) and washed with brine (3 x 3 mL). The organic phase was dried over $MgSO_4$, filtered and concentrated *in vacuo* to give the crude product which was purified by flash column chromatography (SiO_2, 50% EtOAc in hexane) to give **3.13** as a white crystalline solid (33 mg, 0.078 mmol, 44%): m.p. (Acetone): 144-145 °C; ^{1}H NMR (500 MHz, Acetone-D_6) δ_H 7.56-7.51 (2H, m, ArH), 7.41-7.36 (3H, m, ArH), 7.07 (1H, s, NH), 5.90 (1H, s, OCH-1), 5.43 (1H, app dt *J* = 53.6, 7.3

Hz, FCH-4), 5.25-4.86 (4H, overlapping m, FCH-2, FCH-3, FCH-5 and FCH-6), 3.07-2.92 (2H, m, CH_2-2), 2.71-2.54 (1H, m, FCCH-1), 1.31 (9H, s, CH_3); ^{19}F NMR (471 MHz, $CDCl_3$) δ_F -204.0, -211.4, -216.9; ^{13}C NMR (126 MHz, Acetone-D_6) δ_C 171.1 (C=O), 168.2 (C=O), 137.2 (ArC), 129.6 (ArH), 129.4 (ArH), 128.6 (ArH), 89.6 (FC), 88.1 (FC), 86.7 (FC-3 and FC-5), 77.1 (O*C*H-1), 51.9 (*C*$(CH_3)_3$), 31.6 (H_2C-2), 28.9 (H_3C); HRMS m/z (ESI$^+$) (Calculated $C_{20}H_{24}F_5O_3NNa^+$ = 444.1569) found 444.1561 $[M+Na]^+$; ν_{max}/cm^{-1} 2970br (C-H), 1742, 1670 and 1526 (C=O), 1366, 1134 and 1049 (C-F).

1-(*tert*-Butylamino)-3-methyl-1-oxobutan-2-yl 2-((*1r,2R,3R,4s,5S,6S*)-2,3,4,5,6-pentafluorocyclohexyl)acetate 3.15

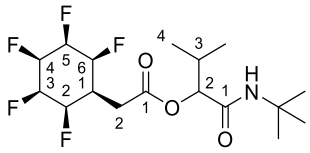

Isobutyraldehyde (24 µL, 0.26 mmol) and *tert*-Butyl isocyanide (24 µL, 0.21 mmol) were added to a suspension of **2.58** in water (5 mL) and MeOH (1 mL) and the suspension was stirred at r.t. for 16 h. The suspension was extracted into EtOAc (3 x 20 mL) and the combined organic phase was washed with brine (3 x 60 mL), dried over $MgSO_4$, filtered and concentrated *in vacuo* to give the crude product which was purified by flash column chromatography (SiO_2, 40-60% EtOAc in hexane) to give **3.15** as a white crystalline solid (42 mg, 0.11 mmol, 52%): m.p. (Acetone): 94-95 °C; ^{1}H NMR (700 MHz, Acetone-D_6) δ_H 6.74 (1H, s, NH), 5.51-5.37 (1H, app d *J* = 53.7 Hz, FCH-4), 5.19-4.90 (4H, overlapping m, FCH-2, FCH-3, FCH-5 and FCH-6), 4.79 (1H, d *J* = 4.9 Hz, OCH-2), 3.00 (1H, dd *J* = 16.7, 7.0 Hz, CH_2-2a), 2.94 (1H, dd *J* = 16.7, 7.6 Hz), 2.69-2.51 (1H, m, FCCH-1), 2.22-2.17 (1H, m, $(H_3C)_2$CH-3), 1.34 (9H, s, $(CH_3)_3$), 0.98-0.95 (6H, m, $(CH_3)_2$); ^{19}F NMR (659 MHz, Acetone-D_6) δ -205.4, -212.2, -212.7, -217.5; ^{13}C NMR (126 MHz, Acetone-D_6) δ_C 171.4 (C=O), 168.8 (C=O), 89.2 (FC), 87.6 (FC), 86.4 (FC), 79.5 (OC-2), 51.6 ($(CH_3)_2$H*C*-3), 36.0 (FCC-1), 31.35 (H_2C-2), 28.9 ($(H_3C)_3$), 19.1 (H_3C-4), 17.5 (H_3C-4); HRMS m/z (ESI$^+$) (Calculated $C_{17}H_{26}F_5O_3NNa^+$ = 410.1725) found 410.1720 $[M+Na]^+$; ν_{max}/cm^{-1} 2968 (C-H), 1736, 1665 and 1526 (C=O), 1134 and 1049 (C-F).

***N*-Allyl-*N*-(2-(*tert*-butylamino)-1-(4-fluorophenyl)-2-oxoethyl)-2-((*1r,2R,3R,4s,5S,6S*)-2,3,4,5,6-pentafluorocyclohexyl)acetamide 3.17**

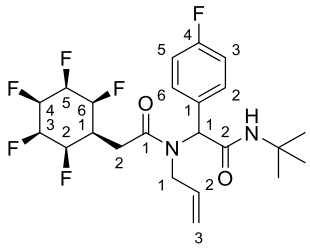

Allylamine (0.017 mL, 0.22 mmol,) and $MgSO_4$ (0.01 g) were added to a solution of 4-fluorobenzaldeyde (0.023 mL, 0.22 mmol) in CH_2Cl_2 (1 mL). The solution was stirred at r.t. until NMR showed complete consumption of the aldehyde starting material. To this *tert*-butyl isocyanide (0.025 mL, 0.22 mmol) in methanol (0.5 mL) and **75** (0.050 g, 0.22 mmol) in methanol (0.5 mL) were added. The solution was stirred at r.t. for 24 h before being concentrated *in vacuo*. The crude product was purified directly by flash column chromatography (SiO_2, 60% EtOAc in 40-60 petroleum ether) and then by HPLC (gradient water to MeCN) to give **3.17** as a fine white powder (0.021 g, 0.044 mmol, 20%): m.p. (MeOH): 173-174 °C; ^{1}H NMR (500 MHz, CD_3OD) δ_H 7.40- 7.37 (2H, m, ArH), 7.14-7.11 (2H, m, ArH), 6.06 (1H, s, OCCH-1), 5.50-5.41 (1H, m, NCCH-2), 5.37-5.21 (1H, app d *J* = 53.9 Hz, FCH-4), 5.07-4.90 (4H, overlapping m, FCH-2, FCH-6 and NCH_2-1), 4.79-4.65 (2H, m, FCH-3 and FCH-5), 4.16-4.08 (1H, m, NCCCH-3a) 3.98-3.90 (1H, m, NCCCH-3b), 2.97-2.94 (2H, m, $OCCH_2$-2), 2.60-2.39 (1H, m, FCCH-1), 1.38 and 1.34 (9H, s (rotamers), C(C*H*$_3$)$_3$); ^{19}F NMR (470 MHz, CD_3OD) δ_F -115.4, -206.2, -211.8, -212.8, -218.25; ^{13}C NMR (126 MHz, CD_3OD) δ_C 171.5 (C=O), 165.2 (C=O), 135.3 (NC*C*H-2), 133.2 (ArCH), 133.1 (ArCH), 132.9 (ArC), 132.85 (ArC), 116.8 (NCH_2-1), 116.5 (ArCH), 116.35 (ArCH), 88.0 (FC), 87.1 (FC), 86.4 (FC), 62.9 (OC*C*H-1), 52.3 ((CH$_3$)$_3$*C*), 49.3 (NCC*C*-3), 36.7 (FCC-1), 31.3 (OC*C*H$_2$-2), 28.8 (H_3C); HRMS m/z (ESI$^+$) (Calculated $C_{23}H_{28}F_6N_2O_2Na^+$ = 501.1947) found 501.1941 $[M+Na]^+$; ν_{max}/cm^{-1} 2968br (C-H), 1630 (C=O).

_N_-Allyl-_N_-(1-(benzylamino)-1-oxo-3-((*1r,2R,3R,4s,5S,6S*)-2,3,4,5,6-pentafluorocyclohexyl)propan-2-yl)benzamide 3.20

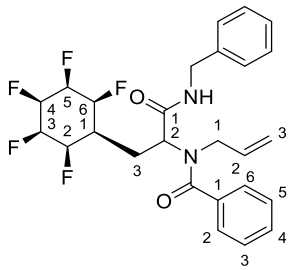

Allylamine (0.028 mL, 0.37 mmol,) and $MgSO_4$ (0.005 g) were added to a solution of **2.87** (0.067 g, 0.31 mmol) in CH_2Cl_2 (2 mL). The solution was stirred at r.t. for 16 h until NMR showed complete consumption of the aldehyde starting material. Then, benzyl isocyanide (0.045 mL, 0.37 mmol) in CH_2Cl_2 (1 mL) and benzoic acid (0.045 g, 0.37 mmol) in CH_2Cl_2 (0.4 mL) were added. The solution was stirred at r.t. for 16 h before being diluted with CH_2Cl_2 (5 mL) and washed with brine (3 x 5 mL). The organic phase was dried over $MgSO_4$, filtered and concentrated *in vacuo*. The crude product was purified by flash column chromatography (SiO_2, 40% EtOAc in hexane to 70% EtOAc in hexane) to give **3.20** as a white crystalline solid (0.131 g, 0.265 mmol, 85%): m.p. (Acetone): 153-154 °C; ^{1}H NMR (500 MHz, Acetone-D_6) δ_H

7.88 (1H, s, NH), 7.47-7.23 (10H, overlapping m, ArCH), 6.18-5.64 (1H, m, NCH_2CH-2) 5.45-5.32 (1H, m, FCH-4), 5.26-4.76 (7H, overlapping m, NCH-2, NCH_2CHCH_2-3, FCH-2, FCH-3, FCH-5 and FCH-6), 4.52-4.37 (2H, m, $PhCH_2$), 4.08-3.94 (2H, m, NCH_2-1), 2.70-2.53 (1H, m, $FCCCH_2$-3a), 2.36-2.21 (1H, m, $FCCCH_2$-3b), 2.21-2.03 (1H, m, FCCH-1); ^{19}F NMR (659 MHz, CD_3OD) δ_F −205.95, −212.8, −218.2; ^{13}C NMR (126 MHz, Acetone-D_6) δ_C 170.4 (*C*=O), 157.7 (*C*=O), 140.3 (ArC), 137.55 (ArC), 135.6 (NCH_2*C*H-2) 130.5 (Ar*C*H), 130.4 (Ar*C*H), 129.2 (Ar*C*H), 128.5 (Ar*C*H), 127.8 (Ar*C*H), 127.7 (Ar*C*H), 118.4 (NCH_2CHCH_2-3) 89.2 (*C*F), 88.1 (*C*F), 86.6 (*C*F), 60.54, 50.7 (NCH_2-1) 43.8 ($PhCH_2$), 36.2 (FCC-1), 26.6 ($FCCCH_2$-3); HRMS m/z ESI$^+$ (Calculated $C_{26}H_{28}F_5N_2O_2^+$ = 495.2065) found 495.2066 $[M+H]^+$; ν_{max}/cm^{-1} 1670 and 1620 (C=O), 1526, 1456 and 1410 (C=C Ar).

N-Allyl-*N*-(1-(benzylamino)-1-oxo-3-((*1r,2R,3R,4s,5S,6S*)-2,3,4,5,6-pentafluorocyclohexyl)propan-2-yl)butyramide 3.21

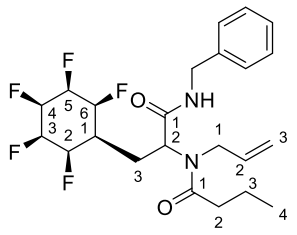

Allylamine (0.025 mL, 0.33 mmol) and $MgSO_4$ (0.005 g) were added to a solution of **2.87** (0.060 g, 0.28 mmol) in CH_2Cl_2 (5 mL). The solution was stirred at r.t. for 16 h until NMR showed complete consumption of the aldehyde starting material. Then, benzyl isocyanide (0.029 mL, 0.32 mmol) in CH_2Cl_2 (1 mL) and butyric acid (0.029 mL, 0.32 mmol) in CH_2Cl_2 (0.5 mL) were added. The solution was stirred at r.t. for 16 h before being diluted with CH_2Cl_2 (10 mL) and washed with brine (3 x 15 mL). The organic phase was dried over $MgSO_4$, filtered and concentrated *in vacuo*. The crude product was purified by flash column chromatography (SiO_2, 20% EtOAc in hexane to 90% EtOAc in hexane) to give **3.21** as a white crystalline solid (0.056 g, 0.12 mmol, 43%): m.p. (Acetone): 121-122 °C; ^{1}H NMR (500 MHz, Acetone-D_6) δ_H 7.68 (1H, s, NH), 7.31-7.21 (5H, overlapping m, ArH), 5.90-5.82 (1H, m, NCCH-2), 5.44-4.70 (8H, m, FCH-1, FCH-2, FCH-3, FCH-4, FCH-5, FCH-6, NCH-2, NCH_2CHCH_2-3), 4.42-4.34 (2H, m, $PhCH_2$), 4.13 (1H, app dd *J* = 17.6, 5.0 Hz, $NCCH_2$-3a), 4.00 (1H, app dd *J* = 17.6, 6.2 Hz, $NCCH_2$-3b), 2.53-2.45 (1H, m, $FCCCH_2$-3a) 2.37-2.29 (2H, m, $NC(O)CH_2$-2), 2.18-2.11 (1H, m, $FCCCH_2$-3b), 2.08-1.91 (1H, m, FCCH-1), 1.60-1.53 (2H, m, $NC(O)CCH_2$-3), 0.87 (3H, t *J* = 7.4 Hz, CH_3-4); ^{19}F NMR (470 MHz, $CDCl_3$) δ_F -203.6, -211.4, -216.7; ^{13}C NMR (126 MHz, Acetone-D_6) δ_H 174.9 (C=O), 170.7 (C=O), 140.2 (ArC), 136.2 (NC*C*H-2), 129.2 (Ar*C*H), 128.4 (Ar*C*H), 127.8 (Ar*C*H), 117.2 (NCH_2CHCH_2-3), 88.9 (FC), 88.7 (FC), 87.5 (FC), 54.5 (NCH-2), 48.1 (NCH_2-1), 43.6 ($PhCH_2$), 36.1 (FCC-1), 35.8 ($NC(O)CH_2$-2), 26.6 ($FCCCH_2$-3), 19.1

(NC(O)CCH_2-3), 14.1 (H_3C-4); HRMS m/z ESI$^+$ (Calculated $C_{23}H_{29}F_5N_2O_2Na^+$ = 483.2041) found 483.2031 $[M+Na]^+$; ν_{max}/cm^{-1} 2963 (C-H), 1622 (C=O), 1132 and 1047 (C-F).

_N_-Benzyl-_N_-(1-(benzylamino)-1-oxo-3-((*1r,2R,3R,4s,5S,6S*)-2,3,4,5,6-pentafluorocyclohexyl)propan-2-yl)propiolamide 3.22

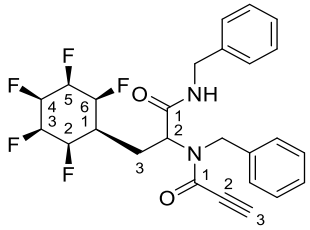

Benzylamine (0.066 mL, 0.61 mmol) and $MgSO_4$ (0.005 g) were added to a solution of **2.87** (0.110 g, 0.509 mmol) in CH_2Cl_2 (10 mL). The solution was stirred at r.t. for 16 h until NMR showed complete consumption of the aldehyde starting material. Then, benzyl isocyanide (0.063 mL, 0.51 mmol) and propiolic acid (0.032 mL, 0.51 mmol) were added. The solution was stirred at r.t. for 16 h before being diluted with CH_2Cl_2 (10 mL) and washed with brine (3 x 20 mL). The organic phase was dried over $MgSO_4$, filtered and concentrated *in vacuo*. The crude product was purified by flash column chromatography (SiO_2, 30% EtOAc in hexane to 70% EtOAc in hexane) to give **3.22** as a white crystalline solid (0.167 g, 0.339 mmol, 67%): m.p. (Acetone): 186-187 °C; Rotamers are present and observable in NMR spectra: ^{1}H NMR (500 MHz, Acetone-D_6) δ_H 8.09 and 7.86 (1H, s, NH), 7.59-7.24 (10H, overlapping m, ArH), 5.39-5.35 and 5.19-5.12 (1H, m, NCH-2), 5.29-3.80 (10H, overlapping m, FCH-2, FCH-3, FCH-4, FCH-5, FCH-6, PhCH_2, C≡CH-3), 2.52-1.94 (2H, overlapping m (rotamers), FCCCH_2-3), 1.79-1.63 (1H, m, FCCH-1); ^{19}F NMR (470 MHz, Acetone-D_6) δ_F −205.2, −212.4, −217.5; ^{13}C NMR (126 MHz, Acetone-D_6) δ_C 169.3 (C=O), 155.8 (C=O), 155.5 (C=O), 140.0 (ArC), 139.6 (ArC), 138.6 (ArC), 129.5 (ArCH), 129.35 (ArCH), 129.2 (ArCH), 128.9 (ArCH), 128.8 (ArCH), 128.55 (ArCH), 128.5 (ArCH), 128.2 (ArCH), 127.9 (ArCH), 127.8 (ArCH), 89.5 (*C*F), 88.6 (*C*F), 87.4 (*C*F), 82.8 (C≡C-2a), 82.0 (C≡C-2b), 60.5 (N*C*H-2a), 55.3 (N*C*H-2b), 51.45, 46.9, 43.9 (Ph*C*H$_2$), 43.8 (Ph*C*H$_2$), 35.8 (FCC-1), 27.5 (FCCC-3a), 26.9 (FCCC-3b); HRMS m/z ESI$^+$ (Calculated $C_{26}H_{25}F_5NO_2Na^+$ = 515.1728) found 515.1708; ν_{max}/cm^{-1} 2106 (C≡C), 1620 (C=O), 1134 and 1049 (C-F).

2-(*N*-Allylacetamido)-*N*-benzyl-3-((*1r,2R,3R,4s,5S,6S*)-2,3,4,5,6-pentafluorocyclohexyl)propenamide 3.23

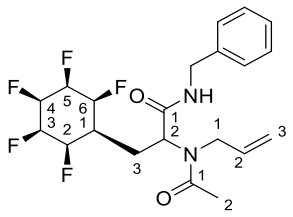

Allylamine (0.012 mL, 0.16 mmol) was added to a solution of **2.87** (0.034 g, 0.16 mmol) in MeOH (0.5 mL) in a microwave vial and the solution was stirred for 5 mins. Then, acetic acid (0.0080 mL, 0.13 mmol) and benzyl isocyanide (0.016 mL, 0.13 mmol) were added and the vial sealed. The solution was heated in a 2.45 GHz microwave reactor targeting 45 °C for 45 mins before being concentrated *in vacuo*. The residue was redissolved in EtOAc (5 mL) and washed with brine (3 x 5 mL). The organic phase was dried over $MgSO_4$, filtered and concentrated *in vacuo* to give the crude product which was purified by flash column chromatography (SiO_2, 70% EtOAc in hexane to 90% EtOAc in hexane) to give **3.23** as a white crystalline solid (0.040 g, 0.093 mmol, 72%): m.p. ($CDCl_3$): 158-159 °C; ^{1}H NMR (500 MHz, $CDCl_3$) δ_H 7.33-7.22 (5H, overlapping m, ArH), 5.71 (1H, ddt *J* = 17.1, 10.5, 5.3 Hz, NCH_2CH-2), 5.35-5.13 (4H, overlapping m, NCH_2CHCH_2-3, NCH-2 and FCH-4), 4.95 (2H, d *J* = 49.0 Hz, FCH-2 and FCH-6), 4.46-4.20 (4H, overlapping m, $PhCH_2$, FCH-3 and FCH-5), 4.03-3.89 (2H, m, NCH_2-1) 2.47 (1H, ddd *J* = 14.8, 9.8, 5.4 Hz, $FCHCHCH_2$-3a), 2.21-2.13 (1H, m, $FCHCHCH_2$-3b), 2.07 (3H, s, CH_3), 1.73-1.54 (1H, m, FCHCH-1); ^{19}F NMR (470 MHz, $CDCl_3$) δ_F −203.4, −211.45, −216.7; ^{13}C NMR (126 MHz, $CDCl_3$) δ_C 173.1 (C=O), 170.0 (C=O), 138.1 (ArC), 133.3 (C=C-2), 128.9 (Ar*C*H), 127.9 (Ar*C*H), 127.7 (Ar*C*H), 117.9 (C=C-3), 88.2 (*C*F), 87.2 (*C*F), 86.2 (*C*F), 54.0 (N*C*H-2), 48.35 (NCH_2-1), 43.6 ($PhCH_2$), 35.9 (FCH*C*H-1), 25.5 ($FCHCHCH_2$-3), 22.1 (H_3C-2); HRMS m/z ESI$^+$ (Calculated $C_{21}H_{25}F_5O_2N_2Na^+$ = 455.1728) found 455.1718 $[M+Na]^+$; ν_{max}/cm^{-1} 1624 (C=O), 1134 and 1049 (C-F).

2-(*N*-Allyl-2,2,2-trifluoroacetamido)-*N*-benzyl-3-((*1r,2R,3R,4s,5S,6S*)-2,3,4,5,6-pentafluorocyclohexyl)propenamide 3.24

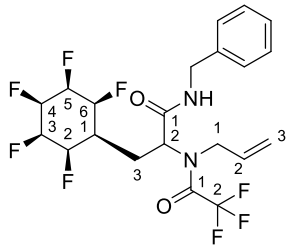

Allylamine (0.017 mL, 0.19 mmol) was added to a solution of **2.87** (0.050 g, 0.23 mmol) in MeOH (0.5 mL) in a microwave vial and the solution was stirred for 5 mins. Then, trifluoroacetic acid (0.015 mL, 0.19 mmol) and benzyl isocyanide (0.023 mL, 0.19 mmol) were added and

the vial sealed. The solution was heated in a 2.45 GHz microwave reactor targeting 45 °C for 45 mins before being concentrated *in vacuo*. The residue was redissolved in EtOAc (5 mL) and washed with brine (3 x 5 mL). The organic phase was dried over $MgSO_4$, filtered and concentrated *in vacuo* to give the crude product which was purified by flash column chromatography (SiO_2, 50% EtOAc in hexane) to give **3.24** as a white crystalline solid (0.061 g, 0.13 mmol, 68%): m.p. (MeOH): 141-142 °C ^{1}H NMR (400 MHz, CD_3OD) δ_H 7.34-7.23 (5H, overlapping m, ArH), 5.84 (1H, ddt *J* = 16.6, 10.9, 6.0 Hz, C=C-H-2), 5.34-4.50 (8H, overlapping m, FCH-2, FCH-3, FCH-4, FCH-5, FCH-6, NCH_2CHCH_2-3, NCH-2), 4.40-4.31 (2H, m, $PhCH_2$), 4.27-4.13 (2H, m, NCH_2-1), 2.61-2.51 (1H, m, $FCHCHCH_2$-3a), 2.29-2.16 (1H, m, $FCHCHCH_2$-3b), 1.95-1.73 (1H, m, FCHCH-1); ^{19}F NMR (377 MHz, CD_3OD) δ_F −70.1 (CF_3), −206.0, −212.6, −213.1, −218.1; ^{13}C NMR (126 MHz, CD_3OD) δ 168.9 (C=O), 157.8 (C=O), 138.2 (ArC), 133.1 (C=C-2), 128.2 (ArH), 127.3 (ArH), 126.9 (ArH), 118.5 (C=C-3), 87.6 (*C*F), 87.5 (*C*F), 86.2 (*C*F), 57.0 (N*C*H-2), 49.0 (N*C*H_2-1) 43.0 (Ph*C*H_2), 35.3 (FCH*C*H-1), 25.5 (FCHCH*C*H_2-3); HRMS m/z ESI$^+$ (Calculated $C_{21}H_{22}F_8O_2N_2Na^+$ = 509.1446) found 509.1442 $[M+Na]^+$; ν_{max}/cm^{-1} 1682 (C=O), 1150 and 1136 (C-F).

_N_-Benzyl-2-(_N_-benzylacetamido)-3-((*1r,2R,3R,4s,5S,6S*)-2,3,4,5,6-pentafluorocyclohexyl)propenamide 3.25

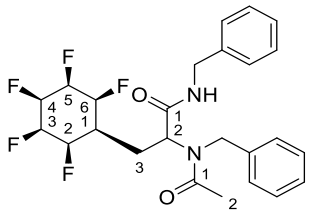

Benzylamine (0.030 mL, 0.28 mmol) was added to a solution of **2.87** (0.054 g, 0.25 mmol) in MeOH (0.5 mL) in a microwave vial and the solution was stirred for 5 mins. Then, acetic acid (0.016 mL, 0.28 mmol) and benzyl isocyanide (0.033 mL, 0.28 mmol) were added and the vial sealed. The solution was heated in a 2.45 GHz microwave reactor targeting 45 °C for 45 mins before being concentrated *in vacuo*. The residue was redissolved in EtOAc (5 mL) and washed with brine (3 x 5 mL). The organic phase was dried over $MgSO_4$, filtered and concentrated *in vacuo* to give the crude product which was purified by flash column chromatography (SiO_2, 80% EtOAc in hexane) to give **3.25** as a white crystalline solid (0.049 g, 0.10 mmol, 41%): m.p. (MeOH): 142-143 °C; ^{1}H NMR (500 MHz, $CDCl_3$) δ_H 7.36-7.17 (10H, overlapping m, ArH, 5.30-5.16 (1H, m, FCH-4), 5.10-5.03 (1H, m, NCH-2), 4.91-4.78 (1H, m, FCH-2a and FCH-6a), 4.70-4.60 (2H, m, $PhCH_2$), 4.54-4.44 (1H, m, FCH-2b and FCH-6b), 4.38-4.27 (1H, m, $PhCH_2$), 4.35-4.04 (2H, m, FCH-3 and FCH-5), 2.48-2.39 (1H, m, $FCHCHCH_2$-3a), 2.15 (3H, s, CH_3-2), 2.16-2.07 (1H, m, $FCHCHCH_2$-3b), 1.64-1.47 (1H, m, FCHCH-1); ^{19}F NMR (470 MHz, $CDCl_3$) δ_F −203.4, −203.5, −211.4, −211.8, −216.9; ^{13}C NMR (126 MHz, $CDCl_3$) δ_C 173.4

(*C*=O), 170.0 (*C*=O), 138.0 (ArC), 136.8 (ArC), 129.3 (Ar*C*H), 128.9 (Ar*C*H), 128.2 (Ar*C*H), 127.8 (Ar*C*H), 127.75 (Ar*C*H), 126.5 (Ar*C*H), 87.8 (*C*F), 86.9 (*C*F), 86.0 (*C*F), 54.85 (N*C*H-2), 50.0 (Ph*C*H_2), 43.6 (Ph*C*H_2), 35.6 (FCH*C*H-1), 25.55 (FCHCH*C*H_2-3), 22.5 (H_3C-2); HRMS m/z ESI$^+$ (Calculated $C_{25}H_{27}F_5N_2O_2Na^+$ = 505.1885) found 505.1875 $[M+Na]^+$; v_{max}/cm^{-1} 1641 (C=O), 1140 (C-F).

tert-Butyl ((*2S*)-1-(benzyl(1-(benzylamino)-1-oxo-3-((*1r,2R,3R,4R,5S,6S*)-2,3,4,5,6-pentafluorocyclohexyl)propan-2-yl)amino)-3-methyl-1-oxobutan-2-yl)carbamate 3.26

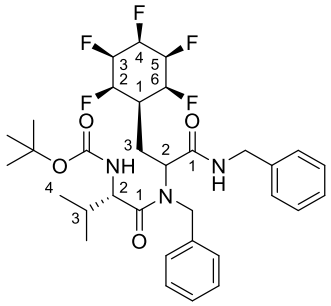

Benzylamine (0.031 mL, 0.29 mmol) was added to a solution of **2.87** (62 mg, 0.29 mmol) in MeOH (0.5 mL) in a microwave vial and the solution was stirred for 5 mins. Then, Boc-L-valine (0.052 g, 0.24 mmol) and benzyl isocyanide (0.029 mL, 0.24 mmol) were added and the vial sealed. The solution was heated in a 2.45 GHz microwave reactor targeting 45 °C for 45 mins before being concentrated *in vacuo*. The residue was redissolved in EtOAc (5 mL) and washed with brine (3 x 5 mL). The organic phase was dried over $MgSO_4$, filtered and concentrated *in vacuo* to give the crude product which was purified by flash column chromatography (SiO_2, 80% EtOAc in hexane) to give **3.26** as a white crystalline solid (0.088 g, 0.14 mmol, 58%): m.p. ($CHCl_3$): 178-179 °C; ^{1}H NMR (500 MHz, $CDCl_3$) δ_H 7.38-7.09 (10H, overlapping m, ArH), 5.32-5.09 (1H, m, FCH-4), 5.14-4.96 (1H, m, CH_2CH-2), 4.88-4.75 (1H, m, FCH-2a and FCH-6a), 4.72-4.60 (2H, m, PhCH_2), 4.59-4.12 (7H, m, PhCH_2, FCH-2b, FCH-6b (CH_3)$_2$CHCH-2, FCH-3, FCH-5, CH_2CH-2), 2.58-2.37 (1H, m, CH_2-3a), 2.11-2.03 (1H, m, CH_2-3b), 1.94-1.87 (1H, m, (CH_3)$_2$CH-3), 1.91-1.76 (1H, m, FCCH-1), 1.43 (9H, s, (CH_3)$_3$), 0.93-0.79 (6H, m, (CH_3)$_2$-4); ^{19}F NMR (471 MHz, $CDCl_3$) δ_F −203.65, −211.55, −216.8; ^{13}C NMR (126 MHz, $CDCl_3$) δ_C 174.8 (*C*=O), 169.9 (*C*=O), 156.25 (*C*=O), 137.8 (ArC), 136.0 (ArC), 129.2 (Ar*C*H), 128.9 (Ar*C*H), 128.7 (Ar*C*H), 128.1 (Ar*C*H), 127.7 (Ar*C*H), 127.5 (Ar*C*H), 87.9 (*C*F), 86.7 (*C*F), 85.1 (*C*F), 80.3 ((CH_3)$_3$*C*), 56.4 ((*C*H_3)$_2$-4), 51.1 (Ph*C*H_2), 43.6 (Ph*C*H_2), 35.8 (FCC-1), 28.3 ((*C*H_3)$_3$), 25.8 (*C*H_2-3), 19.8 (H_3C-4a), 17.1 (H_3C-4b); HRMS m/z ESI$^+$ (Calculated $C_{33}H_{42}F_5N_3O_4Na^+$ = 662.2988) found 662.2984 $[M+Na]^+$; v_{max}/cm^{-1} 2965br (C-H), 1672 and 1639 (C=O), 1136 and 1047 (C-F).

2-(*N*-Allyl-2-(2-chlorophenyl)acetamido)-*N*-benzyl-3-((*1r,2R,3R,4s,5S,6S*)-2,3,4,5,6-pentafluorocyclohexyl)propenamide 3.27

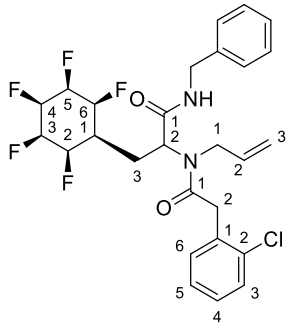

Allylamine (0.017 mL, 0.23 mmol) was added to a solution of **2.87** (50 mg, 0.23 mmol) in MeOH (0.5 mL) in a microwave vial and the solution was stirred for 5 mins. Then, 2-chlorophenylacetic acid (0.032 g, 0.19 mmol) and benzyl isocyanide (0.023 mL, 0.19 mmol) were added and the vial sealed. The solution was heated in a 2.45 GHz microwave reactor targeting 45 °C for 45 mins before being concentrated *in vacuo*. The residue was redissolved in EtOAc (5 mL) and washed with brine (3 x 5 mL). The organic phase was dried over $MgSO_4$, filtered and concentrated *in vacuo* to give the crude product which was purified by flash column chromatography (SiO_2, 20% EtOAc in hexane to 40% EtOAc in hexane) to give **3.27** as a white crystalline solid (0.082 g, 0.15 mmol, 79%): m.p. ($CHCl_3$): 182-183 °C; ^{1}H NMR (500 MHz, $CDCl_3$) δ_H 7.38-7.19 (9H, overlapping m, ArH), 6.92 (1H, t *J* = 5.4 Hz, NH), 5.77 (1H, ddt *J* = 17.0, 10.5, 5.4 Hz, C=CH-2), 5.35-5.20 (3H, overlapping m, FCH-4 and C=C-H_2-3), 5.08 (1H, t *J* = 7.3 Hz, NCH-2), 5.02-4.96 (1H, m, FCH-2a and FCH-6a), 4.92-4.85 (1H, m, FCH-2b and FCH-6b), 4.39-4.25 (4H, overlapping m, FCH-3, FCH-5 and PhCH_2), 4.13-4.00 (2H, m, NCH_2-1), 3.77 (2H, s, ArCH_2) 2.56 (1H, dt *J* = 14.6, 7.3 Hz, FCHCHCH_2-3a), 2.22 (1H, dt *J* = 14.4, 7.3 Hz, FCHCHCH_2-3b), 1.84-1.54 (1H, m, FCHCH-1); ^{19}F NMR (471 MHz, $CDCl_3$) δ_F −203.3, −203.6, −211.2, −211.65, −216.75; ^{13}C NMR (126 MHz, $CDCl_3$) δ_C 172.6 (C=O), 169.8 (C=O), 137.8 (ArC), 134.1 (ArC), 133.1 (C=C-2), 131.6 (Ar*C*H), 129.6 (Ar*C*H), 129.05 (Ar*C*H), 128.9 (Ar*C*H), 128.0 (Ar*C*H), 127.8 (Ar*C*H), 127.4 (Ar*C*H), 118.6 (C=C-3), 88.2 (*C*F), 86.3 (*C*F), 85.1 (*C*F), 54.9 (N*C*H-2), 48.3 (NCH_2-1), 43.8 (PhCH_2), 38.9 (ArCH_2), 35.9 (FCH*C*H-1), 25.4 (FCHCHCH_2-3); HRMS m/z ESI$^+$ (Calculated $C_{27}H_{28}F_5ClN_2O_2Na^+$ = 565.1652) found 565.1650 $[M+Na]^+$; ν_{max}/cm^{-1} 1682 and 1626 (C=O), 1136 (C-F).

2-(*N*-Allylacetamido)-*N*-benzyl-3-phenylpropanamide 3.28

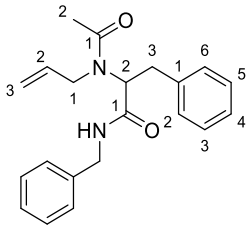

Allylamine (0.034 mL, 0.46 mmol) was added to a solution of phenylacetaldehyde (0.055 g, 0.46 mmol) in MeOH (1 mL) in a microwave vial and the solution was stirred for 5 mins. Then, acetic acid (0.022 mL, 0.38 mmol) and benzyl isocyanide (0.046 mL, 0.38 mmol) were added and the vial sealed. The solution was heated in a 2.45 GHz microwave reactor targeting 45 °C for 45 mins before being concentrated *in vacuo*. The residue was redissolved in EtOAc (5 mL) and washed with brine (3 x 5 mL). The organic phase was dried over $MgSO_4$, filtered and concentrated *in vacuo* to give the crude product which was purified by flash column chromatography (SiO_2, 30% EtOAc in hexane to 100% EtOAc in hexane) to give **3.28** as a colourless oil (0.060 g, 0.18 mmol, 47%): ^{1}H NMR (500 MHz, $CDCl_3$) δ_H 7.31-7.21 (8H, overlapping m, ArH), 7.09-7.06 (2H, m, ArH), 6.80 (1H, t *J* = 5.5 Hz, NH), 5.70-5.62 (1H, m, C=CH-2), 5.20-5.12 (3H, overlapping m, C=CH_2-3 and NCH-2), 4.42 (1H, dd *J* = 15.0, 6.3 Hz, PhCH_2-a), 4.28 (1H, dd *J* = 15.0, 5.6 Hz, PhCH_2-b), 4.02-3.93 (2H, m, NCH_2-1), 3.33 (1H, dd *J* = 13.8, 8.9 Hz, PhCH_2-3a), 3.06 (1H, dd *J* = 13.8, 7.0 Hz, PhCH_2-3b), 2.04 (3H, s, CH_3); ^{13}C NMR (126 MHz, $CDCl_3$) δ_C 172.7 (*C*=O), 170.1 (*C*=O), 138.05 (ArC), 137.2 (ArC), 133.85 (C=C-2), 129.3 (Ar*C*H), 128.6 (Ar*C*H), 127.6 (Ar*C*H), 127.3 (Ar*C*H), 126.75 (Ar*C*H), 117.1 (C=C-3), 58.9 (N*C*H-2), 48.65 (N*C*H_2-1), 43.3 (Ph*C*H_2), 34.7 (Ph*C*H_2-3), 22.1 (H_3C-2); HRMS m/z ESI$^+$ (Calculated $C_{21}H_{24}N_2O_2Na^+$ = 359.1730) found 359.1723 $[M+Na]^+$; ν_{max}/cm^{-1} 1624 (C=O), 1410 (C=C Ar).

2-(*N*-Allylacetamido)-*N*-benzyl-3-cyclohexylpropanamide 3.31

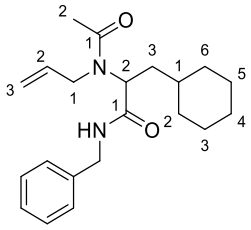

Allylamine (0.017 mL, 0.23 mmol) was added to a solution of cyclohexylacetaldehyde (0.029 g, 0.23 mmol) in MeOH (0.5 mL) in a microwave vial and the solution was stirred for 5 mins. Then, acetic acid (0.011 mL, 0.19 mmol) and benzyl isocyanide (0.023 mL, 0.19 mmol) were added and the vial sealed. The solution was heated in a 2.45 GHz microwave reactor targeting 45 °C for 45 mins before being concentrated *in vacuo*. The residue was redissolved in EtOAc (5 mL) and washed with brine (3 x 5 mL). The organic phase was dried over $MgSO_4$, filtered

and concentrated *in vacuo* to give the crude product which was purified by flash column chromatography (SiO_2, 10% EtOAc in hexane to 50% EtOAc in hexane) to give **3.31** as a colourless oil (0.029 g, 0.085 mmol, 45%): ^{1}H NMR (700 MHz, $CDCl_3$) δ_H 7.33-7.20 (5H, overlapping m, ArH), 6.75 (1H, t *J* = 5.5 Hz, NH), 5.72-5.65 (1H, m, C=CH-2), 5.16-5.06 (3H, overlapping m, C=CH_2-3 and NCH-2), 4.40 (1H, dd *J* =15.0, 6.0 Hz, PhCH_2-a), 4.34 (1H, dd *J* = 15.0, 5.9 Hz, PhCH_2-b), 3.96 (1H, app ddt *J* = 17.7, 5.7, 1.6 Hz, NCH_2-1a), 3.87 (1H, app ddt *J* = 17.7, 5.0, 1.7 Hz, NCH_2-1b), 2.08 (3H, s, CH_3-2), 1.90-1.83 (1H, ddd *J* = 13.8, 7.5, 7.2 Hz, CyCH_2-3a), 1.76-1.61 (5H, overlapping m, CyH), 1.53-1.49 (1H, ddd *J* = 13.8, 7.5, 6.8 Hz, CyCH_2-3b), 1.21-1.10 (4H, overlapping m, CyH), 0.95-0.86 (2H, overlapping m, CyH); ^{13}C NMR (176 MHz, $CDCl_3$) δ_C 172.8 (*C*=O), 171.1 (*C*=O), 138.4 (ArC), 134.1 (C=C-2), 128.7 (Ar*C*H), 127.8 (Ar*C*H), 127.5 (Ar*C*H), 117.1 (C=C-3), 54.3 (N*C*H-2), 47.8 (N*C*H_2-1), 43.4 (Ph*C*H_2), 35.5 (Cy*C*H_2-3), 34.5 (CyC), 33.4 (CyC), 26.5 (CyC), 26.3 (CyC), 26.3 (CyC), 22.2 (H_3C-2); HRMS m/z ESI$^+$ (Calculated $C_{21}H_{30}N_2O_2Na^+$ = 365.2199) found 365.2197; ν_{max}/cm^{-1} 1626 (C=O), 1414 (C=C Ar).

_N_-Benzyl-2-(_N_-benzylacetamido)-3-phenylpropanamide 3.29

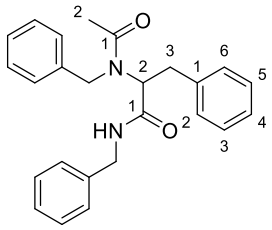

Benzylamine (0.025 mL, 0.23 mmol) was added to a solution of phenylacetaldehyde (0.025 mL, 0.23 mmol) in MeOH (0.5 mL) in a microwave vial and the solution was stirred for 5 mins. Then, acetic acid (0.011 mL, 0.19 mmol) and benzyl isocyanide (0.023 mL, 0.19 mmol) were added and the vial sealed. The solution was heated in a 2.45 GHz microwave reactor targeting 45 °C for 45 mins before being concentrated *in vacuo*. The residue was redissolved in EtOAc (5 mL) and washed with brine (3 x 5 mL). The organic phase was dried over $MgSO_4$, filtered and concentrated *in vacuo* to give the crude product which was purified by flash column chromatography (SiO_2, 50% EtOAc in hexane to 70% EtOAc in hexane) to give **3.29** as a colourless oil (0.030 g, 0.078 mmol, 35%): ^{1}H NMR (500 MHz, $CDCl_3$) δ_H 7.30-7.01 (15H, overlapping m, ArH), 6.68 (1H, app t *J* = 5.5 Hz, NH), 5.12 (1H, dd *J* = 9.0, 6.8 Hz, NCH-2), 4.61 (1H, d *J* = 17.7, PhCH_2a) 4.55 (1H, d *J* = 17.7, PhCH_2b), 4.41 (1H, dd *J* =14.9, 6.4 Hz, PhCH_2a'), 4.18 (1H, dd, *J* = 14.9, 5.4 Hz, PHCH_2-b'), 3.25 (1H, dd *J* = 13.6, 9.0 Hz, PhCH_2-3a), 3.00 (1H, dd *J* = 13.6, 6.8, PhCH_2-3b), 2.04 (3H, s, CH_3-2); ^{13}C NMR (126 MHz, $CDCl_3$) δ_C 173.0 (*C*=O), 170.0 (*C*=O), 138.0 (ArC), 137.3 (ArC), 129.4 (ArCH), 129.0 (ArCH), 128.7 (ArCH), 127.6 (ArCH), 127.5 (ArCH), 127.4 (ArCH), 126.8 (ArCH), 126.2 (ArCH), 60.0 (N*C*H-2), 50.2 (Ph*C*H_2), 43.3 (Ph*C*H_2), 34.9 (Ph*C*H_2-3), 22.5 (H_3C-2); HRMS m/z ESI$^+$

(Calculated $C_{25}H_{26}O_2N_2Na^+$ = 409.1886) found 409.1875 $[M+Na]^+$; ν_{max}/cm^{-1} 1626 (C=O), 1452 (C=C Ar).

2-(*N*-Allyl-2-(2-chlorophenyl)acetamido)-*N*-benzyl-3-phenylpropanamide 3.30

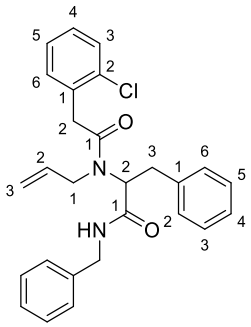

Benzylamine (0.025 mL, 0.23 mmol) was added to a solution of phenylacetaldehyde (0.025 mL, 0.23 mmol) in MeOH (0.5 mL) in a microwave vial and the solution was stirred for 5 mins. Then, acetic acid (0.011 mL, 0.19 mmol) and benzyl isocyanide (0.023 mL, 0.19 mmol) were added and the vial sealed. The solution was heated in a 2.45 GHz microwave reactor targeting 45 °C for 45 mins before being concentrated *in vacuo*. The residue was redissolved in EtOAc (5 mL) and washed with brine (3 x 5 mL). The organic phase was dried over $MgSO_4$, filtered and concentrated *in vacuo* to give the crude product which was purified by flash column chromatography (SiO_2, 50% EtOAc in hexane to 70% EtOAc in hexane) to give **3.31** as a colourless oil (0.030 g, 0.067 mmol, 35%): ^{1}H NMR (500 MHz, $CDCl_3$) δ_H 7.35-7.05 (14H, overlapping m, ArH), 6.75 (1H, app t *J* 5.5 Hz, NH), 5.70-5.61 (1H, m, C=CH-2), 5.21-5.12 (3H, overlapping m, NCH-2 and $C=CH_2$-3), 4.36 (1H, dd *J* = 14.9, 6.1 Hz, $PhCH_2$a), 4.30 (1H, dd *J* = 14.9, 5.8 Hz, $PhCH_2$b), 4.05 (1H, app ddt *J* = 17.9, 5.0, 1.7 Hz, NCH_2-1a), 3.99 (1H, app ddt *J* = 17.9, 5.5, 1.6 Hz, NCH_2-1b), 3.71 (2H, s, $OCCH_2$-2), 3.34 (1H, dd *J* = 14.0, 8.2 Hz, $PhCH_2$-3a), 3.13 (1H, dd *J* = 14.0, 7.8 Hz, $PhCH_2$-3b); ^{13}C NMR (126 MHz, $CDCl_3$) δ_C 172.1 (C=O), 170.0 (C=O), 138.0 (ArC), 137.1 (ArC), 134.2 (ArC), 133.55 (C=C-2), 133.2 (ArC), 129.4 (ArCH), 129.3 (ArCH), 128.6 (ArCH), 128.6 (ArCH), 128.55 (ArCH), 127.6 (ArCH), 127.3 (ArCH), 127.0 (ArCH), 126.7 (ArCH), 117.5 (C=C-3), 59.4 (N*C*H-2), 48.35 (NCH_2-1), 43.3 (PhCH_2), 38.8 (OCCH_2-2), 34.4 (PhCH_2-3); HRMS m/z ESI$^+$ (Calculated $C_{27}H_{27}O_2N_2ClNa^+$ = 469.1653) found 469.1643; ν_{max}/cm^{-1} 1636 (C=O), 1454 (C=C Ar).

***N*,*N*-Dibenzyl-2-((*1r,2R,3R,4s,5S,6S*)-2,3,4,5,6-pentafluorocyclohexyl)ethan-1-amine 3.32**

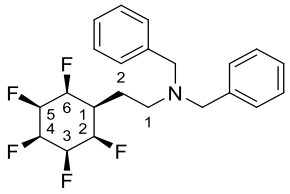

Dibenzylamine (0.17 mL, 0.88 mmol) and 4 Å molecular sieves (0.500 g) were added to a solution of **2.87** (0.166 g, 0.769 mmol) in CH_2Cl_2 (13 mL) and the suspension was stirred at r.t. for 16 h. After TLC showed complete consumption of **2.87**, sodium triacetoxyborohydride (0.488 g, 2.30 mmol) and acetic acid (0.102 mL 1.78 mmol) were added and the suspension was stirred for a further 1 h at r.t.. The suspension was filtered, and the filtrate was quenched by the addition of saturated $NaHCO_3$ solution (10 mL). The phases were separated, and the aqueous layer was extracted into CH_2Cl_2 (2 x 10 mL). The combined organic phase was washed with brine, dried over $MgSO_4$, filtered and concentrated *in vacuo* to give the crude product which was purified by flash column chromatography (SiO_2, 20% EtOAc in hexane to 40% EtOAc in hexane) to give **3.32** as a white crystalline solid (0.199 g, 0.501 mmol, 65%): m.p. (acetone): 147-148 °C ^{1}H NMR (300 MHz, Acetone-D_6) δ_H 7.39-7.20 (10H, overlapping m, ArH), 5.28 (1H, app dt *J* = 53.0, 7.7 Hz, FCH-4), 4.95-4.34 (4H, overlapping m, FCH-2, FCH-3, FCH-5 and FCH-6), 3.57 (4H, s, $PhCH_2$), 2.57 (2H, t *J* = 6.3 Hz, CH_2-1), 2.35-2.08 (1H, m, FCHCH-1), 1.98-1.90 (2H, m, CH_2-2); ^{19}F NMR (471 MHz, $CDCl_3$) δ_F −203.3, −212.0, −216.75; ^{13}C NMR (126 MHz, $CDCl_3$) δ_C 139.7 (ArC), 129.3 (Ar*C*H), 128.6 (Ar*C*H), 127.6 (Ar*C*H), 87.45 (*C*F), 87.35 (*C*F), 86.2 (*C*F), 59.5 (Ph*C*H_2), 49.1 (H_2C-1), 35.3 (FCC-1), 24.0 (H_2C-2); HRMS m/z ESI$^+$ (Calculated $C_{22}H_{25}F_5N^+$ = 398.1902) found 398.1893 $[M+H]^+$; ν_{max}/cm^{-1} 1452 (C=C Ar), 1090 and 1047 (C-F).

4-(2-((*1r,2R,3R,4s,5S,6S*)-2,3,4,5,6-Pentafluorocyclohexyl)ethyl)morpholine 3.35

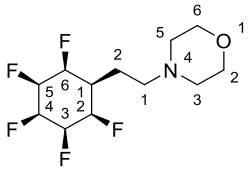

Morpholine (0.025 mL, 0.29 mmol) was added to a solution of **2.87** (0.053 g, 0.24 mmol) in CH_2Cl_2 (4 mL) and the solution was stirred at r.t. for 16 h. After TLC showed complete consumption of **2.87**, sodium triacetoxyborohydride (0.106 g, 0.500 mmol) and acetic acid (0.015 mL 0.26 mmol) were added and the solution was stirred for a further 1 h at r.t.. The solution was quenched by the addition of saturated $NaHCO_3$ solution (4 mL). The phases were separated, and the aqueous layer was extracted into CH_2Cl_2 (2 x 4 mL). The combined organic phase was washed with brine, dried over $MgSO_4$, filtered and concentrated *in vacuo* to give the crude product which was purified by flash column chromatography (SiO_2, 10% MeOH in CH_2Cl_2) to give **3.35** as white crystalline solid (0.044 g, 0.15 mmol, 63%): m.p. (acetone): 163 °C (decomposition); ^{1}H NMR (500 MHz, Acetone-D_6) δ_H 5.38 (1H, app dt *J* = 53.9, 7.4 Hz, FCH-4), 5.16-5.00 (2H, m, FCH-2 and FCH-6), 4.99-4.78 (2H, m, FCH-3 and FCH-5), 3.58 (4H app t *J* = 4.6 Hz, $CyCH_2$), 2.51 (2H, t *J* = 6.7 Hz, NCH_2-1), 2.41 (4H, br s, $CyCH_2$), 2.31-2.13 (1H, m, FCHCH-1), 2.00-1.96 (2H, m, $FCCCH_2$-2); ^{19}F NMR (471 MHz, Acetone-D_6) δ_F

−204.8, −212.45, −217.45; ^{13}C NMR (126 MHz, Acetone-D_6) δ_C 89.0 (*C*F), 88.6 (*C*F), 87.3 (*C*F), 67.4 (CyC), 55.7 (N*C*H_2-1), 54.4 (CyC), 36.5 (FCC-1), 23.2 (FCC*C*H_2-2); HRMS m/z ESI$^+$ (Calculated $C_{12}H_{19}F_5NO^+$ = 288.1381) found 288.1374 $[M+H]^+$; ν_{max}/cm^{-1} 1115 and 1042 (C-F).

1-(2-((*1r,2R,3R,4s,5S,6S*)-2,3,4,5,6-Pentafluorocyclohexyl)ethyl)piperidine 3.36

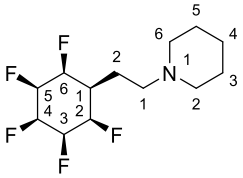

Piperidine (0.047 mL, 0.48 mmol) was added to a solution of **2.87** (0.051 g, 0.23 mmol) in 1,2-Dichloroethane (2.3 mL) and the solution was stirred at r.t. for 16 h. After TLC showed complete consumption of **2.87**, sodium triacetoxyborohydride (0.078 g, 0.37 mmol) and acetic acid (1M in CH_2Cl_2, 0.28 mL 0.28 mmol) were added and the solution was stirred for a further 16 h at r.t.. The solution was quenched by the addition of saturated $NaHCO_3$ solution (4 mL). The phases were separated, and the aqueous layer was extracted into CH_2Cl_2 (2 x 4 mL). The combined organic phase was washed with brine, dried over $MgSO_4$, filtered and concentrated *in vacuo* to give the crude product which was purified by flash column chromatography (SiO_2, 50% MeOH in CH_2Cl_2) to give **3.36** as white crystalline solid (0.019 g, 0.067 mmol, 29%): m.p. (MeOH): 167-168 °C; ^{1}H NMR (500 MHz, CD_3OD) δ_H 5.23 (1H, app d *J* = 54.4 Hz, FCH-4), 4.96-4.87 (2H, m, FCH-2 and FCH-6), 4.64 (2H, app dt *J* = 40.1, 28.2 Hz, FCH-3 and FCH-5), 2.50-2.41 (6H, overlapping m, NCH_2-1 and CyCH_2), 2.00-1.94 (2H, m, FCCCH_2-2), 1.93-1.75 (1H, m, FCHCH-1), 1.62-1.58 (4H, m, CyCH_2), 1.51-1.44 (2H, m, CyCH_2); ^{19}F NMR (471 MHz, CD_3OD) δ_F −205.9, −213.3, −218.2; ^{13}C NMR (126 MHz, CD_3OD) δ_C 89.9 (*C*F), 88.4 (*C*F), 87.1 (*C*F), 57.0 (N*C*H_2-1), 55.5 (CyC), 37.6 (FCC-1), 26.6 (CyC), 25.3 (CyC), 23.8 (FCCC-2); HRMS m/z ESI$^+$ (Calculated = $C_{13}H_{20}F_5N$ = 286.1589) found 286.1579 $[M+H]^+$; ν_{max}/cm^{-1} 1128 and 1043 (C-F).

Ethyl (*E*)-4-((*1r,2R,3R,4s,5S,6S*)-2,3,4,5,6-pentafluorocyclohexyl)but-2-enoate 3.38

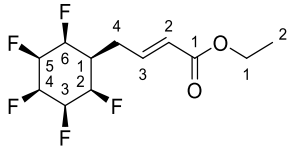

(Carbethoxymethylene)triphenylphosphorane (0.201 g, 0.578 mmol) was added to a solution of **2.87** (0.052 g, 0.24 mmol) in CH_2Cl_2 (1 mL). The solution was stirred for 4h and then concentrated *in vacuo*. The residue was purified directly by flash column chromatography (SiO_2, 10% EtOAc in hexane to 60% EtOAc in hexane) to give **3.38** as a white crystalline solid

(0.047 g, 0.16 mmol, 68%): m.p. (acetone): 111-112 °C; **3.38** was isolated in an *E*:*Z* 9:1 ratio, only peaks of the major stereoisomer are assigned: ^{1}H NMR (500 MHz, Acetone-D_6) δ_H 6.98 (1H, dt *J* = 15.6, 7.5 Hz, C=CH-3), 6.03 (1H, app dt *J* = 15.6, 1.4 Hz, C=CH-2), 5.51-5.33 (1H, m, FCH-4), 5.13-4.84 (4H, overlapping m, FCH-2, FCH-3, FCH-5 and FCH-6), 4.17 (2H, q *J* = 7.1 Hz, OCH_2-1), 2.76 (2H, app t *J* = 7.5 Hz, CH_2-4), 2.42-2.22 (1H, m, FCHCH-1), 1.26 (3H, t *J* = 7.1 Hz, OCH_2CH_3-2); ^{19}F NMR (659 MHz, Acetone-D_6) δ_F −205.3, −213.1, −217.5; ^{13}C NMR (126 MHz, Acetone-D_6) δ_C 165.3 (*C*=O), 144.3 (C=C), 124.25 (C=C), 88.5 (*C*F), 86.9 (*C*F), 85.65 (*C*F), 59.8 (OCH_2-1), 59.6 (H_2C-4), 37.2 (FCC-1), 13.65 (OCH_2CH_3); HRMS m/z ESI$^+$ (Calculated $C_{12}H_{15}F_5O_2Na^+$ = 309.0884) found 309.0876 $[M+Na]^+$; ν_{max}/cm^{-1} 1715 (C=O), 1655 (C=C).

(2-((*1r,2R,3R,4s,5S,6S*)-2,3,4,5,6-Pentafluorocyclohexyl)ethyl)triphenylphosphonium bromide 3.39

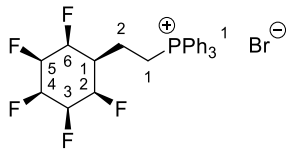

Triphenylphosphine (0.168 g, 0.640 mmol) was added to a solution of **2.82** (0.090 g, 0.32 mmol) in toluene (1.5 mL) and the solution was heated to 111 °C for 16 h. A white precipitate was isolated from the solution by filtration and was washed with hexane (10 mL) and cold Et_2O (3 mL) to give **3.39** as a fine white powder (0.161 g, 0.296 mmol, 93%): m.p. (MeOH): >350 °C (no melt observed); ^{1}H NMR (500 MHz, CD_3OD) δ_H 7.91-7.75 (15H, overlapping m, ArH), 5.27 (1H, app d *J* = 54.3 Hz, FCH-4), 5.07 (2H, d *J* = 49.4 Hz, FCH-2 and FCH-6), 4.87-4.59 (2H, m, FCH-3 and FCH-5), 3.64-3.58 (2H, m, CH_2-1), 2.27-1.97 (3H, overlapping m, FCCH-1 and CH_2-2); ^{19}F NMR (471 MHz, CD_3OD) δ_F −206.3, −213.3, −218.4; ^{31}P NMR (202 MHz, CD_3OD) δ_P 24.1; ^{13}C NMR (126 MHz, CD_3OD) δ_C 135.1 (Ar*C*H), 133.4 (Ar*C*H), 130.2 (Ar*C*H), 118.4 (ArC), 117.7 (ArC), 88.0 (*C*F), 86.3 (*C*F), 85.4 (*C*F), 38.5 (FCC-1), 19.3 (H_2C-2), 18.6 (H_2C-1); HRMS m/z ESI$^+$ (Calculated $C_{26}H_{25}F_5P^+$ = 463.1609) found 463.1600 $[M]^+$; ν_{max}/cm^{-1} 1439 (C=C Ar), 1130 and 1113 (C-F).

Dimethyl 2-(2-((*1r,2R,3R,4s,5S,6S*)-2,3,4,5,6-pentafluorocyclohexyl)ethoxy)terephthalate 3.48

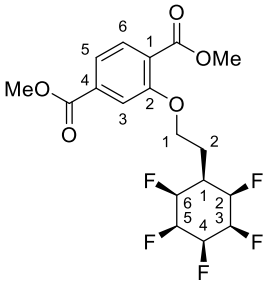

K_2CO_3 (23 mg, 0.17 mmol) and **2.82** (48 mg, 0.17 mmol) were added to a solution of dimethyl 2-hydroxyterephthalate (29 mg, 0.14 mmol) in DMF (3 mL). The suspension was heated to 90 °C for 14 h before being diluted with water (30 mL) and then extracted into CH_2Cl_2 (3 x 30 mL). The combined organic phase was washed with water (3 x 30 mL), dried over $MgSO_4$, filtered and concentrated *in vacuo*. The residue was purified by flash column chromatography (SiO_2, hexane to 20% EtOAc in hexane) to give **3.48** as a white crystalline solid (40 mg, 0.097 mmol, 69%): m.p. ($CHCl_3$): 165 °C; ^{1}H NMR (700 MHz, $CDCl_3$) δ_H 7.82 (1H, d *J* = 7.9 Hz, ArCH), 7.67-7.65 (2H, overlapping m, ArCH), 5.36 (1H, app d *J* = 53.0 Hz, FCH-4), 5.02 (2H, app d *J* = 49.2 Hz, FCH-2, FCH-6), 4.65-4.51 (2H, m, FCH-3, FCH-5), 4.32 (2H, t *J* = 5.7 Hz, OCH_2-1), 3.94 (3H, s, OCH_3), 3.84 (3H, s, OCH_3), 2.53-2.35 (3H, overlapping m, FCCH-1, CH_2-2); ^{19}F NMR (470 MHz, $CDCl_3$) δ_F −203.5, −212.1, −216.8; ^{13}C NMR (176 MHz, $CDCl_3$) δ_C 166.0 (C=O), 165.6 (C=O), 157.9 (ArC), 134.9 (ArC), 131.7 (Ar*C*H), 124.1 (ArC), 122.0 (Ar*C*H), 114.4 (Ar*C*H), 88.1 (*C*F), 86.9 (*C*F), 85.9 (*C*F), 65.4 (O*C*H_2-1), 52.75 (O*C*H_3), 52.3 (O*C*H_3), 34.7 (FCC-1), 25.6 (*C*H_2-2) HRMS m/z ESI$^+$ (Calculated $C_{18}H_{19}F_5O_5Na^+$ = 433.1045) found 433.1041 $[M+Na]^+$; ν_{max}/cm^{-1} 1724 (C=O), 1292 (C-O), 1227 (C-O).

2-(2-((*1r,2R,3R,4s,5S,6S*)-2,3,4,5,6-Pentafluorocyclohexyl)ethoxy)terephthalic acid 3.49

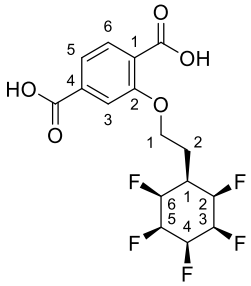

A round bottom flask was charged with **3.48** (37 mg, 0.090 mmol) and HCl (6 M, 10 mL) and heated to reflux for 14 h. The solution was basified to pH 9 with saturated $NaHCO_3$ solution and residual starting material was extracted into EtOAc (3 x 50 mL). The aqueous phase was reacidified by addition of HCl (1M) and extracted into EtOAc (3 x 50 mL). This second extract

was dried over $MgSO_4$, filtered and concentrated *in vacuo* to give **3.49** as a white crystalline solid (33 mg, 0.086 mmol, 96%): m.p. (Acetone): 235-236 °C; ^{1}H NMR (700 MHz, CD_3OD) δ_H 7.78 (1H, d *J* = 7.9 Hz, ArCH), 7.73 (1H, s, ArCH), 7.65-7.64 (1H, m, ArCH), 5.27 (1H, app d *J* = 53.9 Hz, FCH-4), 5.02 (2H, app d *J* = 49.8 Hz, FCH-2, FCH-6), 4.68 (2H, app dt *J* = 40.5, 27.6 Hz, FCH-3, FCH-5), 4.32 (2H, t *J* = 5.6 Hz, OCH_2-1), 2.36-2.22 (3H, overlapping m, FCCH-1, CH_2-2); ^{19}F NMR (659 MHz, CD_3OD) δ_F −205.9, −213.55, −218.4; ^{13}C NMR (176 MHz, CD_3OD) δ_C 169.4 (C=O), 168.7 (C=O), 158.9 (ArC), 136.4 (ArC), 132.1 (ArCH), 126.9 (ArC), 122.85 (ArCH), 115.4 (ArCH), 89.8 (FC), 88.5 (FC), 87.3 (FC), 67.0 (O*C*H_2-2), 36.2 (FCC-1), 26.8 (*C*H_2-2); HRMS m/z ESI$^-$ (Calculated $C_{16}H_{14}F_5O_5$ = 381.0767) found 381.0766 $[M-H]^-$; ν_{max}/cm^{-1} 2922 (C-H), 1686 (C=O), 1439 (O-H).

Dimethyl 5-(2-((*1r,2R,3R,4s,5S,6S*)-2,3,4,5,6-pentafluorocyclohexyl)ethoxy)isophthalate 3.50

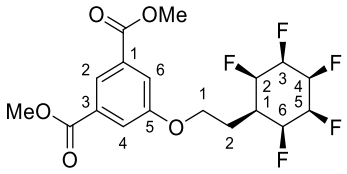

K_2CO_3 (70 mg, 0.51 mmol) and **2.82** (147 mg, 0.52 mmol) were added to a solution of dimethyl 5-hydroxyisophthalate (89 mg, 0.42 mmol) in DMF (9 mL). The suspension was heated to 90 °C for 14 h. The reaction was diluted with water (90 mL) and then extracted into CH_2Cl_2 (3 x 90 mL). The combined organic phase was washed with water (3 x 90 mL) and the organic phase was dried over MgSO4, filtered and concentrated in vacuo. The residue was purified by flash column chromatography (SiO_2, hexane to 20% EtOAc in hexane) to give **3.50** as a white crystalline solid, (105 mg, 0.256 mmol, 62%): m.p. (Acetone): 143-144 °C; ^{1}H NMR (500 MHz, DMSO-D_6) δ_H 8.09 (1H, t *J* = 1.4 Hz, ArCH-2), 7.72 (2H, d *J* = 1.4 Hz, ArCH-4, ArCH-6), 5.46-5.32 (1H, m, H-4), 5.15-5.02 (2H, m, FCH-2, FCH-6), 4.99-4.76 (2H, m, FCH-3, FCH-5), 4.28 (2H, t *J* = 6.0 Hz, OCH_2-1), 3.89 (6H, s, OCH_3), 2.29-2.11 (3H, overlapping m, FCCH-1, CH_2-2); ^{19}F NMR (471 MHz, DMSO-D_6) δ_F −203.4, −211.5, −216.3; ^{13}C NMR (176 MHz, Acetone-D_6) δ_C 165.4 (*C*=O), 159.1 (ArC), 132.0 (ArC), 122.3 (Ar*C*H), 119.4 (Ar*C*H), 88.4 (*C*F), 87.4 (*C*F), 86.1 (*C*F), 65.3 (O*C*H_2-1), 51.9 (CO_2CH_3), 35.1 (FCC-1), 25.7 (*C*H_2-2); HRMS m/z (ESI$^+$) (Calculated $C_{18}H_{20}F_5O_5^+$ = 411.1225) found 411.1225 $[M+H]^+$; ν_{max}/cm^{-1} 1717 (C=O), 1248 (C-F).

1-(2-((*1r,2R,3R,4s,5S,6S*)-2,3,4,5,6-Pentafluorocyclohexyl)ethyl)-1H-1,2,3-triazole-4-carboxylic acid 3.51

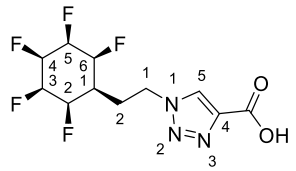

Propiolic acid (0.020 g, 0.29 mmol), sodium ascorbate (0.008 g, 0.04 mmol) and copper sulfate pentahydrate (0.002 g, 0.009 mmol) were added to a solution of **2.83** (0.071 g, 0.29 mmol) in EtOH (1 mL) and water (1 mL). The reaction was warmed to 65 °C and stirred for 15 h. The reaction was basified with saturated sodium hydrogen carbonate solution and organic impurities were extracted into EtOAc (3x 5 mL). The remaining aqueous phase was acidified with HCl (1M) and extracted into EtOAc (3x 10 mL). The organic phase was dried over $MgSO_4$, filtered and concentrated *in vacuo* to give **3.51** (0.072 g, 0.23 mmol, 79%) as white powder: m.p. (Acetone): >300 °C (no melt); ^{1}H NMR (500 MHz, DMSO-D_6) δ_H 8.75 (1H, s, C=CH-5), 5.41-5.27 (1H, m, FCH-4), 5.05 (2H, app d *J* = 50.5 Hz, FCH-2 and FCH-6), 4.93-4.74 (2H, m, FCH-3 and FCH-5), 4.59 (1H, t *J* = 6.8 Hz, CH_2-1), 2.28-2.23 (2H, m, CH_2-2), 1.96-1.72 (1H, FCCH-1); ^{19}F NMR (471 MHz, DMSO-D_6) δ_F −203.6, −211.7, −216.3; ^{13}C NMR (126 MHz, DMSO-D_6) δ_C 162.2 (*C*=O), 140.2 (C=C-4), 129.7 (C=C-5), 88.7 (*C*F), 87.0 (*C*F), 85.8 (*C*F), 47.0 (H_2C-1), 34.8 (FCC-1), 26.6 (H_2C-2); HRMS m/z ESI$^-$ (Calculated $C_{11}H_{11}F_5O_2N_3^-$ = 312.0777) found 312.0775 [M−H]$^-$; v_{max}/cm^{-1} 1680 (C=O), 1053 (C-F).

1-(1-(2-((*1r,2R,3R,4s,5S,6S*)-2,3,4,5,6-Pentafluorocyclohexyl)ethyl)-1H-1,2,3-triazol-4-yl)cyclohexan-1-ol 3.53

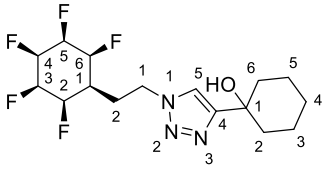

1-Ethynyl-1-methylcyclohexane (0.036 g, 0.29 mmol), sodium ascorbate (0.008 g, 0.04 mmol) and copper sulfate pentahydrate (0.002 g, 0.008 mmol) were added to a solution of **2.83** (0.071 g, 0.29 mmol) in ethanol (1 mL) and water (1 mL). The solution was warmed to 65 °C and stirred for 4 h before being extracted into EtOAc (3 x 5 mL). The combined organic phase was washed with brine (5 mL), dried over $MgSO_4$, filtered and concentrated *in vacuo*. The crude product was purified by flash column chromatography (SiO_2, 70% EtOAc in hexane) to give **3.53** as a white crystalline solid (0.025 g, 0.068 mmol, 23%): m.p. (Acetone): 209 °C; ^{1}H NMR (700 MHz, Acetone-D_6) δ_H 7.88 (1H, s, C=CH-5), 5.40 (1H, app d *J* = 54.1 Hz, FCH-4), 5.17-5.08 (2H, m, FCH-2 and FCH-6), 4.99-4.81 (2H, m, FCH-3 and FCH-5), 4.63 (2H, t *J* = 7.1 Hz, CH_2-1), 3.82 (1H, s, OH), 2.43-2.38 (2H, m, FCCCH_2-2), 1.98-1.94 (2H, m, CyCH_2),

1.80-1.73 (4H, overlapping m, $CyCH_2$), 1.60-1.47 (3H, overlapping m, FCCH-1 and $CyCH_2$), 1.37-1.27 (2H, m, $CyCH_2$); ^{19}F NMR (659 MHz, Acetone-D_6) δ_F −205.2, −212.75, −217.5; ^{13}C NMR (126 MHz, Acetone-D_6) δ_C 121.3 (C=C-5), 89.15 (*C*F), 87.6 (*C*F), 86.7 (*C*F), 47.4 (H_2C-1), 39.05 (Cy*C*H_2), 27.7 (CyC), 26.4 (FCC*C*H_2-2), 25.1 (FCC-1), 22.7 (Cy*C*H_2); HRMS m/z ESI$^+$ (Calculated $C_{16}H_{22}F_5N_3ONa^+$ = 390.1575) found 390.1571 $[M+Na]^+$; v_{max}/cm^{-1} 1132 and 1051 (C-F).

1-(2-((*1r,2R,3R,4s,5S,6S*)-2,3,4,5,6-Pentafluorocyclohexyl)ethyl)-4-(p-tolyl)-1H-1,2,3-triazole 3.54

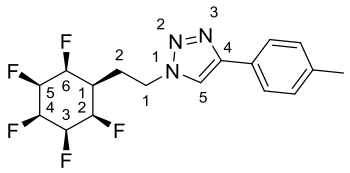

4-Ethynyltoluene (0.034 g, 0.29 mmol), sodium ascorbate (0.008 g, 0.04 mmol) and copper sulfate pentahydrate (0.002 g, 0.008 mmol) were added to a solution of **2.83** (0.071 g, 0.29 mmol) in ethanol (1 mL) and water (1 mL). The solution was warmed to 65 °C and stirred for 4 h before being extracted into EtOAc (3 x 5 mL). The combined organic phase was washed with brine (5 mL), dried over $MgSO_4$, filtered and concentrated *in vacuo*. The crude product was purified by flash column chromatography (SiO_2, 50% EtOAc in hexane) to give **3.54** (0.090 g, 0.25 mmol, 86%) as a white powder: m.p. (Acetone): 230-231 °C; ^1H NMR (500 MHz, Acetone-D_6) δ_H 8.40 (1H, s, C=CH-5, 7.77-7.75 (2H, m, ArH), 7.26-7.24 (2H, m, ArH), 5.50-5.32 (1H, m, FCH-4), 5.26-5.10 (2H, m, FCH-2 and FCH-6), 5.03-4.83 (2H, m, FCH-3 and FCH-5), 4.72 (2H, t *J* = 6.8 Hz, NCH_2-1), 2.51-2.47 (2H, m, FCCCH_2-2), 2.35 (3H, s, CH_3), 2.18-2.05 (1H, m, FCCH-1); ^{19}F NMR (470 MHz, Acetone-D_6) δ_F −205.2, −212.8, −217.5; ^{13}C NMR (126 MHz, Acetone-D_6) δ_C 148.1 (C=C-4), 138.3 (ArC), 130.23 (Ar*C*H), 129.5 (ArC), 126.14 (Ar*C*H), 121.2 (C=C-5), 88.5 (*C*F), 88.4 (*C*F), 87.3 (*C*F), 47.5 (N*C*H_2-1), 36.1 (FCC-1), 27.6 (FCC*C*H_2-2), 21.2 (H_3C); HRMS m/z ESI$^+$ (Calculated $C_{17}H_{19}F_5N_3^+$ = 360.1494) found 360.1486 $[M+H]^+$; v_{max}/cm^{-1} 1520 (C=C Ar).

4-([1,1'-Biphenyl]-4-yl)-1-(2-((*1r,2R,3R,4s,5S,6S*)-2,3,4,5,6-pentafluorocyclohexyl)ethyl)-1H-1,2,3-triazole 3.55

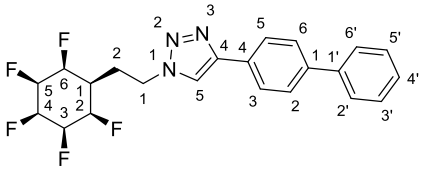

4-Ethynylbenzene (0.067 g, 0.37 mmol), sodium ascorbate (0.034 g, 0.17 mmol) and copper sulfate pentahydrate (0.008 g, 0.03 mmol) were added to a solution of **2.83** (0.076 g,

0.31 mmol) in EtOH (1 mL) and water (1 mL). The solution was heated to 65 °C and stirred for 16 h before being extracted into EtOAc (3 x 5 mL). The combined organic phase was washed with brine (5 mL), dried over $MgSO_4$, filtered, and concentrated *in vacuo*. The crude product was purified by flash column chromatography (SiO_2, 70% EtOAc in hexane) to give **3.55** as a white crystalline solid (0.083 g, 0.20 mmol, 65%): m.p. (acetone): 267-268 °C; ^{1}H NMR (700 MHz, Acetone-D_6) δ_H 8.51 (1H, s, C=CH-5), 7.99-7.97 (2H, m, ArCH), 7.76-7.74 (2H, m, ArCH), 7.72-7.70 (2H, m, ArCH), 7.49-7.46 (2H, m, ArCH), 7.39-7.36 (1H, m, ArCH), 5.41 (1H, app d *J* = 53.7 Hz, FCH-4), 5.23-5.16 (2H, m, FCH-2 and FCH-6), 4.93 (2H, dt *J* = 40.6, 28.3 Hz, FCH-3 and FCH-5), 4.76 (2H, t *J* = 6.8 Hz, NCH_2-1), 2.53-2.50 (2H, m, $FCCCH_2$-2), 2.17-2.06 (1H, m, FCCH-1); ^{19}F NMR (659 MHz, Acetone-D_6) δ_F −205.2, −212.75, −217.5; ^{13}C NMR (176 MHz, Acetone-D_6) δ_C 147.7 (C=C-4), 141.3 (ArC), 141.2 (ArC), 131.3 (ArC), 129.8 (ArCH), 128.3 (ArCH), 128.1 (ArCH), 127.6 (ArCH), 126.7 (ArCH), 121.7 (C=CH-5), 88.95 (*C*F), 87.9 (*C*F), 86.9 (*C*F), 47.6 (NCH_2-1), 36.1 (FCC-1), 27.6 (FCCC-2); HRMS m/z ESI$^+$ (Calculated $C_{22}H_{21}F_5N_3^+$ = 422.1650) found 422.1641 $[M+H]^+$; ν_{max}/cm^{-1} 1693 (C=C), 1485 (C=C Ar), 1130 and 1049 (C-F).

4-(1-(2-((*1r,2R,3R,4s,5S,6S*)-2,3,4,5,6-Pentafluorocyclohexyl)ethyl)-1H-1,2,3-triazol-4-yl)benzoic acid 3.56

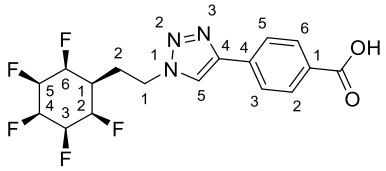

Sodium ascorbate (0.017 g, 0.086 mmol) and copper sulfate pentahydrate (0.021 g, 0.086 mmol), ^{i}PrNEt$_2$ (0.060 mL, 0.34 mmol) and **2.83** (0.050 g, 0.21 mmol) were added to a suspension of 4-ethynylbenzoic acid (0.025 g, 0.17 mmol) in MeOH (1 mL) and water (1 mL) The solution was heated to 65 °C and stirred for 16 h. After cooling to r.t. the crude product was precipitated from solution by addition of HCl (1M, 1 mL). The precipitate was isolated by filtration and then partitioned between EtOAc (3 mL) and saturated $NaHCO_3$ (3 mL). The aqueous phase was acidified by addition of HCl (2M) and then extracted into EtOAc (3 x 10 mL). The combined organic phase was washed with brine (30 mL), dried over $MgSO_4$, filtered and concentrated *in vacuo* to give **3.56** as a white crystalline solid (0.042 g, 0.11 mmol, 63%): m.p. (Acetone): >300 °C (no melt observed); ^{1}H NMR (500 MHz, DMSO-D_6) δ_H 12.94 (1H, br s, CO_2H), 8.80 (1H, s, C=CH-5), 8.03-7.96 (4H, overlapping m, ArCH), 5.46-5.28 (1H, m, FCH-4), 5.19-4.77 (4H, overlapping m, FCH-2, FCH-3, FCH-5 and FCH-6), 4.63 (1H, t *J* = 7.1 Hz, NCH_2-1), 2.33-2.28 (2H, m, $FCCCH_2$-2), 2.04-1.83 (1H, m, FCCH-1); ^{19}F NMR (470 MHz, DMSO-D_6) δ_F −203.6, −211.6, −216.3; ^{13}C NMR (126 MHz, DMSO-D_6) δ_C 167.0 (*C*=O), 145.5 (C=C-4), 134.9 (ArC), 130.0 (Ar*C*H), 129.85 (ArC), 125.05 (Ar*C*H), 122.8 (C=C-5), 88.1

(*C*F), 86.6 (*C*F), 85.45 (*C*F), 46.6 (N*C*H$_2$-1), 34.5 (FCC-1), 26.25 (FCC*C*H$_2$-2); HRMS m/z ESI$^+$ (Calculated $C_{17}H_{15}F_5N_3O_2^-$ = 388.1090) found 388.1086 [M−H]$^-$; ν_{max}/cm^{-1} 1670 (C=O), 1427 (C=C Ar), 1132, 1103 and 1053 (C-F).

1,4-*Bis*(1-(2-((*1r,2R,3R,4s,5S,6S*)-2,3,4,5,6-pentafluorocyclohexyl)ethyl)-1H-1,2,3-triazol-4-yl)benzene 3.57

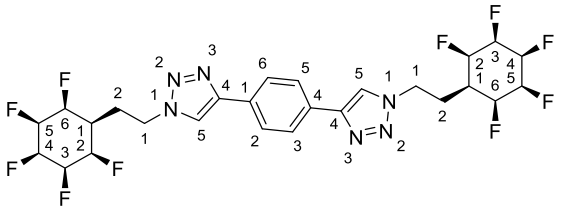

Sodium ascorbate (0.008 g, 0.04 mmol) and copper sulfate pentahydrate (2 mg, 0.008 mmol) were added to a solution of **2.83** (0.050 g, 0.21 mmol) and 1,4-diethynylbenzene (0.013 g, 0.10 mmol) in ^{t}BuOH (3 mL) and water (3 mL). The solution was heated to 80 °C for 3 h. After cooling to r.t. a white precipate was isolated by filtration and washed with cold Et$_2$O (5 mL) to give **3.57** as a fine white powder (0.051 g, 0.083 mmol, 83%): m.p. (Acetone): >300 °C (no melt); ^{1}H NMR (500 MHz, DMSO-D$_6$) δ_H 8.70 (2H, s, C=CH-5), 7.93 (4H, s, ArCH), 5.37 (2H, d *J* = 54.1 Hz, FCH-4), 5.18-5.05 (4H, m, FCH-2 and FCH-6), 4.88 (4H, dt *J* = 39.6, 28.8 Hz, FCH-3 and FCH-5), 4.61 (4H, t *J* = 7.1 Hz, NCH$_2$-1), 2.32-2.28 (4H, m, FCCCH$_2$-2), 2.06-1.86 (2H, m, FCCH-1); ^{19}F NMR (471 MHz, DMSO-D$_6$) δ_F −203.7, −211.6, −216.3; ^{13}C NMR (126 MHz, DMSO-D$_6$) δ_C 146.1 (C=C-4), 130.2 (ArC), 125.6 (Ar*C*H), 121.7 (C=C-5), 88.2 (*C*F), 86.8 (*C*F), 85.5 (*C*F), 46.55 (N*C*H$_2$-1), 34.5 (FCC-1), 26.3 (FCC*C*H$_2$-2); HRMS m/z ESI$^+$ (Calculated $C_{26}H_{27}F_{10}N_6^+$ = 613.2132) found 613.2122 [M+H]$^+$; ν_{max}/cm^{-1} 1132 (C-F).

6.3.3. Chapter 4

(10-Carboxydecyl)triphenylphosphonium bromide 4.7

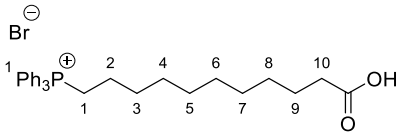

Triphenylphosphine (0.188 g, 0.716 mmol) was added to a solution of 12-Bromododecanoic acid (0.200 g, 0.716 mmol) toluene (1.1 mL). The solution was heated to 111 °C and stirred for 16 h. After cooling to r.t. a viscous oil separated out of solution. Excess solvent was decanted and the viscous oil was washed with toluene (2 x 10 mL) and Et_2O (2 x 10 mL) to give **4.7** as a viscous yellow oil (0.301 g, 0.571 mmol, 80%): ^{1}H NMR (400 MHz, $CDCl_3$) δ_H 7.87-7.67 (15H, overlapping m, ArCH), 3.80-3.70 (2H, m), 2.39 (2H, t *J* = 7.3 Hz), 1.67-1.56 (6H, overlapping m, CH_2), 1.35-1.18 (12H, overlapping m, CH_2) data are in agreement with literature.[5]

Diethyl ((perfluorophenyl)methyl)phosphonate 4.11[2]

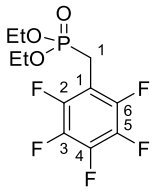

A microwave vial was charged with pentafluorobenzyl bromide (522 mg, 2.00 mmol) and triethyl phosphite (332 mg, 2.00 mmol) and then sealed using a Teflon cap. The vial was heated in a 2.45 GHz microwave reactor targeting 140 °C for 5 mins and then trace starting material was removed *in vacuo* to give **4.11** as a colourless oil (631 mg, 1.98 mmol, 99%); ^{1}H NMR (300 MHz, $CDCl_3$) δ_H 4.08 (4H, dqd *J* = 8.1, 7.1, 1.3 Hz, OCH_2CH_3), 3.17 (1H, dtd *J* = 21.2, 1.7, 0.6 Hz, PCH-1a), 1.26 (6H, td *J* = 7.1, 0.6 Hz, OCH_2CH_3); ^{13}C NMR (126 MHz, $CDCl_3$) δ_C 145.15 (Ar*C*F), 140.4 (Ar*C*F), 137.7 (Ar*C*F), 107.0 (Ar), 62.78 (OCH_2CH_3), 21.71 (PC-1b), 20.58 (PC-1a), 16.43 (OCH_2CH_3); ^{31}P NMR (162 MHz, $CDCl_3$) δ_P 21.63; ^{19}F NMR (376 MHz, $CDCl_3$) δ_F -141.40 (ArCF), -155.84 (F-4), -162.32 (ArCF); HRMS m/z (ESI^+) (calculated $C_{11}H_{12}O_3F_5NaP^+$ = 341.0336) found 341.0327 $[M+Na]^+$; ν_{max}/cm^{-1} 2984 (C-H), 1522 and 1506 (C=C Ar), 1269 (C-F).

Methyl 12-hydroxydodecanoate 4.15[2]

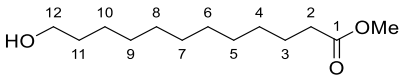

Acetyl chloride (2.14 mL, 30 mmol) was added dropwise to a solution of 12-hydroxydodecanoic acid (4.059 g, 18.78 mmol) in MeOH (60 mL). The solution was heated to

reflux for 14 h before being neutralised by careful addition of NaOH to pH 7. Excess MeOH was removed *in vacuo* and the residue was extracted into EtOAc (3 x 50 mL). The organic phase was dried over $MgSO_4$, filtered and concentrated *in vacuo* to give **4.15** as a colourless oil (4.105 g, 95%) which was used without further purification: ^{1}H NMR (500 MHz, $CDCl_3$) δ_H 3.66 (3H, s, OCH_3), 3.63 (2H, t *J* = 6.5 Hz, H-12), 2.30 (2H, t *J* = 7.5 Hz, H-2), 1.65-1.52 (5H, overlapping m, CH_2, OH), 1.35-1.25 (14H, overlapping m, CH_2); ^{13}C NMR (126 MHz, $CDCl_3$) δ_C 174.5 (C=O), 63.2 (C-12), 51.6 (O*C*H$_3$), 34.25 (C-2), 32.9 (CH_2), 29.7 (CH_2), 29.6 (CH_2), 29.5 (CH_2), 29.4 (CH_2), 29.3 (CH_2), 25.85 (CH_2), 25.1 (CH_2); HRMS m/z (ESI$^+$) (calculated $C_{13}H_{26}O_3Na^+$ = 253.1774) found 253.1768 $[M+Na]^+$; ν_{max}/cm^{-1} 3400br (O-H), 1738 (C=O).

Methyl 12-oxododecanoate 4.12[2]

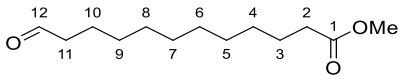

DMSO (2.6 mL, 37 mmol) in CH_2Cl_2 (8.8 mL) was added to a solution of $(COCl)_2$ (2.31 g, 18.2 mmol) in CH_2Cl_2 (44 mL) at -78 °C. The solution was stirred for 30 mins at -78 °C before **4.12** (3.82 g, 16.6 mmol) in CH_2Cl_2 (17.6 mL) was added dropwise. The solution was stirred at −60 °C for 45 mins before triethylamine (11.6 mL, 83.2 mmol) was added and the solution warmed to r.t.. The solution was stirred for 1 h at r.t. before being diluted with water (100 mL) and then extracted into CH_2Cl_2 (2 x 100 mL). The organic phase was washed with brine, dried over $MgSO_4$, filtered and concentrated *in vacuo*. The residue was purified by flash column chromatography (SiO_2, hexane to 10% EtOAc in hexane) to give **4.12** as a colourless oil, (2.84 g, 12.3 mmol, 74%); ^{1}H NMR (500 MHz, $CDCl_3$); δ_H 9.75 (1H, s, H-12), 3.66 (OCH_3), 2.41 (2H, t *J* = 7.1 Hz, H-11), 2.29 (2H, t *J* = 7.5 Hz, H-2), 1.63-1.59 (4H, overlapping m, CH_2), 1.33-1.23 (12H, overlapping m, CH_2); ^{13}C NMR (126 MHz, $CDCl_3$) δ_C 203.1 (C-12), 174.5 (C-1), 51.6 (O*C*H$_3$), 44.0 (C-11), 34.2 (C-2), 29.5 (CH_2), 29.5 (CH_2), 29.45 (CH_2), 29.3 (CH_2), 29.3 (CH_2), 29.25 (CH_2), 25.1 (CH_2), 22.2 (CH_2); data are in agreement with literature.[6]

Methyl 13-(perfluorophenyl)tridec-12-enoate 4.8[2]

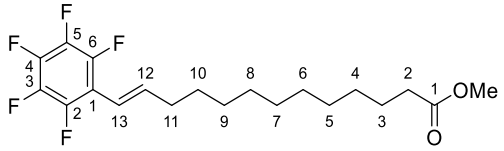

NaH (60% in oil, 0.350 g, 8.76 mmol) was added to a solution of **4.11** (1.394 g, 4.381 mmol) in THF (12 mL) at 0 °C. The suspension was stirred for 5 mins at 0 °C before **4.12** (1.00 g, 4.38 mmol) was added dropwise. The solution was heated to 50 °C for 14 h before being quenched by the careful addition of water (5 mL) at 0 °C. The mixture was extracted into

EtOAc (3 x 20 mL) and the combined organic phase was washed with saturated brine. The organic phase was dried over $MgSO_4$, filtered and concentrated *in vacuo*. The residue was purified by flash column chromatography (SiO_2, hexane to 50% EtOAc in hexane) to give **4.8** as a colourless oil (0.995 g, 4.36 mmol, 58%) which was a mixture of E:Z (5:1) diastereomers (only peaks of the major isomer are assigned): ^{1}H NMR (500 MHz, $CDCl_3$) δ_H 6.54 (1H, dt *J* = 16.2, 7.1 Hz, H-12), 6.25 (1H, d *J* = 16.2, H-13), 3.66 (3H, s, OCH_3), 2.30 (2H, t *J* = 7.5 Hz, H-2), 2.25 (2H, app q *J* = 7.1 Hz, H-11), 1.64-1.58 (2H, m, CH_2), 1.50-1.45 (2H, m, CH_2), 1.36-1.26 (12 H, overlapping m, CH_2); ^{19}F NMR (471 MHz, $CDCl_3$) δ_F −143.9, −158.1, −163.5; ^{13}C NMR (126 MHz, $CDCl_3$) δ_C 174.5 (C=O), 144.7 (Ar*C*F), 141.5 (C-12), 139.6 (C-F), 137.4 (C-F), 114.1 (C-13), 112.7 (ArC), 51.6 (O*C*H$_3$), 34.45 (C-11), 34.25 (C-2), 29.6 (CH_2), 29.6 (CH_2), 29.5 (CH_2), 29.5 (CH_2), 29.4 (CH_2), 29.3 (CH_2), 29.0 (CH_2), 25.1 (CH_2); HRMS m/z (ESI$^+$) (calculated $C_{20}H_{25}O_2F_5Na^+$ = 415.1667) found 415.1657 $[M+Na]^+$; ν_{max}/cm^{-1} 1740 (C=O).

Methyl 13-((*1r,2R,3R,4s,5S,6S*)-2,3,4,5,6-pentafluorocyclohexyl)tridecanoate 4.9[2]

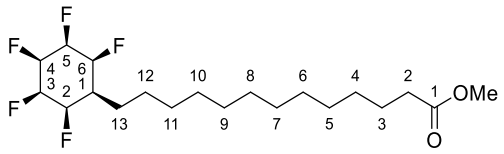

Silica gel (8.5 g), **4.8** (1.360 g, 3.466 mmol) and **2.14** (39 mg, 0.090 mmol, 3 mol%) were suspended in hexane (50 mL) in a vial and the vial placed inside an autoclave. The autoclave was pressurised with hydrogen to 50 Bar and the reaction mixture stirred at room temperature for 24 h. After depressurising and removing the vial, the suspension was filtered and concentrated in vacuo to give the crude product, which was purified by flash column chromatography (SiO_2, 50% EtOAc in hexane to 100% EtOAc) to give **4.9** as a white crystalline solid, (0.300 g, 0.749 mmol, 22%): ^{1}H NMR (500 MHz, $CDCl_3$) δ_H 5.41-5.25 (1H, m, FCH-4), 4.94 (2H, app d *J* = 49.1 Hz, FCH-2, FCH-6), 4.54-4.32 (2H, app dt *J* = 41.1, 26.4 Hz, FCH-3, FCH-6), 3.66 (3H, s, OCH_3), 2.30 (2H, t, *J* = 7.6 Hz, CH_2-2), 1.88-1.83 (2H, m, CH_2), 1.72-1.48 (5H, overlapping m, FCCH-1, CH_2-3, CH_2), 1.46-1.41 (2H, m, CH_2), 1.35-1.25 (16H, overlapping m, CH_2); ^{19}F NMR (471 MHz, $CDCl_3$) δ_F −203.1, −212.1, −216.7; ^{13}C NMR (126 MHz, $CDCl_3$) δ_C 174.5 (C=O), 87.4 (FC), 87.3 (FC), 86.4 (FC), 51.6 (O*C*H$_3$), 38.6 (FC*C*-1), 34.25 (*C*H$_2$-2), 29.7 (*C*H$_2$), 29.7 (*C*H$_2$), 29.6 (*C*H$_2$), 29.6 (*C*H$_2$), 29.5 (*C*H$_2$), 29.4 (*C*H$_2$), 29.3 (*C*H$_2$), 26.8 (*C*H$_2$), 26.6 (*C*H$_2$), 26.0 (*C*H$_2$), 25.1 (*C*H$_2$); HRMS m/z (ESI$^+$) (calculated $C_{20}H_{33}O_2F_5Na^+$ = 423.2293) found 423.2286 $[M+Na]^+$; ν_{max}/cm^{-1} 1734 (C=O), 1047 (C-F).

13-((*1r,2R,3R,4s,5S,6S*)-2,3,4,5,6-Pentafluorocyclohexyl)tridecanoic acid 4.1[2]

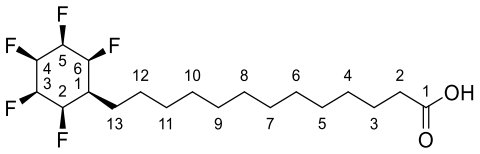

A round bottom flask was charged with **4.9** (90 mg, 0.22 mmol) and HCl (6N, 100 mL). The suspension was heated to reflux and stirred for 14 h before being cooled to 0 °C basified by careful addition of saturated $NaHCO_3$ solution. Residual starting material was extracted into EtOAc (3 x 200 mL) and the aqueous phase was re-acidified by addition of HCL (1M). The re-acidified solution was extracted into EtOAc (3 x 200 mL) and this organic phase was dried over $MgSO_4$, filtered and concentrated *in vacuo* to give **4.1** as a white crystalline solid (81 mg, 0.21 mmol, 95%): m.p. 178 °C; ^{1}H NMR (500 MHz, Acetone-D_6) δ_H 10.40 (COOH), 5.38 (1H, app dt *J* = 53.9, 8.1 Hz, FCH-4), 5.12-4.95 (2H, m, FCH-2, FCH-6) 4.97-4.77 (2H, m, FCH-3, FCH-5), 2.27 (2H, t *J* = 7.5 Hz, CH_2-2), 2.06-1.90 (1H, m, FCCH-1), 1.83-1.78 (2H, m, CH_2), 1.61-1.55 (2H, m, CH_2), 1.52-1.46 (2H, m, CH_2), 1.37-1.29 (16H, overlapping m, CH_2); ^{19}F NMR (471 MHz, Acetone-D_6) δ_F −204.8, −213.0, −217.5; ^{13}C NMR (126 MHz, Acetone-D_6) δ_C 174.7 (C=O), 88.95 (FC-2, FC-6), 88.75 (FC-4), 87.6 (FC-3, FC-5), 38.6 (FC*C*-1), 34.2 (*C*H_2-2), 30.4 (*C*H_2), 30.4 (*C*H_2), 30.4 (*C*H_2), 30.3 (*C*H_2), 30.2 (*C*H_2), 30.1 (*C*H_2), 30.1 (*C*H_2), 30.0 (*C*H_2), 27.1 (*C*H_2), 26.7 (*C*H_2), 25.7 (*C*H_2); HRMS m/z (ESI$^+$) (calculated $C_{19}H_{31}O_2F_5Na^+$ = 409.2136) found 409.2132 $[M+Na]^+$; ν_{max}/cm^{-1} 1701 (C=O), 1126 and 1049 (C-F).

13-((*1r,2R,3R,4s,5S,6S*)-2,3,4,5,6-Pentafluorocyclohexyl)tridecan-1-ol 4.2[2]

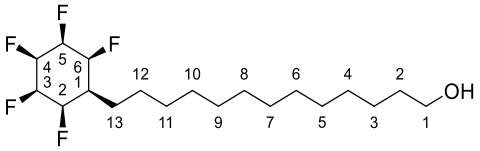

Diisobutylaluminium hydride solution (1M in hexane, 0.49 mL, 0.49 mmol) was added to a solution of **4.9** (79 mg, 0.197 mmol) in CH_2Cl_2 (1.5 mL) at −78 C. The reaction was warmed to r.t. and stirred for a further 1 h. The reaction was diluted with Et_2O (10 mL), cooled to 0 °C and quenched by the sequential addition of water (0.02 mL), NaOH (15% w/w, 0.02 mL) and water (0.05 mL). The mixture was warmed to r.t and $MgSO_4$ was added. The suspension was stirred for 15 mins before being filtered and concentrated *in vacuo* to give the crude product, which was purified by flash column chromatography (SiO_2, 80% EtOAc in hexane to 100% EtOAc) to give **4.2** as a white crystalline solid (47 mg, 0.126 mmol, 64%): m.p. 140 °C; ν_{max}/cm^{-1} 3325 (O-H), 1126 and 1049 (C-F); ^{1}H NMR (500 MHz, Acetone-D_6) δ_H 5.38 (1H, app dt *J* = 54.1, 8.2 Hz, FCH-4), 5.13-4.72 (4H, overlapping m, FCH-2, FCH-3, FCH-5, FCH-6) 3.54-3.50 (2H, m, CH_2-1), 3.37 (1H, t *J* = 5.2 Hz, OH), 2.08-1.90 (1H, m, FCCH-1), 1.83-1.78 (2H, m, CH_2),

1.53-1.45 (4H, overlapping m, CH_2), 1.35-1.29 (18H, overlapping m, CH_2); ^{19}F NMR (470 MHz, Acetone-D_6) δ_F −204.8, −213.05, −217.4; ^{13}C NMR (126 MHz, Acetone-D_6) δ_C 89.4 (FC), 88.8 (FC), 87.6 (FC), 62.5 (*C*H_2OH), 38.6 (FCC-1), 33.9 (H_2C), 30.5 (*C*H_2), 30.5 (*C*H_2), 30.4 (*C*H_2), 30.4 (*C*H_2), 30.4 (*C*H_2), 30.3 (*C*H_2), 30.3 (*C*H_2), 30.2 (*C*H_2), 27.3 (*C*H_2), 27.1 (*C*H_2), 26.8 (*C*H_2); HRMS m/z (ESI$^+$) (calculated $C_{19}H_{33}OF_5Na^+$ = 395.2344) found 395.2343 $[M+Na]^+$; ν_{max}/cm^{-1} 3325br (O-H).

(*1R,2R,3s,4S,5S,6r*)-1,2,3,4,5-Pentafluoro-6-tridecylcyclohexane 4.3[2]

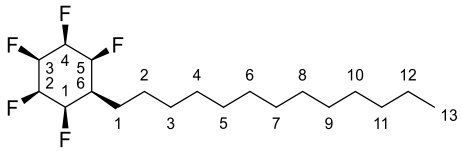

1-Allyl-2,3,4,5,6-pentafluorobenzene (0.306 mL, 2.00 mmol) and 1-dodecene (0.444 mL, 2.00 mmol) were added dropwise and simultaneously to a solution of Grubbs first generation catalyst® (82 mg, 5 mol%) in CH_2Cl_2 (6 mL). The solution was heated to 40 °C for 14 h and was then concentrated *in vacuo* and the residue was filtered through a plug of silica. The silica was washed with hexane. The filtrate was concentrated *in vacuo* to give **4.16** which was used immediately without further purification. **4.16** (530 mg), 4 Å molecular sieves (5.3 g) and **2.14** (25 mg, 0.058 mmol) were suspended in hexane (20 mL) in a vial and the vial placed inside an autoclave. The autoclave was pressurised with hydrogen to 50 Bar and the reaction mixture stirred at room temperature for 24 h. After depressurising and removing the vial, the suspension was filtered and concentrated in vacuo to give the product, which was purified by flash column chromatography (SiO_2, 20% EtOAc in hexane to 40% EtOAc) to give **4.3** as a white crystalline solid, (228 mg, 0.640 mmol, 32% over two steps); m.p. 121 °C; ^1H NMR (400 MHz, $CDCl_3$) δ_H 5.43-5.23 (1H, m, FCH-3), 4.94 (2H, app d *J* = 48.9 Hz, FCH-1, FCH-5), 4.42 (2H, dt *J* = 41.5, 26.6 Hz, FCH-2, FCH-4), 1.89-1.82 (2H, m, CH_2), 1.66-1.51 (1H, m, FCCH-6), 1.48-1.39 (2H, m, CH_2), 1.33- 1.25 (20H, overlapping m, CH_2), 0.88 (3H, t *J* = 6.9 Hz, CH_3-13); ^{19}F NMR (376 MHz, $CDCl_3$) δ_F −203.1, −212.1, −216.6; ^{13}C NMR (101 MHz, $CDCl_3$) δ_C 87.4 (FC), 87.3 (FC), 86.4 (FC), 38.7 (FCC-6), 32.1 (*C*H_2), 29.8 (*C*H_2), 29.8 (*C*H_2), 29.8 (*C*H_2), 29.7 (*C*H_2), 29.6 (*C*H_2), 29.6 (*C*H_2), 29.5 (*C*H_2), 26.7 (*C*H_2), 26.0 (*C*H_2), 26.0 (*C*H_2), 22.8 (*C*H_2), 14.3 (*C*H_3-13); HRMS m/z (ESI$^+$) (calculated $C_{19}H_{33}F_5Na^+$ = 379.2395) found 379.2390 $[M+Na]^+$; ν_{max}/cm^{-1} 1123 and 1051 (C-F).

1,2,3,4,5-Pentafluoro-6-(4-((*1r,2R,3R,4s,5S,6S*)-2,3,4,5,6-pentafluorocyclohexyl)butyl)benzene 4.21

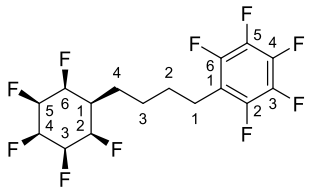

Palladium on carbon (10 % w/w, 7 mg) was added to a solution of **4.17** (50 mg, 0.13 mmol) in MeOH (3 mL). The suspension was stirred under an atmosphere of hydrogen at r.t. for 16 h until TLC showed complete consumption of **4.17**. The suspension was filtered through celite and the filtrate concentrated *in vacuo* to give **4.21** which was used immediately without further purification. A vial was charged with **4.21** (50 mg, 0.13 mmol), 4 Å molecular sieves (500 mg), **2.14** (3 mg, 0.005 mmol) and hexane (2 mL) and the vial placed inside an autoclave. The autoclave was pressurised with hydrogen to 50 Bar and the reaction mixture stirred at room temperature for 24 h. After depressurising and removing the vial, the suspension was filtered and concentrated in vacuo to give the crude product, which was purified by flash column chromatography (SiO_2, 10% EtOAc in hexane to 30% EtOAc in hexane) to give **4.21** as a white crystalline solid (21 mg, 0.053 mmol, 41%): m.p. (acetone): 198-199 °C; ^{1}H NMR (700 MHz, Acetone-D_6) δ_H 5.41 (1H, app d *J* = 53.7 Hz, FCH-4), 5.06 (2H, app d *J* = 50.1 Hz, FCH-2 and FCH-6), 4.91 (2H, app dt *J* = 40.5, 27.7 Hz, FCH-3 and FCH-5), 2.83 (2H, obscured, CH_2-1), 2.11-1.95 (1H, m, FCCH-1), 1.91-1.86 (2H, m, CH_2-4), 1.74 (2H, app p *J* = 7.6 Hz, CH_2-2), 1.63-1.58 (2H, m, CH_2-3); ^{19}F NMR (659 MHz, Acetone-D_6) δ_F −145.8, −160.8, −165.4, −204.9, −213.05, −217.5; ^{13}C NMR (176 MHz, Acetone-D_6) δ_C 145.2 (Ar*C*F), 115.4 (ArC) 89.3 (*C*F), 88.2 (*C*F), 87.0 (*C*F), 38.5 (FCC-1), 29.7 (CH_2-2), 26.5 (CH_2) 26.4 (CH_2), 22.7 (CH_2-1); HRMS m/z ESI$^+$ (Calculated $C_{16}H_{14}F_{10}Na^+$ = 419.0828) found 419.0825 $[M+Na]^+$; ν_{max}/cm^{-1} 1522 and 1499 (C=C Ar), 1126 and 1109 (C-F).

Methyl 11-(perfluorophenyl)undec-10-enoate 4.25[2]

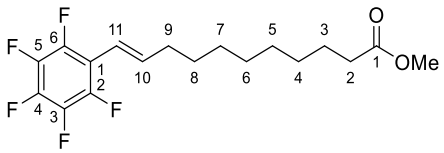

Methyl 10-undecenoate (198 mg, 1.00 mmol) and pentafluorostyrene (388 mg, 2.00 mmol) were added dropwise and simultaneously to a solution of 2nd Generation Hoveyda-Grubbs Catalyst® (12 mg, 0.019 mmol, 2 mol%) in CH_2Cl_2 (5 mL). The solution was heated to reflux for 14 h before being concentrated *in vacuo*. The residue was purified by flash column chromatography (SiO_2, hexane to 10% EtOAc in hexane) to give alkene **4.25** as a colourless oil (195 mg, 0.536 mmol, 54%): ^{1}H {^{19}F} NMR (500 MHz, $CDCl_3$) δ_H 6.55 (1H, dt *J* = 16.2,

7.1 Hz, H-10), 6.26 (1H, d *J* = 16.2 Hz, H-11), 3.68 (3H, s, OCH_3), 2.31 (2H, t *J* = 7.5 Hz, H-2), 2.29-2.24 (2H, m, H-9), 1.66-1.60 (2H, m, H-3), 1.51-1.45 (2H, m, H-8), 1.34-1.29 (8H, overlapping m, H-7, H-6, H-5, H-4); ^{13}C NMR (126 MHz, $CDCl_3$) δ_C 174.4 (C=O), 144.6 (Ar*C*F), 141.4 (C-10), 139.3 (Ar*C*F), 137.75 (Ar*C*F), 114.1 (C-11), 112.65 (ArC-1), 51.5 (O*C*H3), 34.4 (C-9), 34.2 (C-2), 29.3 (*C*H2), 29.3 (*C*H2), 29.2 (*C*H2), 29.2 (*C*H2), 28.9 (*C*H2), 25.0 (C-3); ^{19}F $\{^1H\}$ NMR (470 MHz, $CDCl_3$) δ_F −144.0 (ArCF), −158.2 (F-4), −163.6 (ArCF); HRMS m/z (ESI+) (calculated $C_{18}H_{22}F_5O_2^+$ = 365.1534) found 365.1530 $[M+H]^+$; v_{max}/cm^{-1} 1740 (C=O), 1520 and 1495 (C=C Ar).

11-(Perfluorophenyl)undec-10-enal 4.29[2]

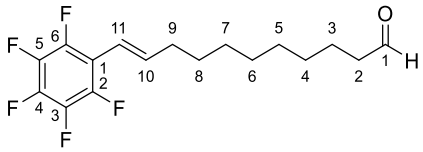

DIBAlH (1.1 mL, 1M in hexane, 1.1 mmol) was added dropwise to a solution of **4.25** (130 mg, 0.357 mmol) in CH_2Cl_2 (9 mL) at -78 °C. The resulting solution was stirred for 40 min at -78 °C before being quenched by the careful addition of MeOH (1 mL). After stirring for 10 min, the solution was warmed to r.t. and saturated rochelle salt solution (10 mL) was added. The biphasic mixture was stirred at r.t. for 12 h and then extracted with CH_2Cl_2 (3 x 10 mL). The combined organic phase was dried over $MgSO_4$, filtered and concentrated *in vacuo* to give **4.29** as a colourless oil, (119 mg, 0.357 mmol, quantitative); ^1H NMR (700 MHz, $CDCl_3$) δ_H 9.76 (1H, t *J* = 1.8 Hz, H-1), 6.53 (1H, dt *J* = 16.2, 7.0 Hz, H-10), 6.24 (1H, dt *J* = 16.2, 1.5 Hz, H-11), 2.42 (2H, td *J* = 7.4, 1.8 Hz, H-2), 2.26-2.23 (2H, m, H-9), 1.63-1.60 (2H, m, H-3), 1.49-1.45 (2H, m H-8), 1.33-1.28 (8H, overlapping m, H-7, H-6, H-5, H-4); ^{13}C NMR (101 MHz, $CDCl_3$) δ_C 203.0 (C=O), 144.6 (Ar*C*F), 141.4 (C-10), 139.5 (Ar*C*F), 137.7 (Ar*C*F), 114.2 (C-11), 112.65 (ArC-1), 44.0 (C-2), 34.4 (C-9), 29.4 (CH_2), 29.3 (CH_2), 29.2 (CH_2), 29.2 (CH_2), 28.9 (CH_2), 22.2 (C-3); ^{19}F NMR (377 MHz, $CDCl_3$) δ_F −143.95 (ArCF), −158.1 (F-4), −163.6 (ArCF); HRMS m/z (EI^+) (calculated $C_{17}H_{19}F_5O^+$ = 334.1351) found 334.1351 $[M-e^-]^+$; v_{max}/cm^{-1} 1726 (C=O), 1520 and 1493 (C=C Ar).

(1*E*,11*E*)-1,12-*Bis*(perfluorophenyl)dodeca-1,11-diene 4.26[2]

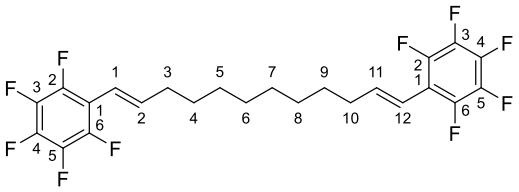

NaH (60% in oil, 58 mg, 1.46 mmol) was added to a solution of **4.11** (230 mg, 0.724 mmol) in THF (2.4 mL) at 0 °C. The suspension was stirred at 0 °C for 5 mins before **4.29** (114 mg, 0.341 mmol) was added dropwise as a solution in THF (3 mL). The reaction was heated to 76 °C for 14 h. The solution was cooled to 0 °C and quenched by the careful addition of water (5 mL). The mixture was extracted into EtOAc (3 x 20 mL) and the combined organic phase was washed with saturated brine. The organic phase was dried over $MgSO_4$, filtered and concentrated *in vacuo*. The residue was purified by flash column chromatography (SiO_2, hexane) to give **16** as a colourless oil, (92 mg, 0.18 mmol, 53%); ^{1}H NMR (700 MHz, $CDCl_3$) δ_H 6.55 (2H, dt *J* = 16.2, 7.1 Hz, H-11, H-2), 6.26 (2H, dt *J* = 16.2, 1.3 Hz, H-1, H-12), 2.28-2.24 (4H, m, H-10, H-3), 1.51-1.46 (4H, m, CH_2), 1.38-1.31 (8H, overlapping m, CH_2); ^{19}F NMR (471 MHz, $CDCl_3$) δ_F −144.0 (ArCF), −158.1 (F-4), −163.6 (ArCF); ^{13}C NMR (176 MHz, $CDCl_3$) δ_C 144.6 (Ar*C*F), 141.4 (H_2C-11, H_2C-2), 139.4 (Ar*C*F), 137.8 (Ar*C*F), 114.2 (H_2C-12, H_2C-1), 112.7 (ArC-1), 34.45 (H_2C-10, H_2C-3), 29.5 (H_2C), 29.3 (H_2C), 29.0 (H_2C); HRMS m/z (EI$^+$) (calculated $C_{24}H_{20}F_{10}^+$ = 498.1400) found 498.1397 [M-e$^-$]$^+$; ν_{max}/cm^{-1} 1520 and 1493 (C=C Ar).

1,12-*Bis*((*1r,2R,3R,4s,5S,6S*)-2,3,4,5,6-pentafluorocyclohexyl)dodecane 4.27[2]

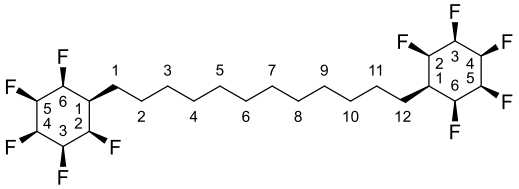

Activated 4 Å molecular sieves (500 mg), **4.26** (50 mg, 0.10 mmol) and **2.14** (2 mg, 0.005 mmol, 5 mol%) were suspended in hexane (2 mL) in a vial and the vial placed inside an autoclave. The autoclave was pressurised with hydrogen to 50 Bar and the reaction mixture stirred at room temperature for 24 h. After depressurising and removing the vial, the suspension was filtered and concentrated in vacuo to give the crude product, which was purified by flash column chromatography (SiO_2, 20% EtOAc in hexane to 100% EtOAc) to give **4.27** as a white crystalline solid (17 mg, 0.033 mmol, 33%): m.p. 188 °C; ^{1}H NMR (500 MHz, $CDCl_3$) δ_H 5.43-5.26 (2H, m, FCH-4), 4.93 (4H, app d *J* = 49.9 Hz, FCH-2, FCH-6), 4.56-4.34 (4H, m, FCH-3, FCH-5), 1.90-1.85 (4H, m, CH_2-1, CH_2-12), 1.74-1.56 (2H, m, FCHCH-1), 1.49-1.43 (4H, m, CH_2-11, CH_2-2), 1.39-1.28 (16H, overlapping m, CH_2); ^{19}F NMR (471 MHz, Acetone-D_6) δ_F −204.8, −213.05, −217.45; ^{13}C NMR (126 MHz, $CDCl_3$) δ_C 87.3 (FC-2, FC-6),

87.1 (FC-4), 86.5 (FC-3, FC-5), 38.6 (FC*C*-1), 32.1 (H_2C), 29.8 (H_2C), 29.7 (H_2C), 29.6 (H_2C), 26.6 (H_2C-11, H_2C-2), 26.0 (H_2C-1, H_2C-12); HRMS m/z (ESI^+) (calculated $C_{24}H_{36}F_{10}Na^+$ = 537.2550) found 537.2540 $[M+Na]^+$; v_{max}/cm^{-1} 1132 and 1049 (C-F).

Methyl 13-phenyltridec-10-enoate 4.31[2]

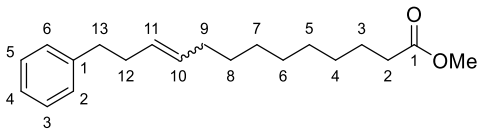

Methyl 10-undecenoate (1.051 g, 5.300 mmol) and 4-phenylbutene (0.700 g, 5.30 mmol) were added dropwise simultaneously to a solution Grubbs first generation Catalyst® (0.217 g, 0.264 mmol, 5 mol%) in CH_2Cl_2 (12 mL). The solution was heated to reflux for 14 h before being concentrated *in vacuo* to give **4.31** as a colourless oil as a mixture of diastereomers (0.626 g, 2.07 mmol, 39%): ^1H NMR (500 MHz, $CDCl_3$) δ_H 7.31-7.16 (5H, overlapping m, ArH), 5.50-5.37 (2H, overlapping m, H-10, H-11), 3.67 (3H, s, OCH_3), 2.70-2.65 (2H, m, CH_2), 2.35-2.29 (4H, overlapping m, CH_2), 1.99-1.95 (2H, m, CH_2), 1.66-1.59 (2H, m, CH_2), 1.35-1.24 (10H, overlapping m, CH_2); ^{13}C NMR (126 MHz, $CDCl_3$) δ_C 174.45 (C=O), 142.3 (ArC-1), 131.2 (C=C), 130.7 (C=C), 129.4 (C=C), 128.8 (C=C), 128.6 (Ar*C*H), 128.3 (Ar*C*H), 125.8 (Ar*C*H), 51.6 (O*C*H_3), 36.3 (*C*H_2), 34.6 (*C*H_2), 34.2 (*C*H_2), 32.65 (*C*H_2), 29.6 (*C*H_2), 29.4 (*C*H_2), 29.3 (*C*H_2), 29.3 (*C*H_2), 29.1 (*C*H_2), 25.1 (*C*H_2); HRMS m/z (ESI^+) (calculated $C_{20}H_{30}O_2Na^+$ = 325.2138) found 325.2133 $[M+Na]^+$; v_{max}/cm^{-1} 1740 (C=O).

Methyl 13-cyclohexyltridecanoate 4.32[2]

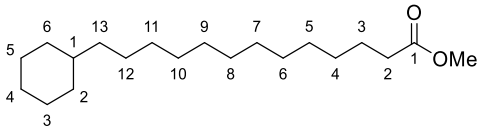

Activated 4 Å molecular sieves (500 mg), **4.31** (54 mg, 0.18 mmol) and **2.14** (6 mg, 0.015 mmol, 8 mol%) were suspended in hexane (2 mL) in a vial and the vial placed inside an autoclave. The autoclave was pressurised with hydrogen to 50 Bar and the reaction mixture stirred at room temperature for 24 h. After depressurising and removing the vial, the suspension was filtered and concentrated in vacuo to give the crude product, which was purified by flash column chromatography (SiO_2, hexane) to give **4.32** as a colourless oil (41 mg, 0.132 mmol, 74%): ^1H NMR (500 MHz, $CDCl_3$) δ_H 3.66 (3H, s, OCH_3), 2.29 (2H, t *J* = 7.6 Hz, OCH_2-2), 1.71-1.57 (7H, overlapping m, CH_2), 1.32-1.10 (24H, overlapping m, CH_2), 0.89-0.79 (2H, m, CH_2); ^{13}C NMR (126 MHz, $CDCl_3$) δ_C 174.5 (C=O), 51.6 (O*C*H_3) , 37.8 (CH_2), 37.7 (CH_2), 34.3 (OC*C*H_2-2), 33.6 (CH_2), 30.15 (CH_2), 29.9 (CH_2), 29.8 (CH_2), 29.8 (CH_2), 29.7 (CH_2), 29.6 (CH_2), 29.4 (CH_2), 29.3 (CH_2), 27.0 (CH_2), 26.9 (CH_2), 26.6 (CH_2), 25.1 (CH_2);

HRMS m/z (ESI$^+$) (calculated $C_{20}H_{38}O_2Na^+$ = 333.2764) found 333.2758 $[M+Na]^+$; ν_{max}/cm^{-1} 1742 (C=O).

13-Cyclohexyltridecanoic acid 4.4[2]

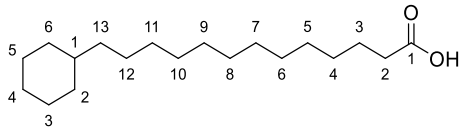

NaOH (1M, 4 mL, 4 mmol) was added to a solution of **4.4** (43 mg, 0.14 mmol) in MeOH (10 mL). The solution was stirred at reflux for 14 h before being acidified by the careful addition of HCl (1M, 30 mL). The mixture was extracted into CH_2Cl_2 (3 x 50 mL) before being dried over $MgSO_4$, filtered and concentrated *in vacuo* to give **4.4** as a crystalline white solid, (41 mg, 0.14 mmol, quant.); m.p. 65 °C; ^{1}H NMR (500 MHz, $CDCl_3$) δ_H 2.34 (2H, t *J* = 7.6 Hz, $OCCH_2$-2), 1.78-1.61 (7H, overlapping m, CH_2), 1.33-1.12 (24H, overlapping m, CH_2), 0.90-0.81 (2H, m, CH_2); ^{13}C NMR (126 MHz, $CDCl_3$) δ_C 180.6 (C=O), 37.85 (*C*H_2), 37.7 (*C*H_2), 34.3 ($OCCH_2$-2), 33.6 (*C*H_2), 30.2 (*C*H_2), 29.9 (*C*H_2), 29.8 (*C*H_2), 29.8 (*C*H_2), 29.75 (*C*H_2), 29.6 (*C*H_2), 29.4 (*C*H_2), 29.2 (*C*H_2), 27.0 (*C*H_2), 26.9 (*C*H_2), 26.6 (*C*H_2), 24.8 (*C*H_2); HRMS m/z (ESI$^-$) (calculated $C_{19}H_{35}O_2^-$ = 295.2643) found 295.2637 $[M-H]^-$; ν_{max}/cm^{-1} 1699 (C=O).

13-Cyclohexyltridecan-1-ol 4.5[2]

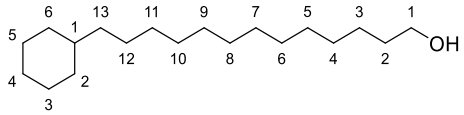

DIBAlH (1M in hexane, 1.05 mL, 1.05 mmol) was added to a solution of **4.4** (0.156 g, 0.419 mmol) in CH_2Cl_2 (3 mL) at −78 °C. The solution was warmed to r.t. and stirred for 1 h before being diluted with Et_2O and cooled to 0 °C. The solution was then quenched by the sequential addition of; water (0.04 mL), NaOH (15% w/w, 0.04 mL) and water (0.1 mL). The solution was then warmed to r.t. and stirred for 15 mins before being dried over $MgSO_4$ and the suspension stirred for a further 15 mins. The suspension was filtered and concentrated *in vacuo* to give **4.5** as a white amorphous solid (0.096 g, 0.34 mmol, 81%): m.p. ($CHCl_3$): 34 °C; ^{1}H NMR (500 MHz, $CDCl_3$) δ_H 3.64 (2H, t *J* = 6.7 Hz, OCH_2-1), 1.76-1.62 (6H, m, CH_2), 1.60-1.54 (2H, m, CH_2), 1.38-1.14 (26H, m, CH_2), 0.91-0.83 (2H, m, CH_2); ^{13}C NMR (126 MHz, $CDCl_3$) δ_C 63.0 (OCH_2-1), 37.7 (*C*H_2), 37.6 (*C*H_2), 33.5 (*C*H_2), 32.8 (*C*H_2), 30.0 (*C*H_2), 29.7 (*C*H_2), 29.7 (*C*H_2), 29.7 (*C*H_2), 29.6 (*C*H_2), 29.5 (*C*H_2), 26.9 (*C*H_2), 26.8 (*C*H_2), 26.5 (*C*H_2), 25.8 (*C*H_2); HRMS m/z ESI$^+$ (calculated $C_{19}H_{38}ONa^+$ = 305.2815) found 305.2798 $[M+Na]^+$; ν_{max}/cm^{-1} 3447br (O-H).

6.4. References

[1] Y. Wei, B. Rao, X. Cong, X. Zeng, *J. Am. Chem. Soc.* **2015**, *137*, 9250–9253.

[2] J. Clark, D. O'Hagan, S. Guldin, A. Slawin, D. B. Cordes, C. Yu, R. A. Cormanich, R. Neyyappadath, A. Geddis, A. Taylor, B. A. Piscelli, *Chem. Sci.* **2021**, *12*, 9712-9719

[3] X. Cui, Y. Li, C. Topf, K. Junge, M. Beller, *Angew. Chem. Int. Ed.* **2015**, *54*, 10596–10599.

[4] G. W. Wong, T. T. Adint, C. R. Landis, *Org. Synth.* **2012**, *89*, 243–254.

[5] C. E. Astete, D. Songe Meador, D. Spivak, C. Sabliov, *Synth. Commun.* **2013**, *43*, 1299–1313.

[6] J. Ternel, J.-L. Couturier, J.-L. Dubois, J.-F. Carpentier, *Adv. Synth. Catal.* **2013**, *355*, 3191–3204.

7. Appendix

Chemical Science

ROYAL SOCIETY OF CHEMISTRY

EDGE ARTICLE

View Article Online
View Journal | View Issue

Cite this: *Chem. Sci.*, 2021, **12**, 9712

All publication charges for this article have been paid for by the Royal Society of Chemistry

Supramolecular packing of alkyl substituted Janus face all-*cis* 2,3,4,5,6-pentafluorocyclohexyl motifs†

Joshua L. Clark,[a] Alaric Taylor,[b] Ailsa Geddis,[a] Rifahath M. Neyyappadath,[a] Bruno A. Piscelli,[c] Cihang Yu,[a] David B. Cordes,[a] Alexandra M. Z. Slawin,[a] Rodrigo A. Cormanich,[c] Stefan Guldin[b] and David O'Hagan[*a]

This study uses X-ray crystallography, theory and Langmuir isotherm analysis to explore the conformations and molecular packing of alkyl all-*cis* 2,3,4,5,6-pentafluorocyclohexyl motifs, which are prepared by direct aryl hydrogenations from alkyl- or vinyl-pentafluoroaryl benzenes. Favoured conformations retain the more polar triaxial C–F bond arrangement of the all-*cis* 2,3,4,5,6-pentafluorocyclohexyl ring systems with the alkyl substituent adopting an equatorial orientation, and accommodating strong supramolecular interactions between rings. Langmuir isotherm analysis on a water subphase of a long chain fatty acid and alcohol carrying terminal all-*cis* 2,3,4,5,6-pentafluorocyclohexyl rings do not show any indication of monolayer assembly relative to their cyclohexane analogues, instead the molecules appear to aggregate and form higher molecular assemblies prior to compression. The study indicates the power and potential of this ring system as a motif for ordering supramolecular assembly.

Received 15th April 2021
Accepted 4th June 2021

DOI: 10.1039/d1sc02130c

rsc.li/chemical-science

Introduction

Organofluorine compounds have long made important contributions to organic materials chemistry and society more generally.[1] Perfluorocarbons where all of the hydrogens in an aliphatic material are replaced by fluorines display very high heat stabilities and are known for their chemical stability as well as their immiscibility with both hydrocarbons and water and ability to dissolve gases.[2] The 'fluorous phase'[3] has been coined to recognise the unique properties of this class of materials which is exemplified most prominently by the 'non-stick' polymer and coating poly(tetrafluoroethylene) (PTFE).[4] Partially fluorinated materials have very different properties and are characterised by an increasing polarity relative to fluorocarbons or hydrocarbons. Selective fluorination will induce polarity, and a polymer such as poly-(vinylidine fluoride)-PVDF displays piezoelectric properties due to dipoles created by the alternating $-CF_2-$ and $-CH_2-$ groups, a property maximised by poling (Fig. 1a).[5] Similarly there are a range of liquid crystalline materials which are used in modern displays and which derive their performance due to an orientated polarity introduced by selective fluorination of an organic material (Fig. 1b).[6]

We have developed an interest in the synthesis and properties of selectively fluorinated cyclohexanes and find that partial fluorination of aliphatic rings can lead to highly polar aliphatic motifs, particularly if isomers are selected that place fluorines on the same side of the cyclohexane ring.[7] All-*syn*-1,2,3,4,5,6-hexafluorocyclohexane **1** shown in Fig. 2a is the prototype compound of this class.[8] Cyclohexane **1** has all of its six fluorines on one face of the ring and is considered to be among the most polar aliphatic compounds known.[9] The molecule decomposes/sublimes at 208 °C, extraordinarily high for a low molecular weight aliphatic, and it has a molecular dipole moment of 6.2 D [calculated at M11/6-311G(2d,p) level], again extraordinarily high for an aliphatic. The polarity arises because there are three axial C–F bonds in the cyclohexane ring which are co-aligned and which generate a strong orientated dipole due to the maximal electronegativity of fluorine. The hydrogens

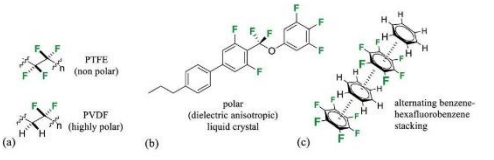

Fig. 1 (a) Minimal structures of (PTFE) and polar (PVDF) organofluorine polymers; (b) selectively fluorinated −ve dieletric anisotropic liquid crystal;[6a] (c) representation of benzene–hexafluorobenzene stacking in the solid state.[11,12]

[a]*School of Chemistry, University of St Andrews, North Haugh, St Andrews, Fife, KY16 9ST, UK. E-mail: do1@st-andrews.ac.uk*
[b]*Department of Chemical Engineering, University College London, Torrington Place, London, WC1E 7JE, UK*
[c]*Chemistry Institute, University of Campinas, Monteiro Lobato Street, Campinas, Sao Paulo, 13083-862, Brazil*

† Electronic supplementary information (ESI) available. CCDC 2068702–2068707. For ESI and crystallographic data in CIF or other electronic format see DOI: 10.1039/d1sc02130c

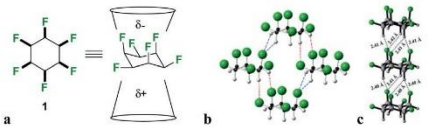

Fig. 2 Hexafluorocyclohexane **1** (a) structure and non-equivalent facial polarity profile; (b) X-ray structure of the prototype Janus face all-*cis* hexafluorocyclohexane **1**; (c) theoretically predicted optimal molecular packing of **1** differs from the observed X-ray derived structure.[11]

around the ring, three of them co-axial, become polarized by the geminal fluorine atoms rendering them electropositive.[7b] Accordingly the molecule has an electrostatically biased negative (fluorine) face and an electrostatically biased positive (hydrogen) face. More generally aromatic rings are electrostatically negative on both faces and cycloalkanes are neutral and hydrophobic, however there is no obvious counterpart ring in organic chemistry that has a −ve and a +ve face. This polarised aspect has led to **1** being described as a 'Janus face' ring system,[10] and it can be envisaged that electrostatic attraction between the fluorine and hydrogen faces of such ring systems could play a role as a motif for ordering and stabilising supramolecular assembly. Perhaps the closest related phenomenon to that described for these Janus face cyclohexanes is the widely celebrated outcome, described in the early 1960's by Patrick and Prosser, when benzene and hexafluorobenzene are mixed equally (Fig. 1c).[11] The two liquid components generate a solid material (mp 24 °C) which has stacked and alternating (offset) aryl- and hexafluoroaryl-rings, an arrangement accommodated by the complementary electrostatic profiles of these ring systems. For benzene the ring core is electronegative and the peripheral hydrogens electropositive, whereas for the hexafluorobenzene the ring core is electropositive and the peripheral fluorines are electronegative. This ordering opened up a wide area of supramolecular exploration which remains active until the present.[12] Janus rings of **1** can be considered to approximate a fusion of benzene and hexafluorobenzene, with the ability to display a similar ordering phenomenon within a single ring system. When rings of **1** associate, they order electrostatically with the fluorine face of one ring contacting the hydrogen face of another (Fig. 2b). Theoretical studies indicate that the interaction energy of two isolated rings of **1** is ~8.2 kcal mol^{-1},[13] about the strength or stronger than a hydrogen bond, an energy that will be substantial in supramolecular ordering. The crystal structure of **1** (Fig. 2b) has the rings arranged such that stacking is offset from the perpendicular, however theoretical studies indicate that perpendicular packing shown in Fig. 2c should be optimal and that there is a relatively low energy between these polymorphic arrangements. In this paper we explore supramolecular ordering of mono-alkyl substituted derivatives of cyclohexane **1**.

A clear challenge in order to explore the properties of these Janus face systems is access to an appropriate syntheses to prepare such compounds. Recent and important progress has been made by the Glorius laboratory,[14] who have demonstrated that multiply-fluorinated aromatics can be directly hydrogenated to generate the corresponding all-*cis* fluorocyclohexane products in one step, without any significant loss of fluorine. The method used the cyclic(alkyl)(amino)carbene (CAAC)/Rh catalyst **2** developed by Zeng[15] for aryl hydrogenations. Glorius demonstrated that cyclohexane **1** could be efficiently prepared from hexafluorobenzene by this approach as illustrated in Fig. 3a reducing the original twelve step protocol to one step. It follows that a range of monosubstituted alkyl derivatives of cyclohexane **1** could now be prepared by direct hydrogenation of alkyl substituted pentafluorobenzenes, an approach that forms the focus of this paper. Indeed, we find that both the R = Me **3** and R = Et **4** (Fig. 4) substituents are accessible directly by hydrogenation of their pentafluoroaryl precursors, as the first examples of alkyl all-*cis* 1,2,3,4,5-pentafluorocyclohexyl derivatives. Developing this further, we also report the synthesis and some properties the bis-cyclohexyl tethered rings **5** and **6** with short and long alkyl spacers between the rings and then systems **7–9**, with longer alkyl chains terminating in either alkyl, alcohol or carboxylic acid residues. These compounds are illustrated in Fig. 3b. In order to gain insight into supramolecular assembly we have determined the solid state structures of the **3** and **4**, bis-ring systems **5** and **6**, as well as **8** and **9** and we have investigated the deposition of the long chain alkyls **7–9** on a water subphase. The outcomes are reported below.

Results and discussion

Hydrogenation (50 bar H_2) of pentafluoroaryl-toluene and pentafluoroaryl-ethylbenzene using catalyst **2** generated the corresponding methyl- and ethyl-functionalised all-*cis* pentafluorocyclohexanes **3** (55% yield) and **4** (76% yield) respectively (Fig. 4). Cyclohexanes **3** (mp = 182 °C) and **4** (mp = 148 °C) have high melting points consistent with strong electrostatic attraction between the rings, and this contrasts with their hydrocarbon or perfluorocarbon analogues which are liquids at ambient temperature. It was of immediate interest in the context of supramolecular assembly to establish if the alkyl substituents preferred an axial over an equatorial orientation as it was not obvious if the steric effect of an axial Me/Et group and two axial C–F bonds would be more or less stabilising than the

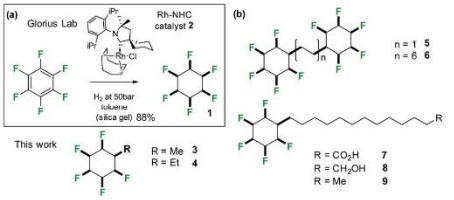

Fig. 3 (a) Aryl hydrogenation developed by Glorius[14b] was adapted to the synthesis of alkyl substituted all-*cis* 1,2,3,4,5-pentafluorocyclohexane rings systems; (b) structures of alkyl substituted all-*cis* pentafluorocyclohexanes **3–9** prepared in this study.

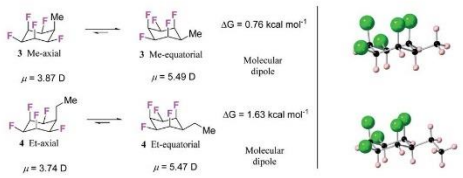

Fig. 4 (a) Calculated (M06L-D3/aug-cc-pVTZ level) equilibrium energies between axial/equatorial conformers of alkyl substituted all-*cis* 1,2,3,4,5,-pentafluorocyclohexanes **3** and **4**; (b) solid state X-ray structures of **3** (upper) and **4** (lower). In each case the equatorial conformer is favoured.

electrostatic repulsion associated with three axial C–F bonds when the Me/Et group is equatorial (Fig. 4a).

Since both **3** and **4** are crystalline solids their crystal structures were determined by X-ray analyses and are illustrated in Fig. 4b. In each case the solid-state structures have the alkyl groups equatorial with triaxial C–F bonds. To gain a deeper insight into the favoured conformations of these mono alkylated cyclohexyl systems a theory study (M06L-D3/aug-cc-pVTZ level) was carried out to establish the relative energies between the axial and equatorial conformers of **3** and **4** in the gas phase.[16] This theory level showed the best results in benchmarking calculations using the DLPNO-CCSD(T)/def2-TZVP level as the benchmark (see ESI†). The results are summarised in Fig. 4a. For cyclohexane **3** it emerged that the equatorial Me conformer is of lower energy despite it having a significantly higher molecular dipole ($\mathbf{3}_{ax} = 3.87$ D *versus* $\mathbf{3}_{eq} = 5.49$ D), although the energy difference between conformers is not large ($\Delta G = 0.76$ kcal mol^{-1}), tending towards an isoenergetic situation, and being significantly less than for example methylcyclohexane (~1.74 kcal mol^{-1}).[17] However the equatorial preference increases significantly ($\Delta G = 1.63$ kcal mol^{-1}) for ethylcyclohexane **4** although the situation is a little more complex due to ethyl group rotation. The equilibrium energy difference was calculated after rotational energy profiles (see ESI†) established the minimum energies for the axial and equatorial conformers of **4**. The conformations in the solid-state structures of **3** and **4** are clearly equatorial, reinforced by the strong intermolecular association between the more polar conformers in the solid state, and this augers well for the reliability of supramolecular packing for this series (alkyl all-*cis* 1,2,3,4,5-pentafluorocyclohexane motifs) more generally.

Natural bond orbital (NBO) analysis[16,18] was carried out to rationalise the significantly larger equatorial preference for **4** over **3** (Table S1 in the ESI†). NBO analysis separates the relative global electronic energy [ΔE(T)] into its Natural Lewis energy [ΔE(L)], which accounts for a chemical structure without any delocalisation and therefore representing steric and electrostatic contributions only, from Natural Non-Lewis energies [ΔE(NL)] which account for hyperconjugation. NBO analysis indicates that the increase in energy difference between the ax/eq conformers of **4** relative to **3** is due to a balance between electrostatics ΔE(NCE) as calculated from the Natural Coulomb Electrostatic (NCE) analysis,[16b] and hyperconjugation ΔE(NL), with electrostatics favouring the axial conformer (−0.95 kcal mol^{-1}) and global hyperconjugation interactions favouring the equatorial conformer in **3** (1.17 kcal mol^{-1}) (Table S1 in ESI†). On the other hand, the Et derivative **4** has a higher preference for the equatorial conformer, because now the electrostatic term [ΔE(L)] (0.68 kcal mol^{-1}) also favours the equatorial conformer. This arises from replacing a positively charged H atom in **3** by a CH_3 group with a negatively charged C atom in **4** (Fig. 5), the interactions with the axial F atoms become destabilising (see Tables S2 and S3 in the ESI† for individual atom–atom interactions) and disfavour the axial geometry to a greater extent ($\Delta G = 1.63$ kcal mol^{-1}).

Another interesting feature of the NBO analysis is the possibility to decompose the total molecular dipole moment quantitatively into the individual bonds and lone pairs that sum to give the overall value.[16] Since the total dipole moment of compounds **1**, **3** and **4** is mainly directed from the hydrogen to the fluorine face of the cyclohexane ring, we analysed the bonds and lone pairs that contribute to this axis (Table S5 in the ESI†). Accordingly, each C–F_{ax} bond contributes ~1.8 D, and the F_{ax} lone pairs ~1.4 D, to the total dipole, whereas the C–F_{eq} bonds and F_{eq} lone pairs contribute only ~0.5 D and 0.4 D, respectively. Thus, by replacing an equatorial C–F_{eq} bond from **1** by an alkyl group as in **3** and **4**, only a small decrease in the total dipole moment occurs, and therefore the mono substituted ring retains high polarity.

The bis-cyclohexane systems **5** and **6** were next prepared, with two all-*cis* 1,2,3,4,5-pentafluorocyclohexyl rings anchored between a shorter and a longer aliphatic spacer. The synthesis routes to **5** and **6** are summarised in Fig. 6 and 7. Compound **5** was prepared by direct hydrogenation of decafluorostilbene **11**, a known substrate readily accessible by a McMurry coupling of pentafluorobenzaldehyde **10**.[19] The hydrogenation reaction (catalyst **2**, 50 bar H_2) proved sluggish and product **5** was notably highly insoluble in standard chromatography solvents. As a consequence, a suitable sample for crystal structure analysis was isolated by recrystallisation rather than column chromatography. It was notable that bis-cyclohexane **5** did not have

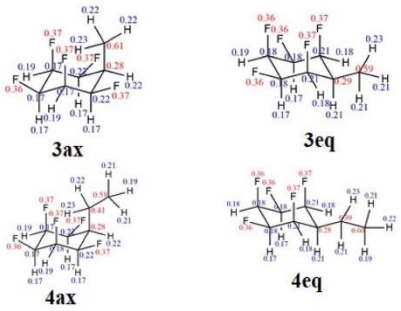

Fig. 5 Calculated NPA charges for the axial and equatorial conformers of **3** and **4** at the M06-2X/aug-cc-pVTZ level. Blue and red represent positive and negative charges, respectively (in au).

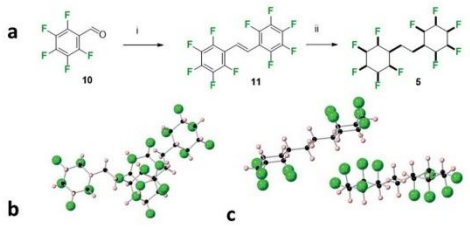

Fig. 6 (a) Synthesis of **5**. (i) Zn, $TiCl_4$, THF, 70 °C, 4 h, 19% yield; (ii) 50 bar H_2 gas, 1 mol% cat (**2**), 4 Å MS, hexane, 24 h, 28% yield. (b) X-ray crystal structure showing two molecules of 1,2-bis-(all-*cis*-2,3,4,5,6-pentafluorocyclohexyl)ethane **5** with one molecule lying above the other and (c) with an orientation highlighting an interdigitated packing.

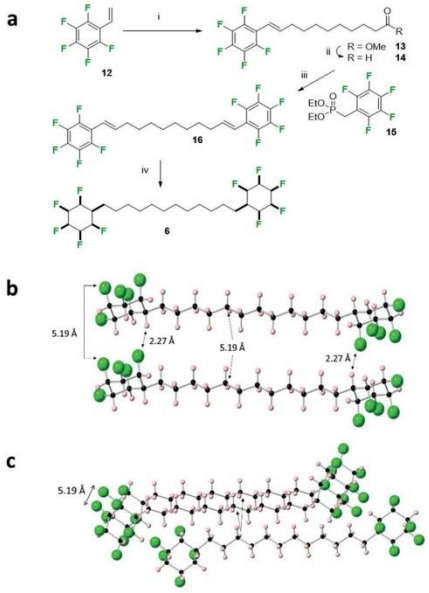

Fig. 7 (a) Synthesis route to **6** involving the exhaustive hydrogenation of **16**. (i) Methyl 10-undecenoate 2nd generation Hoveyda–Grubbs catalyst, CH_2Cl_2, 40 °C, 14 h, 54%; (ii) DIBAlH, CH_2Cl_2, −78 °C, 1 h, quantitative; (iii) NaH, THF, 0 °C then **14**, 0 °C to 66 °C, 53%; (iv) H_2 (50 bar), **2** (5 mol%), 4 Å MS, hexane, r.t., 33%. (b) X-ray crystal structure showing the alignment of adjacent molecules of **6**. Short CF···HC contacts (2.27 Å) are illustrated which suggest a strong electrostatic interaction between the cyclohexane rings. (c) View incorporating a third molecule of an adjacent stack illustrating the condensed packing of the alkyl chains.

a classical melting profile; showing discolouration at 210 °C and remaining unmelted at 300 °C! This unusual behaviour for a relatively low molecular weight aliphatic is similar to that observed for cyclohexane **1** (mp = 208 °C),[8] and it is indicative of the strong electrostatic interactions between the rings in the solid state. A suitable crystal of **5** was selected for crystal structure analysis and views of the resultant structure are shown in Fig. 6.

In the solid state, the linking alkyl chain lies equatorial and molecules of **5** pack in an interdigitated manner rather than one on top of each other. The rings of adjacent molecules associate, with the complementary fluorine and hydrogen faces contacting each other. When two molecules are viewed one above the other (Fig. 6a) an axial fluorine of one ring is pointing directly towards the axial hydrogens of the next ring. The three CF···HC contact distances are almost equidistant, (2.46 Å, 2.46 Å & 2.54 Å) and below the van der Waals contact distance (2.67 Å)[20] for hydrogen and fluorine. The orientation of the peripheral cyclohexyl rings in any molecule of **5** is antiparallel, consistent with an arrangement which reduces the molecular dipole of an isolated molecule and reduces the net polarity of the crystal.

The bis-cyclohexyl system **6** with a longer linker was prepared as illustrated in Fig. 7 after a metathesis reaction[21] between styrene **12** and methyl undec-1-enoate, to generate ester **13**. Selective reduction gave aldehyde **14** which was amenable to a Horner–Wadsworth–Emmons olefination[22] with phosphonate **15** to generate bis-olefin **16**. Exhaustive hydrogenation of both the double bonds and the aryl rings with catalyst **2** generated the desired product **6**, again as a solid material. The melting point of **6** (188 °C) was lower than that of **5** presumably on account of the longer aliphatic spacer.

In the solid state, the structure shows simpler packing than **5**, with the peripheral rings in **6** stacked directly one above another along the *b*-axis, and where the linking chains align, spaced by a repeat distance of 5.19 Å for both the cyclohexane rings and the aliphatic chains, slightly longer than the typical (4.5–5.0 Å) distances for optimal packing in hydrocarbon chain assemblies.[23] There are three CF···HC contacts within stacks of molecules, two at 2.39 Å and 2.46 Å, and one notably short at a CF···HC distance of 2.27 Å. Such distances are among the shortest CF···HC contacts found in the Cambridge Structural Database[24] and well below the sum of the van der Waal's F···H contact distance (2.67 Å)[20] suggesting that the electrostatic attraction between the fluorine and hydrogen faces of the rings is leading to a compression and accommodating these non-classical hydrogen bonds. As well as these contacts within stacks, adjacent stacks are also linked by CF···HC contacts, at 2.32 Å.

The study was then extended to the synthesis of the long chain fatty acid **7** with a terminal pentafluorocyclohexane ring system. The classical amphiphilic nature of fatty acids is such that they adopt organised supramolecular assemblies in the solid state or on the surface of water supported by hydrogen bonding of the carboxylate head groups and van der Waals interactions of the aliphatic chains, typical of lipid membranes.[25] In the solid state such arrangements can be interdigitated to form a repeat monolayer or the molecules can arrange head to head and form bilayers. On water, the carboxylate head groups associate with the aqueous subphase and chains aggregate into monolayer or bilayer assemblies, a process that can be monitored in a Langmuir trough through pressure area isotherm analysis.[26] Therefore long chain fatty

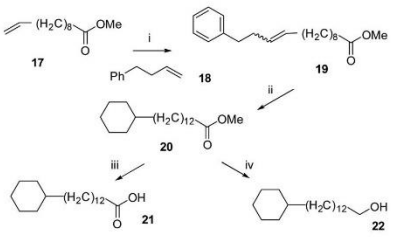

Scheme 1 Synthetic routes to non-fluorinated cyclohexyl fatty acid **12** and long chain alcohol **13**. (i) 4-phenylbutene **18**, Grubbs first generation catalyst ®, CH_2Cl_2, 40 °C, 14 h, 39%; (ii) H_2 (50 bar), **2** (8 mol%), 4 Å MS, hexane, r.t., 74%; (iii) NaOH, H_2O, MeOH, 65 °C; (iv) DIBALH, CH_2Cl_2, −78 °C to r.t., 1 h, 81%.

acid **7** was targeted as a molecular tool in which to further explore the mode of supramolecular assembly of the all-*syn* pentafluorocyclohexyl motif. The study extended to preparing the corresponding alcohol **8** and methyl terminated alkane **9**. The analogous long chain fatty acid **21** and alcohol **22**, without any fluorines, were also prepared as reference compounds for Langmuir isotherm analyses.

The synthesis routes to fatty acid **21** and long chain alcohol **22** are illustrated in Scheme 1. The length of the chain was assembled by fusing together methyl 10-undecenoate **17** and phenylbutene **18** in a cross-metathesis protocol.[21] This proved to be relatively straightforward and the resultant ester **19** was subject to an exhaustive aryl/olefin hydrogenation reaction with catalyst **2**. The product aliphatic ester **20** was either progressed by reduction to generate alcohol **22** or it was hydrolysed to the desired fatty acid **21**. The synthesis of carboxylic acid **7** and alcohol **8** was accomplished as illustrated in Scheme 2. This involved a Horner–Wadsworth–Emmons (HWE) olefination[23] between pentafluoroaryl phosphonate **26** and long chain ester-aldehyde **24** to generate ester **27** as a mixture of *E* and *Z* stereoisomers. Direct aryl hydrogenation under pressure resulted in the formation of the saturated ester **28**. Ester **28** was then hydrolysed to generate fatty acid **7** and was separately reduced to long chain alcohol **8**. In a separate sequence, a cross metathesis reaction between terminal alkene **29** and 1-dodecene to generate olefin **30** generated the resultant olefin **30** which was also submitted to an exhaustive hydrogenation reaction with catalyst **2** (ref. 15) to generate alkylcyclohexane **9**. Melting point comparisons where made between the analogous partially fluorinated and non-fluorinated products as an immediate comparator of the anticipated difference in physical properties between the two series. These are summarised in Table 1.

Table 1 Melting point comparisons between cyclohexyl and all-*cis* 2,3,4,5,6-pentafluorocyclohexyl systems

	Pentafluoro	Hydrocarbon
Fatty acids	**7** = 178 °C	**21** = 65 °C
Long chain alcohols	**8** = 140 °C	**22** = 34 °C
Tridecylcyclohexane	**9** = 121 °C	14 °C[a]

[a] Ref. 25.

It is clear that the melting points are very much higher for the fluorinated analogues consistent with electrostatic

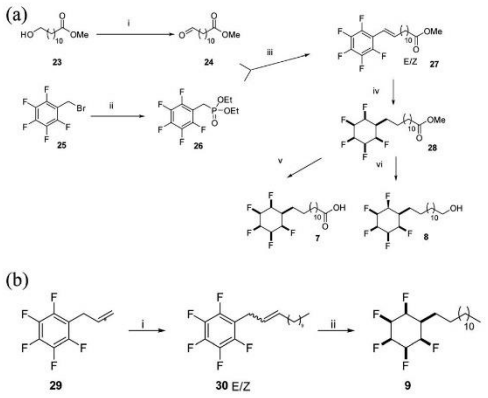

Scheme 2 (a) Synthetic routes to all-*cis* pentafluorocyclohexyl fatty acid **7** and alcohol **8**. (i) $(COCl)_2$, DMSO, Et_3N, CH_2Cl_2, −78 °C, 74%; (ii) $P(OEt)_3$, microwave, 140 °C, 5 min, 99%; (iii) NaH, THF, 0 °C to 50 °C, 14 h, 58%; (iv) **2** (3 mol%), H_2 (50 bar), silica gel, hexane, r.t., 22%; (v) HCl (6 N), H_2O, 100 °C, 14 h, 95%; (vi) DIBAlH, CH_2Cl_2, −78 °C to r.t., 64%. (b) Synthetic route to all-*cis* pentafluorocyclohexyl long chain aliphatic **9**. (i) Grubbs first generation catalyst, 1-dodecene, CH_2Cl_2, 40 °C, 14 h; (ii) H_2 (50 bar), **2** (3 mol%), 4 Å MS, hexane, r.t., 32% over two steps.

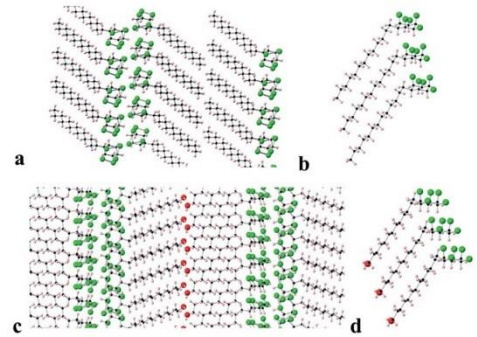

Fig. 8 Views of the X-ray determined crystal structures of tridecyl alkane **9** (upper) and long chain alcohol **8** (lower). (a) Cross sectional view down the *b*-axis of the packing arrangement of tridecyl alkane **9** and (b) the stacking arrangement of three molecules of **9** showing an angled (130°) arrangement between the alkyl chains and the cyclohexyl rings. (c) Cross sectional view down the (1 −1 0) axis of the packing arrangement of long chain alcohol **8** and (d) the stacking arrangement of three molecules of **8** also showing an angled (120°) arrangement optimised for intermolecular contacts between the alkyl chains and cyclohexyl rings.

attraction between the faces of the all-*cis*-2,3,4,5,6-pentafluorocyclohexyl rings in the solid state.

Long chain alkane **9** and alcohol **8** generated suitable crystals for X-ray crystal structure analysis. The resultant packing structures are shown in Fig. 8.

Compound **9** (Fig. 8a and b) adopts a packing structure similar to that found for hexafluorocyclohexane **1** where there is an offset between adjacent cyclohexane rings. The equivalent ring atoms (fluorines or hydrogens) are 5.62 Å apart, which is an increase on the equivalent spacing found in **6** (5.19 Å). The long chain alkane moiety extends linearly in a classical extended anti zig-zag conformation and the terminal methyl groups interface to form a double lamellar (bilayer) hydrophobic domain. The aliphatic chains are compact running parallel to each other at a regular distance of 4.0–4.2 Å along the chains. To accommodate this narrowing relative to the cyclohexane ring spacing (5.62 Å) and to presumably maximise van der Waals interactions, the chains are orientated at an angle 130° with respect to the plane of the cyclohexane rings.

In the case of long chain alcohol **8** (Fig. 8c and d), the molecules arrange in a similar manner but there is an additional extended hydrogen bonding network, forming chains running along the *a*-axis between the terminal alcohol moieties of two molecular domains. The pentafluorocyclohexane rings are again offset, one above another, and the rings associate edge to edge at the molecular interface with the rings of another domain of extended molecules forming an infinite bilayer array. Again, the extended aliphatic chains run parallel and are set at an angle of 120° to the plane of the cyclohexane ring in a similar arrangement to that found in **9**. This angle allows the aliphatic chains to approach closely (4.0–4.1 Å), because the equivalent atoms of the cyclohexane rings are spaced more widely (5.57 Å apart), an arrangement that accommodates close van der Waals contacts between the long chains.

Langmuir isotherm analysis

Surface pressure–area isotherms[26] were recorded after deposition of fatty acids **21** and **7** and long chain alcohols **22** and **8** on a water subphase in a Langmuir trough, in order to compare the influence of cyclohexyl fluorination on the surface behaviour (see ESI†). In the first instance the non-fluorinated fatty acid **21** was deposited onto the water subphase from a solution in chloroform, as a reference. The resultant isotherm for **21** is illustrated in Fig. 9a. There is a very clear monolayer transition at about 28–31 Å^2 per molecule, a little expanded relative to a fatty acid such as stearic acid. With additional compression this monolayer collapses until a second transition is apparent at ~12 Å^2 per molecule, suggesting a thermodynamically stable bi- or multi-layer, before infinite compression. Deposition of the fluorocyclohexyl fatty acid **7** required preparation of a pre-solution with 50% acetone in chloroform to overcome its relatively poor solubility. The resultant isotherm in Fig. 9a shows a clear single transition at about 7–9 Å^2 per molecule for **7**, similar in area to the second compression for the reference fatty acid **21**. The outcome is indicative of the immediate formation of at least a bilayer assembly on the surface. There was no

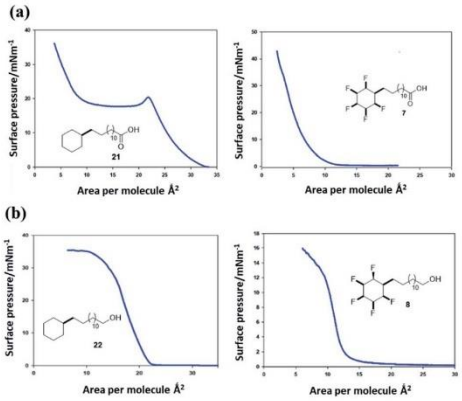

Fig. 9 (a) Pressure–area isotherms[26] on a water subphase of long chain cyclohexyl fatty acids **21** (left) and **7** (right). Fatty acid **21** presents a classical isotherm indicating an initial monolayer collapsing to a bilayer on compression. Fatty acid **7** only displays a low surface area isotherm indicative of a bi- or multi-layer formation. (b) Pressure–area isotherms of long chain cyclohexyl alcohols **22** and **8**. The aliphatic alcohol **22** displays classical monolayer behaviour whereas the fluorinated alcohol **8** displays bilayer behaviour.

evidence at all for an initial monolayer transition for **7**. This is consistent with pre-aggregation of **7** in the 2D-gas phase.

The long chain alcohols **8** and **22** gave more consistent data due to the increased solubility of **8** as illustrated in isotherms in Fig. 9b. The reference isotherm for the nonfluorinated alcohol **22** indicated well behaved monolayer formation on the aqueous subphase with a condensed phase apparent at around 22–23 Å^2 per molecule.

By comparison, isotherms for the pentafluorinated cyclohexyl alcohol **8** did not show monolayer formation. After deposition from a solution in chloroform, a first phase transition is apparent at an area per molecule of 13–14 Å^2, below half that for the transition observed for reference alcohol **22**, indicative of a spontaneous bilayer formation. Interestingly, when the long chain alcohol **8** is deposited from a solution which contains acetone (10% by volume in chloroform), then this perturbs the surface isotherm. A first compression is apparent indicating a more classical monolayer, at an area of 24 Å^2 per molecule. However with further compression a phase transition to the bilayer (at 13 Å^2) becomes favoured as illustrated in the right hand isotherm in Fig. 9b. It would appear that the more polar solvent (acetone), helps disperse pre-formed aggregations such that a monolayer becomes observable, before reorganisation to a bilayer on compression. Repeated compressions and expansion cycles could not recover any evidence of the monolayer. This is illustrated in Fig. 10.

These experiments suggest that the all-*syn* pentafluorocyclohexyl ring systems **7** and **8** pre-aggregate and generate bilayers directly, whereas the non-fluorinated cyclohexane systems **21** and **22** display classical behaviour. It is clear

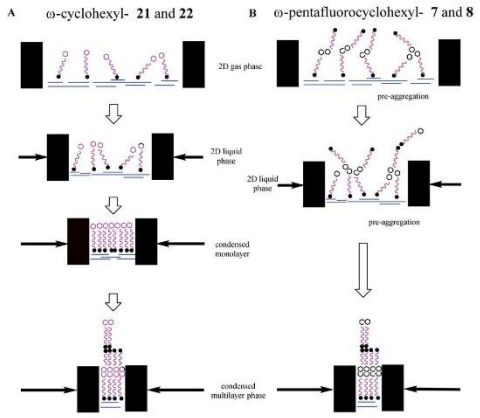

Fig. 10 Schematic illustration of the Langmuir isotherms behaviour of the ω-cyclohexyl and ω-pentafluorocyclohexanol fatty acids and alcohols on the water subphase. Arrows indicate the movement of the barriers to reduce surface area. (A) ω-Cyclohexyl fatty acid **21** and alcohol **22** behave classically to generate a coherent condensed monolayer, which further compresses to a multilayer. (B) ω-Pentafluoroyclohexyl fatty acid **7** and alcohol **8** pre-aggregate due to associations between the terminal rings and compression progresses directly to a multilayer.

that the all-*cis* petafluorocyclohexyl ring systems are self-associating. The interaction energy of these rings has been calculated[13] to be ~6–8 kcal mol^{-1} and competitive with the strength of hydrogen bonding interactions between the polar head groups and water, and this is consistent with the observed deviation from classical behaviour.

In conclusion, in this study we have prepared the first examples of alkyl substituted 2,3,4,5,6-pentafluorocyclohexanes where all of the substituents are *cis*. The bis ring systems **5** and **6** were prepared and structure **6** with the longer alkyl spaces shows a simpler packing arrangement, in that both rings for each molecule associate with both on adjacent molecules, rather than the more interdigitated arrangement observed in **5**. The very high melting points (>210 °C for **5** and 188 °C for **6**) for these bis-ring systems are striking and is also indicative of the strong intermolecular interactions between these cyclohexane rings. Long chain alkane **9**, alcohol **8** and carboxylic acid **7** were prepared and all had very significantly higher melting points relative to their hydrocarbon analogues. These long chain alkyl derivatives were variously subject to crystal structure and pressure–area isotherm analysis in a Langmuir trough. It is notable that in the X-ray determined structures that were solved for **8** and **9**, and also of the shorter chain alkyls **3** and **4**, that the alkyl substituents always lie equatorial to the all-*cis* pentafluorocyclohexane in a conformation where there are three axial C–F bonds rather than the alternative with two axial C–F bonds and the alkyl group adopting an axial orientation. A theory study indicative of behaviour in the gas phase also supported lower energy equatorial conformers for **3** and **4** despite an increased molecular dipole (polarity) with this arrangement. This augurs well for strong intermolecular associations which are not impeded sterically as there will be stronger electrostatic interactions between the more polar equatorial conformers. This conformation is consistently observed in the solid-state structures presented here. The study illustrates that these functionalised rings constitute a novel motif for the design of supramolecular organic frameworks, a prospect that becomes practical due to improved methods for the synthesis of building blocks by the recent developments in perfluoroaryl hydrogenations.[27]

Author contributions

University of St Andrews, UK: Joshua L. Clark (PhD student) synthesised compounds **4**, **7**, **8** and **9**, **21** and **22**. Cihang Yu (PhD student) made and crystallised compound **3**. Rifahath M. Neyyappadath (post doc) and Ailsa Geddis (Master's student) worked together and made and crystallised compound **5**. David Cordes (SEO) and Alexandra Slawin (Professor) are crystallographers, who between them solved the structures of compounds **3**, **4**, **5**, **6**, **8** & **9**. They also deposited cifs and data at the CCDC. David O'Hagan (Professor) guided the work, arranged the collaborations and wrote the manuscript. **University College London, UK:** Alaric Taylor (post doc) and Stefan Guldin (Professor) are surface scientists at UCL London, where the Langmuir isotherm studies were carried out for compounds **7** and **8** and **21** and **22**. **University of Campinas, Brazil:** Rodrigo Cormanich (Professor) and Bruno Piscelli (PhD student) are theorists based at the University of Campinas in Brazil. They carried out the theory analysis of compounds **3** and **4**.

Conflicts of interest

There are no conflicts to declare.

Acknowledgements

We thank EPSRC for a grant (EP/R013799/1) and for Studentships (AT & JC) through a Centre for Doctoral Training (EP/L016419/1) and a Doctoral Training Partnership (EP/M507970/1). FAPESP is also gratefully acknowledged for a studentship (BAP, #2019/03855-3), and a Young Research Award (RAC, #2018/03910-1). CENAPAD-SP, CESUP and SDumont are acknowledged for computational clusters used in theory calculations.

Notes and references

1 (*a*) P. Kirsch, *Modern fluoroorganic chemistry*, Wiley VCH-Verlag GmbH & Co KGaA, Weinheim, Germany, 2nd edn, 2013; (*b*) W. R. Dolbier, *J. Fluorine Chem.*, 2005, **126**, 157–163.
2 (*a*) M. A. Miller and E. M. Sletten, *ChemBioChem*, 2020, **21**, 3451–3462; (*b*) T. Brandenburg, R. Golnak, M. Nagasaka, K. Atak, S. Sreekantan, N. Lalithambika, N. Kosugi and E. F. Aziz, *Sci. Rep.*, 2016, **6**, 31382; (*c*) P. Kirsch, *J. Fluorine Chem.*, 2015, **177**, 29; (*d*) D. M. Lemal, *J. Org. Chem.*, 2004,

69, 1; (*e*) G. Sandford, *Tetrahedron*, 2003, **59**, 437–454; (*f*) M. P Krafft and J. G. Riess, *J. Polym. Sci., Part A: Polym. Chem.*, 2007, **45**, 1185–1198.

3 (*a*) A. P. Dobbs and M. R. Kimberley, *J. Fluorine Chem.*, 2002, **118**, 3–17; (*b*) I. T. Horváth and J. Rábai, *Science*, 1994, **266**, 72–75.

4 (*a*) G. J. Puts, P. Crouse and B. M. Ameduri, *Chem. Rev.*, 2019, **119**, 1763–1805; (*b*) R. A. Cormanich, D. O'Hagan and M. Bühl, *Angew. Chem., Int. Ed.*, 2017, **129**, 7975–7978.

5 (*a*) G. Suresh, S. Jatav, G. Mallikarjunachari, M. S. R. Rao, P. Ghosh and D. K. Satapathy, *J. Phys. Chem. B*, 2018, **122**, 8591–8600; (*b*) H. Kawai, *Jpn. J. Appl. Phys.*, 1969, **8**, 975–976.

6 (*a*) S. Matsui, T. Kondo and K. Sago, *Mol. Cryst. Liq. Cryst.*, 2004, **411**, 127–137; (*b*) P. Kirsch, F. Huber, M. Lenges and A. Taugerbeck, *J. Fluorine Chem.*, 2001, **112**, 69–72; (*c*) Z. Fang, N. Al-Maharik, P. Kirsch, M. Bremer, A. M. Z. Slawin and D. O'Hagan, *Beilstein J. Org. Chem.*, 2020, **16**, 674–680.

7 (*a*) D. O'Hagan, *Chem.–Eur. J.*, 2020, **26**, 7981–7997; (*b*) A. Rodil, S. Bosisio, M. S. Ayoup, L. Quinn, D. B. Cordes, A. M. Z. Slawin, C. D. Murphy, J. Michel and D. O'Hagan, *Chem. Sci.*, 2018, **9**, 3023–3028; (*c*) M. J. Lecours, R. A. Marta, V. Steinmetz, N. Keddie, E. Fillion, D. O'Hagan, T. B. McMahon and W. S. Hopkins, *J. Phys. Chem. Lett.*, 2017, **8**, 109–113; (*d*) T. Bykova, N. Al-Maharik, A. M. Z. Slawin and D. O'Hagan, *Beilstein J. Org. Chem.*, 2017, **13**, 728–733; (*e*) B. E. Ziegler, M. Lecours, R. A. Marta, J. Featherstone, E. Fillion, W. S. Hopkins, V. Steinmetz, N. S. Keddie, D. O'Hagan and T. B. McMahon, *J. Am. Chem. Soc.*, 2016, **138**, 7460–7463.

8 N. S. Keddie, A. M. Z. Slawin, T. Lebl, D. Philp and D. O'Hagan, *Nat. Chem.*, 2015, **7**, 483–488.

9 (*a*) B. S. D. R. Vamhindi, C.-H. Lai, S.-J. Koyambo-Konzapa and M. Nsangoue, *J. Fluorine Chem.*, 2020, **236**, 109575; (*b*) X.-H. Li, X.-L. Zhang, Q.-H. Chen, L. Zhang, J.-H. Chen, D. Wu, W.-M. Sun and Z.-R. Li, *Phys. Chem. Chem. Phys.*, 2020, **22**, 8476–8484; (*c*) W.-M. Sun, B.-L. Ni, D. Wu, J.-M. Lan, C.-Y. Li, Y. Li and Z.-R. Li, *Organometallics*, 2017, **36**(17), 3352–3359.

10 (*a*) B. S. D. R. Vamhindi, C.-H. Laib, S.-J. Koyambo-Konzapa and M. Nsangou, *J. Fluorine Chem.*, 2020, **236**, 109575; (*b*) N. Santschi and R. Gilmour, *Nat. Chem.*, 2015, **7**, 467–468.

11 (*a*) C. R. Patrick and G. S. Prosser, *Nature*, 1960, **187**, 102; (*b*) J. H. Williams, *Acc. Chem. Res.*, 1993, **26**, 593–598; (*c*) C. E. Smith, P. S. Smith, R. Ll. Thomas, E. G. Robins, J. C. Collings, C. Dai, A. J. Scott, S. Borwick, A. S. Batsanov, S. W. Watt, S. J. Clark, C. Viney, J. A. K. Howard, W. Clegg and T. B. Marder, *J. Mater. Chem.*, 2004, **14**, 413–420; (*d*) J. C. Collings, K. P. Roscoe, E. G. Robins, A. S. Batsanov, L. M. Stimson, J. A. K. Howard, S. J. Clark and T. B. Marder, *New J. Chem.*, 2002, **26**, 1740–1746.

12 (*a*) A. Friedrich, I. E. Collings, K. F. Dziubek, S. Fanetti, K. Radacki, J. Ruiz-Fuertes, J. Pellicer-Porres, M. Hanfland, D. Sieh, R. Bini, S. J. Clark and T. B. Marder, *J. Am. Chem. Soc.*, 2020, **142**, 18907–18923; (*b*) M. D. Ward, W.-S. Tang, L. Zhu, D. Popov, G. D. Cody and T. A. Strobel, *Macromolecules*, 2019, **52**, 7557–7563; (*c*) K. Kishikawa, T. Inoue, Y. Sasaki, S. Aikyo, M. Takahashi and S. Kohmoto, *Soft Matter*, 2011, **7**, 7532–7538.

13 S. M. Pratik, A. Nijamudheen and A. Datta, *ChemPhysChem*, 2016, **17**, 2373–2381.

14 (*a*) Z. Nairoukh, M. Wollenburg, C. Schlepphorst, K. Bergander and F. Glorius, *Nat. Chem.*, 2019, **11**, 264–270; (*b*) M. P. Wiesenfeldt, T. Knecht, C. Schlepphorst and F. Glorius, *Angew. Chem., Int. Ed.*, 2018, **57**, 8297–8300; (*c*) M. P. Wiesenfeldt, Z. Nairoukh, W. Li and F. Glorius, *Science*, 2017, **357**, 908–912.

15 (*a*) X. Zhang, L. Ling, M. Luo and X. Zeng, *Angew. Chem., Int. Ed.*, 2019, **58**, 16785–16789; (*b*) Y. Wei, B. Rao, X. Cong and X. Zeng, *J. Am. Chem. Soc.*, 2015, **137**, 9250–9253.

16 (*a*) E. D. Glendening, J. K. Badenhoop, A. E. Reed, J. E. Carpenter, J. A. Bohmann, C. M. Morales, C. R. Landis and F. Weinhold, *NBO 7.0*, Theoretical Chem. Institute, Univ. Wisconsin, Madison, WI, 2018; (*b*) J. K. Badenhoop and F. Weinhold, Natural Bond Orbital Analysis of Steric Interactions, *J. Chem. Phys.*, 1997, **107**(14), 5406–5421.

17 E. E. Eliel and S. H. Wilen, *Stereochemistry of organic compounds*, John Wiley & Sons Inc., 1994.

18 F. Weinhold and C. R. Landis, *Discovering Chemistry with Natural Bond Orbitals*, 2014.

19 (*a*) V. Rauniyar, H. Zhai and D. G. Hall, *J. Am. Chem. Soc.*, 2008, **130**(26), 8481–8490; (*b*) M. I. Donnoli, P. Scafato, S. Superchi and C. Rosini, *Chirality*, 2001, **13**, 258–265.

20 A. Bondi, *J. Phys. Chem.*, 1964, **68**, 441–451.

21 D. Astruc, *New J. Chem.*, 2005, **29**, 42–56.

22 J. A. Bisceglia and L. R. Orelli, *Curr. Org. Chem.*, 2015, **19**, 744–775.

23 J. F. Nagle and D. A. Wilkinson, *Biophys. J.*, 1978, **23**, 159–175.

24 (*a*) C. R. Groom, I. J. Bruno, M. P. Lightfoot and S. C. Ward, *Acta Crystallogr., Sect. B: Struct. Sci., Cryst. Eng. Mater.*, 2016, **72**, 171–179; (*b*) J. D. Dunitz and R. Taylor, *Chem.–Eur. J.*, 1997, **3**, 89–98; (*c*) J. A. K. Howard, V. J. Hoy, D. O'Hagan and G. T. Smith, *Tetrahedron*, 1996, **52**, 12613–12622.

25 M. Milhet, J. Pauly, J. A. P. Coutinho and J.-L. Daridon, *J. Chem. Eng. Data*, 2007, **52**, 1250–1254.

26 (*a*) M. C. Petty, *Langmuir-Blodgett Films,* Cambridge University Press, 2009; (*b*) J. W. Munden, D. W. Blois and J. Swarbrick, *J. Pharm. Sci.*, 1969, **58**, 1308–1312.

27 During revision a report on the living supramolecular polymerization of all-*cis*-2,3,4,5,6-pentafluorocyclohexane containing monomers was published demonstrating a novel application for this motif; O. Shyshov, S. V. Haridas, L. Pesce, H. Qi, A. Gardin, D. Bochicchio, U. Kaiser, G. M. Pavan and M. von Delius, *Nat. Commun.*, 2021, **12**, 3134.

Chemistry–A European Journal | Full Paper doi.org/10.1002/chem.202102819

Janus All-*Cis* 2,3,4,5,6-Pentafluorocyclohexyl Building Blocks Applied to Medicinal Chemistry and Bioactives Discovery Chemistry

Joshua L. Clark,[a] Rifahath M. Neyyappadath,[a] Cihang Yu,[a] Alexandra M. Z. Slawin,[a] David B. Cordes,[a] and David O'Hagan*[a]

Abstract: Monoalkylated derivatives of the unusually polar all-*cis* 2,3,4,5,6- pentafluorocyclohexyl (Janus face) motif are prepared starting from an aryl hydrogenation of 2,3,4,5,6-pentafluorophenylacetate methyl ester **15**. The method used Zeng's Rh(CAAC) carbene catalyst **4** in the hydrogenation following the protocol developed by Glorius. The resultant Janus pentafluorocyclohexylacetate methyl ester **16** was converted to the corresponding alcohol **18**, aldehyde **13**, bromide **29** and azide **14** through functional group manipulations, and some of these building blocks were used in Ugi-multicomponent and Cu-catalysed click reactions. NBoc protected pentafluoroarylphenylalanine methyl ester **35** was also subject to an aryl hydrogenation, and then deprotection to generate the Janus face β-pentafluorocyclohexyl-alanine amino acid **15**, which was incorporated into representative members of an emerging class of candidate antiviral compounds. Log P measurements demonstrate that the all-*cis* 2,3,4,5,6-pentafluorocyclohexyl ring system is more polar than a phenyl ring. In overview the paper introduces new building blocks containing this Janus ring and demonstrates their progression to molecules typically used in bioactives discovery programmes.

Introduction

Over the last two decades or so organofluorine chemistry has experienced a 'Renaissance', driven by an interest in addressing the synthesis and properties of products carrying isolated –F or $-CF_3$ groups, particularly when attached to sp^3 carbons.[1] This is distinct from an immediately previous era which was defined by the perfluorocarbons and fluoropolymers industries or within fine chemicals, with a focus on aryl –F and $-CF_3$ compounds.[2] The prospects of novel bioactives (med-chem and agrochemicals) resulting from stereogenic fluorine has driven this more recent agenda, and innovation has been stoked by the intense international effort and extraordinary growth in new methods development and catalysis, which defines modern organic chemistry.[3] Access to this next generation of selectively fluorinated alkyls has led to a re-evaluation of dogmas such as 'fluorine increases lipophilicity'. In many cases –F or $-CF_3$ substituted alkyls become more polar (less lipophilic) than the hydrocarbon and such fluorine effects are being explored in detail.[4]

We have had a long interest in selective fluorination of alkyl chains, and particularly in a class of molecules which we have termed 'multi vicinal fluoroalkanes' (Figure 1a) that are defined by placing a fluorine on each carbon along a chain and with a defined stereochemistry, to limit isomer mixtures.[5] The programme progressed from linear to cyclic alkanes and most recently we have been exploring the synthesis and properties of cyclohexanes with multiple vicinal fluorines attached around the ring with the all-*cis* stereochemistry.[6–10] The parent structure, all-*cis* 1,2,3,4,5,6-hexafluorocyclohexane **1** adopts a chair conformation resulting in triaxial C–F bonds, and this arrangement imparts a very high polarity to the ring system as demonstrated by the extraordinary polar properties of **1** (Figure 1b). Cyclohexane **1** has a melting point of 208 °C and a dipole moment of 6.5 D which are particularly high values for an aliphatic.[6] This has been termed a 'Janus' ring system as the fluorine and hydrogen faces, face in opposite directions and are responsible for imparting this polarity.[11]

Most recently[10] we have explored monoalkylated structures of all-*cis* pentafluorocyclohexane represented by **2a** and **2b**, where R is either Me or Et respectively. These systems adopt a conformation, both in gas phase calculations and in solid state structures, where the R substituent lies equatorial and there are three triaxial C–F bonds, rather than the R group axial and with two diaxial C–F bonds. Therefore against expectation, the preferred conformation is the more polar for mono alkylated ring systems. There is a recent and developing interest in applying this motif to solution state coordination of anions[12] and for controlled supramolecular assembly of polymers[13] due

[a] J. L. Clark, Dr. R. M. Neyyappadath, C. Yu, Prof. A. M. Z. Slawin, Dr. D. B. Cordes, Prof. D. O'Hagan
School of Chemistry
University of St Andrews
North Haugh, St Andrews, Fife, KY16 9ST (UK)
E-mail: do1@st-andrews.ac.uk

Supporting information for this article is available on the WWW under https://doi.org/10.1002/chem.202102819

Chemistry–A European Journal | Full Paper doi.org/10.1002/chem.202102819 | Chemistry Europe European Chemical Societies Publishing

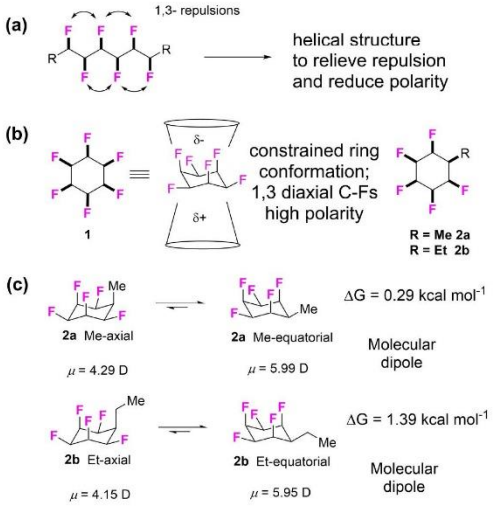

Figure 1. (a) Acyclic multivicinal fluoroalkane chain, adopts a helical conformation. (b) Janus face aspect imparts high polarity to cyclohexane **1** and derivatives **2** with all-*cis* fluorines. (c) Monoalkylated derivatives **2** favour the more polar triaxial C–F conformation with an equatorial alkyl group.[10]

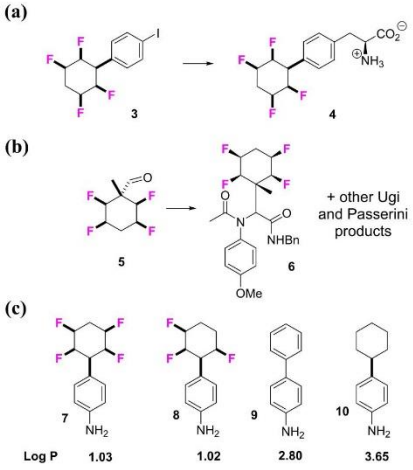

Figure 2. Previous disclosures on all-*cis* 2,3,5,6 - tetrafluorocyclohexane motifs. (a) An amino acid derivative **4**;[14d] (b) aldehyde **5** as an Ugi component. (c). Log P trends across anilines **7–10** indicate increased hydrophilicity with increased fluorination.[16]

to the self association of the polar rings, however these derivatives have yet to be explored in a medicinal chemistry context. In that context the Janus all-*cis* pentafluorocyclohexyl ring system is anticipated to have unique properties not represented by any other substituent in organic chemistry as it has an electronegative fluorine face and an electropositive hydrogen face, and both faces have the potential to interact[8][12] with polar amino acid side chains of opposite electrostatic polarity in protein receptors or enzymes.

Previously[14] we have reported on the preparation of building blocks for the incorporation of all-*cis* 2,3,5,6 - tetrafluorocyclohexane motifs into molecular architectures appropriate to bioactives discovery with illustrative examples shown in Figure 2. For example amino acid **4** could be prepared[14d] in various protected forms and the peptoid product **6**[14c] represents a range of products which were generated through Ugi and Passerini multicomponent reactions.[15] With such compounds in hand it became apparent that the fluorine of the 2,3,5,6 - tetrafluorocyclohexane ring system rendered these compounds significantly more hydrophilic relative to their aromatic and non-fluorinated cyclohexyl analogues.[16] This is a striking feature of the ring system as fluorine is generally considered to impart lipophilicity, however in these ring systems the fluorine imparts hydrophilicity, as determined by comparative Log P measurements, illustrated for the anilines **7**–**10** in Figure 2. This is due to the polar nature of the fluorocyclohexane ring with water associating to the protic face of the Janus rings through hydrogen bonding.[16] In this paper we now explore the all-*cis* 1,2,3,4,5-pentafluorocyclohexane ring system in a similar context. Until recently this arrangement of a substituted cyclohexane and with five fluorine around the ring was not synthetically accessible, however the Glorius lab have developed[17] a catalytic fluoroaryl hydrogenation which we have used here to access this class of compounds. The prototype example shown in Figure 3 demonstrated the efficient hydrogenation of hexafluorobenzene **11** using Zeng's CAAC catalyst **12**[18] to generate hexafluorocyclohexane **1**, and the method was extended to prepare a range of all-*cis* fluorocyclohexanes and also with different functionalities.[17]

In this paper we report the preparation of a range of building blocks incorporating the all-*cis* 2,3,4,5,6-pentafluorocyclohexypentafluoro cyclohexyl motif but with a particular focus on elaborations of aldehyde **13**, azide **14** and amino acid **15** as illustrated in Figure 4.

The utility of aldehyde **13** is explored in Ugi multicomponent reactions,[15] the azide in Cu-catalysed 'click' reactions[19] and the amino acid is incorporated into known coronavirus inhibitor analogues.[20,21] It emerges as a general phenomenon that the replacement of cyclohexyl or aryl ring by the all-*cis*

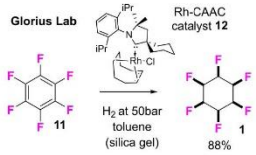

Figure 3. Catalyst and *cis*-selective hydrogenation of hexafluorobenzene **11** to give **1** as reported by Glorius.[17,18]

Chemistry–A European Journal | Full Paper doi.org/10.1002/chem.202102819 | Chemistry Europe European Chemical Societies Publishing

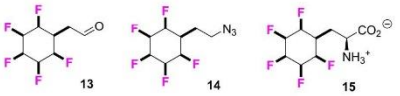

Figure 4. Key building blocks **13**–**15** carrying the all-*cis* 2,3,4,5,6-pentafluorocyclohexyl motif used in this study.

2,3,4,5,6-pentafluorocyclohexyl moiety results in a significant reduction in Log P values, which suggests that these motifs would be quite acceptable starting points, for example as fragments for bioactives and drug discovery programmes.

Results and Discussion

The pentafluoroaryl phenylacetate ester **16** is readily available and offered a convenient starting point for building block development. Aryl hydrogenation using the Zeng catalyst **12**[17] and following Glorius protocols[16] resulted in an efficient conversion to the corresponding cyclohexyl ester **17** as the major product with the 5-defluorinated co-product **18** as a minor product (**17**:**18**, 11:1). The regiospecific nature of the defluorination was established by X-ray crystallography of **18** (Scheme 1). This minor co-product could be removed by chromatography and **17** was progressed to further transformations. Reduction of the ester moiety of **17** to aldehyde **13** was carried out in a two-step protocol as a one-step controlled reduction with DIBAL did not offer any yield advantage. Accordingly, ester **17** was reduced to alcohol **19** with DIBAL and this product was conveniently oxidised to aldehyde **13** after exposure to Dess-Martin periodinane.[22]

^{1}H NMR analysis revealed that aldehyde **13** readily forms a hemiacetal with [$^{2}H_4$]-methanol suggesting a significant electron withdrawing effect of the pentafluorocyclohexane ring system. None- the-less it was a good substrate in a number of 4-component Ugi reactions, of which the products **20**–**25** are summarised in Figure 5.

Two of these products (**20** and **25**) were amenable to X-ray structure analysis as shown in Figure 6 and this assisted in confirming their peptoid like structures. In order to elucidate the effect of the 2,3,4,5,6-all-*cis*-pentafluorocyclohexane ring on

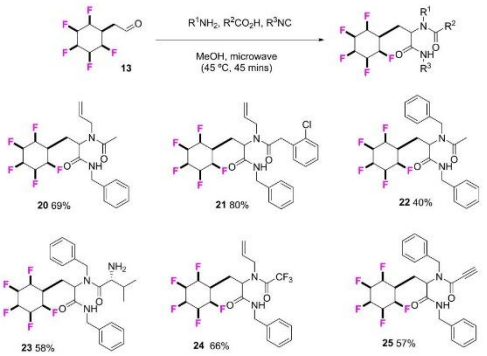

Figure 5. General Ugi multicomponent procedure with aldehyde **13** showing isolated yields and product structures **20**–**25**.

Figure 6. X-ray crystal structures of Ugi multicomponent products **20** and **25**.

lipophilicity of this product class, Log P values were determined for products **20**–**22** and compared to their corresponding analogues **26**–**28** with a phenyl ring in place of the 2,3,4,5,6-all-*cis*-pentafluorocyclohexane rings. The Log P values were determined by HPLC (acetonitrile/water) as described previously[14,16] and the comparative data are presented in Figure 7. It is clear that replacement of a phenyl ring by the all-*cis* 2,3,4,5,6-pentafluorocyclohexyl moiety increases hydrophilicity, with the Log P decreasing by 0.4–0.65 Log P units. This trend is consistent with that previously observed for the phenyltetrafluorocyclohexyl motifs,[14] and also the all *cis*-1,2,3-trifluorocyclopropyl motif,[24] and it suggests that this aspect reinforces its utility as a candidate isostere[25] for hit optimisation studies.

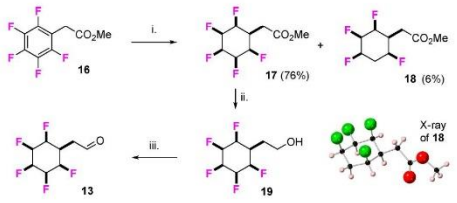

Scheme 1. i. **12** (1 mol%), H_2 (50 bar), hexane, 4 Å MS, r.t., 16h; ii. DIBAL, THF, 0 °C to r.t, 16h, 83%; iii. Dess-Martin periodinane, THF, r.t, 45min, 85%. X-ray structure of **17**.

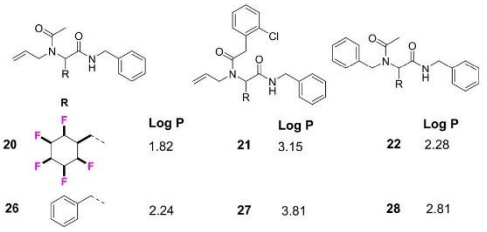

Figure 7. Comparative Log P values of Ugi fluorocyclohexyl products **20**–**22** with the corresponding benzyl products **26**–**28**.

Chemistry–A European Journal | Full Paper doi.org/10.1002/chem.202102819 | Chemistry Europe European Chemical Societies Publishing

In other functional group interconversions, alcohol **19** was readily converted to the corresponding bromide **29** by an Appel reaction,[26] and the bromide to azide **14** as shown in Figure 8a. Azide **14** is a crystalline solid and the corresponding X-ray is also shown in Figure 8a. Azide **14** could be readily reduced under Staudinger conditions[27] to amine **34** to provide another building block. Azide **14** was also a relatively efficient substrate in a series of Cu-catalysed 'click' reactions[19] with phenylacetylenes to give the products **30–33** as illustrated in Figure 8b.

A potentially interesting building block of wide utility is amino acid **15**. We report its synthesis here and then its incorporation into the structural skeleton of a class of antiviral analogues typified by **34** and **35** in Figure 9. This structural series of peptidomimetic aldehydes and esters has emerged as potent inhibitors of the human enterovirus 71(EV-71) and coronavirus (SARS) protease,[20] and interest in this class of compounds has received a particular and recent focus as a starting point to find inhibitors of the COVID-19 coronavirus.[21] In particular those compounds **34** and **35** containing fluoroaryl-phenylalanine and cyclohexyl-amino acid show good antiviral activities.[20] In the context of exploring the all-*cis* 2,3,4,5,6-pentafluorocyclohexyl moiety in drug discovery, the two aldehydes **45** and **48** (Scheme 2) and the two esters **52** and **53** (Scheme 3) of this class of antivirals were prepared carrying the Janus ring in place of phenyl or cyclohexyl. These syntheses required amino acid **15** which could be prepared by aryl hydrogenation of the pentafluoroaryl analogue of fully protected phenylalanine **36**, itself prepared after methylation of the commercially available NBoc protected L-amino acid.[28] Hydrogenation using the Glorius/Zeng protocol[16,17] generated the cyclohexylamino acid **37** in good yield. The pentafluorocyclohexyl ring system is susceptible to base decomposition, and selective ester hydrolysis under acidic conditions proved difficult, therefore the free amino acid **15** was generated and its structure confirmed by X-ray analysis (inset in Scheme 2). This amino acid was then re-protected with the NBoc group to give **38**.[29] The synthesis to the target aldehydes **45** and **48** with either a cinnamate or indole-carboxylate amide could then be completed following the published[20c] protocols as illustrated in Scheme 2. Similarly, the corresponding conjugated ethyl ester analogues **52** and **53**, carrying the pendant cinnamate or indole-carboxylate amides respectively were prepared also from

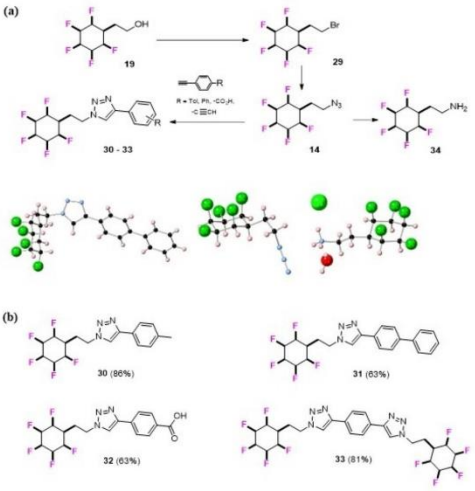

Figure 8. (a) Reactions forming azide **14**, amine **34** and 'click' products **30–33**. X-ray structures of triazole **31**, azide **14**, and amine hydrochloride of **34**. (b) 'Click' triazole products **30–33** derived from **14** and an appropriate phenyl acetylene.

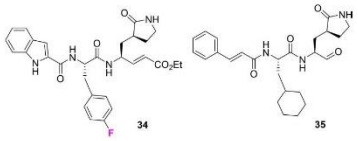

Figure 9. Representatives **34** and **35** of lead Enterovirus-71 and SARS-2 proteases inhibitors.[20]

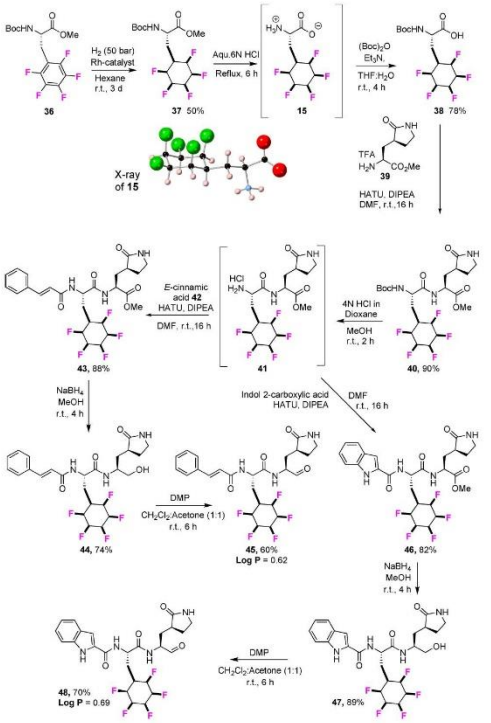

Scheme 2. Synthesis of antiviral candidates **45** and **48** from amino acid **15**.

Chemistry–A European Journal | Full Paper doi.org/10.1002/chem.202102819 | Chemistry Europe European Chemical Societies Publishing

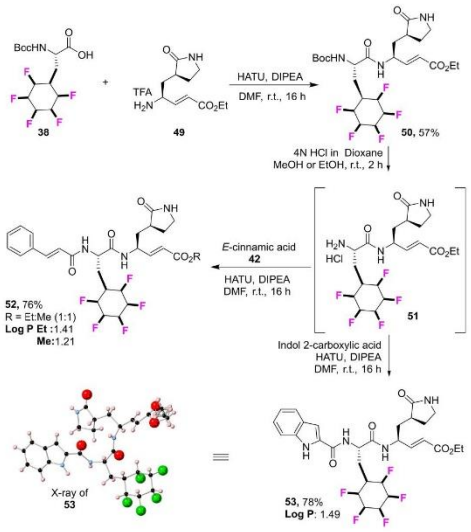

Scheme 3. Syntheses of antiviral candidates **52** and **53**.

NBoc protected amino acid **38** following the previous protocols,[20d] with only minor modifications as illustrated in Scheme 3. During the Boc deprotection of **50** to get **51** in methanol, trans esterification of ethyl ester to methyl ester was observed (1:1 mixture) and the reaction of **51** upon reaction with **42** gave a 1:1 mixture of **52**. Knowing this, the de protection of Boc for the synthesis of **53** was performed in ethanol and achieved pure **53**.

Log P values were determined[10,16] for products **45**, **48**, **52** and **53**. The values were in the range Log P ~1.5–2.0. These are low values and in a good range for candidate drug development, and they indicate again that the all-*cis* 2,3,4,5,6-pentafluoro-cyclohexyl ring system possesses good properties for bioactive molecule discovery. In the event the candidate antivirals **45**, **48**, **52** and **53** were assessed for their antiviral activity against Zika virus and the SARS-CoV-2 virus, however they did not show any activity in these assays.[30]

Conclusion

Several building blocks have been prepared by direct aryl hydrogenation of all- 2,3,4,5,6-pentafluorophenyl acetaldehyde **16** and the NBoc-protected methyl ester of pentafluoroaryl phenylalanine. In particular a series of candidate bioactives were prepared from cyclohexylacetaldehyde **13** and amino acid **15**. Aldehyde **13**, was used to prepare a range of Ugi multicomponent products and the amino acid to access direct analogues of known peptidomimetic aldehydes and esters. Comparative Log P determinations between phenyl and all-*cis* 2,3,4,5,6-pentafluorocyclohexyl analogues illustrates an increase in hydrophilicity for the fluorocyclohexanes and suggests a utility for this motif in bioactives discovery programmes. These results should encourage the further exploration of this motif in medicinal chemistry.

X-ray crystallography

Deposition Number(s) 2098747 (**14**), 2098748 (**15**), 2098749 (**17**), 2098750 (**18**), 2098751 (**19**), 2098752 (**20**), 2098753 (**25**), 2098754 (**31**), 2098755 (**34HCl**), 2098756 (**37**), 2098757 (**53**) contain(s) the supplementary crystallographic data for this paper. These data are provided free of charge by the joint Cambridge Crystallographic Data Centre and Fachinformations-zentrum Karlsruhe Access Structures service.

Acknowledgements

We thank EPSRC for a grant (EP/R013799/1) and Studentships (JLC) through the EPSRC CRITICAT CDT programme and also the Chinese Scholarship Council (CY). We also thank Professor Arvind H Patel at the MRC Centre for Virus Research at the University of Glasgow for antiviral assays.

Conflict of Interest

The authors declare no conflict of interest.

Keywords: aryl hydrogenation · fluorocyclohexanes · Janus motif · organic chemistry · organofluorine chemistry

[1] a) S. Meyer, J. Hafliger, R. Gilmour, *Chem. Sci.* **2021**, *12*, 10686–10695; b) R. Hevey, *Chem. Eur. J.* **2021**, *27*, 2240–2253; c) I. Ojima (Ed.), *'Frontiers of Organic Fluorine Chemistry'*, World Scientific Europe, **2020**; d) Q. H. Liu, C. F. Ni, J. B. Hu Hu, *Nat. Sci. Rev.* **2017**, *4*, 303–325; e) A. Harsanyi, G. Sandford, *Green Chem.* **2015**, *17*, 2081–2086; f) P. Kirsch, *'Modern Fluoroorganic Chemistry. Synthesis, Reactivity, Applications.'* 2nd Edn., Wiley-VCH, Weinheim, **2013**.

[2] a) R. D. Chambers, *'Fluorine in Organic Chemistry'* 2nd Edn., Blackwell Publishing Ltd., Oxford, **2004**; b) M. Hudlicky, A. E. Pavlath, *'Chemistry of Organofluorine Compounds II,'* ACS Monograph 187, American Chemical Society, Washington **1995**.

[3] a) W. Zhu, X. Zhen, J. Wu, Y. Cheng, J. An, X. Ma, J. Liu, Y. Qin, H. Zhu, J. Xue, X. Jiang, *Nat. Commun.* **2021**, *12*, 3957; b) F. Scheidt, M. Schäfer, J. C. Sarie, C. G. Daniliuc, J. J. Molloy, R. Gilmour, *Angew. Chem. Int. Ed.* **2018**, *57*, 16431–16435; *Angew. Chem.* **2018**, *130*, 16669–16673; c) S. M. Banik, J. W. Medley, E. N. Jacobsen, *J. Am. Chem. Soc.* **2016**, *138*, 5000–5003; d) I. G. Molnar, R. Gilmour, *J. Am. Chem. Soc.* **2016**, *138*, 5004–5007; e) T. D. Beeson, D. W. C. MacMillan, *J. Am. Chem. Soc.* **2005**, *127*, 8826–8828; f) L. Hintermann, A. Togni, *Angew. Chem. Int. Ed.* **2000**, *39*, 4359–4362; *Angew. Chem.* **2000**, *112*, 4530–4533.

[4] a) B. F. J. Jeffries, Z. Wang, H. R. Felstead, J. Y. Le Questel, J. Scott, E. Chiarparin, J. Graton, B. Linclau, *J. Med. Chem.* **2020**, *63*, 1002–1031; b) Q. A. Huchet, N. Trapp, B. Kuhn, B. Wagner, H. Fischer, N. A. Kratochwil, E. M. Carreira, K. Müller, *J. Fluorine Chem.* **2017**, *198*, 34–46; c) R. Vorberg, N. Trapp, D. Zimmerli, B. Wagner, H. Fischer, N. A. Kratochwil, M. Kansy, E. M. Carreira, K. M. Müller, *ChemMedChem* **2016**, *11*, 2216–2239; d) H.-J Bôhm, D. Banner, S. Bendels, M. Kansy, B. Kuhn, K. Müller, U. Obst-Sander, M. Stahl, *ChemBioChem.* **2004**, *5*, 637–643.

[5] a) D. O'Hagan, *Chem. Eur. J.* **2020**, *26*, 7981–7997; b) N. Al-Maharik, D. B. Cordes, A. M. Z. Slawin, M. Bühl, D. O'Hagan, *Org. Biomol. Chem.* **2020**,

Chemistry–A European Journal | Full Paper doi.org/10.1002/chem.202102819 | Chemistry Europe European Chemical Societies Publishing

18, 878–887; c) D. O'Hagan, *J. Org. Chem.* **2012**, *77*, 3689–3699; d) L. Hunter, P. Kirsch, A. M. Z. Slawin, D. O'Hagan, *Angew. Chem. Int. Ed.* **2009**, *48*, 5457–5460; *Angew. Chem.* **2009**, *121*, 5565–5568.
[6] N. S. Keddie, A. M. Z. Slawin, T. Lebl, D. Philp, D. O'Hagan, *Nat. Chem.* **2015**, *7*, 483–488.
[7] R. A. Cormanich, N. Keddie, R. Rittner, D. O'Hagan, M. Bühl, *Phys. Chem. Chem. Phys.* **2015**, *44*, 29475–29478.
[8] B. E. Ziegler, M. Lecours, R. A. Marta, J. Featherstone, E. Fillion, W. S. Hopkins, V. Steinmetz, N. S. Keddie, D. O'Hagan, T. B. McMahon, *J. Am. Chem. Soc.* **2016**, *138*, 7460–7463.
[9] M. J. Lecours, R. A. Marta, V. Steinmetz, N. Keddie, E. Fillion, D. O'Hagan, T. B. McMahon, W. S. Hopkins, *J. Phys. Chem. Lett.* **2017**, *8*, 109–113.
[10] J. L. Clark, A. Taylor, A. Geddis, R. M. Neyyappadath, B. A. Piscelli, C. Yu, D. B. Cordes, A. M. Z. Slawin, R. A. Cormanich, S. Guldin, D. O'Hagan, *Chem. Sci.* **2021**, *12*, 9712–9719.
[11] N. Santschi, R. Gilmour, *Nat. Chem.* **2015**, *7*, 467–468.
[12] O. Shyshov, K. A. Siewerth, M. von Delius, *Chem. Commun.* **2018**, *54*, 4353–4355.
[13] O. Shyshov, S. V. Haridas, L. Pesce, H. Qi, A. Gardin, D. Bochicchio, U. Kaiser, G. M. Pavan, M. von Delius, *Nat. Commun.* **2021**, *12*, 3134.
[14] a) T. Bykova, N. Al-Maharik, A. M. Z. Slawin, M. Bühl, T. Lebl, D. O' Hagan, *Chem. Eur. J.* **2018**, *24*, 13290–13296; b) T. Bykova, N. Al-Maharik, A. M. Z. Slawin, D. O'Hagan, *Beilstein J. Org. Chem.* **2017**, *13*, 728–733; c) T. Bykova, N. Al-Maharik, A. M. Z. Slawin, D. O'Hagan, *Org. Biomol. Chem.* **2016**, *14*, 1117–1123; d) M. S. Ayoup, D. B. Cordes, A. M. Z. Slawin, D. O'Hagan, *Org. Biomol. Chem.* **2015**, *13*, 5621–5624; e) M. Salah Ayoup, D. B. Cordes, A. M. Z. Slawin, D. O'Hagan, *Beilstein J. Org. Chem.* **2015**, *11*, 2671–2676; f) A. J. Durie, T. Fujiwara, R. Cormanich, M. Bühl, A. M. Z. Slawin, D. O'Hagan, *Chem. Eur. J.* **2014**, *20*, 6259–6263.
[15] a) Q. Wang, D.-X. Wang, M.-X. Wang, J. Zhu, *Acc. Chem. Res.* **2018**, *51*, 1290–1300; b) I. Ugi, A. Dömling, W. Hörl, *Endeavour* **1994**, *18*, 115–122.
[16] A. Rodil, S. Bosisio, M. S. Ayoup, L. Quinn, D. B. Cordes, A. M. Z. Slawin, C. D. Murphy, J. Michel, D. O'Hagan, *Chem. Sci.* **2018**, *9*, 3023–3028.
[17] a) Z. Nairoukh, M. Wollenburg, C. Schlepphorst, K. Bergander, F. Glorius, *Nat. Chem.* **2019**, *11*, 264–270; b) M. P. Wiesenfeldt, T. Knecht, C. Schlepphorst, F. Glorius, *Angew. Chem. Int. Ed.* **2018**, *57*, 8297–8300; *Angew. Chem.* **2018**, *130*, 8429–8432; c) M. P. Wiesenfeldt, Z. Nairoukh, W. Li, F. Glorius, *Science* **2017**, *357*, 908–912.
[18] a) X. Zhang, L. Ling, M. Luo, X. Zeng, *Angew. Chem. Int. Ed.* **2019**, *58*, 16785–16789; *Angew. Chem.* **2019**, *131*, 16941–16945; b) Y. Wei, B. Rao, X. Cong, X. Zeng, *J. Am. Chem. Soc.* **2015**, *137*, 9250–9253.
[19] a) C. W. Tornøe, C. Christensen, M. Meldal, *J. Org. Chem.* **2002**, *67*, 3057–3064; b) V. V. Rostovtsev, L. G. Green, V. V. Fokin, K. B. Sharpless, *Angew. Chem. Int. Ed.* **2002**, *41*, 2596–2599; *Angew. Chem.* **2002**, *114*, 2708–2711.
[20] a) W. Dai, D. Jochmans, H. Xie, H. Yang, J. Li, H. Su, D. Chang, J. Wang, J. Peng, L. Zhu, Y. Nian, R. Hilgenfeld, H. Jiang, K. Chen, L. Zhang, Y. Xu, J. Neyts, H. Liu, *J. Med. Chem.* **2021**, *64*, https://doi.org/10.1021/acs.jmedchem.0c02258; b) W. Dai, B. Zhang, X.-M. Jiang, H. Su, J. Li, Y. Zhao, X. Xie, Z. Jin, J. Peng, F. Liu, C. Li, Y. Li, F. Bai, H. Wang, X. Cheng, X. Cen, S. Hu, X. Yang, J. Wang, X. Liu, G. Xiao, H. Jiang, Z. Rao, L.-K. Zhang, Y. Xu, H. Yang, H. Liu, *Science* **2020**, *363*, 1331–1335; c) Y. Zhai, X. Zhao, Z. Cui, M. Wang, Y. Wang, L. Li, Q. Sun, X. Yang, D. Zeng, Y. Liu, Y. Sun, Z. Lou, L. Shang, Z. Yin, *J. Med. Chem.* **2015**, *58*, 9414–9420; d) C.-J. Kuo, J.-J. Shie, J.-M. Fang, G.-R. Yen, J. T. A. Hsu, H.-G. Liu, S.-N. Tseng, S.-C. Chang, C.-Y. Lee, S.-R. Shih, P.-H. Liang, *Bioorg. Med. Chem.* **2008**, *16*, 7388–7398; e) K. Anand, J. Ziebuhr, P. Wadhwani, J. R. Mesters, R. Hilgenfeld, *Science* **2003**, *300*, 1763–1767.
[21] a) R. L. Hoffman, R. S. Kania, M. A. Brothers, J. F. Davies, R. A. Ferre, K. S. Gajiwala, M. He, R. J. Hogan, K. Kozminski, L. Y. Li, J. W. Lockner, J. Lou, M. T. Marra, L. J. Mitchell, B. W. Murray, J. A. Nieman, S. Noell, S. P. Planken, T. Rowe, K. Ryan, G. J. Smith, J. E. Solowiej, C. M. Steppan, B. Taggart, *J. Med. Chem.* **2020**, *63*, 12725–12747; b) L. Zhang, D. Lin, Y. Kusov, Y. Nian, Q. Ma, J. Wang, A. von Brunn, P. Leyssen, K. Lanko, J. Neyts, A. de Wilde, E. J. Snijder, H. Liu, R. Hilgenfeld, *J. Med. Chem.* **2020**, *63*, 4562–4578.
[22] D. B. Dess, J. C. Martin, *J. Org. Chem.* **1983**, *48*, 4155–4156.
[23] a) C. Giaginis, A. Tsantili-Kakoulidou, *J. Liq. Chromatogr. Relat. Technol.* **2008**, *31*, 79–96; b) C. M. Du, K. Valko, C. Bevan, D. Reynolds, M. H. Abraham, *Anal. Chem.* **1998**, *70*, 4228–4234.
[24] Z. Fang, D. B. Cordes, A. M. Z. Slawin, D. O'Hagan, *Chem. Commun.* **2019**, *55*, 10539–10542.
[25] a) B. M. Johnson, Y. Z. Shu, X. L. Zhuo, N. A. Meanwell, *J. Med. Chem.* **2020**, *63*, 6315–6386; b) H. Mei, J. Han, S. White, D. J. Graham, K. Izawa, T. Sato, S. Fustero, N. A. Meanwell, V. A. Soloshonok, *Chem. Eur. J.* **2020**, *26*, 11349–11390; c) E. P. Gillis, K. J. Eastman, M. D. Hill, D. J. Donnelly, N. A. Meanwell, *J. Med. Chem.* **2015**, *58*, 8315–8359.
[26] R. Appel, *Angew. Chem. Int. Ed.* **1975**, *14*, 801–811; *Angew. Chem.* **1975**, *87*, 863–874.
[27] Y. G. Gololobov, L. F. Kasukhin, *Tetrahedron* **1992**, *48*, 1353–1406.
[28] P. P. Geurink, N. Liu, M. P. Spaans, S. L. Downey, A. M. C. H. van den Nieuwendijk, G. A. van der Marel, A. F. Kisselev, B. I. Florea, H. S. Overkleeft, *J. Med. Chem.* **2010**, *53*, 2319–2323; N-Boc-L-(pentafluoroaryl)phenylalanine - Fluorochem. Ltd., Catalogue No 008086; CAS Number 34702–60-8.
[29] E. Vaz, M. Fernandez-Saurez, L. Muñoz, *Tetrahedron: Asymmetry* **2003**, *14*, 1935–1942.
[30] Antiviral assays were conducted the MRC-Centre for Virus Research at the University of Glasgow, UK.

Manuscript received: August 3, 2021
Accepted manuscript online: September 6, 2021
Version of record online: October 6, 2021

